UNIVERSITÀ DEGLI STUDI DI SALERNO

DIPARTIMENTO DI INGEGNERIA CIVILE

Dottorato di Ricerca in Rischio e Sostenibilità nei sistemi dell'Ingegneria civile, edile e ambientale

XXX Ciclo (2014-2017)

Optimal seismic retrofitting of existing RC frames through Soft-Computing approaches

Roberto Falcone

Tutor	**Il Coordinatore**
Prof. Enzo Martinelli	*Prof. Fernando Fraternali*

Co-Tutor
Prof. Raffaele Cerulli
Prof. Ciro Faella

"Non è la più forte delle specie che sopravvive, né la più intelligente,

ma quella più reattiva ai cambiamenti"

Charles Robert Darwin

ACKNOWLEDGMENT

Index

1. Introduction

1.1 Motivation and objectives

The seismic risk generally means the expected loss in terms of lives injury, property damage, direct and indirect costs due to potential ground shaking associated with energy release from a fault for a given area and a reference period [1]. It is determined by a combination of earthquake hazard, vulnerability, and exposure. The greater or lesser presence of goods at risk and, therefore, the consequent possibility of suffering damage is defined as "exposure" (of human life, economic assets, and cultural heritage).

Earthquake hazard, also called "seismicity", measures the likelihood that a seismic event of a given magnitude (or intensity) affects a certain area in a certain interval of time. Geological studies and historical records indicate that lower magnitude earthquakes generally occur more frequently than higher magnitude ones [2] [3] [4]. The ground motion at a site depends on the natural evolution of the earth's crust and, hence, seismicity is a physical characteristic of a certain area. The higher the seismicity, the higher the probability of earthquake occurrence in the same interval of time.

Moreover, vulnerability represents the building's susceptibility to damage induced by the seismic event of a given magnitude (or, correspondingly, return period). In fact, the greater the vulnerability (among the other things, due to inadequate design, poor quality materials, construction methods, lack of maintenance as described in Section 1.2) the more serious damage the structure will suffer as a result of the induced seismic shaking [5].

However, the fault rupture that originates the earthquakes does not itself kill people or induce great economic losses. What causes most of the injury and economic losses is the interaction of the earthquake ground motions with the built environment. Seismic "disaster" at any site or region is, hence, the consequence of the interaction of the sources of potential earthquake hazards (created by the local seismic activity associated with energy release from a fault) with the vulnerability of the human-made facilities (either engineered or not). The economic loss induced

by earthquakes depends not only on their magnitude and on the surface propagation of the seismic waves but also on the level of "anthropization" of the affected areas and the human ability to build safe buildings and infrastructures.

That said, Italy is characterized by a medium-to-high seismicity due to the frequency and magnitude of the earthquake phenomena. In the last 150 years, there have been around 30 earthquakes with a destructive character. From the beginning of the 20th century, there have been 6 major earthquakes (Figure 1.1) with a magnitude equal or higher than 6.5 causing a total number of casualties equal to 126,607 [6].

Messina 1908 (deaths: 85,926)

Avezzano 1915 (deaths: 32,610)

Friuli 1976 (deaths: 989)

Irpinia 1980 (deaths: 2,914)

L'Aquila 2009 (deaths: 309)

Amatrice 2016 (deaths: 299)

Figure 1.1: Deadliest earthquakes occurred in last 150 years in Italy

The exposure in Italy stands at high values as a result of the high population density and the presence of an important historical, artistic and monumental heritage [7]. In this sense, it is significant the seismic event in Umbria and Marche occurred in 1997, which severely damaged 600 churches and, particularly, the Basilica of St. Francis of Assisi (Figure 1.2).

(a)   *(b)*
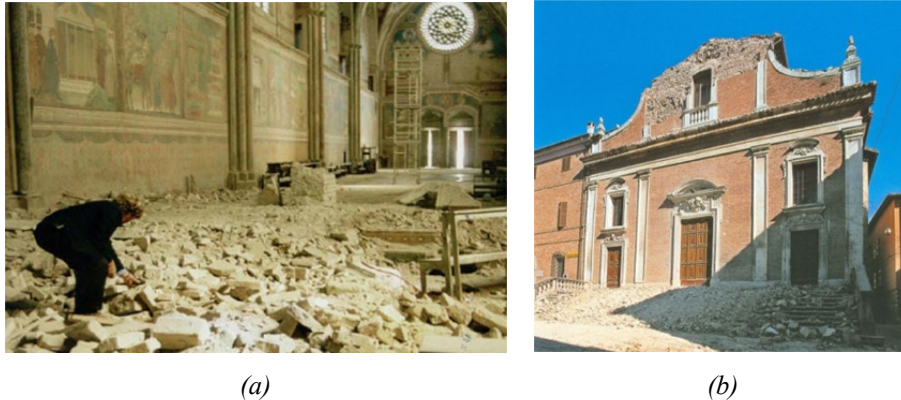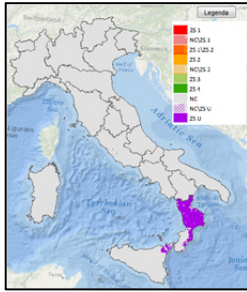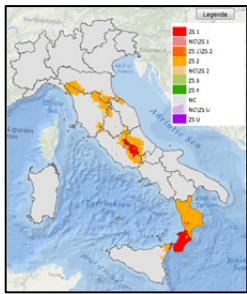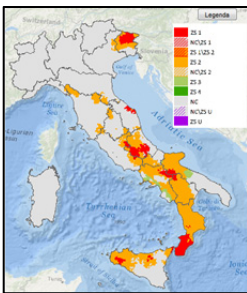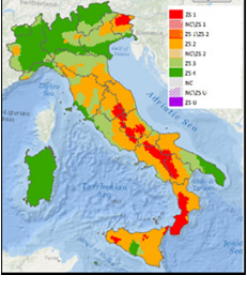
Figure 1.2: Damage to Basilica of St. Francis (a) and San Biagio Church (b)

Hence, Italy is one of the countries facing the highest seismic risk in the Mediterranean area. However, the ratio between occurred damage and the recorded amount of energy released during the events is much higher than other highly seismic countries. Italy with respect to those countries, where the earthquake hazard is even greater, is characterized by a very high vulnerability affecting constructions built even in the recent past and devoted to public and strategic purposes [8]. Some of them have been designed and consequently built prior to the entry into force of the first regulations for construction in the seismic area or in accordance to subsequently replaced or radically amended seismic regulations which over time, due to advancement in engineering knowledge, have improved the degree of analysis and considerably enhanced the magnitude of the design seismic forces [9]. The older buildings usually cannot comply with the more stringent specifications of the latest standards even if constructed in compliance with prevailing standards of the time. Other existing buildings are placed on sites whose seismicity has been upgraded after their construction.

The evolution of the seismic hazard assessment of Italian territories over the years and subsequent application of appropriate design rules have often led to seismic design actions higher than expected during the design stage [10] [11]. The following Table summarizes the time evolution of both seismic codes and hazard classification occurred in Italy during the last century.

Evolution of Italian seismic code			*Evolution of seismic classification*	
R.D. 193, 1909		**1909**	R.D. 143, 1909	
				No Zone
R.D. 2089, 1924	1st generation standards purely prescriptive			
R.D. 431, 1927			R.D. 431, 1927	
R.D. 640, 1935				
R.D. 2228, 1939		**1950**		Zone I – II
Law n. 1684, 1962				
C.M. 6090, 1969				
Law n.64, 1974	2nd generation standards 1-level performance			
D.M. 1975			D.M. 515 1981	
D.M. 1981				
D.M. 1984				
D.M. 1986				Zone I – II - III
D.M. 1996				
		2000		
Testo Unico 2001				
O.P.C.M. 3274, 2003	3rd generation standards 2-levels performance		O.P.C.M. 3274, 2003	
				Zone I – II – III – IV
O.P.C.M. 3431, 2005				
D.M. 2005				
D.M. 2008 [15]	4th generation standards multi-levels	**2010**		

According to the most recent seismic classification [12], 43.5% of the national territory is characterized by high earthquake hazard (seismic zone I or II). According to the 2011 Italian census [13], the number of buildings with a predominantly residential use shown in Table 1.1 is 12,180,131.

More than 35% of the residential buildings are placed in a high-risk area where 21.7 million people live. Particularly, the census states that reinforced concrete structures on which the present Ph.D. thesis is focused are rather spread in all the aforementioned seismic prone regions, representing the 33% of Italian built stock.

However, a percentage equal to 68% of existing residential buildings have been built before 1971 according to the 1st generation (purely prescriptive) standards. Moreover, a percentage lower than 2% of homes were built in the years 2000 when technical standards began to impose far more restrictive criteria.

Table 1.1: Estimated number of homes with potential seismic risk [14]

Region	I generation standards	II generation standards	III - IV generation standards	Total
	< 1971	1972 - 2001	2002-2011	
Abruzzo	193,488	95,891	3,808	293,187
Basilicata	88,184	40,417	1,571	130,172
Calabria	292,312	179,335	1,554	473,201
Campania	646,446	307,505	6,095	960,046
Emilia-Romagna	590,290	260,064	30,046	880,400
Friuli	185,350	81,753	6,258	273,361
Lazio	716,741	310,627	4,394	1,031,762
Liguria	419,296	63,939	1,508	484,743
Lombardia	1,287,572	525,336	52,320	1,865,228
Marche	202,243	93,341	7,419	303,003
Molise	62,613	21,436	1,163	85,212
Piemonte	849,156	210,936	6,607	1,066,699
Puglia	495,199	283,620	1,015	779,834
Sardegna	178,954	144,636	5,911	329,501
Sicilia	675,706	386,492	5,035	1,067,233
Toscana	623,183	174,037	15,958	813,178
Trentino	157,764	68,008	6,798	232,570
Umbria	111,188	53,881	5,671	170,740
Valle d'Aosta	31,994	13,333	1,023	46,350
Veneto	560,107	298,649	34,955	893,711
Total	**8,367,786**	**3,613,236**	**199,109**	**12,180,131**

Although recent progress have been done in the area of seismic prediction, the earthquakes cannot be accurately predicted in time, magnitude or location. Furthermore, despite earthquake resistance requirements in building codes have become more stringent and improved significantly even the last codes are not infallible [15]. Therefore, the main way of decreasing economic and life losses as a

direct consequence of earthquake disasters is making new building earthquake-safe and strengthen existing ones. Therefore, the need for strengthening existing buildings has emerged as a technical challenge [16] and a societal priority [17] as a result of the significant damages and casualties often deriving from seismic events.

Over the last seventy years, around 190 billion euros have been spent in post-event restoration and reconstruction including direct and indirect costs [18]. Retrofitting of vulnerable structures is a major task that many building corporations and government have to address. In future projection, the costs of securing the housing stock from earthquakes depend on the level of risk coverage that is deemed acceptable.

Based on this assumption, referring to the Italy's housing stock and using as a parameter of seismic intensity the impact of the earthquake of L'Aquila [19] (representing, on the scale of historically recorded in Italy, an average destructive event), CNI's Study Center has suggested a possible distribution of the intervention costs based on the age distribution of the buildings and their structural conditions [14]. According to this study, the percentage of structures to be retrofitted based on the examination of the damages recorded to houses in L'Aquila and the housing conditions gathered from census surveys is equal to approximately 40% of houses in the country, regardless of the seismic risk level.

In this perspective, about 12 million properties (with a population of around 23 million people involved) should be involved in rehabilitation and static safety intervention. Applying the average parameters of technical specifications for seismic interventions, there would be an overall cost to secure the Italians' housing stock by average seismic events of about 93 billion euros (Table 1.2). Hence, the financial implication of such a huge task could be mind-boggling.

Nowadays, no well-established and completely accepted procedures are available for obtaining the optimal seismic retrofitting solution. Therefore, the definition of a rational strategy for seismic retrofitting is still an open issue. In the Authors' best knowledge, no relevant study is currently available for approaching seismic retrofitting of existing RC frames as an optimization problem, as recent scientific contributions on optimization algorithms are restricted to seismic design of new structures [20][21].

Conversely, in the current practice, as well as in most relevant scientific contributions on this topic [22]-[26], seismic retrofitting of RC frames are only based on common sense. Considerations about optimization are left to the engineering judgment and, hence, they are not part of a systematic analysis. This is partly due to the complexity of the constrained optimization problem under

6

consideration, which cannot be duly approached by means of analytical techniques commonly employed in structural engineering, as it can only be solved by means of alternative techniques that are not in the background of common structural engineers.

Table 1.2: Cost estimate necessary to make Italian homes safe from seismic risk [14]

Region	Seismic zone 1	Seismic zone 2	Seismic zone 3	Seismic zone 4	Total [€]
Abruzzo	519,608,951	956,819,990	1,026,708,276	-	2,503,137,217
Basilicata	389,756,074	578,689,566	110,593,193	-	1,079,038,833
Calabria	2,261,606,036	1,674,589,040	-	-	3,936,195,076
Campania	757,085,265	6,495,980,770	842,691,565	-	8,095,757,600
Emilia-R.	-	1,886,802,360	4,444,537,374	360,037,192	6,691,376,926
Friuli	175,023,026	912,238,866	282,330,683	668,360,083	2,037,952,658
Lazio	289,653,340	2,251,614,507	4,944,840,424	188,586,014	7,674,694,285
Liguria	-	358,830,381	978,983,635	1,978,397,589	3,316,211,605
Lombardia	-	244,134,343	2,127,065,643	10,530,581,244	12,901,781,230
Marche	21,979,822	2,286,865,047	145,423,612	1,608,381	2,455,876,862
Molise	180,286,210	473,637,420	94,327,642	-	748251272
Piemonte	-	259,827,928	726,379,390	6,400,791,351	7,386,998,669
Puglia	82,257,196	1,206,391,434	2,125,295,858	2,952,326,318	6,366,270,806
Sardegna	-	-	-	2,376,413,502	2,376,413,502
Sicilia	562,630,213	7,477,470,927	11,386,789	637,807,857	8,689,295,786
Toscana	-	1,264,897,651	5,031,170,932	475,004,478	6,771,073,061
Trentino	-	-	272,053,211	1,128,520,230	1,400,573,441
Umbria	238,681,660	1,054,306,951	230,937,694	27,123,598	1,551,049,903
Valle d'A.	-	-	37,820,498	264,450,404	302,270,902
Veneto	-	929,716,300	3,857,865,949	2,497,349,972	7,284,932,221
Total	**5,478,567,793**	**30,312,813,481**	**27,290,412,368**	**30,487,358,213**	**93,569,151,855**

Therefore, this Ph.D. Thesis proposes a soft-computing (Chapter 4) approach capable of selecting and designing the "best" solution (in terms of initial costs) for seismic retrofitting of existing RC buildings.

1.2   Common deficiencies in existing R.C. buildings

Recent devastating earthquakes [27]-[31] have evidenced the vulnerability of many existing reinforced concrete buildings. The seismic vulnerability mainly depends on the seismic deficiency of the building under consideration, which, in turn, is defined as a condition that prevents a building from meeting the required performance. These deficiencies have a strong influence on the potential damage and modes of failure of components during an earthquake when directly affects the structure's ability to sustain the seismic loads and remain stable. More than any

laboratory test or analytic study, the lessons learned from past earthquakes should serve to establish a historical record of what worked well in past earthquakes, as well as what did not.

Damage investigations have demonstrated the poor performance of older buildings designed using out-dated technology. The most important and the most frequently observed deficiencies that have been found to have negative consequences for seismic behavior can be taken as a reference to learn from past mistakes and avoid them in the future. A wide, yet not-exhaustive, list of critical deficiencies contributing to the vulnerability of concrete buildings is proposed in the following subsections. For convenience, the deficiencies have been broadly classified as follows: local deficiencies, when they refer to the deficiencies in individual members, and global deficiencies, when they refer to the deficiencies which are observed in the structure as a whole [32]. Finally, even the common mistakes made in analysis and concrete mixing are described.

1.2.1   Component deficiencies

Component (or local) deficiencies typically include the poor detailing of single structural members or connection between them, the inadequate sizing of cross sections or steel reinforcement and so on. Consequently, the structural members are not able to behave properly under seismic actions.

1.2.1.1   Deficiencies of columns

During an earthquake, columns of frame buildings may fail under shear-compression or bending-compression force. It is often difficult to distinguish such mechanisms, as both failures take place near the column ends and involve concrete crushing. However, shear failure is a result of the opening of diagonal cracks and degradation of the shear transfer mechanism, which is associated with low energy dissipation and sudden failure also known as "brittle failure".

The tensile stresses carried by the concrete before the onset of significant shear cracking cannot be resisted by shear reinforcement once shear cracks open, leading to diagonal tension failure. Further opening of cracks and movement along the diagonal failure plane, in the case of high axial loads and inadequate stirrups, can lead to loss of gravity load-carrying capacity, accompanied by buckling of longitudinal reinforcing bars. As axial capacity is lost, gravity loads should be transferred to neighboring columns, which can lead to a progression of overload, damage and eventually collapse of the buildings.

This type of failure occurs due to several reasons, such as the widely spaced horizontal ties laid in the column, the low strength of shear reinforcement, the reduction in steel area due to corrosion, the inadequate cross-section size of the column (Figure 1.3a). Moreover, if the ends of rectilinear lateral reinforcement are not properly anchored in the core concrete with a bend it may lead to shear failure of columns by pull-out of lateral reinforcement from the anchorage zone (Figure 1.3b).

Another type of shear failure may be caused by interaction with masonry infills during an earthquake. In fact, columns next to openings or short (and stiff) columns, due to infill walls of partial height (Figure 1.3c), attract larger shear force which leads to their failure prior to flexural yielding at their ends because of reinforcement not properly done.

(a)   *(b)*   *(c)*
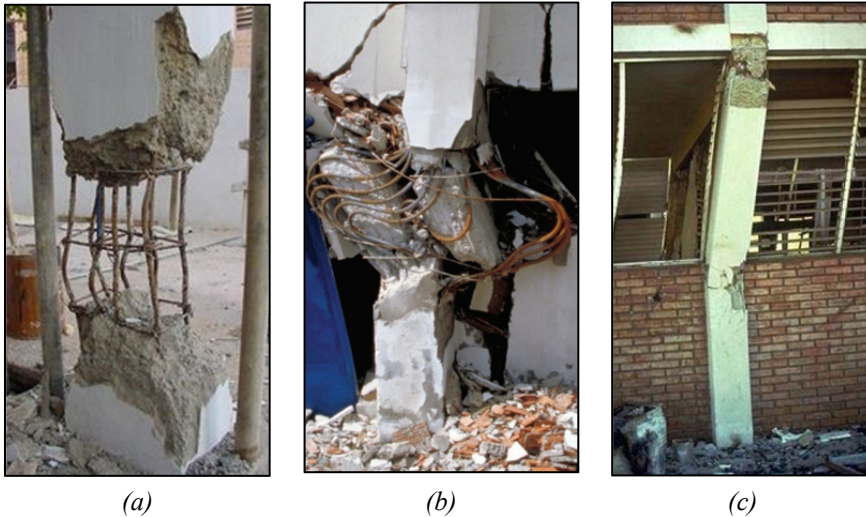
Figure 1.3: a) Corroded re-bars; b) inadequate stirrups [33]; c) short column

If short and tall columns exist within the same story level, then the "short columns" [34] attract several times larger earthquake-induced force and suffer more damage as compared to taller ones. The negative effect can be caused by the free inflection length reduced by the presence of infills for a partial height that acts as a constraint where it is present, subjecting the column to shear stresses only into the short free length. The "short column" effect can also happen when the effective height of some columns in a particular story is reduced by the presence of an intermediate floor.

Bending (or flexural) failure, whereas, may occur either due to the premature crushing of concrete in compression or due to yielding of steel, accompanied by tensile cracking of concrete. Bending failures usually occur because of an inadequate amount of steel bars provided vertically in the columns, inadequate amount of lateral reinforcement, particularly near the beam-column joints or column-foundation junctions, namely the region of plastic deformation. Finally, columns with a large aspect ratio (length to width ratio) are often inadequate under biaxial bending forces.

1.2.1.2   Deficiencies of beams

Under gravitational loads, the beams typically sag in the middle and hog near the column supports, generating a flexural crack pattern in beam span. On the contrary, under seismic conditions, this hogging action increases at one end, but decreases and sometimes reverses to sagging at the other end. The pre-existing cracks may be opened further because of the effects of the vertical component of the earthquake.

During an earthquake, the beams may also fail either in shear or in bending (flexural failure), but their failure is less "catastrophic" than the failure of a column: in contrast to failure of a column which can affect the stability of the whole building, the failure of a beam causes a localized effect. However, shear (brittle) failure is always undesirable, as it decreases the load resisting capacity and prevents the yielding of the longitudinal steel bars (ductile behavior).

These failures mainly occur because of the absence of proper detailing. In fact, the lack of proper stirrup spacing (nearly equal to the beam depth) often designed for gravity shear loads along with the use of smooth longitudinal steel bars can generate the formation of shear cracks that led to a reduction in both flexural and shear strength.

Bending failures often occur because of the poor quality of concrete, inadequate amount of horizontal steel bars, or inadequate anchorage of the re-bars, particularly near the beam-column joints, or. In fact, the yielding of the re-bars under reversed cyclic loading increases the rotation near a beam-column joint, resulting in the formation of the so-called "plastic hinge" that plays a significant role in the seismic response of structures for the dissipation of internal energy. The rotation capacity of a beam near the joint may be inadequate due to lack of confining reinforcement. In fact, the amount of hoops near the joints is often such that the beam doesn't generate their rotation (flexural) capacity before they fail in shear. This may lead to a sudden shear failure before a hinge is formed (Figure 1.4).

Figure 1.4: Example of shear failure in the beam [35]

1.2.1.3   Deficiencies in the beam-column joints

Joints between beams and columns play an important role: their integrity ensures that beams can safely transfer forces to columns and columns, in turn, can transfer forces to foundations. However, in existing frames, beam-column joints (also called "panel zone") sometimes lack adequate confinement and transverse reinforcement (Figure 1.5a).

It is also very common to find eccentric beam-column connections usually located in the perimeters of moment frames structures. In existing structures, top bars have often hooks bent upward, while bottom bars are typically discontinued at the face of the supporting column (anchored in essentially plain concrete) or provided with only a short embedment into the joint. This is in contrast to the preferred detailing for beam longitudinal reinforcement of extending the top and bottom bars through beam-column joints with hooks bending into the joint.

(a)   *(b)*

Figure 1.5: a) Poor beam-column connection; b) failure of a corner joint

In case of a moment-resisting frame characterized by "weak-beam strong-column behavior", the weak detailed joint after the yielding of the beam is not able

to develop the strength of the connected members. Such deficiencies could lead to axial and/or sudden shear failure of the panel zone characterized by diagonal cracking which results in redistribution of gravity loads to neighboring joints (and columns), reduction of the stiffness and progressive collapse of the building.

In principle, interior joints are less vulnerable due to the confinement provided by four beams connected to the column. On the contrary, the corner joints around the building perimeter are usually more prone to fail, as shown in Figure 1.5b.

1.2.1.4   Deficiency of frames

As known, in the 3D configuration of a framed structure, only the frames aligned in one direction form a lateral-force-resisting system capable to react to seismic loads acting in the same direction. However, if the existing buildings were designed to resist only to gravity loads, they generally are not characterized by a specific lateral-force-resisting system.

The presence of frames in one direction and the mono-directional warping of the floors are typical of buildings designed according to the past seismic codes: for designing buildings in non-seismic areas the engineer had to account only the vertical loads. In such cases, sometimes transverse beams (i.e. placed in the frames on which the floor does not directly rest) are completely absent or have very small size. In this situation, the resistance to lateral actions in the direction parallel to the joist is very low. Therefore, under moderate to a large earthquake, the overall lateral resisting strength and stiffness are often inadequate to limit story drifts and/or to resist additional demand due to earthquake loading. Excessive horizontal displacements generate P-Δ effects, thus, impairing the global stability of the frame.

Another deficiency can be due to low structural redundancy, i.e. the ability to redistributed overstress by creating alternative load paths. In the lack of redundancy in a structure, the seismic capacity is mostly dependent on the nonlinear behavior of the lateral load resisting elements. Finally, in curved buildings with non-rectangular grid plans, the frames are not parallel or symmetric about the major orthogonal axes of the seismic force resisting system. This leads to decreasing the lateral strength of the building.

1.2.1.5   Deficiencies of foundations

Foundation deficiencies can occur within the foundation element itself, or due to inadequate transfer mechanisms between foundation and soil. Element deficiencies include inadequate bending or shear strength of spread foundations, inadequate

axial capacity or detailing of isolated foundation system. On the other hand, the overall stability of a building depends, among the others, on the transfer mechanism of the supported loads to the soil (or rock). A deficient transfer of loads to the foundation system often causes an inappropriate behavior of the structure leading to several damages. Many existing structures were built upon isolated footings, not properly designed against seismic forces.

Other dangerous situations occur when the deformations or volume variation of the soil are not caused by the load. It is the case of the building placed on poorly compacted or water-sensitive soil that may result in loss of bearing capacity, uniform or differential settlements and, consequently, in large uniform or differential displacement.

The so-called "liquefaction" phenomenon occurs when a saturated or partially saturated soil substantially loses strength and stiffness in response to sudden change in stress condition (due to earthquake shaking), causing it to behave like a liquid. The earthquake (or other cyclic) loading reduces the soil volume and develops pore water pressure. This reduces the effective stress to zero and the soil cannot support a structure (Figure 1.6a).

The soil liquefaction sometimes is also the cause of the occurrence of global "overturning" mechanism of many multi-story buildings during the earthquake (Figure 1.6b), which results in the excessive rotation. This failure mode happens when the moment at the base of a building due to the lateral seismic forces is larger than the resistance provided by the foundation's uplift resistance and building weight. The global overturning mechanism results in high tensile or compressive forces in the vertical member located close to the end of the lateral force resisting systems.

(a)   *(b)*

Figure 1.6: Example of a) liquefaction of soil; b) overturning mechanism

Sometimes damages may be caused also by the presence of heterogeneous foundation systems on heterogeneous soils. In other cases the construction of large buildings nearby existing frame structures causes the intersection of stresses "bulbs", increasing the settlements in that area.

Another observed source of damage is the construction of additional stories upon weak columns, instead of enhancing the existing foundation system. The load increment usually lead to loss of bearing capacity and/or compaction of soil foundation.

1.2.2   System deficiencies

System (or global) deficiencies are the attributes responsible for degradation of the lateral load resisting mechanism of a building subjected to an earthquake. Typically, such deficiencies are caused by "irregularities" in the structural configuration which result in an irregular load path, damage and eventually failure of the structure.

They are generally classified in plan and vertical irregularities [36]. Both are important factors that decrease the seismic performance of the structures and can result in significant increase of loads and deformations in comparison to those assumed by the conventional linear methods of analysis. The irregularities are broadly classified as plan irregularities and vertical irregularities. The section list the different types of irregular configuration.

1.2.2.1   Plan Irregularities

The plan irregularities can be detected by observation and simple calculations based on the plan of a building. Sever plan irregularities can result in dynamic behavior governed by torsion, leading to large displacement demands and collapse on the "soft" or "weak" side of the building.

The existence of an asymmetric in-plan configuration (e.g. T, L or U-shaped plans) without seismic joints or the asymmetric (or even non-parallel) existence of lateral force-resisting elements are usually leading to an increase in stresses of certain elements that consequently results in a significant damage during an earthquake. Such category includes torsional irregularity, diaphragm inadequacy, and out-of-plane offsets.

1.2.2.1.1   Torsional irregularity

In a multi-story structure, seismic force at each level acts through its center-of-mass and is resisted by the building through resulting shear force applied in the center-of-rigidity of its frames. Centre-of-mass is the point of each floor where the mass of the floor and tributary portions of the adjacent stories can be considered to be lumped for the purpose of analysis. Centre-of-rigidity (or stiffness), whereas, can be identified for each floor as the point such that when the horizontal force along a direction acts at that point, the resulting displacement of the level is a pure translation in the same direction.

Torsional irregularity is caused by plan asymmetry and/or eccentricity between these centers. This is usually due to a particular in-plan configuration, such as the asymmetric in-plan distribution of lateral stiffness or the asymmetrical position of stairs and/or lift, that leads to twisting of the building and increased shear forces especially in the in members away from the center of rigidity (that is on the "flexible side"). Because of torsional effects, different portions of the same floor move horizontally by different amounts and this induces larger damage (higher inelastic demands) in the exterior columns and walls.

This problem is especially common in buildings at the corner of a block, where common walls as the back of the building provide large resistance while the street sides provide less resistance. Another example occurs in office buildings in which an elevator hall surrounded by structural walls may be placed on one side of the floor to leave large open office area in the remainder of the floor.

1.2.2.1.2   Diaphragm inadequacy

Structural diaphragms are required to span between vertical elements of the lateral-force-resisting system and, thus, to transfer forces in the horizontal plane. A rigid floor slab acts as a horizontal diaphragm that mobilizes the frames to resist the lateral load and to undergo the same displacement at the floor level.

A diaphragm discontinuity refers to a large cut-out or open areas in a floor slab which generates stress concentration in the corners of the cut-out. Large openings in floor diaphragms (usually greater than 50% of the gross enclosed diaphragm area) due, for instance, to the presence of stairwells and/or lift are considered structural deficiency.

As consequence of this deficiency, the diaphragm action of the slab may be reduced and the global behavior of the existing building could be inadequate. Moreover, buildings having diaphragms that span large distances between vertical

elements of the lateral-force-resisting system usually become overstressed in moment or shear, leading to unexpected inelastic behavior in the diaphragm.

1.2.2.1.3   Out-of-plane offsets

The out-of-plane offset refers to the discontinuity (or interruption) of the lateral load resisting systems which are shifted within their own plane in a certain story.

An example is a peripheral column in the upper stories that is interrupted at the ground floor. In this case, the columns are supported on cantilever overhang beams and they are termed as "floating" columns. This leads to a discontinuity in load path from the perimeter frame in the upper stories to the outer columns in the ground story.

This deficiency usually occurs when there is a limitation for moving space along the border of the building at ground level. This type of frame may be adequate for gravity loads but perform poorly when subjected to earthquakes.

1.2.2.2   Vertical Irregularity

The vertical irregularities can be detected by observation and simple calculations based on the elevation of a building profile. Discontinuity of vertical elements in the seismic-force-resisting system can result in excessive earthquake-induced deformations and force demands concentrate just above the vertical irregularity.

Such category includes geometric irregularity, mass irregularity, stiffness irregularity, strength irregularity, and deficiency in separation joints

1.2.2.2.1   Geometric irregularity

A geometric irregularity generally occurs with "setback buildings", where the horizontal dimension of the story is greater than the adjacent one. An example of setback building can be found in existing building with a small appendage, such as a penthouse, at the upper levels. Such configuration can cause large deformation just above the setback during an earthquake.

1.2.2.2.2   Stiffness irregularity

Stiffness irregularity refers to the variation in terms of lateral stiffness between consecutive levels. The substantial reduction in lateral stiffness in any story with respect to that in the upper story may lead to a "soft story" failure.

A soft story is a relatively flexible story in which its relative horizontal displacement is much larger than the corresponding displacements of other stories.

This mechanism is highly undesirable because significantly increases the deformation demand and puts the burden of energy dissipation concentrated on the columns of the same level, with almost irrelevant damage to the remaining part of the building (both lower and upper floors).

As a matter of fact, if the columns have not been well detailed, or in case of large axial forces (particularly at ground-story), the columns are unable to follow the large story drift without failure (Figure 1.7a).

Soft stories are especially common in multi-story residential buildings where the infill walls, which affect the stiffness of the story, are absent to meet the change in use. In this case, the first story often is used for "open space" (like the "pilotis" configuration), commercial facilities or garages. Moreover, soft intermediate stories have also been observed in buildings with large windows on the façade (Figure 1.7b).

(a)   *(b)*
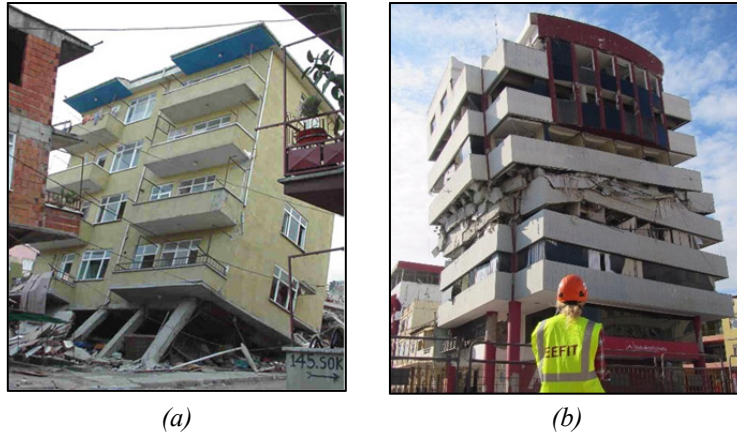
Figure 1.7: Example of a) ground soft story; b) soft intermediate story

1.2.2.2.3   Strength irregularity

The strength irregularity refers to substantial discontinuity in terms of lateral strength in any story with respect to the upper story. The story strength is the total strength of all seismic-resisting elements sharing the story shear for the direction under consideration. Inadequate story shear strength caused by an insufficient number of columns and/or walls is referred to as "weak story".

Figure 1.8a shows an example of weak story mechanism that usually occurs in buildings with an "open" story at the first floor, while infill or structural walls in the upper stories. Moreover, it can also occur in many residential buildings characterized by massive beams and smaller designed columns (also called ''weak

column-strong beam'') in which yielding mechanism of columns is possible at any story.

The weak story can lead to an undesirable "sway" mechanism under seismic load and, eventually, in "pancake" failure (Figure 1.8b). The sway mechanism generally refers to the movement of the upper stories like a single block with severe deformation of the ground story columns. The process results in a concentration of inelastic deformation demands in the columns of one story which are exacerbated by P-Δ effects in taller buildings.

<div align="center">(a)   (b)</div>

Figure 1.8: Example of a) weak story; b) pancake failure

1.2.2.2.4   Mass irregularity

Existing buildings are sometimes used for a different purpose from their original intended function. The observed substantial difference in mass (or weight) between two consecutive stories due to heavy equipment in a particular floor is accounted in this category. The concentration of mass at a particular story attracts higher seismic forces and generally results in the creation of a "weak" story.

1.2.2.2.5   Deficiency in separation joints

Inadequate separation joints (gap) between two adjacent buildings, especially those with different heights, different materials, different dynamic properties and free to oscillate independently, may lead to "pounding" (or "hammering") mechanism when they collide between them during the vibration (Figure 1.9a).

This condition is particularly adverse when the floor levels of the adjacent buildings do not match. If the floor slabs of adjacent buildings do not line up horizontally, the top slab of the shorter building can severely damage the columns of the adjacent building leading to axial load failure due to excessive demands

caused by dynamic horizontal vibrations of the two buildings. This mechanism is called "mid-column" pounding whose example is shown in Figure 1.9b.

On the other hand, if the buildings are located within in a block of similar height buildings, collapse due to pounding is less likely to occur since differential movement and dynamic effects are "constrained" by the presence of the adjacent structures.

(a)   *(b)*

Figure 1.9: Example of a) pounding mechanism [33]; b) mid-column pounding

1.2.3   Deficiencies in concrete mixing and placement

Due to insufficient mixing, placement, and workmanship, the compressive strength of concrete is often smaller than half of the expected strength. In order to achieve workability, the water-cement ratio is usually exceeded compromising the strength of concrete [37].

Quality and shape (mostly rounded) of fine and coarse aggregates can lead to low stiffness and improper binding of concrete [38]. In addition, aggregate dimensions used in the concrete are sometimes larger than the allowable diameter: segregation and bleeding have been commonly observed in the damaged buildings in the seismic-affected area.

The aging of materials and aggressive environmental conditions can unavoidably lead to their deterioration with an adverse effect on the potential seismic performance of a building [39]. In addition, the inadequate bar cover, poor or cracked concrete may cause moisture and oxygen to penetrate to the steel reinforcement leading to its corrosion. Another source of deficiency has been found in many existing frames built in stages: the non-homogenous and non-monolithic construction can lead to a variation in terms of structural performance.

1.2.4   Deficiencies in analysis

The most important source of deficiency in the analysis is related to the acting loads. Existing buildings have been often designed to resist under gravity loads, while the seismic loads have been underestimated or completely neglected in the analysis.

Moreover, practitioners usually do not take into account the modifications to the structural system happened for functional reasons over time. Both addition and removal of elements commonly observed in existing building result in significant increases in dead and live loads which are sometimes neglected in the analysis.

As regards the nonstructural elements, despite they are placed for the purpose of building function (the case of partition walls), they are commonly neglected in the analysis for design calculations. For instance, the contribution of unreinforced masonry in infill walls is often neglected in the analysis leading to a longer time period and, as consequence, lower seismic forces [40]. Although the infill walls are not designed to absorb seismic actions, actually they can absorb still part of these actions in proportion to their stiffness and affect the shear resistance of the story. Moreover, the stiffness of an infill wall can influences also the location of the center of rigidity of the lateral load resisting system in a story. For instance, if infill walls are present only on one side, neglecting them analysis may lead to overlooking a torsional irregularity.

On the one hand, damage occurring in infill wall could contribute to the dissipation of input energy and reduce the seismic forces on the frame. On the other hand, when stiff and strong nonstructural elements are placed in contact with structural elements the interaction can result also in structural element damage. In the examples of Figure 1.10 a-b, the compressed rod forming in the wall acts in a concentrated area of the frame where it may cause brittle failure in the columns.

(a)   *(b)*

Figure 1.10: Example of a) interaction with the column; b) diagonal rod in infill wall

Moreover, the engineer sometimes did not account for the P-Δ effect in the analysis. This effect is due to the increase of lateral displacement response of structure during the seismic event which leads to a higher eccentricity of the vertical loads, causing additional moment in the columns. Neglecting this effect can result in the under-estimation of the design forces.

Regarding the foundation system, whereas, it is sometimes designed without adequate information on geotechnical data such as the type of soil, bearing capacity, locations of fill and fault. Therefore, the amplification effects due to the interference of the earthquake waves are neglected in the analysis.

2. State of practice on seismic analysis for design and assessment

2.1 Simulation process

Seismic analysis of structures is a typical example of simulation problem, in which both earthquake-induced actions and mechanical properties of structural components are known and the mechanical response of the system is searched for.

Key issues in simulation include the acquisition of valid source information about the relevant properties of materials and models, the use of simplifying approximations and assumptions, and the validation results. Figure 2.1 shows the main steps characterizing the simulation problem are idealization, discretization, and solution.
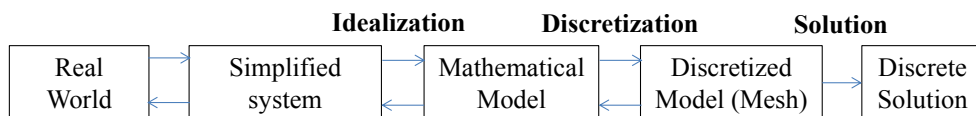
Figure 2.1: A simplified view of the physical simulation process

2.1.1 Idealization

Engineering systems often tend to be highly complex. Hence, for simulation, it is necessary to reduce that complexity to manageable proportions by developing a reasonably simplified model intended to predict the key characteristics and aspects of the selected system's behavior. Complexity reduction can be achieved by filtering out the physical details of the system that are not relevant to the analysis process. Engineers often approach the simulation problem intuitively by creating an analogy between the real world and the simplified system.

The idealization is a simplifying process by which an engineer passes from the real system to its mathematical model. Hence, idealization is an abstraction tool by which complexity is tamed. It is the most important step in engineering practice because it must be done by humans. Models introduce approximations and

assumptions, but allow the description of a property over a wide range which cannot be covered by real data.

According to an "extension" of the scientific method whose flow-chart is shown in Figure 2.2, mathematical models allow exploring system behavior in an articulated way which is often either impossible or too risky in the real world. Mathematical models also enable the search for conditions outside the range of known properties.
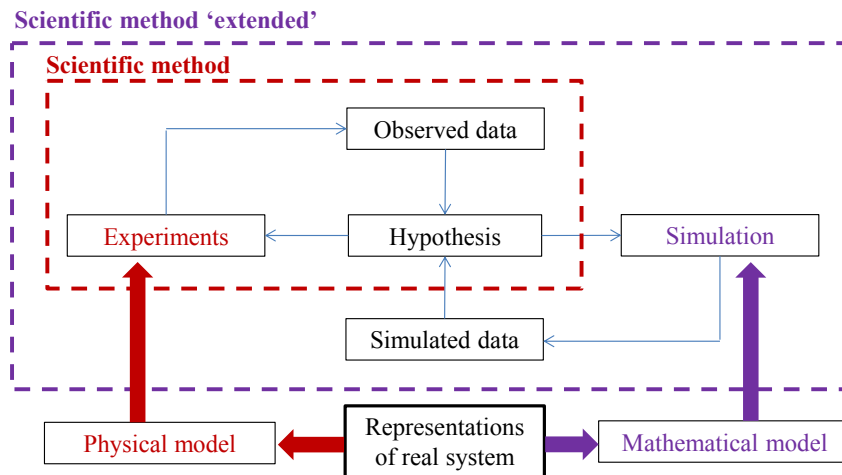
Figure 2.2: Flow-chart of scientific method based on a mathematical model

Two types of models can be distinguished: rather simple equations, where parameters are fitted to experimental data, and predictive methods, where properties are estimated. The equations are normally preferred because they describe the property almost exactly. To obtain reliable parameters it is necessary to have experimental data which are usually derived from data banks or from measurements.

Despite using predictive methods is much cheaper than experimental work, predicted properties are normally only used in early steps of simulation because these estimation methods normally introduce higher errors than equations (or correlation) obtained from real data.
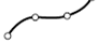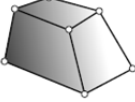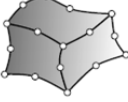
Moreover, the modeling can be further divided into implicit or explicit modeling. The former means choosing a specific component system from a "catalog" which automatically implies fully aware of the choice (including the mathematical models on which the component are based). The other extreme is explicit modeling: a mathematical model of the physical problem is selected on the basis of own technical expertise, resources, and maturity.

2.1.2   Discretization

In "continuous" systems the simulation problem can only be defined by using coupled partial differential equations in space and time subject to boundary and/or interface conditions which imply a huge number of unknowns (degrees of freedom). However, since the capacity of all computers is limited, the models of continuous systems can be solved by mathematical manipulation: it is necessary to reduce the number of unknowns to a finite number.

The process of sub-dividing a system into its individual well-defined components, whose behavior is readily understood, and then assemble the original system from a finite number components is called "discretization" (or "meshing"). This approximation approaches in the limit the true continuum solution as the number of components increases. The basic concept of discretization is the subdivision of the mathematical model into a finite number of disjoint components of simple geometry (Table 2.1) whose behavior is expressed in terms of a finite number of degrees of freedom.

Table 2.1:Typical element geometry defined by nodal location [41]

The response of the mathematical model of the complete system is then considered to be approximated by the response of the discrete model obtained by assembling the collection of all elements.

In particular, two main discretization strategies characterized by an increasing level of accuracy and complexity can be employed in the analysis of structures [42]:

- – discrete finite element models, where a structural model is obtained through the assembly of a reasonable number of interconnected members;
- – microscopic finite element models, where members and joints are modeled through a large number of two or three-dimensional elements connected between each other [43][44].

On the one hand, microscopic models are typically suitable for the detailed study of critical regions as a result of its complication and high-cost computational process. On the other hand, member element models often guarantee the best balance between simplicity and accuracy.

2.1.3   Solution

Analytical solutions (also called "closed-form solutions") tend to be restricted to very simple problems of regular geometries with simple boundary conditions. Practical problems either do not yield to analytical treatment or the domain is geometrically complex and the likelihood of obtaining an exact analytical solution is very low.

Once formulated, the resulting mathematical models can be often hard to solve, especially when the governing equations are nonlinear partial differential equations. Alternatively, approximate solutions based on numerical methods are most often obtained in engineering analyses of complex problems (Figure 2.3).
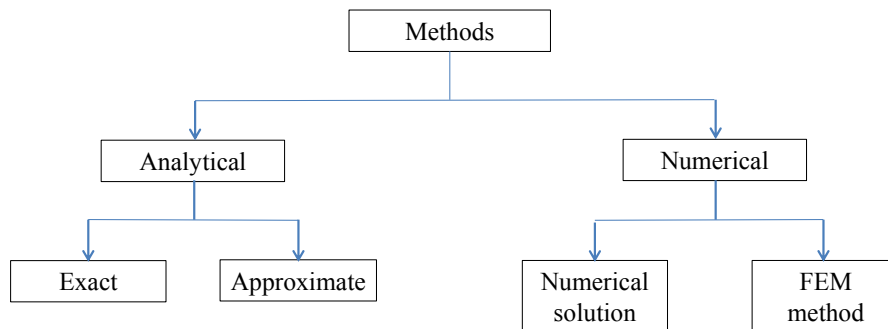
Figure 2.3: Classification of solution methods for a mathematical model

Nowadays, the Finite Element Method (FEM) [45] is considered as one of the most powerful numerical methods for obtaining approximate solutions with good accuracy of complex boundary value (or field) problems in different fields of engineering.

A boundary value problem is a mathematical problem in which one or more dependent variables must satisfy a differential equation everywhere within a known domain and specific conditions on the boundary of the domain. The field is the domain of interest and most often represents a physical structure, while the field variables are the dependent variables of interest governed by the differential equation.

The FEM solution process consists of the following steps:

1) discretization of the structure domain into regular finite elements with nodes (specific points at which the value of the field variable is to be explicitly calculated);
2) assembly of the elements at the nodes to form an approximate system of equations for the whole structure;
3) solving of the system of equations involving unknown values of the primary field variables (such as the displacements) at the nodes;
4) computation of desired additional quantities (derived variables) at selected elements.

The software executing the calculations is termed "solver" because it solves a set of mathematical equations for each node of the "meshed" model. It is worth highlighting that the way of assembling finite elements should ensure the following conditions:

− the field variables at the shared node of adjacent finite elements are equal (compatibility requirement);
− the elemental forces are in equilibrium with the external forces applied to the system nodes (equilibrium requirement);
− the system satisfies the boundary constraints (boundary conditions).

The constraints are fixed values of the field variables (or their derivatives) on the boundaries of the field. Moreover, the values of the field variable computed at the nodes are used to approximate the values at non-nodal points (in the element interior) by interpolation of the nodal values. The interpolation functions, also known as "shape" (or blending) functions, are most often predetermined polynomial functions of the independent variables, derived to satisfy certain required conditions at the nodes and can be expressed by the displacement field of the real problem [46][47][48].

Based on the law of conservation of energy, the Finite Element Method has to solve the energy balance to find a stable operating point for the examined system. This is based on the Principle of Virtual Works which postulates that if a particle is under equilibrium, the work done by internal forces must be equal to the work done by the external forces acting on it. The FEM obtains the solution of desired field variables by minimizing the total potential energy Π of the discretized structure which can be expressed as follows:

$$\Pi = \frac{1}{2} \int_{\Omega} \sigma^{T} \varepsilon dV - \int_{\Omega} d^{T} b dV - \int_{\Gamma} d^{T} q dS \qquad (2.1)$$

where σ and ε are the vectors of the stress and strain components at any point, respectively, d is the vector of displacement at any point, b is the vector of body force components per unit volume, and q is the vector of applied surface force components at any surface point.

The volume and surface integrals are defined over the entire domain of the system Ω and that part of its boundary subject to load Γ. The first term on the right-hand side of this equation represents the internal strain energy, while the second and third terms are, respectively, the potential energy contributions of the body force loads and distributed surface loads.

However, the displacement is assumed to have unknown values only at the nodal points, and the variation within the element can be described in terms of the nodal values by means of interpolation functions. Thus, within any single element, the displacement **d** can be replaced by **N u**, where **N** is the matrix of interpolation functions and **u** is the vector of unknown nodal displacements. Likewise, the strains within the element can be expressed in terms of the element nodal displacements as $\varepsilon = \mathbf{B} \mathbf{u}$ where **B** is the strain displacement matrix. Finally, the stresses may be related to the strains by use of an elasticity matrix (e.g., Young's modulus) as $\sigma = \mathbf{E} \varepsilon$.

The total potential energy Π of the discretized structure is the sum of all the energy contributions associated with each individual finite element which is given by the following equation (Eq. 2.2):

$$\Pi_{e} = \frac{1}{2} \int_{\Omega_{e}} u^{T} \left(B^{T} E B \right)^{T} u dV - \int_{\Omega_{e}} u^{T} N^{T} u dV - \int_{\Gamma} u^{T} N^{T} q dS \qquad (2.2)$$

Applying the principle of minimum potential energy, the stable operating point is found by setting the derivative of the functional with respect to the unknown displacement equal to zero (Eq. 2.3).

$$\frac{\partial \Pi_{e}}{\partial u} = \frac{1}{2} \int_{\Omega_{e}} u^{T} \left(B^{T} E B \right)^{T} u dV - \int_{\Omega_{e}} u^{T} N^{T} u dV - \int_{\Gamma} u^{T} N^{T} q dS = 0 \qquad (2.3)$$

It is possible to rewrite the element equilibrium equation in the form (Eq. 2.4):

$$f = k \cdot u \tag{2.4}$$

where the term f represents the mechanical force (Eq. 2.5):

$$f = \int_{\Omega_e} N^T u \, dV + \int_{\Gamma} N^T q \, dS \tag{2.5}$$

and **k** is known as the finite element stiffness matrix (Eq. 2.6)

$$k = \frac{1}{2} \int_{\Omega_e} \left(B^T E B\right)^T u \, dV \tag{2.6}$$

However, for nonlinear problems, the stiffness matrix of a finite element depends on the actual displacements intensity and Eq. (2.4) must be reformulated as:

$$f = k\left(u\right) \cdot u \tag{2.7}$$

On the one hand, the stiffness matrix of the whole system is nothing more than the summation of each element stiffness matrix. Likewise, the summation of load integrals yields the applied load vector.

Finally, there are two major methods for improving the accuracy of the solution. The aim of both methods is to obtain solutions that exhibit asymptotic convergence to values representing the exact solution. In the first method, the number of elements used to model a given domain is increased and, consequently, the finite element size is reduced (fine meshing).

Element type, size, shape, and quality have a big effect on the accuracy of the results: the more elements, the more accurate the results, but with a longer computational time analysis. In the second method, element size is unchanged but the order of the polynomials used as interpolation functions is increased.

2.2   Methods of analysis

Both Eurocode 8 [9] and Italian Seismic Code [15] allow to assess the seismic performance of a given structure on the base of the following linear and nonlinear methods:

- − Linear Static analysis;
- − Linear Dynamic analysis;

− Non-Linear Static analysis;
− Non-Linear Dynamic analysis.

The complexity of the procedure and the required computational "cost" are generally increasing in the list above: the Linear Static procedure is the easiest and quickest method, while the Non-Linear Dynamic procedure is the most accurate and computation intensive. Conversely, the computational effort decreases as complexity increases as shown in Figure 2.4.

Nowadays, the linear methods are permitted only in few cases, because the conditions for their applicability are very restrictive. They are mainly applied to the design of new structures.
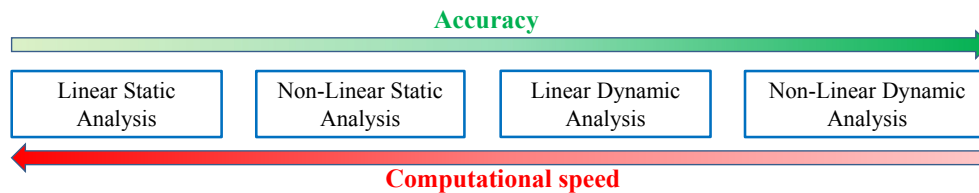
Figure 2.4:Accuracy vs computational speed of most common methods of seismic analysis

According to both Eurocode 8 [9] and Italian Seismic Code [15], the need for accuracy in predicting the building's internal forces and deformations together with the need of simulating particular case of extreme seismic loading direct the structural engineer into using non-linear analysis methods which have widespread applicability mainly in the assessment of existing structures. In fact, non-linear modeling and analysis allow more accurate determination of global capacity and ductility of the structure. The above-mentioned methods will be better discussed in the following Sections pointing out their relevant advantages and limitations.

2.2.1 Linear static analysis

The Linear Static Analysis (LSA) is the simplest method of seismic analysis. The term "static" means that the effect of seismic shaking is simulated by a system of forces constantly applied to the structural model. Linearity comes from the basic hypothesis of the methods: small deformations and elastic material. It implies a linear equation defining the relationship between loads and displacements.

In a linear static procedure, the building is modeled as an equivalent Single-Degree-of-Freedom (SDoF) system with an elastic stiffness and an equivalent viscous damping consistent with components responding at near yield level. The

seismic input is modeled by a set of equivalent lateral static forces applied at the center of the mass in horizontal directions with the aim to produce the same stresses and strains caused by the earthquake they represent. The purpose is to simulate the peak inertia loads due to the horizontal component of the seismic action.

Based on an empirical estimation of the first fundamental period [49][50][51], engineers can calculate the seismic acceleration by mean a given Response Spectrum. The Response Spectrum is a plot of the peak or steady-state response (displacement, velocity or acceleration) of a series of SDoF oscillators of varying natural frequency, that are forced to a motion by the same base vibration. Once known, the seismic acceleration is multiplied by the mass of the building to calculate the equivalent static forces. The lateral shear force is then distributed over the height of the building assuming that the deformed shape associated with the 1st vibration mode is linear.

If the system responds basically elastically to the applied loads, the evaluated internal forces can be considered reasonable approximations of those expected during the design earthquake. As already seen, the linear static procedures are used primarily for design purposes. However, their applicability is restricted to regular buildings for which the 1st mode of vibrating is dominant.

2.2.2   Linear Dynamic analysis

Linear Dynamic Analysis (LDA) removes some of the limitations of LSA and it is nowadays applicable for calculating the linear response of complex structures. Engineers have to model the building as a Multi-Degree-of-Freedom (MDOF) system with a linear elastic stiffness matrix and an equivalent viscous damping matrix. The seismic input can be modeled using either Response Spectrum Analysis or Time History Analysis.

2.2.2.1   Response Spectrum Analysis

The Response Spectrum (or Modal) Analysis [52][53][54][55] uses the peak modal responses calculated through a dynamic analysis of a mathematical model which takes into account the three-dimensional character of seismic acceleration.

The dynamic response of a building is supposed being the superposition of the independent responses of each individual vibrating mode, each characterized by its own pattern of deformation (the mode shape), frequency and modal damping. The first step of Modal Analysis is the determination of the so-called "eigenmodes" and "eigenvalues", meaning the 3D modal shapes and natural frequencies of vibration,

respectively. The minimum number of modes to be taken into account is chosen on the basis of the effective modal participating mass on the X, Y or even Z seismic action components: only those contributing significantly to the response must be considered.

The peak member forces, displacements, and base reactions for each mode of response can be combined by either the SRSS (square root sum of squares) rule or the CQC (complete quadratic combination) rule. On the one hand, if all relevant modal responses can be considered independent of each other, the most likely maximum value may be calculated through the SRSS rule. On the other hand, two consecutive modes cannot be considered as independent of each other, then the most likely procedure for the combination of modal maximum responses must be the CQC rule.

Similarly to LSA, also the Linear Dynamic Analysis takes into account the nonlinear behavior through the behavior factor q. The q-factor derives from the assumptions that greater ductility corresponds to a greater dissipative capacity. As a result, the forces given by the Design Response Spectrum can be reduced.

As noted, such approach does not allow to have information on the inelastic demand distribution while the plastic-ductile mechanisms are evolving. This fact confirms that linear elastic methods are suitable to the structural design as the ductile behavior is guaranteed following the Capacity Design's rule and the plastic hinge detailing proposed by the modern seismic codes.

2.2.2.2   Response-History Analysis

The Response History (or "Time-History") Analysis involves a time-step-by-time-step evaluation of building response, using recorded or synthetic earthquake records as base motion input. In both cases, the corresponding internal forces and displacements are determined using linear elastic analysis. If seven or more consistent pairs of ground motion records are used for Time-History analysis, the average the parameter of interest is allowed.

The advantage of these linear dynamic procedures with respect to linear static procedures is that higher modes can be considered. This feature makes Time-History analysis suitable for irregular buildings. However, it is based on linear elastic response and, hence, its applicability decreases with the increase of global force reduction factor which describes, in summary, the nonlinear behavior of the structure.

2.2.3   Non-Linear Static Analysis

Non-Linear Static (or Pushover) Analysis is essentially an extension of the LSA because the geometric and material nonlinearities of individual components are taken into account into the finite element model [56].

The non-linear force-deformation behavior of the building is obtained by a pushover procedure carried out by subjecting the model to monotonically increasing lateral forces under constant gravity loads. The lateral forces are distributed over the height of the model according to a given load pattern until a target displacement is exceeded or a failure mechanism develops. Usually, a displacement control strategy is employed. The displacement control strategy requires the specification of an incremental displacement and a control node (usually center of gravity of top roof) whose horizontal displacement (or others degree of freedom) is monitored.

According to EC8 [9] and NTC [15], pushover analyses are carried out with two sets of the monotonically increasing lateral forces pattern: uniform and modal pattern. The uniform pattern attempts to simulate the inelastic response dominated by a "soft-story" mechanism (development of plastic hinges at both top and bottom ends of the columns) that concentrates lateral drifts in a story (in general the ground floor, which is subjected to highest lateral forces) and this causes the storeys above to move with roughly the same lateral displacement.

Instead, the modal pattern of lateral loads (which should follow the fundamental elastic translational mode shape) tries to simulate the response up to global yielding, or even beyond that point, if a beam-sway mechanism ("strong" columns which remain elastic except for the base and "weak" beams which develop plastic mechanisms at their ends) governs the inelastic response. In case of existing buildings, the inelastic mechanisms which are likely to develop are, in general, unknown. Therefore, the results obtained using the two standard lateral force patterns should be considered as an envelope of the actual response, which should lie between the results obtained with the two lateral forces pattern.

The main outcome of the pushover analysis is a nonlinear force-displacement capacity curve (also known as "pushover curve") which relates the base shear force and the lateral displacement in the control node. Each step on the pushover curve defines a specific damage state for the structure because the deformation for all components can be related to the global displacement of the structure. Each point of the curve can be used to evaluate important parameters such as the total displacement, the drift, forces, and deformations of the individual member.

Clearly, the advantage of pushover procedure with respect to the linear static analysis is the possibility to account directly the effects of nonlinear material response and hence. Hence, the internal forces and deformations are more reasonable approximations of those expected during an earthquake [57].

The pushover analysis can provide information that can't be obtained from linear methods such as verification of the effective distribution of inelastic demand on the plastic hinges for buildings designed with a q factor; identification of the critic regions where the deformation demands are expected to be high; investigation of the evolution of the plastic mechanism and structural damage as a function of the lateral displacement's magnitude; description of strength, stiffness, deformations in each member of the structure (both brittle or ductile) during the incremental analysis.

Therefore, it is worth to underline that nonlinear static analysis is a good instrument to check subsequently if an appropriate behavior factor q has been chosen and if the value is consistent with the available local and global ductility. For this reason, this method can describe the evolution of the expected plastic mechanisms and of structural damage of existing structures (often not designed to meet the Capacity Design rules), with the limit that the seismic input can simulate only a single horizontal component of the seismic motion and does not reverse.

However, the pushover analysis is restricted to the first mode dominated structures because the procedure fails to account accurately for higher mode dynamic effects. Hence, this method is not suitable for irregular buildings for which higher modes become important. Hence, if a building does not respect the above condition, it is necessary to use a nonlinear dynamic analysis.

2.2.4   Non-Linear Dynamic procedures

The Non-Linear Dynamic (or "Time-History") Analysis is the most sophisticated analysis for predicting force-displacement relationship under seismic input [58].

Nonlinear Dynamic Analysis removes all the limitations of the other approaches but is characterized by a high computational time cost. It requires an appropriate mathematical model that incorporates directly the explicit inelastic load-deformation characteristics of the individual components using finite elements: cyclic nonlinear constitutive materials (for fiber section elements) and moment-rotation law for the plastic hinges (for concentrated plasticity elements).

The numerical models generally require refined relationships between stresses and strains under cyclic action, to possibly simulate strength and stiffness

degradation processes under cyclic actions [59][60]. The seismic input, whereas, is modeled using a set of real ground motion records.

The NLTH analysis involves time-step-by-time-step evaluation of the building response. It starts from the undisturbed static condition of the structure and repeated for the duration of the ground motion record with equal time increments to obtain the complete structural response time-history under a given seismic excitation.

The time-history response of the structure is calculated through the direct numerical integration of the differential equations of motions using a 3D finite element model under a set of ground motions. The step-by-step solution method attempts to satisfy dynamic equilibrium at discrete time steps and often requires several iterations, especially when nonlinearities are developed in the structure and the stiffness of the model must be updated due to degradation of strength and redistribution of forces.

Unlike modal response spectrum analysis which provides only best estimates of the peak response (through statistical function, such as the SRSS and the CQC rules), the nonlinear dynamic analysis calculates the exact peak response quantities. Moreover, the calculated peak response can be very sensitive to the characteristics of the individual ground motion employed as seismic input.

One of the main issues is the appropriate choice of the input ground motions as they have to be representative of the expected seismic event. The choice of a set of representative input signals to be employed for simulating the effect of seismic shaking is still an open issue [61][62][63]. In addition to the reasons briefly outlined above, the high computational effort required and a large amount of output information produced, discourage practitioners from performing an NLTH on all buildings.

Moreover, the computational effort is often unjustified if one takes into account, on the one hand, the high variability affecting the behaviour of structural members due to the aleatoric nature of the mechanical properties of materials [64] and, on the other hand, the incomplete knowledge of "as-built" structural details [65].

Therefore, the main value of NLDA is as a research tool capable to simulate the behavior of a building structure in detail, i.e. to describe the exact displacement profiles, the propagation of cracks, the strength and stiffness degradation, the distribution of vertical and shear stresses, and the shape of the hysteretic curves.

2.3   Material nonlinearities in frame models

A simple linear elastic model of a structure can accurately capture the static and dynamic behavior of the system when stresses in all elements of the structure do not exceed their elastic limit. Beyond this level, a linear model will fail to represent many sources of inelastic response of the structure.

Two categories of nonlinear behavior can be incorporated in the structural model in order to properly represent the expected response under moderate to intense levels of seismic demand: the geometric and the material nonlinearity. The precise definition of geometric and material nonlinearities in the model is not an easy task, as the resulting response values are generally highly sensitive to small variations in the input parameters.

The first category represents second order or P-Δ effects on a structure, where the equilibrium condition is determined under the deformed configuration of the structure. Such nonlinearity category is usually incorporated directly in the analysis algorithm.

The second category consists of inelastic behavior of elements and cross-sections due to nonlinear material stress-strain relationships, as well as the presence of dampers (Section 3.3.1), or nonlinear springs in some components.

The nonlinear mechanical behavior of the structure is generally simulated in numerical studies by using different plasticity models. Inelastic structural models can be differentiated by the way that plasticity is distributed through the member's cross section and along its length. The most common approaches for modeling material nonlinearities in frame inelastic analysis are grouped into two main classes:

i.   concentrated plasticity approach characterized by the presence of discrete nonlinear moment-rotation hinges at the ends of linear elements;
ii.   distributed plasticity approach where nonlinearities can develop not only at the ends but also along the member.

Five idealized model types for simulating the inelastic response of structural members are shown in Figure 2.5. The plastic hinge and non-linear spring hinge are considered concentrated plasticity approaches. Finite length hinge zone, fiber section, and micro-finite element, whereas, belong to the class of distributed plasticity approach.

When selecting the plasticity model, it is important to keep in mind the approximations inherent to the proposed model type. As a matter of fact, while more sophisticated formulations may seem to offer better capabilities of modeling certain aspects of behavior, simplified models may capture more effectively the relevant feature with the same or lower approximation.

The additional level of sophistication of the nonlinear model will increase the computational effort required for the analysis, as well as the difficulty in the interpretation of results. Therefore, in the modeling stage, the engineer has to find a right balance between model complexities and the accuracy of the results.
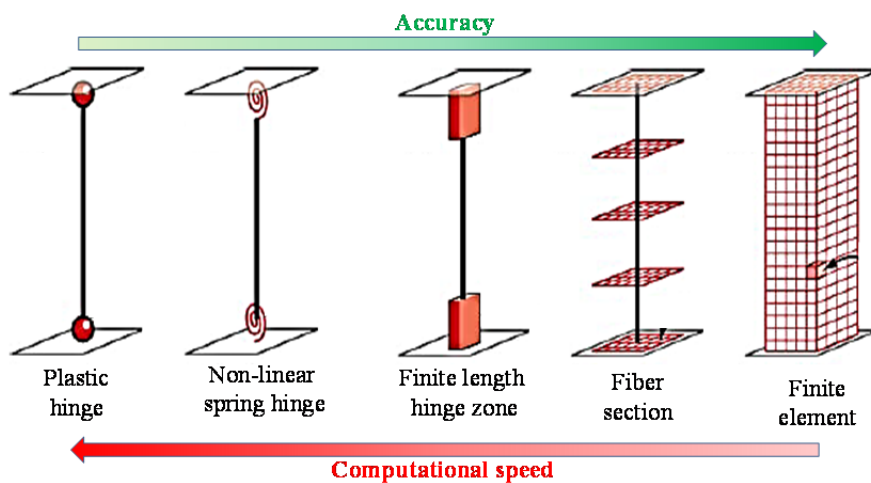
Figure 2.5: Accuracy vs computational speed of methods for modeling nonlinearity

2.3.1   Concentrated plasticity model

In the concentrated (or lumped) plasticity approach, the body of the structural element is modeled as linear elastic part while the inelastic deformations are concentrated where nonlinear behavior is expected to develop, i.e. at the bottom-end nodes of the element [66].

The simplest nonlinear model concentrates the inelastic deformations in specific zero-length regions called "plastic-hinges" [67]. The plastic hinges, which control the post-yielding phase, are modeled as a nonlinear link element. In this case, these regions change their behavior abruptly from rigid to fully plastic when the extremity forces achieve a predefined yield criterion. That is an inelastic rigid-plastic rotational spring which behaves differently in the elastic and the plastic phase: in the elastic phase, the stiffness of the hinge is very high, so basically the flexibility of the combined system (element + spring) is the flexibility of the elastic

element; conversely, in the inelastic phase, after reaching the yield moment, the flexibility of the system depends mainly on the capacity of the spring. In the second case, the hinge serves as rotational springs and behaves in a more complex manner, according to theoretical moment-rotation relationships.

Therefore, there is the need to identify these zones in terms of location, extension, and properties of hysteretic behavior [68], defined through the M-θ curve. Regarding the structural members of new buildings, there is an exhausting literature of possible M-θ models as those shown in Figure 2.6. Despite the springs are zero length elements, their sizes are greatly exaggerated for clarity.
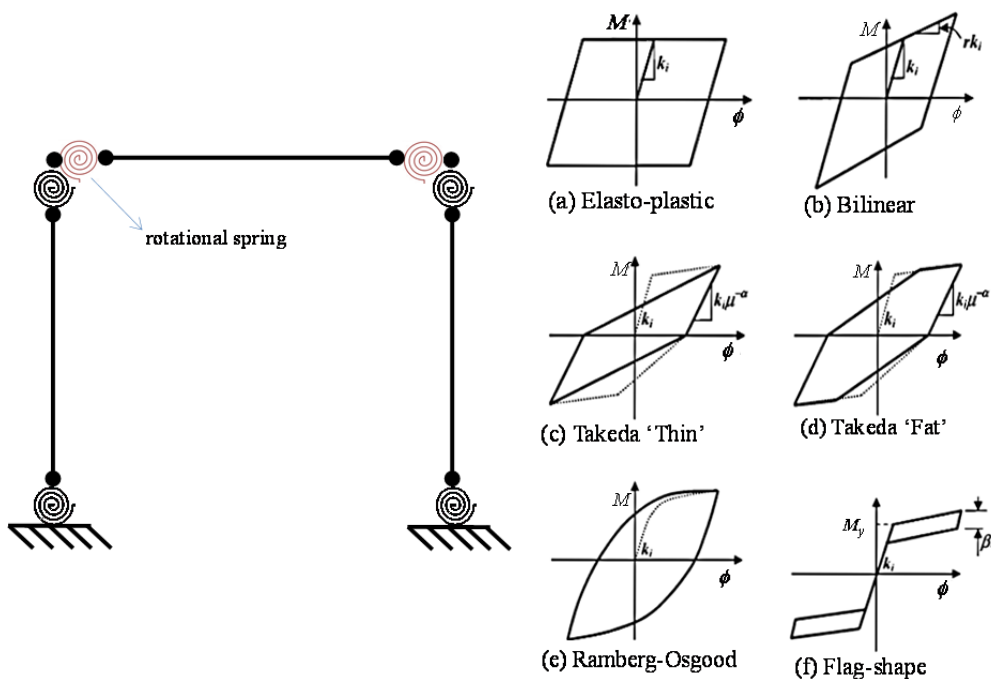
Figure 2.6: Rotational spring hinge and moment-rotation nonlinear models (a-f)

Therefore, this methodology is suitable for the verification of new seismically designed buildings, for which it is easy to identify the location of plastic hinges thanks to the respect of capacity design procedures.

On the one hand, these elements have relatively condensed numerically efficient formulations and their basic assumptions reduce computational effort and the complexity of the model. Lumped inelasticity models, in fact, have been widely used in earthquake engineering applications because their simple formulation allows running very fast analyses.

On the other hand, these assumptions increase the risk of inaccuracy, or inadequacy, of the analysis outcomes. Unfortunately, concerning the assessment of existing buildings, it is hard to understand a priori where the plastic hinges can develop and to define correctly not only their location but also their extension and behavior.

A great experience is, therefore, needed in order to model in a correct way the structure using concentrated plastic hinges. Therefore, accurate results cannot be obtained when the knowledge of the users about the properties of inelastic behavior, defined through the M-θ curve, is inadequate. Thus, it can result in limited applicability [69].

2.3.2   Distributed plasticity model

According to distributed plasticity models, the inelastic behavior is defined at a material level and the whole structure is modeled as nonlinear: all the sections can have excursions in the nonlinear field of the response. As previously seen, several approaches exist to create a distributed plasticity model: finite length hinge model, fiber section, and micro-finite element.

The finite length hinge model is a distributed plasticity formulation with designated hinge zones at the member ends. For reinforced concrete members, cross sections in the inelastic hinge zones are characterized by either nonlinear moment-curvature relationships or explicit fiber-section integrations that enforce the assumption that the cross sections remain plane.

The length of the inelastic hinge can be determined from the moment-curvature characteristics of the section together with the concurrent moment gradient and axial force. Integration of deformations along the hinge length captures the spread of yielding more realistically than the concentrated hinges, while the finite hinge length facilitates calculation of hinge rotations.

The fiber section models, whereas, distribute plasticity through the member cross sections and along the member length. The source of inelasticity is defined by discretizing the members both along their length in a finite number of so-called "Gauss points" and through their cross-section to track the gradual development of inelastic zones as shown in Figure 2.7.

Since the stresses and strains are, in general, not constant on the sections of structural members and the σ-ε relationship is nonlinear, each section is subdivided in a grid of small areas called "fiber", each of them is associated with the uniaxial stress-strain law according to the defined constitutive materials.
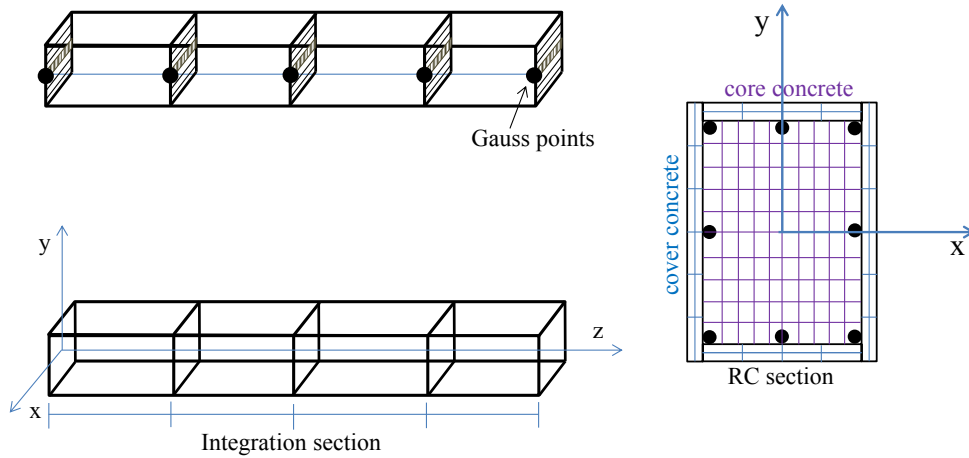
Figure 2.7: Typical fiber model of an RC element

Such uniaxial models are defined to capture the nonlinear hysteretic stress-strain characteristics in the cross-sections. The global nonlinearity of the member is then obtained by integrating the contribution provided by each controlling section.

For R.C. structure, the element is divided into three types of fibers (Figure 2.8): some fibers are used for modeling of longitudinal steel reinforcing bars; other fibers are used to define the nonlinear behavior of confined "core" concrete, and other fibers are used to define the nonlinear behavior for unconfined "cover" concrete.
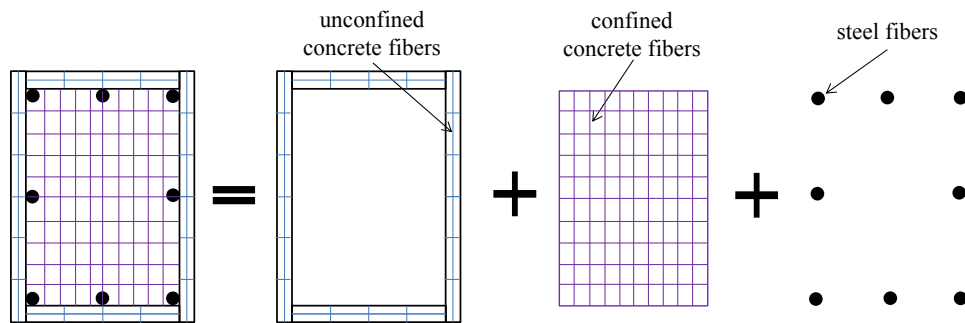
Figure 2.8: Discretization of RC cross-section into three types of fibers

The uniaxial material "fibers" are numerically integrated over the cross-section to obtain force-strain relations. The cross-section parameters are then integrated numerically into discrete sections along the member length, using displacement or

force interpolation functions [70][71][72]. The use of exact interpolation functions in the element need few elements for the representation of the non-linear behavior of the structure. Finally, the most complex models discretize the continuum along the member length and through the cross sections into small micro-finite elements with nonlinear hysteretic constitutive properties that have numerous input parameters.

Distributed plasticity model is undoubtedly one of the closer approximation to the real nonlinear behavior of the structure. As a main advantage of the distributed plasticity models, there is no need to recognize location and extension of nonlinear zones because they are automatically identified.

However, the integration procedure requires long computational time, especially if a huge number of fibers is needed to achieve the wished precision. Moreover, only the flexural behavior can be modeled. Hence, neglecting the shear deformation may yield inaccurate results.

Despite these shortcomings, the "nonlinear fiber element" approach is the most suitable in the case of the assessment of existing R.C. In technical literature different approaches for considering the nonlinear behavior of reinforced concrete structures based on the distributed plasticity concept have been presented [73].

2.4   Seismic assessment

2.4.1   Performance levels

Over the years, several design procedures have been explored to build structures that will survive earthquakes. The prescriptive force-based design procedures were generally unable to simultaneously satisfy both the engineer's desire for a logical explanation of the rules on which decision-making process was based and the owner's desire for sound evaluation of cost-benefit balance for earthquake protection of their properties.

The advances in computational software, new information on earthquake hazards and structural behavior have encouraged the development of an alternative approach called "Performance-Based-Design" (PBD) [74].

PBD is aimed at maximizing the utility from the use of an earthquake-resistant facility by minimizing its expected total cost, including the expected cost of any consequences of damage (in terms of cost of repair, loss of use, etc.) that may occur as a result of future earthquakes. Therefore, the performance-based design can be applied to any phase of the whole life cycle of the building process. It

allows the design of new buildings or the enhancement of existing ones with a realistic understanding of the risk of casualties, occupancy interruption, and economic loss due to future earthquakes.

In the lexicon of PBD, the term "performance level" means the ability of the structure to protect occupants and contents. It is a discrete physical condition identified from a continuous spectrum of possible damage state under a certain level of the earthquake [74]. The performance level of a building is a combination of the performance levels of the structural components, the non-structural parts, and the contents. It can be described by the extent of damage to structural/nonstructural components, which affects the safety of occupants during and after the seismic event, and the cost for repairing and restoring the building to the pre-earthquake condition.

The term "performance objective", whereas, represents a statement of the acceptable risk of damage, and the consequent losses that occur as a result of damage, at a specified level of seismic hazard. Hence, each performance objective expresses what performance levels are expected to be met for a given earthquake hazard level.

The latter can be described either by a deterministic method or by a probabilistic method. In the first case, the engineering characteristics of the shaking at a site due to an earthquake are represented by Response Spectra or ground motion Time Histories.

The second type of method defines the earthquake levels through a probability of exceedance for a given return period. The comprehensive set of relevant performance objective is usually established by the stakeholders (users, owner, regulatory framework, design team, and manufacturers).

The Performance-Based approach has improved the engineer decision-making process leading to more reliable and cost-effective decisions because gives to the designer more choices about the performance of the building than only human life safety objective, as shown in Figure 2.9.

Given the above, the PBD approach can guide designer's decisions on the basis of anticipated performance of the structural system in order to derive the detailed design of the structural and non-structural part of a new building.

In case of existing building, the PBD approach, whereas, can balance the short-term costs and the disruption against the possible benefits of a retrofitting program (read Section 3.3). As a matter of fact, the retrofitting program can effectively raise the performance of an existing building against earthquakes to the desired level, according to the requirements of the modern seismic code [9][15].

Buildings Performance Level
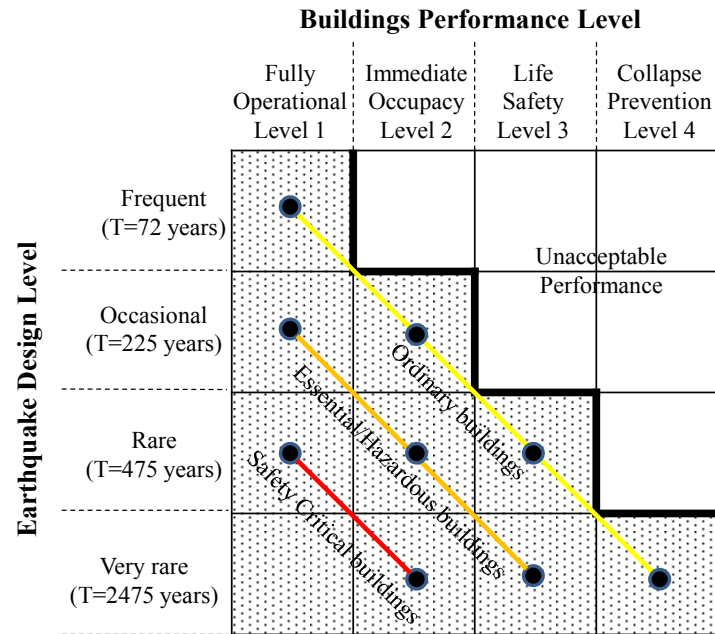
Figure 2.9: Performance Level to be achieved for each type of building [75][76][77]

2.4.2   N2-Method

Once the performance objectives are defined, seismic analyses of the building need to be executed in order to estimate the probable performance of the building under the various scenario.

In principle, seismic analysis can be carried out by means of a variety of linear or nonlinear methods (Section 2.2). However, the performance-based approach prefers a nonlinear analysis able to simulate accurately the seismic response of the structure and the level of damage it is expected to suffer as a result of the excursion in the non-linear range.

To this end, it is worth to mention the Equivalent SDOF Method (or N2-Method) proposed by Fajfar [78]-[82] and currently adopted by the most recent European codes for seismic design and assessment of existing structures [83]. The method provides a clear graphical representation of how a building responds to earthquake ground motion, leading to a comprehensive representation of its deficiencies.

It develops into two fundamental stages. In the first step, the capacity curve describing the evolution of the structural response with increasing seismic intensity

must be determined. This is obtained through a pushover analysis of a nonlinear model of the structure, in which static lateral forces are monotonically increased until structural collapse [84] (Figure 2.10).
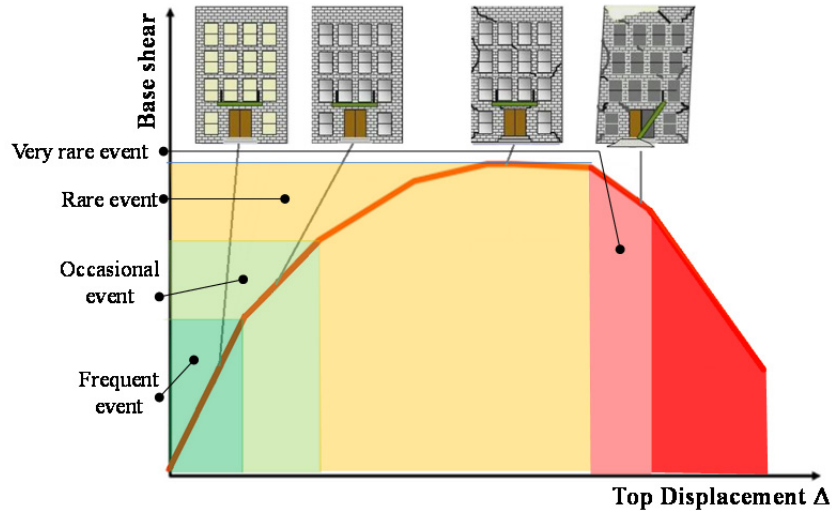
Figure 2.10: Representation of seismic intensity vs damage

In the second step, the expected performance of the building under an assigned design seismic events is then estimated as the point on the capacity curve which corresponds to the so-called "target displacement" of the "control node" and to the total base shear demand.

Since the "target displacements" are defined in terms of spectral quantities, the methodology is referred to the assumption that the response of a real Multi-Degree-of-Freedom (MDoF) system may be represented by a simpler Single-Degree-of-Freedom (SDoF) equivalent system with a specific hysteretic characteristic. Such a transformation is possible if the behavior of an MDOF system is well described by fundamental mode with a modal shape constant during the monotonic increase of the lateral forces.

Hence, the capacity curve which provides the relationship between the global shear force and the horizontal displacement of a control node is transformed into the so-called "Capacity Spectrum" [85] obtained by scaling the capacity curve with the modal participation factor. The Capacity Spectrum is represented in Acceleration Displacement Response Spectra (ADRS) diagram which depicts the spectral displacement S_d on the x-axis and the spectral acceleration S_a on the y-axis.

Even the engineering characteristics of the earthquake are represented in a deterministic way in the same ADRS diagram, through the so-called "Demand (Response) Spectrum" which depends on the selected performance level.

The intersection between the Capacity Spectrum of the equivalent SDOF (idealized as an elastic-perfectly plastic curve) and Inelastic Demand Spectrum [86] is named "Performance Point" and represents the probable performance of the building as a whole in terms of inelastic displacement of the roof.

The Inelastic Demand Response Spectrum (IDRS) can be obtained by scaling the Elastic Response Spectrum of a force reduction factor proportional to the dissipative capacity of the building. To this end, the N2-Method adopts direct relationships between the ductility, the elastic period and the force reduction factor (μ-T-R_μ in the following) based on well-established rules [87] derived the study of the hysteretic response of structures with an ideal elastic-plastic behavior [88].

However, it is worth to mention the work of Martinelli et al. [89] intended at generalizing the above relationships adopted for defining the Inelastic Design Response Spectra. The authors proposed new relationships to take into account the actual dissipative capacity of structural systems.

The field of application of Inelastic Spectra for structures characterized by a hysteretic behavior significantly different (and dissipative capacity possibly lower) than the ideal elastic-perfectly plastic system employed in formulating and calibrating the N2 Method.

However, in the case of existing structures for which an exact value of the force reduction factor is not known a priori, the nonlinear static analysis allows calculating the available ductility through the pushover curve.

The relationships of Eq. (2.8) based upon a formulation derived from an original proposal calibrated on two highly dissipative hysteretic laws [88] can be used for predicting the R_μ value (needed to calculate the IDRS):

$$R_\mu = \begin{cases} 1 + (\mu - 1) \cdot \dfrac{T}{T_C} & \text{if } T \leq T_C \\[2mm] \mu & \text{if } T > T_C \end{cases} \qquad (2.8)$$

As shown in the Figure 2.11, in the case of a rigid structures (characterized by an elastic period lower than the critical period T_C), the spectral displacement of the SDoF system with elastic behavior (S_{de}) is lower than the spectral displacement (S_d) required by the system characterized by an elastic-plastic behavior (equal energy rule).
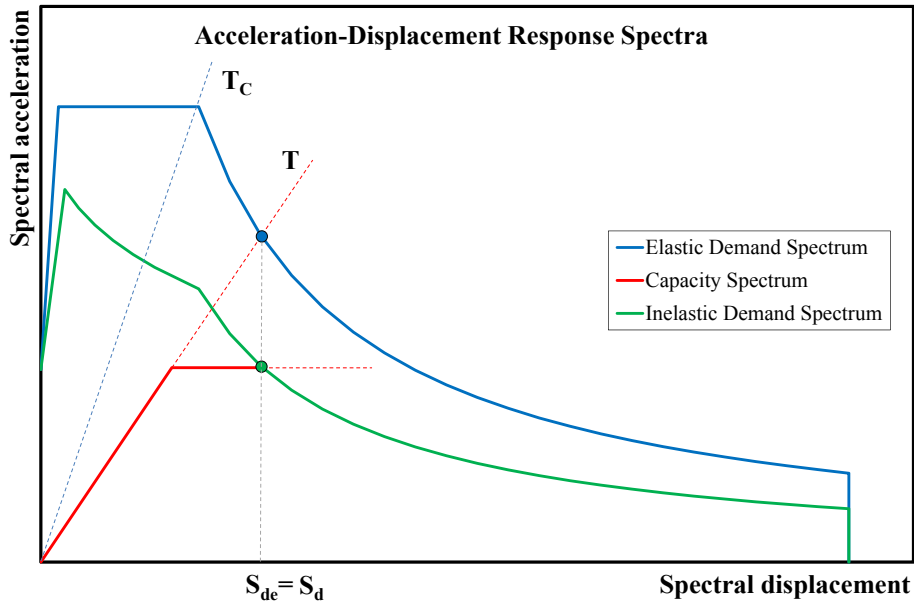
Figure 2.11: Equal displacement rule for long period SDoF system [90]

Conversely, in the case of flexible structures (characterized by an elastic period T greater than critical period T_C), the spectral displacement of the SDoF system with a bilinear behavior is equal to the steady-state peak displacement of an elastic system (equal displacement rule), as shown in Figure 2.12.
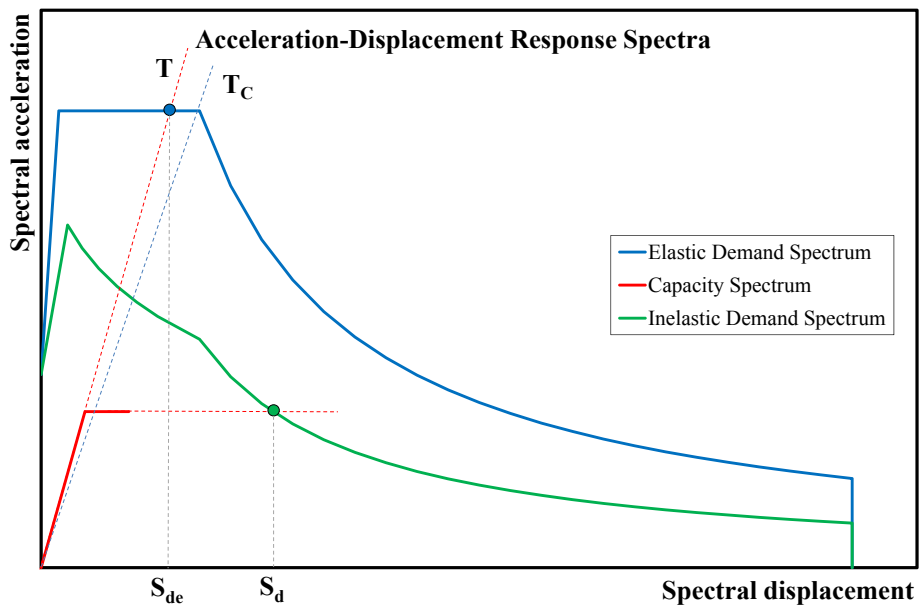
Figure 2.12: Equal energy rule for short period SDoF system

After establishing the Performance Point and once the displacement demand at the control node is known for a given performance level, it is possible to extract all the internal forces and deformations, attained when the "control node" displacement reaches the "target displacement", taken from the capacity curve as the demand values of the structural members.

This is necessary because the assessment of existing buildings is a force based procedure regarding the brittle mechanisms but also a displacement-based method concerning the ductile mechanisms. In particular, in the case of R.C. structures, the ductile modes should be checked in terms of flexural deformation, while the brittle modes should be assessed in terms of shear forces.

As a matter of fact, the structural members (beams and columns) are, in most of the cases, slender elements. The shear forces are, therefore, low compared to the bending moments and, consequently, flexural deformations dominate the behavior. The chord rotation at member ends is the most important and convenient flexural deformation measure for concrete members because unlike curvatures, which are difficult to measure experimentally, deflections can be reliably measured.

On the other hand, the chord rotation capacity depends on both geometrical and mechanical properties of the element and on the seismic input since the same member may develop different values of capacity as the seismic action changes.

3. State of practice on retrofitting strategies and systems

3.1 Performance-based retrofit program

Seismic retrofit is the modification of an existing structure aimed to reduce its vulnerability and, hence, the economic impact of the damage expected for a future earthquake. Sometimes, the terms "seismic rehabilitation" is used in lieu of "seismic retrofit".

Nevertheless, seismic rehabilitation is undertaken in a building that is already damaged, while retrofit refers to structural interventions (as a preventive measure) aimed at mitigating the effect of a future earthquake.

The primary goal of seismic retrofit is to overcome the main weakness and deficiencies relating to the seismic performance in the "as-built" configuration. It can effectively raise the performance of a building against earthquakes to the desired level, and even to achieve the requirements of the modern seismic code [9].

Although seismic performance can be greatly enhanced through the retrofit scheme, it is worth to keep in mind that earthquake-proof structures don't exist. In qualitative terms, seismic retrofit aims to increase the lateral strength and stiffness, to increase the ductility; to reduce the effects of irregularities; to enhance redundancy in the lateral load resisting system; to ensure adequate stability against overturning mechanism (Section 1.2.).

Several important performance-based design guidelines and codes provide sources of reference for performance-based seismic retrofitting.

The first guidelines for seismic retrofitting of existing buildings were SEAOC Vision 2000 report [74]; FEMA 273 instructions [75]; FEMA 274 instructions [76].

Later, a comprehensive and detailed vademecum on performance-based-design in the field of seismic retrofitting was published: Pre-standard and Commentary for Seismic Rehabilitation of Buildings, FEMA 356 [77].

In FEMA 356, performance levels are defined by reference to the damage status described in a qualitative manner. Similar performance levels are found in the

Italian Code in the description of the Limit States against seismic actions, as reported in the current Technical Standards for Construction [15].

The seismic hazard levels associated with each Limit State (at both Serviceability Limit State and Ultimate Limit State) are expressed in terms of probability of exceeding P_{VR} in a reference time V_R as shown in Table 3.1.

Table 3.1: Qualitative description of Limit States according to NTC 2008 [15]

Limit State	P_{VR}	Description
SLO	81%	the building as a whole, including structural, non-structural elements, equipment relevant to its function, must not suffer significant damage and interruption of use.
SLD	63%	the building as a whole, including the structural and non-structural elements, along with the relevant equipment undergoes damage such that does not to put at risk the users and does not significantly affect the resistance and stiffness against the vertical and horizontal actions, remaining immediately usable despite the interruption of use of part of the equipment.
SLV	10%	the building undergoes breakdowns and collapses of non-structural and installation components and significant damage to structural components associated with a significant loss of stiffness against horizontal actions; the building is still characterized by a residual strength and stiffness for vertical actions and a safety margin against collapse for horizontal seismic actions.
SLC	5%	the building is subject to severe breakdowns, collapses of non-structural components and very serious damage to structural components; the building still has a safety margin against vertical actions and a small safety margin against collapse for horizontal seismic actions.

According to the aforementioned guidelines and taking into account the key principles adopted in Performance-Based Seismic Engineering [91][92], before undertaking a retrofit program the designer should be aware of each step to be implemented. In particular, the steps suggested by FEMA 356 [77] are summarized in Figure 3.1.
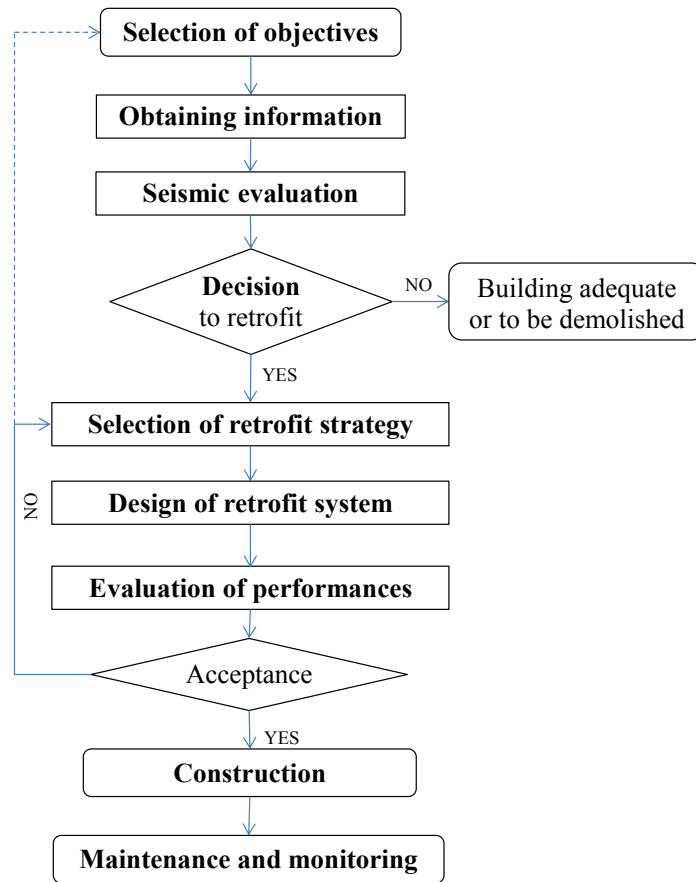
Figure 3.1: General flow-chart for a performance-based retrofit process

i.   Selection of the objective of retrofit

The first step of a retrofit program is the selection of the objectives that give a quantitative "target" to achieve under a certain level of earthquake hazard.

As previously seen, the objective is usually drawn from performance-based approach: the performance objective can be selected among a wide range, ranging from damage limitation to collapse prevention as described in Figure 2.9.

The selection of the performance levels is based on recommended guidelines in accordance with the type of building, economic considerations and engineering judgment.

ii.   Obtaining information about the building

Once the performance objectives are selected, the designer should search for any information and documents about the existing structure construction, including the architectural and structural drawings dating back to the year of construction.

iii.   Seismic evaluation

A series of seismic displacement-based-analysis are then carried out with the aim to identify the deficiencies and the seismic vulnerability level. Those analyses have to be intended to evaluate the deformation of the members and the building as a whole, under the lateral forces of an earthquake of a given level of seismic hazard.

The seismic evaluation can be performed in the two stages: preliminary evaluation to identify areas of potential weaknesses followed by a detailed evaluation of the seismic response of as-built configuration through an FE analysis.

iv.   Decision to repair, retrofit or demolish

Based on the importance of the building, the degree of deficiencies found, the economic viability, the availability of materials and technical resources, the stakeholders are responsible for undertaking a decision.

In particular, the engineer should carefully examine the results of the initial seismic performance evaluation in order to design an applicable, effective, and economical solution. However, although the seismic behavior of the existing building is accurately simulated using nonlinear analyses, a false interpretation of the results may lead to an ill-designed or inapplicable retrofit solution.

Hence, the decision can be one of the following:

a) if the safety of the building is adequate the building needs just some possible repair and regular maintenance;
b) if the safety of the building is inadequate, a seismic retrofit is needed;
c) if the safety of the building is inadequate, and any retrofit solution is not economically feasible, the building is to be declared unfit for use and demolished.

v.   Selection of retrofit strategy

If the building needs a seismic retrofit program, it is necessary to choose the most suitable one. The retrofit strategies suitable for each type of building is discussed in Section 3.2. The knowledge of "pros and cons" of several retrofit strategies commonly adopted is essential for the selection which depends, among the others, on the technical expertise of the designer. Each retrofit strategy should consistently and reliably achieve the performance objectives.

vi.   Preliminary design of the retrofit system

After the selection of a suitable retrofit strategy, one or more systems can be used in a synergistic combination to meet performance objectives under a feasible and economical retrofit scheme to realize the selected strategy. A review of the technical intervention is discussed in Section 3.3.

In practice, the retrofit systems realize a modification in the dynamic features of the structure. Their design and detailing should address the transfer of loads and the compatibility of deformation among the existing members, modified members, and the new ones.

vii.   Verification of the retrofit scheme

After the preliminary design of a retrofit system, engineers should assess the seismic performance of retrofitted configuration through the structural analysis.

Alteration of the load path, redistribution of the member-forces and variation in the failure mode need to be studied.

If the retrofit scheme is acceptable according to Eq. (3.1) and the performance meets or exceeds the objectives, then the design is complete and construction documents can be prepared.

Otherwise, the retrofit system and/or the performance objectives should be changed until the above verifications are met.

viii.   Construction

Once the technical system is acceptable it can be built. Attention should be given to the detailing which greatly affects the effectiveness of the retrofit scheme.

ix.   Maintenance and monitoring

Maintenance and monitoring are two long-term activities that should be undertaken after the construction phase. In particular, the maintenance of retrofitted buildings aims at achieving the selected performance of the building during a future earthquake. On the other hand, monitoring the performance of the buildings during an earthquake, wherever possible, is important to detect any deficiency in the retrofit strategy.

3.2   Retrofit strategy

Seismic retrofitting strategy can be defined as the basic approach adopted to mitigate the effect of a future earthquake on an existing undamaged building and to achieve an overall seismic performance objective. As a matter of fact, the problem of the rational selection of a suitable retrofit strategy for an existing building can be conceptually described by the following inequality:

$$C_{LS,i} - D_{LS,i} \geq 0 \qquad \forall i = 1...n_{LS} \tag{3.1}$$

On the right side, the term C_{LS} is the supplied Capacity features of the strengthened structure at the Limit State (LS) or Performance Level under consideration and it is related to how the structure behaves under seismic loads.

On the left side, D_{LS} is the corresponding demand (target requirement) at the same Limit State (namely, induced by a seismic event whose probability of occurrence is compatible with the Performance Objective under consideration).

Capacity and Demand can be intended in terms of both displacement (for ductile mechanisms) and forces (for brittle mechanisms). Moreover, similar relationships should be checked at all the n_{LS} relevant Limit States.

In seismic-prone areas, Eq. (3.1) is often not met by many existing structures in their "as built" configuration. However, an engineer can meet the inequality by:

   a.   decreasing the seismic hazard demands;
   b.   improving the dynamic characteristics supplied to the existing building.

It should be noted that the above-mentioned strategies (a) and (b) are interrelated because the demands of seismic excitations depend on the capacity supplied to the whole facility system. The following sections collect the most common retrofit strategies.

3.2.1   Global strengthening/stiffening

The global strengthening/stiffening strategy implies an increase in strength and stiffness of existing structural systems. With this strategy, the capacity is almost unchanged while the seismic demand can be reduced down to the available displacement capacity.

This strategy is often preferred when the structure has many structural members found to fail at a small lateral deflection, such as existing columns whose details are insufficient to prevent premature shear failure. It can be less expensive and less disruptive than retrofitting of individual members.

Figure 3.2 depicts the structural behavior before and after the implementation of such retrofitting strategy which can be illustrated schematically with the help of capacity curves in ADRS diagram.
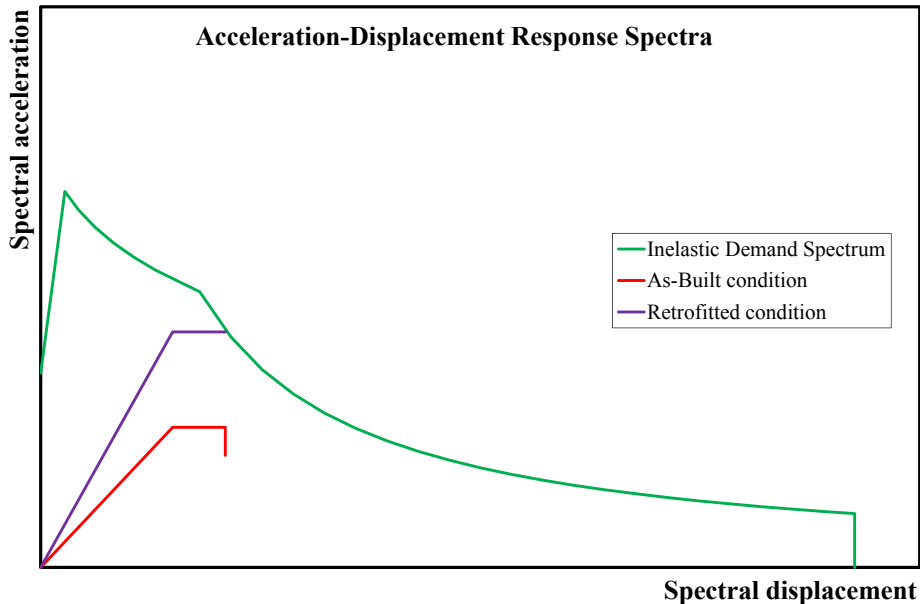
Figure 3.2: Capacity Spectrum before and after global strengthening/stiffening

3.2.1.1   Strategy 1: adding elements

Aside from strengthening and stiffening the existing building, the advantage of adding new lateral-force-resisting-systems is the possibility to reduce pre-existing plan or vertical irregularities.

It is important to take into account the architectural and functional constraints that restrict the frame where new LFRSs can be installed. The upgraded loads to be

carried by new elements should be adequately delivered to other existing components by not creating another source of deficiency in the load path.

Moreover, another important aspect is the transfer of the seismic action from the ground through the foundation: foundation system should be enlarged to respond to the increase of dead loads associated with the new building.

3.2.2   Increasing of deformation capacity

This strategy improves the seismic performance of the building by selectively increasing the local capacity (ductility, strength or stiffness) of individual components without appreciably modifying the global behavior of the structure as a whole. Hence, displacement demands of the earthquake are not changed as can be seen in the ADRS diagram in Figure 3.3.

This strategy is usually adopted when the structure has a low number of members known to fail at a small lateral deflection.
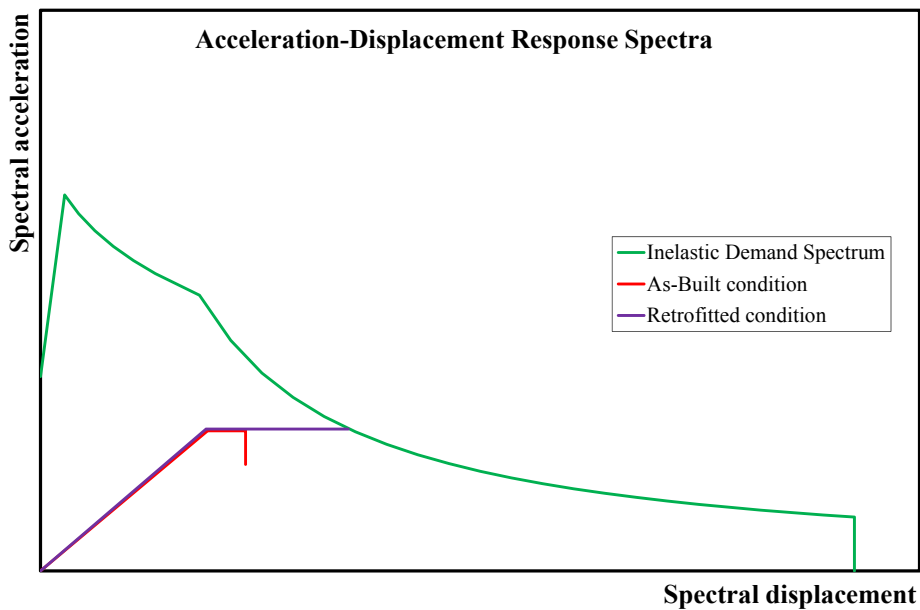
Figure 3.3: Capacity Spectrum before and after increasing of ductility

3.2.2.1   Strategy 2: enhancement of members' ductility

The deformation capacity of structural members can be increased by altering the member in a way that allows additional deformation. According to this strategy, the global deformation capacity is increased, while the ultimate strength and the

stiffness are only slightly increased. The ductility can be enhanced locally also by uncoupling brittle elements from the deforming structure, or by removing them completely, i.e. by shifting brittle failure modes to ductile ones.

3.2.2.2   Strategy 3: improvement of connections between members

The acceptable performance level can be achieved also by local improvement of connections rather than an increase of existing members' ductility.

As a matter of fact, a deficiency in the load path is most often created by a weak connection, rather than by a completely missing one. Connections with non-ductile behavior caused a threat for the partial or complete collapse in the past earthquakes.

3.2.2.3   Strategy 4: selective weakening

A structural member can fail in a variety of different modes, but it fails in the mode characterized by the lowest strength under seismic loads. Normally, an undesirable failure mode is avoided by strengthening the member against failure in that mode.

An alternative seismic retrofitting approach consists in decreasing the strength of some desired mode so that the desired mode becomes the weak link in the system. This is a counter-intuitive strategy to change the inelastic mechanism of the structure and increase the global deformation capacity.

3.2.3   Reduction of seismic demand

This section includes three strategies for reducing seismic demand in terms of both deformations and forces.

3.2.3.1   Strategy 5: softening

The engineers can decrease the input energy by the so-called "softening" strategy. A softening of the structural system basically implies a reduction in stiffness and, as consequence, an increase of the period and the spectral displacement demand as shown in Figure 3.4.

Nevertheless, the displacement is concentrated in a specific region and therefore do not adversely affect the drift-sensitive components of the building. This approach can be highly effective in protecting brittle structural elements as well as acceleration-sensitive building contents.
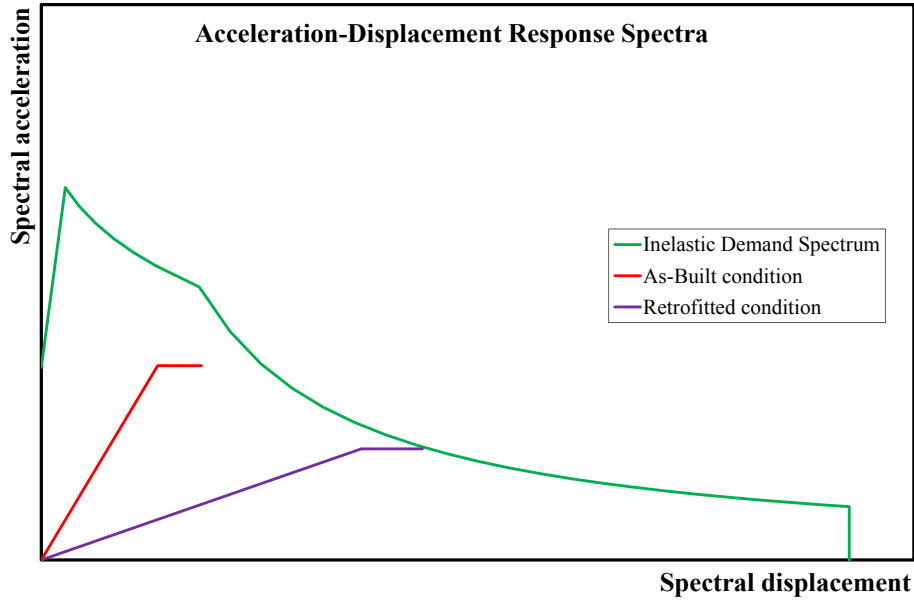
Figure 3.4: Capacity Spectrum before and after softening

3.2.3.2 Strategy 6: increasing of damping

Two ways exist to obtain the energy dissipation: a) within the structural members, by the formation of flexural plastic hinges; b) externally, by damper devices. The scale factor for IDRS is proportional to the dissipated energy (Figure 3.5).
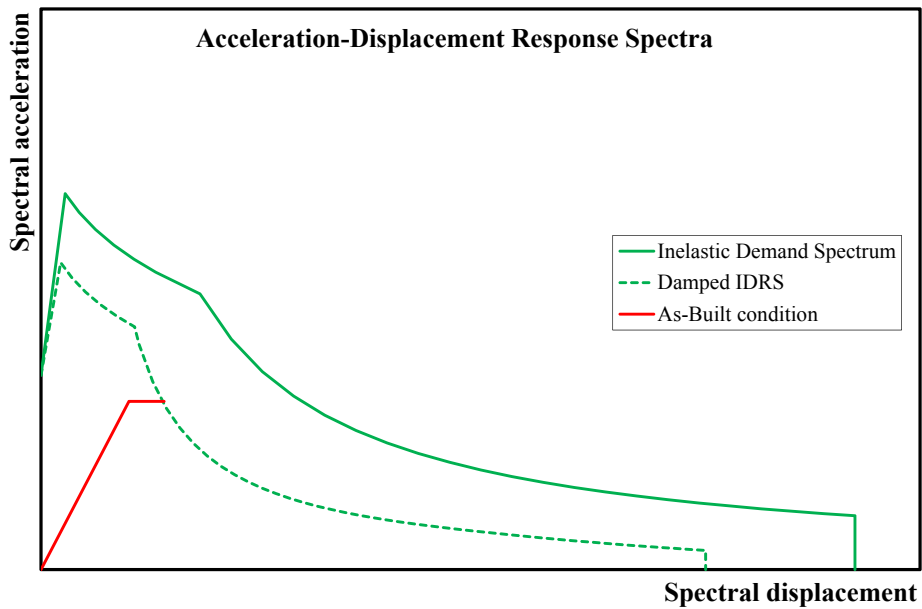
Figure 3.5: Demand Spectrum before and after increasing of damping

3.2.3.3   Strategy 7: reduction of reactive mass

The seismic demand can be reduced by decreasing the reactive masses. In this way, the vibration period of the structures is shortened, and the inertia forces and displacement demand are reduced.

Mass reduction can be achieved by removing heavy non-structural elements (heavy contents such as equipment and storage). In the extreme, the mass reduction can involve the removal of the one or more upper stories in the existing building.

3.2.3.4   Strategy 8: change of intended use

A reduction of seismic demand can be achieved not only through structural measures. A common "non-structural" strategy employed in the field of the seismic retrofitting of existing structures is the restriction or change of the intended use, such as the "declassification" of the building to a lower "importance class" [15].

3.2.4   Existing procedures for selecting an optimal strategy

One of the first systematic approaches for selecting an optimum retrofit strategy was the UNIDO/UN method [93] proposed in 1985 in the form of a procedure based on empirical estimations and engineering judgment.

ATC-40 [56] adopted a different approach based on nonlinear analysis to compare alternative strategies and select the best one. An overall grade was obtained for each strategy by adding the product of the relative weights of the design constraints (such as cost or time) with the grade (on a scale of 1 to 10) that represented the impact of each constraint on a particular strategy (with 10 representing little impact and the most desirable effect). The highest overall grade indicated the optimum strategy to be selected.

Baros and Dristos [94] introduced a simplified procedure for the selection of an optimal retrofit strategy for existing building. The authors proposed quantitative criteria for the accurate evaluation of structural deficiencies which along with the engineering judgment could lead to a well-established retrofit solution.

The procedure was mainly based on the accurate evaluation of the capacity curve of the building in its "as built" configuration through a static nonlinear analysis. The authors classified the available strategies into three groups by considering their effect on the behavior of the building.

–   Group A includes strategies whose basic aim is to improve the overall ductility of the building without affecting the overall stiffness and strength of the structural system as shown in Figure 3.6;
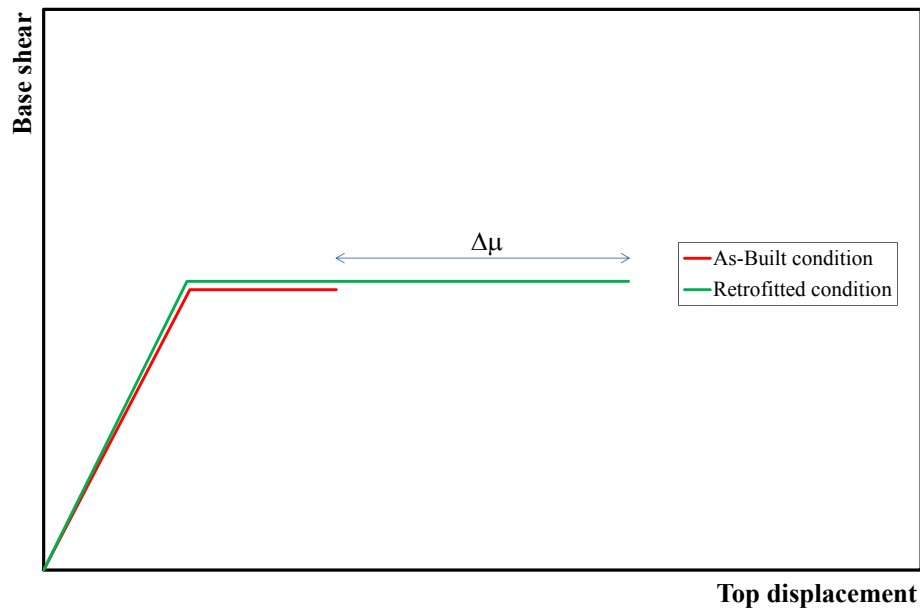
Figure 3.6: Increasing of deformation capacity (strategy A)

- Group B included strategies that imply a strengthening/stiffening while a negligible increment of ductility as shown in Figure 3.7;
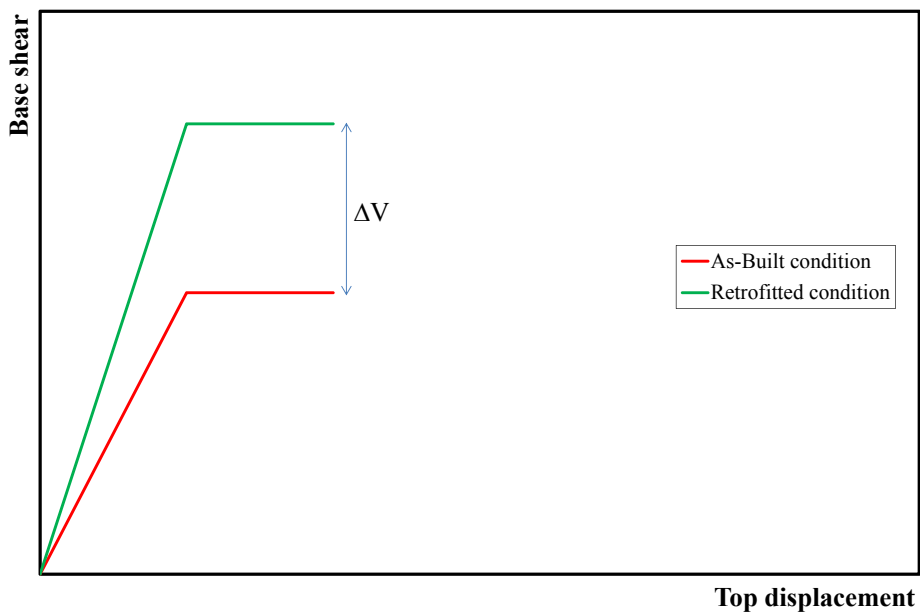
Figure 3.7: Increasing of global strength and stiffness (strategy B)

– Group C included strategies that increase both strength and ductility as shown in Figure 3.8.
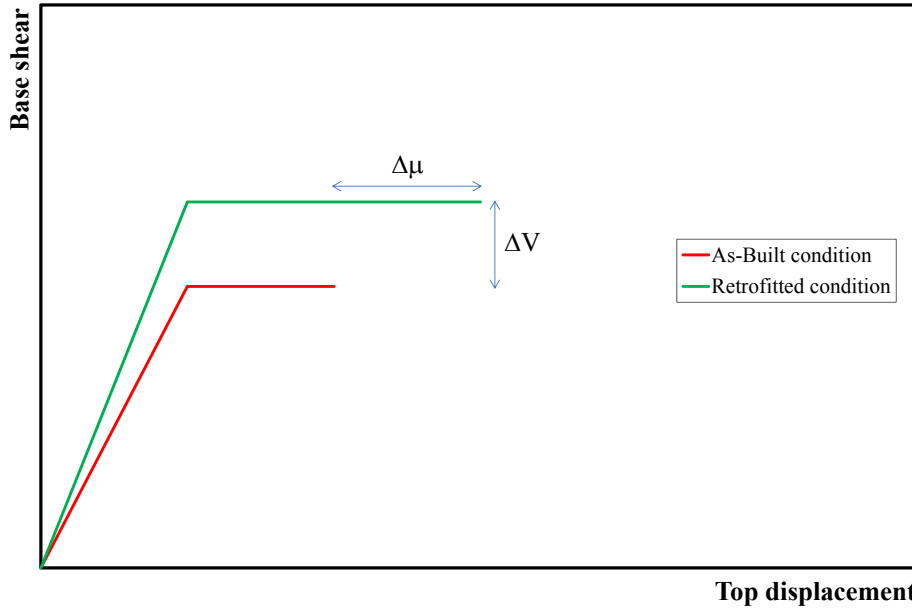
Figure 3.8: Strength, stiffness and ductility enhancement (strategy C)

The alternative strategies could be mainly compared on the basis of quantitative dimensionless parameters which represents the required increase in strength or ductility. In particular, the authors proposed to calculate the required increase in ductility according to the ratio in Eq. (3.2):

$$\lambda_D = \frac{\mu_{req}}{\mu_{av}} \tag{3.2}$$

where μ_{av} is the available ductility factor and μ_{req} is the required ductility to meet the performance objective. Likewise, the required increase in strength was quantified by the following ratio:

$$\lambda_S = \frac{V_{b,ret}}{V_{b,av}} \tag{3.3}$$

where $V_{b,ret}$ is the base shear of the retrofitted building and $V_{b,av}$ is the strength value needed to meet the performance objective. The efficiency of the examined strategies was evaluated by comparing the values of λ_S and λ_D with appropriate empirical limiting values. In addition to the above ratios, the authors proposed to

evaluate also the inter-story drift which is related to the damage at non-structural components which, in turn, affects the occupancy of the building during and after an earthquake.

Therefore, the selection of optimal strategy was based on three parameters: the required ductility, the required strength, and the expected inter-story drift. Summarizing the above, the authors proposed the Table 3.2 for the selection of an effective retrofit strategy for an existing R.C. building.

Table 3.2: Proposed strategies for low, medium and high drift values [94]

Drift (%) < 0.3 x maximum drift					
Strength Ratio λ_S	Ductility Ratio λ_D				
	$\lambda_D < 1.0$	$1.0 < \lambda_D < 1.4$	$1.4 < \lambda_D < 1.8$	$1.8 < \lambda_D < 2.5$	$2.5 < \lambda_D < 4.5$
$\lambda_S < 1.0$	No or light local intervention				
$1.0 < \lambda_S < 1.4$		A	A or C	B or C	B
$1.4 < \lambda_S < 1.7$		A	C	B or C	B or C
$1.7 < \lambda_S < 2.0$		A	C	B or C	C
$2.0 < \lambda_S < 3.0$		A or C	A or C	C	Rebuild

0.3 x maximum drift < Drift (%) < 0.7 x maximum drift					
Strength Ratio λ_S	Ductility Ratio λ_D				
	$\lambda_D < 1.0$	$1.0 < \lambda_D < 1.4$	$1.4 < \lambda_D < 1.8$	$1.8 < \lambda_D < 2.5$	$2.5 < \lambda_D < 4.5$
$\lambda_S < 1.0$	No or light local intervention				
$1.0 < \lambda_S < 1.4$		A	C	B	B
$1.4 < \lambda_S < 1.7$		A or C	A or C	B	B
$1.7 < \lambda_S < 2.0$		A or C	A or C	B	B
$2.0 < \lambda_S < 3.0$		C	A	B	Rebuild

Drift (%) > 0.7 x maximum drift					
Strength Ratio λ_S	Ductility Ratio λ_D				
	$\lambda_D < 1.0$	$1.0 < \lambda_D < 1.4$	$1.4 < \lambda_D < 1.8$	$1.8 < \lambda_D < 2.5$	$2.5 < \lambda_D < 4.5$
$\lambda_S < 1.0$	No or light local intervention				
$1.0 < \lambda_S < 1.4$		A or C	C	B	B
$1.4 < \lambda_S < 1.7$		A or C	B or C	B	B
$1.7 < \lambda_S < 2.0$		A or C	B	B	B
$2.0 < \lambda_S < 3.0$		A or C	B	B	Rebuild

The possible optimum strategy needs anyway to be verified through a detailed design of the retrofit system.

3.3 Retrofit systems

Retrofit systems are specific interventions that might be used to achieve the adopted strategy [56].

These possible technical solutions, partially derived by the seismic protection techniques for new structures, can be classified into two broad classes, generally not mutually exclusive, which collect, on one hand, the local intervention (also known "member-level" techniques) and, on the other hand, the global intervention (also called "structure-level" techniques) [16].

A global retrofit system targets the performance of the entire building under seismic loads. A local retrofit system, whereas, targets the seismic resistance of a member, without significantly affecting the overall resistance of the building.

Furthermore, conventional and innovative techniques can be distinguished. The former mainly include the addition of elements or improvement of individual members, while the latter are based on controlling the seismic responses.

A list of systems designed for the seismic retrofitting of old existing reinforced concrete buildings is presented in the following sections.

3.3.1 Global intervention techniques

When a building is found to be severely deficient under seismic forces, the first attempt in a seismic retrofit program is usually a global intervention so that the displacement demand on the existing structural and non-structural components is less than supplied capacity.

This group includes also the so-called "protective systems" (damping and isolator devices). The most common global intervention are presented hereafter.

3.3.1.1 Base isolation

Seismic isolation is a classic example of "softening" strategy aimed at reducing the seismic input energy.

It basically consists of one or more discontinuities (isolator devices) that separate the structure into two or more parts, i.e. the substructure, connected to the foundations, and the superstructures.

Isolator devices are characterized by a high rigidity for vertical loads and a limited rigidity against horizontal loads. They are interposed between "sub-

structure" and "super-structure" typically at the foundation level, as shown in Figure 3.9.

Figure 3.9: Example of isolator devices at the foundation level

Thereby, a substantial "filter" is applied between the motion of the substructure and the motion of the superstructure, so as to reduce the transmission of the kinetic energy.

The isolator devices are simply considered as global techniques, as they modify the seismic-induced actions on the existing members by modifying the global properties of the structure under consideration (i.e., the fundamental period of vibration).

For the isolation devices to be effective, the period of vibration of the retrofitted structure should be shifted to the descending part of the spectral acceleration. The installation of seismic isolators into an existing structure requires specialized engineering expertise and careful construction planning. In fact, inserting an isolator within an existing column is not so simple because of the necessity of cutting the element, temporarily supporting the weight of the above structure, putting in place the isolators and then giving back the load to the column, without causing damages to structural and non-structural parts.

Seismic isolation is relatively expensive compared to other techniques. For this reason, it is mostly adopted for rehabilitation of critical or essential facilities, buildings with expensive and valuable contents, for historic preservation of occupancies that cannot be disturbed, and structures for which performance well above performance levels is required.

3.3.1.2   Dissipation device

The increasing of damping aimed at reducing the seismic demand can be realized through the installation of energy dissipation devices (Figure 3.10).

Different types of devices are typically used, such as visco-elastic (fluid) dampers, visco-elastic (solid) dampers, hysteretic energy dissipation dampers and friction dampers.

In particular, the visco-elastic dampers exploit the viscoelastic behavior of certain materials (usually plastics, mineral oils, silicon) to dissipate energy with a viscous behavior; elastic-plastic dampers exploit the plasticization of metallic materials (yielding metals and lead) to dissipate energy in hysteresis cycles; the friction dampers dissipate energy by exploiting the friction phenomena that arise between metal surfaces, suitably treated, in relative sliding between them.

The devices are usually installed in the plain-frame in combination with a vertical bracing system, which results also in the stiffening of the existing building. The damping devices are mainly intended for application of important and strategic structures and infrastructures.

Figure 3.10:Example of visco-elastic dampers

3.3.1.3   Addition of RC walls

An efficient system for controlling global lateral drift and reducing displacement demand (which affects the damage status) in framed structures is the addition of new RC walls as shown in Figure 3.11.

This system is designed to increase the lateral strength and the stiffness of an existing building [95].

Figure 3.11: Example of a reinforced concrete wall built between existing columns

The designer has to pay attention to several aspects: the distribution of the walls in plan and elevation (in order to avoid irregular configuration), the shift of the center of rigidity, and the connection of the walls into the existing frame (it is necessary to ensure full interaction between the existing structure and the new one).

A major issue is the strengthening of the foundation system to respond to the increased weight and the overturning moment. As a matter of fact, the foundation intervention is usually expensive and disruptive, so this technique is often unsuitable for buildings without an existing adequate foundation system.

A simpler case is whether the RC walls are built on the "border" of the building where it is easier to realize the strengthening of existing foundation. However, this poses an architectural problem about the "aesthetic" impact of the intervention.

Such an intervention is particularly suitable in case of "soft-story" mechanism and structures with torsional irregularity.

3.3.1.4   Addition of infill walls

Figure 3.12 shows an example of infill walls that are an efficient system aimed at increasing the lateral stiffness of one or more stories. In fact, this intervention is easy to realize and it reduces the inter-story drift without affecting the ductility.

Due to the "strut action" of the infilled walls, the flexural and shear forces attracted by columns in the "weak" story are substantially reduced. However, the increase of lateral stiffness results in greater values of weight, acceleration and seismic forces.

The addition of infill walls is typically a viable option for seismic retrofitting of vulnerable buildings with an "open ground story".

Figure 3.12: Example of infill wall

3.3.1.5   Addition of steel braces

Figure 3.13*a* shows an example of steel bracing system can be realized in an existing flexible frame to increase the lateral stiffness, strength or any combination of these. Alternative configurations of bracing systems can be used: concentric or eccentric. In both configurations, energy dissipation devices can be incorporated to absorb seismic energy as shown in Figure 3.13*b*. To achieve an adequate seismic performance, the engineer has to pay attention to several aspects.

The connection between the bracing system and the existing frame is an important detail. If the connection fails before the brace, the maximum strength and/or lateral stiffness cannot be achieved. If the braces are connected directly to the frames at the beam-column joints, the resisting forces of the bracing elements are transferred to the joints.

While the addition of compressive forces may be tolerated, the resulting tensile forces may be of concern. Strengthening of columns, beams and beam-column joints of braced is usually needed for the adequate performance of the whole system. The designer has to pay attention also to buckling mechanism of the steel members: when a brace suffers global buckling during cyclic loading, it can lose a large percentage of its original strength. Hence, it is necessary to protect the system against local instability and post-buckling ruptures phenomena.

Some of the advantages of such system are the ability to accommodate the openings, the minimal increase in terms of weight and reactive mass, the distribution of loads-induced over the whole foundation system and the minimum disruption to the function of the building and its occupants.

However, in the scientific literature, not enough attention has been paid so far about the topic of the optimal shape of bracings and distribution of their members for a seismic retrofitting intervention of an existing RC frame.

| (a) | (b) |

Figure 3.13: Example of steel braces installed on the ground floor (a); with dampers (b)

3.3.2   Local intervention techniques

This group includes the repairs, reinforcement or replacement intervention of individual structural elements found to be inadequate to their function. Such interventions do not significantly modify the overall behavior of the structure, meaning the lateral strength or the stiffness.

In a framed structure, the columns and the beams are usually retrofitted to increase their flexural and/or shear strength and the deformation capacity of the beam-column joints. However, the retrofitting of the columns is more important than the retrofitting of beams since they are susceptible to brittle failure.

On the one hand, these interventions are adequate if the number of elements that need a higher strength is not excessive, on the other hand, they are inappropriate when the stiffness of the existing structure must be enhanced.

The local retrofit systems fall under three different types: concrete jacketing, steel jacketing (or use of steel plates) and fiber-reinforced polymer (FRP) sheet wrapping.

3.3.2.1   Concrete Jacketing

Figure 3.14a shows an example of concrete jacketing that consists of the application of a layer of concrete, longitudinal bars, and closely spaced stirrups in order to increase the strength of individual members.

The variation in terms of stiffness, whereas, depends on the thickness of the jacket which affects the size of the element.

If the jacket is applied at floor level of vertical elements, both axial and shear strength are improved, while flexural strength and strength of the beam-column joints remain unchanged. If the jacket runs through two consecutive floors, then stiffness, strength, and ductility are enhanced.

(a)   *(b)*

Figure 3.14: Example of concrete jacketing of columns (a); of a beam-column joint (b)

To increase also the flexural strength, additional longitudinal bars should be anchored to the foundation and they should be continuous through the floor slab. It is important to note that with the increase in flexural strength, the shear demand (based on flexural capacity) also increases: additional ties are provided to meet the shear demand. To ensure the composite action of the existing and the new concrete, the preparation of the surface of the existing concrete is needed.

The main disadvantages are the drilling of holes in the existing concrete that may weaken the section and the addition of concrete that increases the weight of the member and requires proper bonding to the existing concrete. Another difficulty lies in placing the bars that should be continuous through the beam-column joints (see Figure 3.14b).

In conclusion, concrete jacketing is suitable in case of insufficient lateral strength, deformation capacity and stiffness discontinuity between successive floors ("soft-story" mechanism).

3.3.2.2   Steel Jacketing

Steel jacketing can enhance the global displacement capacity without affecting the strength capacity. Figure 3.15a shows an example of this technique that consists of

a total encasement of the element with thin steel plates placed at a small distance from the column surface, with grouts used for infilling the gap between the steel jacket and the existing member.

Therefore, there is a minimal increase in member size and no stiffness increase. Since the steel plates cannot be anchored to the foundation and cannot be continuous through the floor slab, the steel jacketing cannot be designed for improving the flexural strength and carrying any axial load.

Sometimes it is employed for enhancing the behavior of beams (Figure 3.15b).

(a)   *(b)*
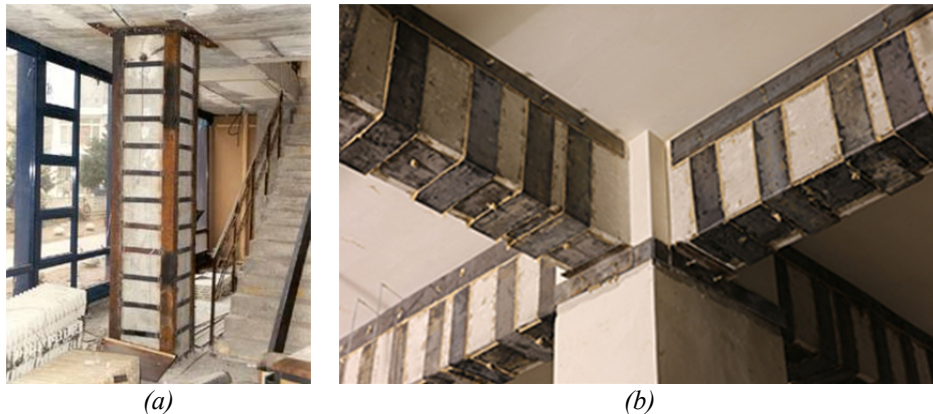
Figure 3.15: Example of steel jacketing of column (a); of beam elements (b)

Steel jacket is effective for enhancing the inadequate shear strength and providing passive confinement of columns which increase the ductility (lateral confining pressure is induced as the concrete expands laterally).

For increasing the deformation capacity in the potential plastic hinge regions, the jacket is usually provided at the top and bottom of the column.

In the case of a rectangular jacket, steel plates are welded to corner angles. However, circular jackets are more effective than rectangular ones because they can be considered equivalent to continuous stirrup reinforcement.

Finally, experienced personnel is required in the execution phase and steel plates need protection against corrosion and fire.

3.3.2.3   Fiber Reinforced Polymer wrapping

Fiber Reinforced Polymer (FRP) wrapping improves mostly deformation capacity of columns and, as consequence, ductility at the structural level. FRP

laminates are sometimes attached also to beams to increase their flexural and shear strengths.

Either complete (Figure 3.16a) or partial (Figure 3.16b) wrapping are generally adopted: the former results in a high increase of ductility and shear strength without significantly modify stiffness, the latter increase only ductility with limited effect on the stiffness and strength.

Choosing the type of fibers, the number of layers, orientation, and thickness it is an engineer's task aimed at achieving the desired level of confinement for a single member without a noticeable increase in size.

The effectiveness of the intervention depends, among the others, on the bond conditions and the available anchorage length. The main drawbacks of FRP are high cost, brittle behavior, and inadequate fire resistance.

(a)   *(b)*

Figure 3.16: Example of complete (a) and partial (b) FRP wrapping of a column

In fact, composites behave in a linear elastic manner without any significant yielding or plastic deformation capacity. Moreover, the wraps are very sensitive to transverse forces and unable to transfer local shear.

Additionally, due to their anisotropic behavior, the large differences in strength and coefficients of thermal expansion can result in bond deterioration and splitting of concrete.

However, the ease of application of FRP composite, the high tensile strength to weight ratio and corrosion resistance renders them attractive for use in structural applications, especially in cases where dead weight, space or time restrictions exist.

3.3.3   Common criteria for selecting an optimal system

Based on what has been described in the Section 3.3.2, it is clear that engineers, asked to design a seismic retrofit intervention, must select the most appropriate technique within a very wide range.

The choice can be anything but simple, taking into account many different criteria according to which, generally, it is necessary to compare the alternative solutions. As a matter of fact, a variety of factors affect such decisions and selections and therefore no general rules apply.

Thermou and Elnashai [96] grouped the selection criteria into two distinct families and provided the following list of possible aspects to consider when comparing different seismic intervention solutions. From an economic and social point of view, the following aspects should be taken into account:

- the cost to be incurred in relation to the importance of the structure;
- the workman-force capacities;
- the duration of the work and the disturbance to normal activities;
- the disturbance to the occupants;
- the achievement of the selected performance objectives;
- the functional and aesthetic compatibility of the intervention;
- the reversibility of the intervention;
- the level of quality control;
- the political and/or historical importance of the structure.

Moreover, the following technical aspects should be considered, as they have an important impact on the selection of the final solution [96]:

- structural compatibility with the pre-existing structural system;
- regularity of stiffness, strength, and ductility;
- adequacy of local stiffness, strength, and ductility;
- protection against non-structural damage;
- capacity of the foundation system;
- availability of materials and technologies necessary for the intervention.

The list of criteria mentioned above is not necessarily to be understood as exhaustive and always valid. Moreover, it may indeed be necessary to add other criteria and, in any case, to take into consideration only those that can actually be discriminating for the final choice.

The retrofit intervention can be characterized in terms of other quantitative/qualitative criteria which can be introduced to assess their actual effectiveness.

For the selection of the best retrofit intervention for an existing building, it seems reasonable to consider a finite number of possible alternatives and to apply, therefore, the discrete Multi-Criteria Decision-Making (MCDM) Method which is a valid support to the decision in multiple and varied real cases [97].

However, MCDM is not aimed at identifying an "optimal" solution in an absolute, rigorously mathematical sense, but rather to draw up a classification of the considered solutions, according to pre-established and discriminating criteria [98][99].

Few studies have been carried out for selecting the most structurally efficient and cost-effective seismic retrofitting solution. A rational procedure was conceptually formulated by Faella et al. [100] with the aim to select the optimal retrofit system in terms of total cost by solving a constrained optimization problem.

The authors took into account two wide classes of strengthening techniques combined with the aim to obtain a synergistic action in increasing the seismic capacity of under-designed members and reducing demand on the whole structure.

4. Engineering application of Soft-Computing: a literature review

In many fields of modern science and technology, such as civil engineering, the solution of problems generally relies on practitioners' "subjective" skills, such as intuitions and past experience, that could be incomplete and imprecise.

A more "objective" approach to the aforementioned problems can be based on Artificial Intelligence (AI) [101], namely *the science and engineering of making intelligent machines*" capable to mimic cognitive functions of human minds, such as "learning", "reasoning" and "problem solving" [102].

Since its first formulations, AI has played an important role because it aims, on the one hand, at exploiting how to help experienced users to enhance the quality of their work and, on the other hand, how to enable inexperienced users to solve real-world problems for most of which conventional algorithmic approaches cannot be formulated.

Over the years, the wide research field of Artificial Intelligence has been subdivided into two broad branches (Figure 4.1): Hard Computing and Soft Computing [103].
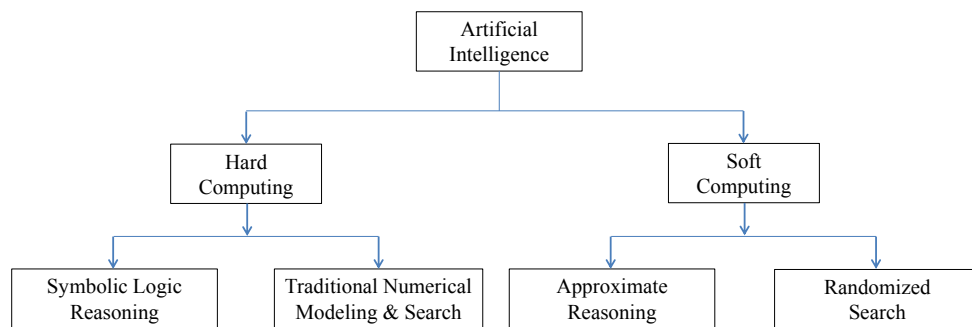
Figure 4.1: Classification of Artificial Intelligence problem-solving techniques [104]

Hard Computing attempts to mimic human intelligence through symbol manipulation and symbolically structured knowledge bases. It mostly involves

methods classified as *machine learning* that makes heavy use of symbolic formalism, logic, and statistics to generate patterns or rules from large datasets [105]. Conversely, the definition of "Soft Computing", introduced by Lotfi Zadeh [103] in 1992, refers to the collection of methodologies that aim at solving problems without an extensive mathematical formulation [106].

Soft Computing is inspired by the reasoning, intuition, consciousness, and wisdom possessed by human beings and it mostly involves iterative developments or learning based on empirical data. The "soft" methods are rather tolerant to imprecision, uncertainty and partial truth in order to return approximated solutions in quick time [106].

However, it is worth highlighting that AI includes also a third category named "Hybrid Computing" which generally refers to the synergistic use of Hard and Soft Computing tools, having their inherent advantages and disadvantages (Figure 4.2). In this way, hybridization encourages users to derive the best advantages from the combined techniques so that the overall algorithm (i.e. the procedure of problem-solving) works more efficiently than the individual components.

Precisely analytical model		Approximate model
Exact algorithms		Clever algorithms (Heuristic)
Huge computational time		Reasonable comput. time
Exact input data	Hard Computing Soft Computing	Ambiguous/noisy input data
Precision and categoricity		Approximation,
Rigidly written programs		Trainable and adaptive
Deterministic		Stochastic
Strictly sequential		Parallel computations
Precise answer		Approximate answer

Figure 4.2: Main differences between Hard-Computing and Soft-Computing

This chapter focuses on Soft Computing techniques that employ a variety of statistical and probabilistic tools to learn from past examples, classify new data, identify new patterns or predict novel trends [107].

Soft Computing is divided into two disciplines: Approximate Reasoning [108] (Figure 4.3) and Randomized Search [109] (Figure 4.4).
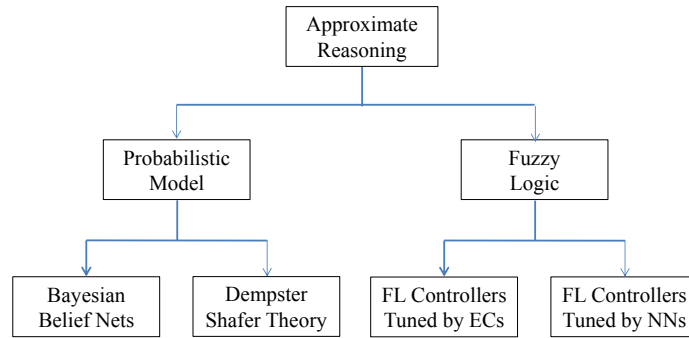
Figure 4.3: Classification of Approximate Reasoning
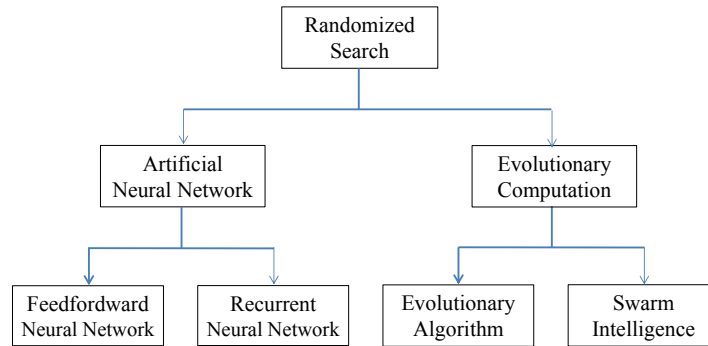
Figure 4.4: Classification of Randomized Search techniques [104]

Approximate Reasoning collects a set of knowledge-driven methods that sacrifice soundness or completeness for a significant speedup of reasoning: it is subdivided into Probabilistic Model and Fuzzy Logic (FL) reasoning systems [110].

Conversely, Randomized Search is a family of numerical optimization methods, such as direct-search, derivative-free, or black-box methods, that work by iteratively moving in the search-space towards better positions which are sampled from a hypersphere surrounding the current position [109].

This class consists of two techniques: Artificial Neural Network (ANN) [111] and Evolutionary Computation (EC) [112]; it does not require gradient information and, hence, it is particularly suitable to be used with objective functions that are not continuous and not differentiable. As a matter of fact, Soft Computing techniques have become promising tools able to provide practice and reasonable solution in different fields [104].

As finding a solution to highly nonlinear and very large-scale problems is often a very challenging task in the civil engineering field, Soft Computing methods are becoming an important class of efficient tools for developing intelligent systems and providing solutions to complex problems in this field. In fact, most of the problems to be addressed by civil engineers are characterized by extensive and undefined aspects leading them to the broader category of unstructured and potentially ill-posed problems that can be consistently formulated only in "soft" terms.

More specifically, this chapter proposes an overview of the recent literature regarding the applications of Soft Computing methods in structural engineering, which is a branch of civil engineering aimed at understanding, predicting and calculating the mechanical response of members and structures [113].

Attention is also given to issues raised within earthquake engineering that is a sub-field of Structural Engineering dealing with the behavior of civil structures subjected to seismic ground motions [114].

Among the first, Chandwani et al. [115] and, later, Fister et al. [116] have already written a short overview of Soft Computing techniques in civil and earthquake engineering, respectively. However, the present chapter does not only aim at updating the aforementioned studies, but it is intended at proposing a consistent critical classification of the main contributions.

As known, the wide domain of general problems arisen in structural engineering can be divided into three broad classes [117]: modeling, simulation, and optimization.

Modeling problems generally deal with describing the mechanical behavior of materials and structures by means of analytical and/or numerically defined relationships capable to portray the consequences of a given load history on a given material or structural elements. The identification of stress-strain relationships, as well as the formulation of consistent yielding for inelastic materials, are among the typical "constitutive" modeling problems.

Simulation problems are the main target of structural analysis procedures, in which both external actions and mechanical properties of structural components are known and the resulting mechanical response/performance of the system, also fulfilling all the assigned constraints, is the main unknown. Seismic analysis of structures, which can be executed by means of a variety of linear or nonlinear methods (read Section 2.2), is a typical example of "simulation" problem.

Optimization generally refers to the inverse procedure aiming to find the best solution for a given problem (e.g. cost optimization, but also optimization of the

structural response in terms of some of their relevant features, such as forces or displacements). Structural optimization problems can be further classified into two sub-classes [118]: synthesis and control problems. On the one hand, synthesis problems aim at optimizing the design of a structural system with the aim to obtain a structural response characterized by a specific feature. On the other hand, control problems aim at determining external actions capable to modify the system response as desired by the designer.

That said, this chapter collects the main contributions published in the scientific literature over the last two decades. It is organized into three main sections devoted to the main classes of Soft Computing techniques. Section 4.1 deals with Fuzzy Logic, Section 4.2 with Artificial Neural Networks and, finally, Section 4.3 covers Evolutionary Computation.

The first part of each section outlines the general theoretical background of the methods under consideration, whereas, the second part summarises the main scientific contributions: for the sake of clarity, the distinction among modeling, simulation, and optimization are retained throughout the three sections.

4.1 Fuzzy logic

Fuzzy-Logic (FL) is a Soft Computing technique based on the definition of "degrees of truth" rather than on the usual "true or false" (1 or 0) Boolean logic of computers. The term "*Fuzzy Logic*" has been introduced in 1965 by Lotfi Zadeh [110] of the University of California at Berkeley, but the idea of a third logic state, called "possible", set against the dual-purpose logic traces the origin up to the Greek philosopher Plato [119].

In the 1960s Zadeh was working on the problem of computers to understand natural language and he observed that unlike computers, whose conventional logic block takes precise input and produces a definite output as "*true*" or "*false*", the approach of FL imitates the way of decision making in human beings, which involves some intermediate possibilities between digital values "*yes*" and "*no*".

Therefore, if 0 and 1 are the extreme cases of the aforementioned "degrees" of truth, FL also includes the various states of partial truth in between ensuring the opportunity to shape conditions of uncertainty.

The ability to treat linguistic variables (like high and low) and making uncertain reasoning, the adaptability for problems without an exact mathematically description, the robustness with respect changing environments and rules [120], make FL fit for solving problems in many fields of sciences and engineering.

4.1.1   Applications of FL in modeling problems

The identification of stress-strain "constitutive" relationships characterizing the mechanical response of materials is a crucial task in structural engineering.

However, analytical approaches are not generally capable to capture the wide set of aspects and parameters that may play a role in controlling the resulting mechanical behavior of materials. Therefore, several FL-based approaches have been recently proposed with the aim to overcome the limits of analytical formulations and, in some cases, take into account heterogeneous uncertainties and heuristic knowledge [121].

Zarandi et al. [122] developed Fuzzy Polynomial Neural Networks (FPNNs), a combination of Fuzzy Neural Networks (FNNs) and Polynomial Neural Networks (PNNs), to predict the compressive strength of concrete mix-design. Six different architectures were constructed, trained and tested by using experimental data obtained from 458 different concrete mixtures.

Doran et al. [123] implemented a FL methodology based on the experimental data set found in the literature, with the aim to model the axial strength of Reinforced Concrete (RC) columns confined by Carbon Fiber Reinforced Polymer (CFRP) strips. Statistical indicators clearly revealed that the proposed prognostic approach produced very smaller deviations with a superior predictive performance compared to the conventional non-linear regression-based method.

Ozbulut and Hurlebaus [124] proposed a neuro-fuzzy model of Nickel-Titanium Shape Memory Alloy (SMA) wires that was capable of capturing the superelastic response at different temperatures and at various loading rates, though remaining simple enough to realize numerical simulations of an isolated bridge provided with dampers made of SMA subjected to seismic excitations.

4.1.2   Applications of FL in simulation problems

Due to the uncertainties involved in structural engineering, the geometrical and mechanical properties defining the structural problem cannot be considered as deterministic quantities. Among the scientific literature, such uncertainties have been often described by following FL-based approaches.

Provenzano and Bontempi [125] demonstrated the suitability of fuzzy variables in the structural analysis to calculate the bounds on mechanical behavior for all possible scenarios.

Savoia [126] used extended fuzzy operations to perform reliability analysis against buckling of a simple structure with geometric and force imperfections. The numerical examples demonstrated that fuzzy number theory can be used to obtain conservative values for lower bounds of buckling limit loads and to estimate the sensitivity of the structural behavior to the uncertainties characterizing the imperfection definition.

Biondini et al. [127] presented a methodological approach for reliability assessment of reinforced and pre-stressed concrete structures. In their study all the uncertainties affecting the geometrical and mechanical properties were modeled by means of a fuzzy criterion: the model was not defined through a set of fixed values, but through bands of values, bounded between the suitable minimum and maximum extremes.

Biondini et al. [128] performed structural reliability assessment of reinforced and pre-stressed concrete frames in the presence of uncertain data in the framework of fuzzy theory, by assuming relevant parameters ranging between a minimum and a maximum value.

Moller et al. [129] introduced the fuzzy probabilistic safety concept and formulated a Fuzzy First Order Reliability Method (FFORM) to analyze the time-varying uncertain safety level and to simulate the uncertain damage process. In their work, the uncertainty of structural models and parameters was appropriately mapped onto safety prognoses.

Marano et al. [130] developed an efficient approach for time-dependent reliability analysis of reinforced concrete beams subject to pitting corrosion, in which non-probabilistic parameters have been treated as fuzzy variables and probabilistic parameters have been mutated into equivalent fuzzy variables. A worked example illustrated the effectiveness and robustness of the proposed approach, useful to support the decision-making in economic analysis and planning of maintenance and reparation interventions.

Dordoni et al. [131] proposed a fuzzy approach for reliability assessment of bridges piers against scouring risks taking into account uncertainties regarding flow, sediments, structural and geotechnical parameters. The obtained results showed how a deterministic approach could disregard variations making the output more severe with respect to structural safety.

Nieto-Morote and Ruz-Vila [132] presented a risk assessment methodology based on the Analytic Hierarchy Process (AHP) and on the FL. The proposed methodology incorporated knowledge and experience acquired from many experts

and also the subjective judgments of the parameters expressed by fuzzy numbers to assess the overall risk factor: risk impact, risk probability, and risk discrimination.

Sobhani and Ramezanianpour [133] developed a soft computing system to estimate the service life of reinforced concrete bridge decks. The proposed system utilized fuzzy interfaces to quantify the exposure condition, required cover thickness, corrosion current density and pitting corrosion ratio.

Darain et al. [134] presented a model inspired to the FL approach and intended at predicting the serviceability performance of RC beams strengthened with near surface mounted FRP reinforcements. Specifically, load and bonded length were used as input parameters, whereas deflection and crack widths were assumed as output quantities. The proposed model showed excellent agreement with the experimental results.

4.1.3 Applications of FL in optimization problems

Since the beginning of the years 2000, the Fuzzy Logic Control (FLC) theory has attracted the attention of engineers interested in controlling the response of structures under seismic actions [135].

Zhou et al. [136] successfully applied an adaptive FLC strategy for controlling linear and nonlinear structural behaviour. The authors found that the adaptive feature of a fuzzy controller has various advantages in the control of a building including magneto-rheological (MR) damper systems.

Kim et al. [137] proposed a multi-input, single-output (MISO) semi-active fuzzy controller for vibration control of seismically excited small-scale buildings. Numerical examples demonstrated that the proposed method was effective to control seismically excited responses of a building structure employing MR dampers.

Guclu and Yazici [138] designed FL and Proportional-Derivative (PD) controllers for a Multi-Degree of Freedom (MDOF) structure with Active Tuned Mass Damper (ATMD) with the aim to control and reduce earthquake-induced vibrations. The results showed a good performance by the FLCs for different loads and the earthquakes.

Ozbulut and Hurlebaus [139] proposed two FLCs for operating control force of piezoelectric friction dampers used for seismic protection of base-isolated buildings against various types of earthquake excitations. For several historical ground motions, the results showed that the developed FLCs could effectively reduce isolation system deformations.

Meng et al. [140] presented a fuzzy control arithmetic based on mode identification used in the semi-active control. The control efficiency of the proposed control arithmetic compared with other control strategy was investigated by numerical simulation.

Zoric et al [141] dealt with active free vibrations control of smart cantilever composite beams. The authors proposed an integration of self-tuning method, where scaling factors of the input variables in the fuzzy logic controller were adjusted via peak observer, with optimization of membership functions using the particle swarm optimization algorithm.

The development of a FL control system has been sometimes obtained in combination with Genetic Algorithms (GA): the latter will be treated into details in Section 4.3.2.1.

Pourzeynali et al. [142] proposed a combination between the GAs and FLC, named Genetic Adaptive Fuzzy Controller (GAFC), intended to design and optimize the different parameters of semi-active MR dampers placed between adjacent buildings with the aim to reduce undesirable vibrations and structural pounding effects.

Uz et Hadi [143] proposed an optimal design strategy based on GA and an integrated fuzzy controller for nonlinear hysteretic devices intended at preventing pounding damage and achieving the best results in seismic response mitigation of two adjacent structures. The fuzzy controller was used in order to provide the interactive relationships between damper forces and input voltages for MR dampers.

Song et al. [144] designed a FLC based on a GA intended to perform numerical simulation and experiments for a complex floating raft active vibration isolation system. Specifically, the fuzzy control was able to provide an intelligent path for the active control while the GA was adopted in order to simultaneously optimize the quantization, scale factors and control rules. The results showed that the fuzzy controller based on GA outperformed the conventional FLC in terms of vibration suppression effect.

Finally, Rosko [145] dealt with the optimal topology design of the structure in order to eliminate the danger of the resonance vibration. The uncertainty of the loading was defined with the help of fuzzy loading and special fuzzy constraint was created from exciting frequencies.

4.2   Artificial Neural Networks

Artificial Neural Networks (ANNs) are computational data-driven methods based on the idea to mimic the learning and memory capability of the human brain. They were first introduced by McCelloch et al. [146] in the mid 40's of the last century.

More recently, Haykin [147] described a neural network as a massively parallel distributed processor made up of simple processing units called "*nodes*", like neurons of the human brain.

These densely interconnected nodes operate in parallel and exchange messages between each other. Each connection is characterized by a number that controls the transfer of signals between the two nodes called "*synaptic weight*".

These number can be tuned on the basis of experience, making the neural networks adaptive to inputs and capable of learning key elements of a neural network. Such learning ability is attributed to the adjustment in the architecture of inter-neuron connection or the synaptic weight values.

The weights are adjusted until an acceptable output: in case of either poor output or errors, then the system updates the weights in order to improve subsequent results, otherwise, there is no need to adjust the weights. ANNs can be classified into two major categories (Figure 3): Feed-Forward Neural Networks (FFNN) [148] and Recurrent Neural Networks (RNN) [149].

In FFNN the information moves in only one direction, forward, from the input nodes, through the hidden nodes, and to the output nodes. Conversely, the connections between nodes in RNN form a loop in the architecture of the network.

Although the ANNs are "black box" methods with limited ability to identify possible causal relationships and add data to the existing network, they show great ability to capture unknown or complex nonlinear relationships between independent/dependent variables and adaptability to changing input-output data pairs. For a long time, the theory of ANNs remained out of interest in applied sciences and engineering, but over the last decade, ANNs have emerged as a powerful tool that could be used to replace time-consuming procedures in various branches of those disciplines.

Some of the fields where ANNs have been successfully applied are pattern recognition, decision making, regression (function approximation/fitting) and optimization.

4.2.1   Applications of ANN in modeling problems

The mathematical relationships commonly used to describe the material behavior are available in the form of empirical formulae derived from experimental results.

Although these empirical relationships in the form of regression equations are widely used, they cannot be yet applied wherein the modeling problem involves a large number of independent variables and the relationships are too complex to be captured by sufficiently compact analytical expressions. In such cases, the traditional regression technique fails to yield the expected accuracy and predictability.

However, ANN can address problems whose solutions require prior knowledge which can be explicitly derived from historical data or experimental observations. Due to its peculiar characteristics, ANN has made the complex problems of modeling much easier than most empirical and statistical methods already in practice.

As matter of fact, in the scientific literature there are successful implementations in predicting and modeling compressive strength of concrete mixtures [150], FRP confined concrete [151], rubberized concrete [152], self-compacting concrete [153], recycled aggregate concrete [154], drying shrinkage of concrete [155].

Ni and Wang [156] used neural networks to predict the 28-day compressive strength of concrete using Multilayer Feed-forward Neural Networks (MFNNs) with the purpose to overcome the inadequacy of other methods when dealing with multiple variable and nonlinear problems. The results demonstrated that this computational intelligent method could be practical and beneficial for civil engineers, technologists and concrete mixture designers to predict with high accuracy the concrete strength.

Oreta and Kawashima [157] explored the capability of ANN to predict the compressive strength and corresponding strain of circular concrete columns. The ANN-based model was compared to some analytical models and was found to produce reasonable results limited to the range of values used in the training database.

Gupta et al. [158] used ANN for accurate prediction of concrete strength based on several parameters like concrete mix design, size, and shape of the specimen, curing technique and period, environmental conditions, etc. The back propagation-learning algorithm was employed to train the network and to extract knowledge

from training examples (concrete specimens casted for compressive strength measurement).

Ozturan et al. [159] used ANN for predicting the 28-day strength of ready-mixed concretes having low to medium strength. The accuracies of prediction by ANN and multiple linear regression (MLR) models were compared on the basis of the coefficient of determination. The results showed that the best results were obtained by the ANN models using data for the fresh concrete and early strength simultaneously.

Aggarwal and Aggarwal [160] presented the comparative performance of models developed to predict 28-day compressive strengths of self-compacting concrete using ANN techniques for data taken from literature and data developed experimentally.

Pham and Hadi [161] proposed the use of ANNs to estimate the compressive strength and strain of FRP–confined square/rectangular columns with better accuracy than the existing conventional methods.

Nikoo et al. [162] predicted the compressive strength of concrete by using an ANN model where the number of layers, the nodes, and the weights were optimized by using GA. The results verified that the recommended ANN model had more flexibility, capability, and accuracy in predicting the compressive strength of concrete compared with MLR model.

In the scientific literature, there are successful applications of ANN also for predicting elastic modulus of normal and high strength concrete [163], the durability of high-performance concrete [164].

Chandwani et al. [165], whereas, explored the usefulness of hybridizing ANN and GA for modeling slump of ready-mix concrete. The trained hybrid model based on past experimental data was used for predicting slump of concrete in quick time, without performing multiple trials with different design mix proportions. The study showed that by hybridizing ANN with GA, the convergence speed of ANN and its accuracy of prediction were improved.

Likewise, in the scientific literature, there are also successful implementations of ANN in predicting and modeling shear, bending and torsional strength.

Sanad and Saka [166] used ANN to predict the ultimate shear strength of RC deep beams. The result of the ANN was compared with various empirical relationships and proved that ANNs provided a good prediction of shear strength.

Cladera and Mari [167][168] developed an ANN model to predict the shear strength of reinforced concrete beams without and with web reinforcement. A

parametric study was carried out to determine the influence of each parameter affecting the shear strength and to propose new design formula.

Lee and Lee [169] presented a theoretical model based on an ANN for predicting shear strength of slender FRP reinforced concrete flexural members without stirrups. Comparisons between the predicted values and the test data showed that the developed ANN model resulted in improved statistical parameters with better accuracy than other existing equations empirically developed for a limited number of influential parameters.

Pendharkar et al. [170] presented a ANN-based methodology aimed at quickly predicting the ultimate bending capacity of composite beams taking into account both instantaneous cracking and time effects in continuous composite beams. The models were validated for four example beams and the errors were shown to be small.

Bagci [171] used ANN to predict the moment-curvature relationship of reinforced concrete governed by a large number of variables and non-linear material behavior. A multilayer, backpropagation and feed-forward algorithm were used to train the data. The authors demonstrated that, on the one hand, ANN algorithms were not able to replace the conventional analytical techniques completely since they need some key values for training and, on the other hand, they can be implemented as an efficient supplementary tool to drastically reduce the computational cost.

Erdem [172] investigated the application of neural networks for predicting the ultimate moment capacity of RC slabs in fire. The moment capacities predicted by ANN were very accurate within the range of input parameters and in line with the results provided by the ultimate moment capacity equation.

Jasim and Mohammed [173] used ANNs for predicting the ultimate torsional strength of spandrel beams. To this end, they compared the results obtained by a resilient backpropagation training algorithm with those obtained by the steepest descent algorithm.

Ghaboussi and Elnashai [174] proposed ANN for modeling complex behavior of beam-column connections. A neural-network-based inelastic hysteretic model was combined with a new component-based model under self-learning simulation framework that used the structural response to learn the cyclic behavior of the beam-column connection and extract material models.

Alacali et al. [175] presented an application of ANN capable of providing accurate estimates of lateral confinement coefficient in concrete columns by using six design parameters. The accuracy of the confinement coefficient was proved to

depend strongly on the data provided to the neural network as well as the number of input variables and the number of examples available for testing.

Jakubek [176] demonstrated that the application of a properly trained neural network could provide a useful surrogate model for predicting load capacity for eccentrically loaded reinforced concrete columns.

Asteris et al. [177] used ANNs to predict the fundamental period of infilled RC structures. The comparison of the predicted values with analytical ones indicated the potential of using ANNs for the prediction of the fundamental period taking into account the crucial parameters that influence its value.

Chou et al. [178] used several advanced artificial intelligence techniques, among which ANNs, to predict pitting corrosion risk of steel reinforced concrete and marine corrosion rate of carbon steel. The findings of this study provided civil engineers with a promising and practical methodology for tracking of steel corrosion and scheduling the maintenance processes.

4.2.2 Applications of ANN in simulation problems

ANNs have been used for probabilistic reliability analysis of structures [179][180]. In particular, Rogers [181] developed guidelines aimed at designing and training an inexpensive neural network to simulate a slow, computationally expensive structural analysis of the large degree of freedom systems.

Tsompanakis et al. [182] presented applications of ANNs in computationally demanding tasks, such as parameter identification and probabilistic seismic analysis of structures. On the one hand, they used ANN based meta-models in order to replace the time-consuming repeated structural analyses. On the other hand, for inverse and parameter identification problems they proposed the direct use of ANNs for the approximation of the inverse structural mapping.

Arslan [183] evaluated the effective design parameters and earthquake performance of RC buildings using ANN models.

ANNs have been used also for structural damage assessment [184][185]. For instance, Parhi and Dash [186] analyzed the dynamic behavior of a beam structure containing multiple transverse cracks using neural network controller. From the comparison with the output of the theoretical, finite-element and experimental analysis it was observed that the developed method could be used as a crack diagnostic tool in the domain of dynamically vibrating structures.

Li et al. [187] presented a non-destructive global, vibration-based damage identification method that employed damage pattern changes in frequency response functions FRFs and artificial neural networks ANNs to identify defects.

Meruane and Mahu [188] developed a real-time damage assessment algorithm using ANN and anti-resonant frequencies capable of detecting, locating and quantifying structural damage in a short period of time. In two experimental cases, the algorithm was successful in assessing the damage that corresponded closely with the experimental damage in all cases.

Hakim et al. [189] developed a faster and more accurate method for predicting the extension and location of damage for I-beam structures using ANN instead of visual inspection which is constrained by the availability of qualified personnel.

Arangio and Bontempi [190] proposed a Bayesian neural networks with the aim to formulate a multilevel strategy for monitoring the integrity of long-span bridges subjected to environmental actions: in the first level the occurrence of damage was detected; at a subsequent level the specific damaged element was identified and the intensity of damage was quantified.

The same authors [191] proposed a Bayesian neural network procedure able to detect anomalies in the behavior of the structures, which can be related to the presence of damage. The dataset employed to test the proposed approach included vibration data of a bridge before and after the damage. The authors validated the method by comparing the results with those obtained by using a traditional approach for vibration-based structural identification.

4.2.3   Applications of ANN in optimization problems

As noted in the previous sections, ANN-based procedures are often adopted in modeling and simulation as they can be more time-efficient than "mechanistic" approaches.

Obtaining optimal solutions typically requires numerous iterations involving analysis and optimization programs. This process becomes prohibitive due to the amount of computer time required for convergence to an optimum solution.

Hence, the higher efficiency of ANN is often the motivation to employ them as part of general optimization procedures requiring that a huge number of simulations are executed.

As a matter of fact, ANN algorithms have been also used in the context of optimal structural design [192][193]. Park and Adeli [194] developed a neural

model, called "neural dynamics model", whose topology consisted of variable layer and constraint layer, for the optimum plastic design of low-rise steel frames.

Mukherjee and Deshpande [195] developed an ANN to predict initial design of reinforced-concrete rectangular single-span beams (i.e., tensile reinforcement required, depth of the beam, width, cost per meter and the moment capacity) for a given set of input parameters (i.e., span, dead load, live load, concrete grade, and steel type).

Yeh [196] described a method, based on ANN and nonlinear programming, for optimizing high-performance concrete mix for a given workability and compressive strength. The proposed methodology provided a guideline to select appropriate materials and mix proportions as a starting trial batch of high-performance concrete and reduce the number of trial mixes required.

Hadi [197] found the optimum design of simply supported concrete beams and reinforced fibrous concrete beams through an ANN able to extract significant information from a massive set of data and cope with ill-defined problems. Based on the applications, the author proved the effectiveness of ANNs compared to conventional design techniques in terms of CPU requirements. Moreover, they demonstrated that the uncertainty of outputs can be reduced, and hence the robustness of ANNs can be improved, by adjusting learning rate and reducing error goal. ANN-based procedures have been often adopted in minimizing the weight of the structure.

Hajela and Berke [198] presented an overview of the neural computing approaches to structural analysis and design. Special features of such learning strategies, which have a direct influence on numerical accuracy and efficiency, were examined in the context of representative structural optimization problems, such as the weight optimization of a truss.

Papadrakakis and Lagaros [199] examined the application of ANN for reliability-based structural optimization of large-scale structural systems to substantially reduce the required computational effort. The use of ANN was aimed, on the one hand, at reaching an optimized design with controlled safety margins with regard to various model uncertainties, and, on the other hand, at minimizing the weight of the structure.

Cost optimization of single and multiple spans reinforced concrete slabs with various boundary conditions subjected to all constraints was presented by Ahmadkhanlou and Adeli [200]. The problem was formulated as a mixed integer-discrete variable optimization problem with three design variables: thickness of the slab, steel bar diameter, and bar spacing. The algorithm based on the neural

dynamic model of Park and Adeli [194] had excellent convergence properties towards the optimum cost solutions.

Papadrakakis et al. [201] examined two methodologies that combined Evolution Strategies and Neural Networks (ES–NN) for a multi-criteria optimization problem aimed at minimizing both the weight of a steel structure and the variance of the structural response. Specifically, in the first part of the study, they used NN as a valuable tool to predict the response of the structure in terms of deterministic/probabilistic constraint and replace the time-consuming repeated analyses in Reliability-Based Design Optimization (RBDO) of large-scale structural systems.

In the scientific literature, ANNs have been successfully applied also for controlling linear and nonlinear structural behavior. For instance, Cho et al. [202] developed an ANN to control the nonlinear response of bridge systems in randomly generated earthquake excitation.

Gu et al. [203] presented numerical studies of linear and nonlinear MDoF structural vibration control based on the approach of the back-propagation algorithm to the Diagonal Recurrent Neural Network (DRNN) control method.

Benchmark and Narasimhan [204] presented a direct adaptive control scheme for the active control of a nonlinear highway bridge benchmark. The control force was calculated by using a single hidden layer nonlinearly parameterized ANN in conjunction with a proportional-derivative type controller. The results showed that the proposed controller scheme could achieve good response reduction in the structure, without the need for the exact description of the nonlinearities, or extensive structural system information.

Laflamme and Connor [205] proposed an adaptive neural network composed of Gaussian radial functions for mapping the behavior of civil structures controlled with MR dampers. The proposed controller was tested by considering several types of ground motions as input action.

Wang and Adeli [206] proposed an adaptive control algorithm for nonlinear vibration control of large structures subjected to dynamic loading through the integration of a Self-Constructing Wavelet Neural Network (SCWNN) with an adaptive fuzzy sliding mode control approach characterized by a good adaptive ability to the changes of structural parameters and external dynamic loading. Specifically, the model was developed for the functional approximation of the nonlinear behavior of large structures whereas a fuzzy compensator was developed to incorporate system uncertainty and to reduce the chattering problem.

Abdeljaber et al. [207] developed an ANN to control the optimal voltage signal applied on the piezoelectric sensor/actuator pairs for active control of plates. The ANN controller was trained based on an algorithm that incorporated a set of emulator neural networks which were also trained to predict the future response of the cantilever plate. By comparing the uncontrolled and controlled responses, the neuro controller was proved to be successful in mitigating the accelerations of the flexible cantilever plate under various types of dynamic excitations.

4.3   Evolutionary Computation

Evolutionary Computation (EC) is a wide family of metaheuristic bio-inspired algorithms with a stochastic nature.

The idea that the evolution could be used as a "metaphor" for problem-solving was already suggested by Alan Turing in a technical report in 1948 [208], although this branch saw a significant development only after the 1970's, as computational devices and computers became more available to the scientific community [209].

The essence of an evolutionary approach is to regard candidate solutions of a generic problem as "*individuals*" of a set called "*population*" and to introduce the notion of "*fitness*" as a formal measure of perceived performance (or quality) of the individual with respect to the optimization objective [210]. Hence, EC can be understood as a group of population-based problem-solvers in which a population of individuals undergoes an iterative process of gradual changes and evolves to achieve the desired optimization objective.

The evolutionary process depends on the fitness of the individual solutions as defined by the environment (objective function). The entire searching process is called "*evolution*" and goes on until a convergence criterion is met [211].

In the last decades EC, which most notably divides into Swarm Intelligence (SI) [212] and Evolutionary Algorithms (EA) [112], has proven to be highly successful for a wide range of engineering problems, such as optimization, machine learning, automatic design and modeling [213].

More specifically, EC is particularly suitable for parallel implementation: this means that the search method is parallel, i.e. several individuals can be examined at the same time, encouraging the users to choose the best solution from a pool of multiple alternatives. However, EC has been mainly applied as an effective method for solving complex optimization problems as consequence of deficiencies of formal conventional methods.

It is worth to mention that the structural optimization problems are typically divided into three categories sometimes combined in the same process [214]: Topological Optimization, Sizing Optimization and Shape Optimization.

Topology Optimization (TO) aims at optimizing material layout within a given design space, for a given set of loads, boundary conditions and with the best possible performance of the system.

Shape Optimization (SO) deals with optimizing the overall shape, or the contour of a structural system whose topology is fixed.

Sizing Optimization is aimed at optimizing geometrical parameters, such as length, width or thickness of elements of a structural system whose topology and shape are fixed.

State of the art (SOTA) in traditional mathematical approaches to continuum shape optimization problems were firstly presented in [215][216]. Instead, SOTA reviews of current research in formal methods for topology optimization design problems can be found in the work of Bendsoe Sigmund [217].

4.3.1   Swarm Intelligence

Swarm Intelligence (SI) is a family of population-based metaheuristic algorithms that takes inspiration from the collective behaviors of insects, such as ants, termites, bees, wasps and other animals able to perform some inherent social actions.

For instance, ants are characterized by a decentralized way of working in the group while searching for food. The communication between them is carried out indirectly by a chemical substance called "*pheromone*" whose amount determines the shortest path to food.

The expression "*Swarm Intelligence*" was introduced by Gerardo Beni and Jing Wang in 1989, in the context of cellular robotic systems [218]. SI simulates a population of simple individuals called "*particles*" which evolve by interacting with each other and with the external environment.

The population of particles flies across the search space. Specifically, each particle moves towards the position of the best particle and thereby discovers a new possible more promising region of the search space. The position is evaluated with the fitness function that reflects the nature of the problem.

The algorithms included in SI domain are: Particle Swarm Optimization (PSO) [219], Artificial Bee Colony (ABC) [220], Firefly Algorithm (FA) [221][222], Harmony Search (HS) [223] and Ant Colony Optimization (ACO) [224]. Among them, PSO is the most common algorithm.

4.3.1.1   Particle Swarm Optimization

Particle Swarm Optimization (PSO) algorithm was originally proposed in 1995 by Kennedy and Eberhart [219] to imitate system where multiple candidate solutions coexist and collaborate simultaneously.

PSO is a population-based global optimization technique that enables an initial random population of particles to iteratively move through a hyperdimensional

space to search for the optimal solution. A communication structure is also defined, assigning neighbors for each individual particle to interact with them.

The particles iteratively evaluate the fitness of the candidate solutions and remember the location where they have had their best success, called the "*local best particle*". Each particle makes this information available to their neighbors. Each particle is also able to see where their neighbors have had success.

The position of each particle is influenced by the best position visited by itself and its own neighborhood, i.e. by the experience of the local best particle and neighboring particles. When the neighborhood of a particle is the entire swarm, the best position in the neighborhood is referred to as the "*global best particle*" and the resulting algorithm is referred to as the *gbest-PSO*.

When smaller neighborhoods are used, the algorithm is generally referred to as the *lbest-PSO*. Each particle in the swarm has an updating position vector and updating velocity vector which is adjusted over the iterations by learning from a local best found (by the particle itself) and a current global best found (by the whole swarm). Poli et al. [225] propose an extensive review of successful applications of the PSO method.

4.3.1.1.1   Applications of PSO in modeling problems

In the present literature review, only two applications of PSO method has been found for modeling problems, i.e. parameters identification.

Quaranta et al. [226] evaluated the performances of PSO algorithms for the parameters identification of Van der Pol-Duffing non-linear oscillators. The results showed that the investigated soft computing techniques behave very well.

The same authors [227] demonstrated that PSO and differential evolution can be effectively exploited for the parametric identification from experimental dynamic tests of the Bouc-Wen model parameters considered to simulate the hysteretic response of seismic isolators.

4.3.1.1.2   Applications of PSO in simulation problems

The relative simplicity, the fast convergence rate, the limited number of parameters to be adjusted and the population-based feature [228] have made PSO a high competitor in solving multi-objective problems when compared to other methods.

Perera et al. [229] developed a multi-objective model updating method, solved by an extension of the PSO method, integrated into the context of structural health

monitoring and based on strain measurements under controlled loading, essential to prevent intermediate crack-induced (IC) debonding of the FRP substrate from the concrete.

Zhang et al. [230] proposed a methodology for crack modeling, modal analysis and crack database construction based on multivariable wavelet finite element method and PSO where the measured modal parameters and the analyzed cracked vibration database were taken as input for PSO to achieve intelligent quantitative identification.

Chatterjee et al. [231] proposed a PSO trained neural network (NN-PSO) capable of predicting structural failure of multi-story RC buildings via detecting the failure possibility. Specifically, the PSO was employed to find an optimal weight vector with minimum root-mean-square error (RMSE) for the NN classifier. The experimental results established the superiority of the proposed NN-PSO compared to the traditionally well-known models based on neural networks.

4.3.1.1.3 Applications of PSO in optimization problems

PSO has shown promising performance on many complex problems and has proven to be a valuable tool for obtaining approximate solutions to optimization problems in a reasonable amount of computation time.

Pereza and Behdinan [232] implemented a PSO algorithm suitable for constrained structural optimization tasks. In their work improvements, the effect of the different setting parameters, and functionality of the algorithm were shown.

Salajegheh et al. [233] proposed a hybrid Radial Basis Function-Binary Particle Swarm Optimization (RBF-BPSO) method to achieve fast optimization with high computational performance. In particular, the BPSO was used to find the optimum design.

Plevris and Papadrakakis [234] presented an enhanced PSO algorithm combined with a gradient-based quasi-Newton sequential quadratic programming (SQP) method for handling structural optimization problems. The proposed PSO explored the design space thoroughly and detected the neighbourhood of the global optimum.

Behbahan [235] replaced the conventional trial and error design process of RC structures under gravity or earthquake loads and assigned standards constraints, with an automated process based on PSO algorithm that included both the economic and practical aspects. The entire process was summarized in a computer programming using a link between MATLAB platform and the open source object-

oriented software OpenSEES. PSO have been sometimes used also to minimize the weight of the structure.

Gholizadeh and Salajegheh [236] proposed a meta-modeling PSO-based framework that reduces the computational effort required to find the optimum weight of a plane steel shear frame.

Gholizadeh and Moghadas [237] proposed an Improved Quantum Particle-Swarm Optimization (IQPSO) metaheuristic algorithm to minimize the structural weight of steel frames subjected to performance constraints on inter-story drift ratios at the immediate occupancy, life safety, and collapse prevention performance levels. Moreover, a high number of applications exist in the scientific literature regarding optimization of truss structures.

Fourie and Groenwold [238][239] were the first to successfully apply PSO method in the optimal shape and size design of truss structures. After that, other variations of the algorithm have been proposed and implemented for structural optimization [240][241].

PSO method was employed for the reliability-based optimal design of statically determinate truss structures [242] where the design variables to be optimize were, on the one hand, the cross-sectional areas of the groups which controlled the size of the truss and, on the other hand, the heights and lengths which controlled the shape.

Kaveh and Talatahari [243] combined a particle swarm optimizer with the passive congregation (PSOPC), ant colony optimization (ACO) and harmony search scheme (HS) to reach to an efficient algorithm, called discrete heuristic particle swarm ant colony optimization (DHPSACO) employed to optimize truss structures with discrete variables. In particular, the DHPSACO applied a PSOPC for global optimization and the ant colony approach as an auxiliary tool to improve local search.

De Oliveira and Gomes [244] investigated the use of a PSO algorithm as an optimization engine in structural truss mass optimization on size and shape, taking into account frequency constraints. To deal with such highly non-linear dynamic optimization problem, the PSO algorithm was chosen instead of other gradient-based methods.

Zeng et al. [245] presented a hybrid optimization algorithm, named Particle Swarm-Group Search Optimization (PS-GSO) algorithm for the optimal design of spatial truss structures with discrete variables. Felkner et al. [246] explored the potential of interactive optimization framework based on PSO for the architectural design of truss tower structures based on aesthetic criteria.

Kaveh and Javadi [247] performed size and shape optimization of truss structures using an efficient hybrid combination Harmony Search [223] Particle Swarm Optimization (HR-PSO) in which PSO acted as the main engine, while additional Harmony Search improved the local search ability for a better exploitation. Results showed that the proposed algorithm outperformed the previously developed mathematical and heuristic algorithms.

PSO algorithm has been often adopted for obtaining the optimal parameters of damper devices and for the optimal control of the vibrating system.

Leung et al. [248] applied PSO algorithm to obtain the optimum parameters (including the optimum mass ratio, damper damping, and tuning frequency) of the Tuned Mass Damper (TMD) system attached to a viscously damped Single-Degree-of-Freedom (SDoF) main system subject to non-stationary excitation.

Shayeghi et al. [249] applied the PSO to design and optimize the parameters of the TMD control scheme for achieving the best results in the reduction of building response under earthquake excitations.

Ali and Ramaswamy [250] presented an optimal FLC algorithm for a better vibration mitigation of buildings under earthquake excitations using magneto-rheological (MR) dampers. The voltage monitoring of MR damper was accomplished using the evolutionary fuzzy system, while the FLC parameters were optimized using PSO.

Schmidt [251] analyzed the design of an active control system as a minimization problem of the building stories' acceleration solved by a modified PSO method.

Marinaki et al. [252] proposed a PSO for the optimal design of the free parameters in active fuzzy control systems. The results of numerical applications on smart piezo-elastic beams were very efficient for a sinusoidal loading pressure using the fuzzy control system optimized by PSO.

Raju et al. [253] proposed PSO for the active vibration control of piezo-actuated flexible beam. The numerical simulation showed that sufficient vibration suppression can be achieved by means of these methods.

Successful applications of GA are currently available in the literature regarding the optimization of strength and stiffness properties.

Sorkhabi et al. [254] used PSO to obtain the optimization process of honeycomb beams with higher strength and lower cost. Loja [255] studied the use of PSO technique to maximize bending stiffness of a functionally graded material (FGM) thin sandwich beam without violating the mass constraint.

4.3.2   Evolutionary Algorithms

Evolutionary Algorithms (EAs) are population-based metaheuristic (or stochastic heuristic) algorithms that simulate Darwin's theory of evolution [256] based on the "survival of the strongest" principle.

As already seen for EC, candidate solutions play the role of individuals in a population, while a fitness function determines the quality of the solutions. Starting from a random population of strings, EA generates successive populations using mechanisms inspired by biological evolution like reproduction, crossover, and mutation operators that refine the search and help the algorithm to bring forth the best candidate solutions satisfying the objective.

More specifically, reproduction is the process by which individual are copied according to the fitness function value: those individuals characterized by a higher value of fitness have a higher probability of contributing to one or more descendants (called "offspring") in the next generation. The crossover mechanism allows mixing of parental information while passing it to their offspring.

Mutation is an occasional random and partial alteration of the string needed to introduce innovation into population because occasionally some potentially useful genetic material could be lost.

The evaluation of objective function and the application of evolutionary operators are repeated until the so-called "termination criterion" is satisfied. Usual these criteria are the number of population, small or no change in the best fitness, or reaching a close approximation of the optimum.

However, the various EAs have different capabilities and the choice of the most appropriate algorithm depends on the type and characteristics of the problems concerned. The variety of EAs share a common set of underlying assumptions but can differ in data type, breeding strategy to be used and genetic representation of individuals.

The similar techniques are: Genetic Algorithms (GAs) [257], Evolution Strategies (ES) [258], Evolutionary Programming (EP) [259], Genetic Programming (GP) [260] and Differential Evolution (DE) [261]. So far, the first one has been the most used one.

4.3.2.1   Genetic Algorithms

Genetic Algorithms (GAs) [257] is the most applied evolutionary algorithm. According to the definition of Koza [260], "*the genetic algorithm is a highly parallel mathematical algorithm that transforms a solutions set, each with an*

associated fitness value, into a new population using operations patterned after the Darwinian principle of reproduction and survival of the fittest and after naturally occurring genetic operations", GAs were developed to simulate some of the biological mechanisms observed in natural evolution operating on chromosomes (organic devices for encoding the structure of living being).

As a matter of fact, GAs encode a potential solution to a specific problem on a simple chromosome-like data structure, a chain of concatenated variables that describe each solution. Basic assumptions include population size, selection strategy, crossover type and the probability of mutation.

By varying these parameters and strategies, the convergence of the algorithm may be altered. Therefore, it is important to tune appropriate values for these parameters in order to maintain the robustness of the algorithm.

Due to their ability to explore/exploit the solution space, their possibility to take into account constraints to the solution space using the penalty function and thanks to their ability to deal with mixed variables and arbitrary nature of constraints and objectives, GAs are particularly suitable for a wide variety of optimization problems.

In fact, in the case of multi-objective optimization and scheduling problems for which more than one individual solution is admitted, the GA is potentially useful in identifying these alternative solutions simultaneously.

It is worth reminding that the GA provides a number of potential solutions to a given problem and the final choice is left to the user.

4.3.2.1.1   Applications of GA in modeling problems

In the present literature review, three applications of GA have been found for identification problems.

Marano et al. [262] proposed a modified real-coded GA to identify two shear-type mechanical systems subject to the dynamic loads, assuming as unknown parameters the mass, the stiffness, and the damping coefficients. The algorithm included an operator based on the auto-adaptive asexual reproduction of the best individual in order to avoid a long stagnation at the start of the evolutionary process due to insufficient exploration and to attempt an improved local exploration around the current best solution.

Chisari et at. [263] successfully applied a GA for identification problem applied to base-isolated, post-tensioned concrete bridge. In their work, inverse techniques were based on in-situ test measurements obtained under static and dynamic loading

conditions. They proved that the main advantage deriving from the use of inverse approaches based on GAs typically was in the possibility to estimate a greater number of material parameters (e.g. properties of concrete, the stiffness of the bearing isolators, etc.).

Chisari et al. [264] proposed a novel method based on GA for optimal sensor placement in structural identification problems. Two numerical applications confirmed that the proposed method could be effective in decreasing the instability of the parameter identification process.

Chisari et al. [265] presented a multi-objective optimization framework based on GA for calibrating relevant parameters in cyclic models of steel members suffering local buckling. With the purpose to overcome the traditional calibration (based on matching the experimental and numerical cyclic responses under loading protocols), they critically discussed a procedure based on the minimization of response misfit thanks to the capability of GA.

4.3.2.1.2   Applications of GA in simulation problems

In the Authors' best knowledge, GA has been applied in three relevant cases for simulation problem in structural engineering.

Sgambi et al. [266] proposed a method based on the combined application of GA and a FE Method aiming at the serviceability assessment of long-span suspension bridge. The stochastic exploration of the load scenarios space was formulated by mean of GA able to get trustworthy evaluations of such important design parameter.

Cha and Buyukoztutk [267] proposed a novel approach based on hybrid multi-objective GA optimization algorithms and Modal Strain Energy (MSE) to detect the exact locations and extents of the induced minor damages in various three-dimensional steel structures.

Silva et al. [268] proposed an unsupervised and nonparametric Genetic Algorithm for Decision Boundary Analysis (GADBA) to support the structural damage detection process in bridges, also considering the effects of environmental and operational actions.

4.3.2.1.3   Applications of GA in optimization problem

Goldberg and Samtani [269] were the first to use GA for structural optimization by taking the example of a 10-bar plane truss.

Rajeev and Krishnamoorthy [270] used a simple GA for optimizing structural systems with discrete design variables, such as a three-bar truss. In their work, a

penalty-based method was used to transform the constrained problem into an unconstrained one.

Azid et al. [271] applied a GA with real-valued representations to optimize topologies (the layout) of three-dimensional trusses without setting up a pre-restricted topology prior to the optimization process. It was found that there was a saving in weight in the optimized structure.

Woon et al. [272] investigated alternative encodings of GAs for continuum shape optimization, based on stiffness and weight criteria, using the actual coordinates of boundary nodes. The method was shown to be able to identify and remove material particles that give a negligible contribution to stiffness, as well as adding material to regions where it effectively increases the structure fitness toward the minimal cost to weight ratio.

Lagaros et al. [273] investigated the efficiency of various EAs, such as GAs and ES, when applied to large-scale structural sizing optimization problems. The computational effort that was required by GA was less than the corresponding effort by ES but they were hindered by premature convergence either to non-optimal or to infeasible designs. It is worth saying that the applications of GAs in the field of structural engineering deal also with optimization of reinforced concrete and steel structures [274].

Deb [275] applied GA for the optimal design of welded beam, namely in the case of nonlinear objective function and nonlinear constraints.

Chau and Albermani [276] successfully implemented GA for the optimum design of liquid retaining structures involving discrete variables such as slab thickness, reinforcement diameter, and reinforcement spacing. Only after examining a minute portion of the design alternatives, GA was proved to be able to locate the optimal solution quickly.

Jarmai et al. [277] applied GA to minimize the volume of welded I-section frames with constraints on both lateral-torsional buckling and local buckling of the beam and column webs and flanges. The authors compared their performance with other nonlinear optimization algorithms operating in a constrained representation space.

Fu et al. [278] used simple GA with elitism to find the optimum weight and cost of welded steel plate girder bridges having a single span and two-equal continuous spans. The GA provided meaningful conclusions for the design variables and for verifying engineers' past design experiences.

Senouci and Ansari [279] presented a GA-based model to optimize an objective function formulated by incorporating the major decision variables (not only the cost) affecting the design of composite beams.

Kociecki and Adeli [280] presented a two-phase GA for simultaneous sizing and topology optimization of free-form steel space frame roof structures with complex curvatures in multiple planes. The final design was lighter and less expensive than the initial solution based on the traditional "engineer's judgment".

The same authors [281] extended the previous algorithm for simultaneous sizing, topology, and shape optimization of free-form steel space-frame roof structures with complex geometries using GA. The authors imposed heuristic limits to avoid drastic or undesirable changes in the architectural form.

Jenkins [282] used GA to create an optimum design environment for a general class of plane frames. The authors recommended defining suitably the objective function and the constraints with the associated violation penalties.

Koumousis and Arsenis [283] used the GA technique for the optimal design of RC members of multi-story buildings. The detailed design was chosen on the basis of a multi-criterion objective representing a compromise between a minimum weight design, a maximum uniformity and the minimum number of bars for a group of members.

Sarma and Adeli [284] presented the cost optimization of realistic three-dimensional concrete structures. After a review of articles about reliability-based cost optimization and cost optimization of concrete structures published in archival journals, they suggested minimizing life-cycle cost of structures instead of the initial cost of construction only.

Camp et al. [285] presented a design procedure based on GA to minimize the material of RC frames and the construction costs subjected to serviceability and strength requirements.

Noguchi et al. [286] developed a GA integrating the concept of Pareto optimality, named MixGA, for solving multi-criteria optimization problems in proportioning of concrete mixture.

Amirjanov and Sobolev [287] developed self-adaptive GA for linear-constrained optimization problem related to the selection and proportioning of concrete aggregates. Unlike conventional GA, the authors implemented a self-adaptive mechanism dynamically to change the mutation rate and concentrate the search of an optimal solution on the feasible region.

Xie et al. [288] used GA to optimize the mix proportion design of high-performance concrete, taking into account the requirements of cost, durability, strength, workability and dimensional stability of concrete.

Rahman and Jumaat [289] used GA to derive a generalized formulation for determining the optimal quantity of materials used to produce non-slump concrete having minimum possible cost. The optimum formulation was based to meet compressive strength and workability requirements.

Aydin and Ayvaz [290] investigated the effective use of GA for overall cost optimization of pre-stressed concrete bridges to determine the optimum span number and the optimum cross-sectional properties of multi-span bridges. The solutions reached by GA were realistic and constructible because of using discrete design variables.

Sgambi et al. [291] investigated the spalling crack formation that takes place during pre-stressing of steel in the Hollow Core Slabs (HCS). They focused on the optimization of geometric and mechanical characteristics investigating the influence of the tendon position and the web width on the spalling stress. After an extensive literature review on soft computing, the authors performed the optimization by means of GA coupled with the 3D FEM models.

Moreover, GAs have been often adopted for the optimal control of the response of the vibrating system. Kim and Ghaboussi [292] applied GAs to design controllers for the wind-excited vibration reduction of tall buildings. Design criteria and constraints including the comfort requirement for building occupants and the control robustness were directly incorporated in the formulation and evaluation of the fitness and penalty function of the genetic algorithm-based control design. The results showed that GA was efficient in obtaining optimal design with multiple constraint conditions.

Wongprasert and Symans [293] used GA to identify the optimal distribution of dampers to control the seismic response of a multi-story benchmark building.

Hejazi et al. [294] used GA to optimize the control systems to protect structures against severe earthquake excitation in order to minimize the effects of the earthquake.

Xu et al. [295] presented an optimization method for design of viscoelastic damping structures with the aim of obtaining low structural mass and high damping. A modified reference point based Non-dominated Sorting Genetic Algorithm (NSGA-II) was used to solve the multi-objective constrained optimization problem. It was shown that the method, combining the advantages of the layerwise finite element analysis with multi-objective search ability of GA, was

computationally efficient and able to achieve concurrently the optimization of material layout and geometry.

Greco and Marano [296] focused on the optimum design of a passive seismic control strategy realized by a linear dissipative connection in a wall-frame system. A multi-objective optimum design was formulated with two conflicting objective functions: the displacement of the frame and the shear in the wall. The authors adopted a NSGA-II to obtain the optimum solution in terms of Pareto set.

Greco et. al [297] dealt with the optimum design of single ATDM for a better control of vibrations induced in building structures under low-moderate earthquakes. A multi-objective optimization was carried out by considering the cost of the device and the performance described by the ratio between the absolute accelerations of the protected structure and the unprotected one. The authors used the NSGA-II to achieve Pareto optimum solutions.

Poh'Sie et al. [298] searched for the optimal design parameters of the TMDs, (i.e. damping and frequency ratios), as a means to reduce the seismic accelerations of high-rise cross-laminated timber buildings by using a GA.

Asadi et al. [299] presented a multi-objective optimization model combining the rapidity of evaluation of ANNs with the optimization power of GAs to quantitatively assess technology choices in a building retrofit project. The proposed approach showed a great potential for the solution of multi-objective (energy consumption, retrofit cost, and thermal discomfort hours) building retrofit problems, and could be used as an aid to decision-making in the context of a retrofit project.

5. A soft-computing approach to seismic retrofitting

5.1 Formulation of the optimization problem

This Ph.D. Thesis mainly aims at replacing the conventional trial-and-error flow-chart shown in Figure 5.1, and usually followed by a civil engineer in the design of a seismic retrofit intervention, with an automatic procedure capable of selecting the "best" retrofitting solution according to the flow-chart in Figure 5.2.
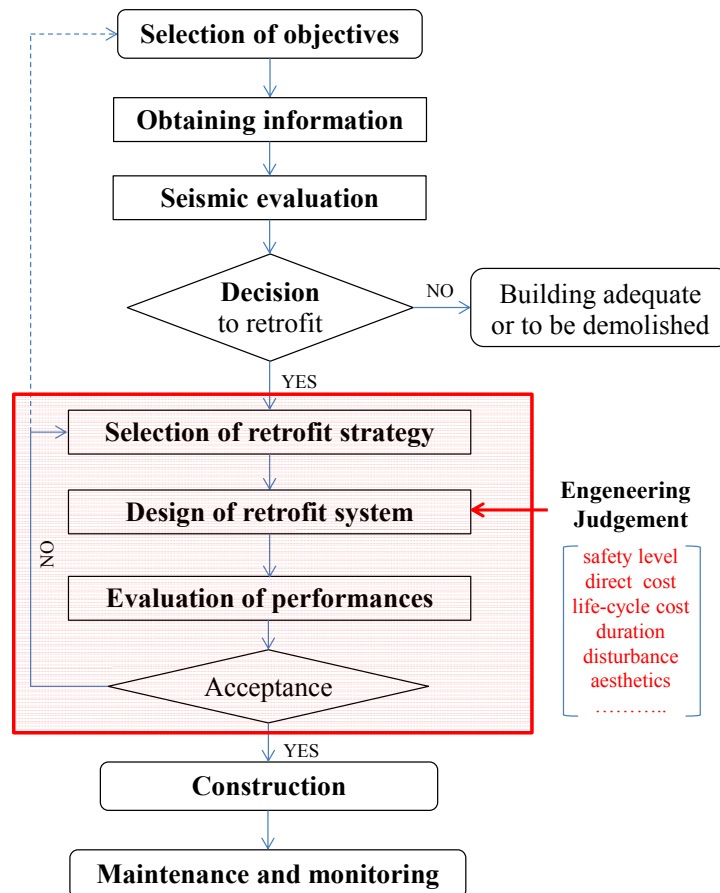

Figure 5.1: Conventional trial-and-error flow-chart for a PBD retrofit process

The selection of the "best" retrofitting system defines an optimization problem which reduces to selecting the "best" element within a given (wide but not infinite) domain.

In the current practice and in most of the available scientific contributions on this topic [95][96][300]-[302], except in the cases of Faella [100] and Chisari [303], the issue of retrofitting RC frames is not approached as an optimization problem.

In fact, it is simplistically addressed as a technical problem, seldom taking into account the Multi-Level nature of verifications according to the principles of Performance-Based Design. Thus, any consideration about optimization (even under the simply "economical" standpoint) is based on subjective experience and the so-called "engineering judgment".

However, the optimization problems need to be re-formulated in mathematical terms in order to define the objective function so that the formal relationship between the values of the design variables and constraints can be established. In the simplest case, an optimization problem consists of maximizing (or minimizing) a real function by choosing input values within an available space.

In many other cases, a set of competitive objectives lead to a more complex multi-objective optimization problem whose solution generally relies on a decision-making process. In the current work, the optimal solution is found by solving the following constrained optimization problem stated in Eq. (5.1):

$$\overline{x}_{opt} = \arg \underset{x}{opt}[f(x)] \quad \text{with } \overline{x}_{opt} \in \Omega_f \tag{5.1}$$

where **x** is the vector of design variables defining the generic retrofit interventions, and f(x) is the aforementioned objective function. On the right side of the equation, Ω_f is the "feasible" region consisting of all the solutions that satisfy the constraints given in Eq. (5.2):

$$g_{LS,i}(x) = C_{LS,i}(x) - D_{LS,i}(x) \geq 0 \quad \forall i = 1...n_{LS} \tag{5.2}$$

where g_{LS} is the Limit State function (as a matter of principle, not met by an existing structure in its "as built" condition) given by the difference between the capacity $C_{LS,i}$ and the corresponding demand $D_{LS,i}$ to be checked at the relevant Limit States.

In particular, two main performance-objectives dealing with the safety check of the strengthened structure at both Serviceability Limit State (in terms of Damage Limitation) and Ultimate Limit State (in terms of Life Safety) are taken into

account. The most comprehensive and rational objective function can be obtained by taking into account a series of concurrent criteria within the framework of a Multi-Criteria optimization problem [97].

Such criteria can be based on both strictly quantitative measures, such as specific parameters related to the seismic response of the retrofitted structures or with the levels of reliability of its seismic performance [304][305], or qualitative measures, possibly related to either the users' opinion or aesthetical aspects of the final solutions [306], as shown in Section 3.3.3.

A less comprehensive objective function can be represented by the life-cycle cost [307], which allows taking into account both the "live-costs" needed for construction and demolition operations and also other cost terms such as the "economic loss" deriving by the downtime periods and the required maintenance.

However, in the present work, the easiest and more simplistic choice is taken by assuming only the actual cost of the intervention as the objective function whose minimization leads to the optimal solution for the problem of under consideration [308].

The solution of such problem may be obtained by using different approaches. The most primitive strategy is to generate all feasible solutions 'step by step', for every solution calculate the cost function and find the best solution. In practice, this procedure cannot be used because exploring all possible solutions would request a huge computation time.

In principle, the cheapest solving methods in terms of computational cost (i.e., number of evaluations of the objective function) are the analytical optimization methods [309][310], based on the grounds of classical mathematical analysis and closed-form formula.

However, such methods are based on the evaluation of the gradient of the objective function (steepest descend [311]; trust region [312]). Therefore, they require that the objective function is sufficiently regular. Since the assumed objective function is not explicitly known and no information about the convexity of the function is present, the solution of optimizations problem cannot be obtained through the aforementioned methods.

When the users are not interested in any "exact" solution, but rather an approximate solution is satisfactory, the problem under consideration can be more properly solved by applying less efficient but more general tools. These alternative methods, called "Soft-Computing" methods (Chapter 4) are fit for handling a multi-objective and multi-criteria optimization problem, such as the search for

optimal seismic retrofitting of existing structures within the framework of performance-based design.

Therefore, the final goal of the present Ph.D. project has been the implementation of a procedure that assembles a numerical model for seismic analysis of structures within a soft-computing-driven optimization algorithm able to solve the aforementioned constrained optimization problem.

It is clear that the purpose of the procedure is to support the engineering judgment (being far from the ambition to rule it out) in the selection of the "best" seismic retrofitting solution of existing Reinforced Concrete frames.

In general terms, the issue of developing such a procedure requires the selection of three main components: the Optimization Algorithm; the Simulation Framework; and the Software Environment. Each will be better described in the next Section.
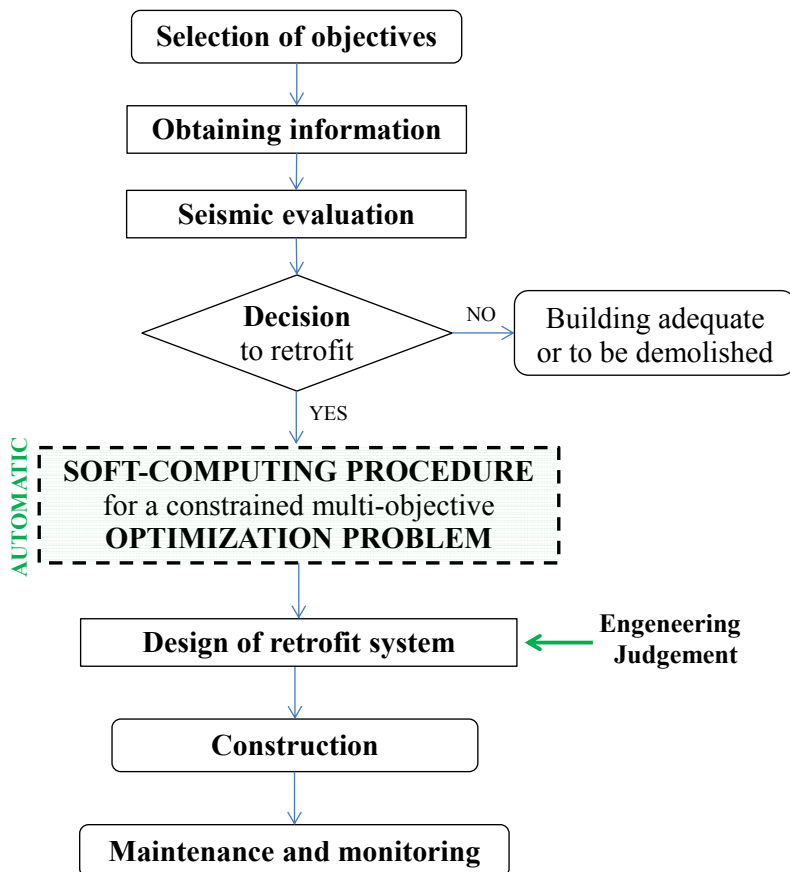

Figure 5.2: Soft-Computing aided procedure for a PBD retrofit process

5.2   Optimization algorithms

The issue of selecting a proper algorithm for the optimization problem described by Eq. (5.1) is not trivial and it is usually based on a number of considerations [313] such as the nature of design variables (continuous, discrete or both), the presence of constraints (constrained or unconstrained), the nature of objective functions (linear or nonlinear, convex or non-convex, continuous or discontinuous, uni-modal or multi-modal, differentiable or non-differentiable, computationally expensive or inexpensive), the characteristics of the problem (static or dynamic), the performance of potential algorithms which have similar features. Table 5.1 presents a classification of mostly-used families and their relevant characteristics.

Table 5.1: Classification of mostly-used optimization algorithms [314]

Family	Strength/Weakness	Typical algorithms
Direct search family	➢ derivative-free methods; ➢ can be used even if cost function has small discontinuities; ➢ may be attracted by a local optimum; ➢ often have problems with non-smooth functions.	- Exhaustive search - Hooke-Jeeves algorithms - Coordinate search algorithm - Mesh adaptive search algorithm - Simplex algorithm
Integer programming family	➢ solving problems which consist of integer or mixed-integer variables.	- Branch and Bound methods - Exact algorithms - Simulated annealing - Tabù search - Hill climbing method
Gradient-based family	➢ fast convergence; ➢ sensitive to discontinuities in the cost function; ➢ sensitive to multi-modal function.	- Bounded BFGS - Levenberg-Marquardt algorithm - Discrete Armijo Gradient algorithm

Meta-heuristic Population-based family	➢ not to "get stuck" in local optima; ➢ a large number of cost function evaluation; ➢ global optimum cannot be guaranteed.	- Genetic algorithm - Genetic programming - Evolutionary programming - Differential evolution - Particle Swarm Optimization - Ant colony algorithm - Bee colony algorithm
Trajectory Search family	➢ easy implementation even for complex problems; ➢ appropriate for discrete optimization problems; ➢ only effective in discrete search space; ➢ unable to tell whether the obtained solution is optimal.	- Simulated annealing - Tabù search - Hill climbing method
Hybrid family	➢ combining strength and limiting the weakness of the other approaches.	- PSO-HJ - GA-GPS - HS-BFGS

As already said, the most "primitive" strategy of searching the "best" solution is to generate all feasible solutions "step by step". However, the exhaustive approach in practice cannot be used because it is impossible to store the infinite number of solutions into the computer's memory and explore all possible values of in a suitable time.

The heuristic nature of optimization problems encountered in structural engineering poses challenges to the engineers thereby making them careful in time and resources saving. Instead of exploring all the possible solution, engineers would rather prefer to handle a limited number of trial solutions, which are potentially capable to reach every point in the search space.

For instance, heuristic methods use some kind of "clever" strategy aimed at finding a near-optimal solution, which may not exactly be optimal, but closer to the optimal solution. The near-optimal solution is based on the trade-off between the satisfaction level and the computational time cost.

In this perspective, recent trends in computational optimization move away from the conventional methods (direct-search, integer-programming, gradient-based family) to nature-inspired meta-heuristic algorithms.

In particular, the population-based algorithms (Swarm Intelligence, Hybrid Algorithms, Evolutionary Algorithms) are the most used methods employed for solving highly nonlinear optimization problems encountered in the civil engineering field, according to the Figure 5.3.
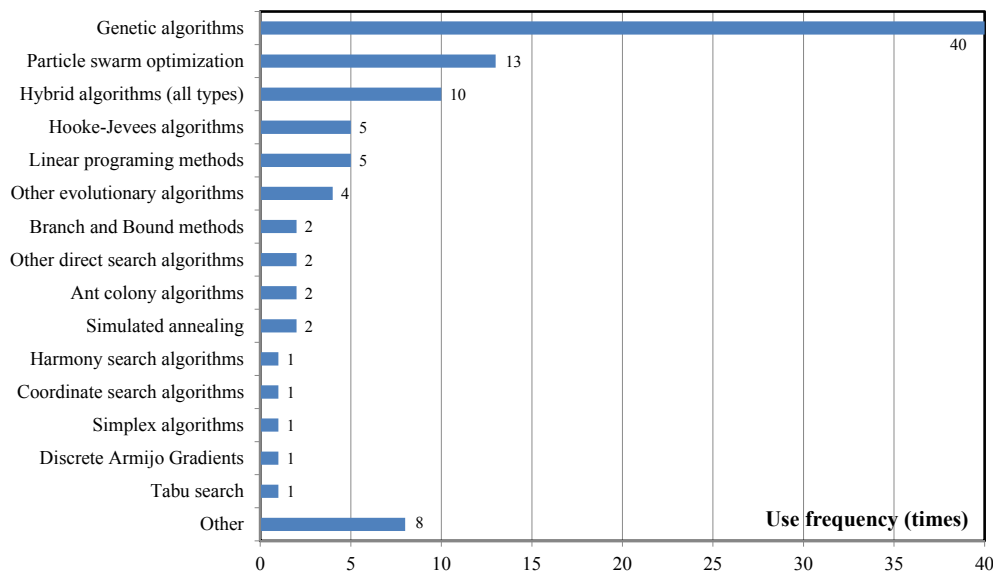
Figure 5.3: Use frequency of different optimization algorithms [314]

One of the reasons for such popularity is that these methods are easy to understand and implement, as they require little efforts for new users to learn. They use stochastic components or randomization techniques to increase the "ergodicity" of the iterative search path.

Among these search techniques, Genetic Algorithm (GA) is a well-known technique for optimization of a complex problem with large search space. As known, the GA belongs to the class of stochastic optimization methods because the evolutionary process is driven by one or more random number generators.

The strategy of searching the optimum through the solution space used by GA is inspired by the natural evolution. The essence of a GA is to equate possible solutions to individuals of a population and to introduce the notion of "fitness" as a measure of solution's quality. Since they are simplified versions of the biological process that operates on chromosomes (organic devices which encode the structure of living being), GAs encode a potential solution of a specific problem on a simple chromosome-like data structure.

Each of these artificial chromosomes consists of strings (or genes) of a certain length which contain information for the corresponding parameter. GAs search for the optimum solution, starting from an initial population of strings and "improving" successive population in accordance with the "survival of the fittest" principle. The evolution of the population is based on a particular algorithmic framework whose main components are the variation operators (mutation and crossover) and the selection operators (parent selection and survivor selection) as shown in Figure 5.4.
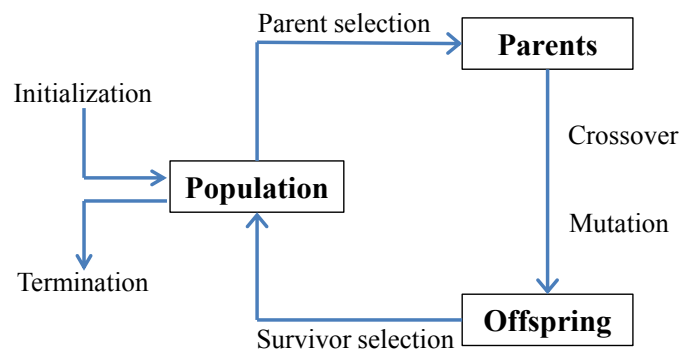
Figure 5.4: Flow-chart of a canonical genetic algorithm

As said in section 4.3.2, the selection is the process by which individual strings are copied into a "mating pool" according to their fitness. This means that strings that have shown to be good temporary solutions have a higher probability of contributing one or more offspring to next population. This is an artificial version of natural selection where the best individuals have greater chance to survive and to become parents of new offspring.

The crossover mechanism allows mixing genetic information of the selected parents while passing it to their descendants. Therefore, the offspring exhibit some traits of the "father" and some traits of the "mother".

Mutation operator is an occasional random alteration of the string position value needed because the reproduction and recombination sometimes lose some

potentially useful genetic materials. The mutation prevents such an irrecoverable loss by introducing (locally in the strings) new genetic information.

Once a new population is created, the evaluation of fitness function of all the individuals and the application of genetic operators are iterated until termination criteria are met. One cycle of these operators and the subsequent fitness evaluation procedure is known as a "generation" in GAs terminology.

In recent years, such algorithm has been used for solving a variety of engineering design problems (Section 4.3.2.1). Goldberg [315][316] discussed how genetic algorithms have several fundamental advantages that allow them to be more robust than other optimization methods:

- − GAs work with a string-coding of the parameter set, not the parameters values themselves: this is advantageous because the parameters may be in different units or measurement scales and may be very difficult to model;

- − GAs search parallel from a population of n individuals, allowing parallel computing on multi-processor computers: this is beneficial when there are multiple local optima because the GA will avoid premature convergence to locally optimal solutions or false-peaks;

- − GAs use objective function information, not derivatives or other auxiliary information (only the fitness levels influence the directions of search): this is beneficial if the objective function is not smooth, or is nonlinear, or if there are a large number of parameters to which the gradient information is not known;

- − GAs use probabilistic transition rules, not deterministic ones making them quite robust in handling discontinuity, multi-modal and highly-constrained problems without being trapped at a local minimum, even with NP-hard problems.

Although there is no absolute guarantee that a GA will find a global optimum, its appeal comes from the simplicity (it practically does not demand the knowledge of mathematics), the elegance as robust search algorithms and its power to discover "good" solutions rapidly for high-dimensional problems. In particular, GAs are useful and efficient when the search space is large, complex or poorly understood.

Moreover, GA provides a number of potential solutions to a given problem and the choice of final solution is left to the user. In cases where a particular problem does not have one individual solution, GA is potentially useful in identifying these alternative solutions. For all the above reasons, GAs have been considered as the most suitable optimization algorithm for the proposed numerical procedure.

5.3   Simulation Framework

The simulation framework chosen for the procedure is the Open System for Earthquake Engineering Simulation (OpenSees) [317][318]. It is an object-oriented software framework for finite element analysis developed by PEER (Pacific Earthquake Engineering Research Center), one of the most important research institutes for seismic engineering.

The software allows users to create both serial and parallel finite element computer applications for simulating the response of structural and geotechnical systems subjected to earthquakes and other hazardous actions. As an open source object-oriented program, OpenSees is free and it can be collaboratively developed and updated rapidly by anyone. The developers and researchers can use the extensible features of the software architecture to add additional capability.

A key feature of OpenSees is the interchangeability of components (modularity) and the ability to integrate existing libraries and new components into the framework without the need to change the existing code (extensibility).

The existing library includes a wide set of both finite elements solution procedures and algorithms that the user can adapt to solve difficult nonlinear problems. OpenSees is based on the Tool Command Language (TCL) that is a string-based scripting language [319] that supports, other than specific OpenSees commands, basic operations, such as variables and variable substitution; mathematical-expression evaluation; basic control structures (if, while, for, foreach); procedures; file manipulation.

The Interpreter is an extension of the TCL scripting language which adds commands to TCL for finite element analysis. Each of these commands is associated with a C++ procedure that is called upon by the interpreter to parse the command. OpenSees does not contain a user graphical interface that allows users to have real-time interaction while building the structural model.

Its "interface" is based on a command which enables the user to create more-versatile input files. Therefore, it lacks the common tools that are available in many other popular applications, such as help menu and debugger, in the model-development environment.

However, there are several helpful media provided by the PEER community to solve these problems. The most popular option is the help documents managed and made available to users and developers through the OpenSees official website (http://opensees.berkeley.edu). This website provides detailed explanations of each

commonly used OpenSees command and offers numerous useful examples to illustrate the functions of the commands. Such simulation framework is able to accommodate any advanced - linear or nonlinear, static or dynamic - analysis procedure.

It is suitable to work under dynamic environment because the construction of the finite element model and the following analysis are written as command lines.

It is comprised of a set of modules (abstracted objects) to perform creation of the finite element model, specification of an analysis procedure, selection of quantities to be monitored during the analysis, and the output of results. In each finite element analysis, the OpenSees interpreter constructs four types of objects, as shown in Figure 5.5:

a. Model Builder Object, which defines the characteristics of the physical model to be analyzed;

b. Domain Object, which stores the objected created by the Model Builder, provides the Analysis access to these objects and holds the state of the model at time t_i and $(t_i + dt)$ for Recorder;

c. Analysis Object, which moves the model from the state at time t_i to state at time $t_i + dt$ and encapsulate algorithms that direct the Domain components to form and solve the governing equations of structural equilibrium at each integration step;

d. Recorder Object, which records and stores into output files the user-defined structural response parameters obtained through the analysis.
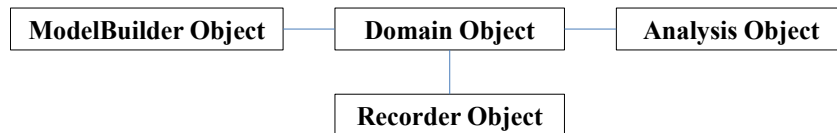
Figure 5.5: OpenSees objects needed to execute a finite element analysis

It is worth highlighting that the OpenSees interpreter constructs objects in the same order they are specified by the user. These objects along with their components are better described in the following paragraphs.

5.3.1   Model Builder Object

The Model Builder is the object responsible for building the components in the model and adding them to the domain. The aggregation of these components defines the type of model that is being analyzed. The modeling commands that

have been added to OpenSees interpreter to create these components of the FE model are the following:

- Model Command: it is used to define the spatial dimension of model and number of degrees-of-freedom at nodes. Once issued additional commands are added to the interpreter;
- Node Command: it is used to assign coordinates and/or masses to nodes;
- Mass Command: it is used to set the mass at a node;
- ConstraintHandler Command: it is used to determine how the constraint equations are enforced in the analysis;
- UniaxialMaterial Command: it is used to construct a uniaxial material object which represents uniaxial stress-strain relationships;
- Section Command: it is used to construct a section which represents force-deformation (or resultant stress-strain) relationships at sample points.
- Element Command: it is used to construct a finite element;
- Geometric Transformation Command: it is used to construct a coordinate-transformation object, which transforms beam element stiffness and resisting force from the basic system to the global coordinate system;
- TimeSeries Command: it is used to represents the relationship between the time in the domain, and the load factor λ applied to the loads in the load pattern with which the Time Series object is associated, i.e. $\lambda = F(t)$;
- Pattern Command: it is used to construct a Load Pattern.

5.3.2   Domain Object

Domain in OpenSees is a collection (an aggregation in object-oriented terms) of elements, nodes, single-and multi-points constraints and load patterns created by the Model Builder Object as shown in Figure 5.6. It provides the Analysis and Recorder object access to these objects.
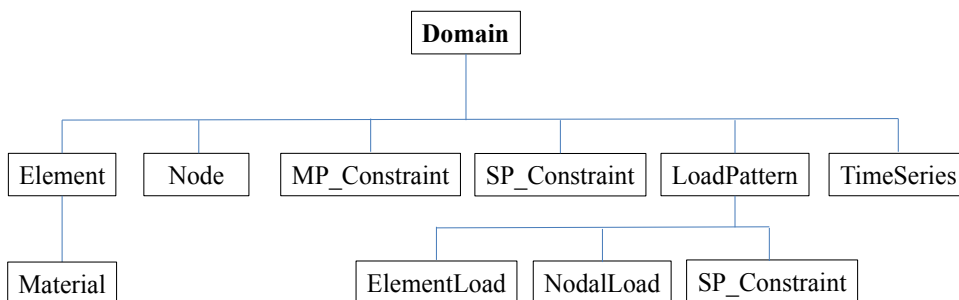

Figure 5.6: Aggregation of components in the Domain object

5.3.3   Analysis Object

The Analysis Objects shown in Figure 5.7 are responsible for performing the analysis, i.e. they move the model from the state at time **t** to the state at time **t+dt**. It is composed by the aggregation of several components objects, defining the type of analysis that is performed on the model.
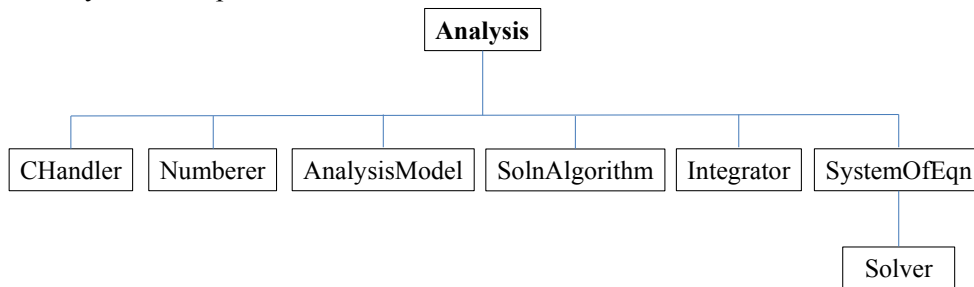

Figure 5.7: Aggregation of components in the Analysis object

5.3.3.1   Constraint Handler

The Constraint Handler object determines how the constraint equations are enforced in the analysis. Constraint equations enforce a specified value for a degree-of-freedom or a relationship between them. In OpenSees library there are several options to specify boundary conditions:

- Plain Constraints Method: it is used to enforce homogeneous single-point constraints, such as the case of homogeneous boundary conditions, where all boundary conditions are fixed;
- Penalty Method: it applies very stiff elements (numerically) at the boundary conditions by adding large numbers to the stiffness matrix (i.e. the potential energy equation which makes up the system of equations is augmented by a penalty function) and the restoring-force vectors to impose a prescribed zero or nonzero DOF;
- Lagrange Multipliers Method: it applies the method of Lagrange multipliers to the system of equations, thus enlarging the size of the matrices (the resulting stiffness matrix is no longer positive definite);
- Transformation Method: it transforms the stiffness matrix by condensing out the constrained DOF's, thus reducing the size of the system for multi-point constraints.

5.3.3.2   Numberer

This command is used to determine the mapping between equation numbers and DOF, namely how degrees-of-freedom are numbered. There are two main rules:

- Plain Numberer: this rule assigns degrees-of-freedom to the nodes based on how the input file of nodes are stored in the domain nodes (i.e arbitrarily);
- RCM Numberer: this rule assigns degrees-of-freedom to the nodes using the Reverse Cuthill-McKee algorithm which optimizes node numbering to reduce bandwidth using a numbering gap.

The latter can output a warning when, for instance, the structure is disconnected.

5.3.3.3   System

This command is used to construct a linear system of equation (LinearSOE) and LinearSolver objects to store and solve the system of equations in the analysis. There are six different System of Equation:

- BandGeneral SOE: it is used to construct an un-symmetric banded system of equations which will be factored and solved during the analysis using the Lapack band general solver;
- BandSPD SOE: it is used to construct a Symmetric Positive Definite (SPD) Banded system of equations which will be factored and solved during the analysis using the Lapack band SPD solver;
- ProfileSPD SOE: it is used to construct Symmetric Positive Definite Profile system of equations which will be factored and solved during the analysis using a profile solver;
- SparseGeneral SOE: it is used to construct a general Sparse System of equations which will be factored and solved during the analysis using the SuperLU solver;
- UmfPack SOE: it is used to construct a general sparse system of equations which will be factored and solved during the analysis using the UmfPack solver;
- SparseSPD SOE: it is used to construct a Sparse Symmetric positive Definite system of equations which will be factored and solved during the analysis using the Kincho Law' sparse solver.

5.3.3.4 Test command

The test object is used to determine if the convergence of an algorithm has been achieved at the end of an iteration step. The convergence test is applied to the Eq. (2.7) F=KΔU. The test objects available in OpenSees are listed below:

- Norm Unbalance Test: it is used to construct a *CTestNormUnbalance* object which tests positive force convergence if the 2-norm of the F vector ($\sqrt{F \cdot F}$) in the LinearSOE object is less than the specified tolerance;
- Norm Displacement Increment Test: it is used to construct a *CTestNormDispIncr* object which tests positive force convergence if the 2-norm of the displacement increment ($\sqrt{\Delta U^T \Delta U}$) in the LinearSOE object is less than the specified tolerance;
- Energy Increment Test: it is used to construct a *CTestEnergyIncr* object which tests positive force convergence if one half of the inner-product of the displacement increment and unbalance ($\sqrt{\Delta U^T F}$) in the LinearSOE object is less than the specified tolerance.

5.3.3.5 Algorithm Command

This command is used to determines the sequence of steps taken to solve the non-linear equation at the current time step. OpenSees includes the following algorithms:

- Linear Algorithm: it is used to construct a Linear algorithm object which takes one iteration to solve the system of equations;
- Newton Algorithm: it is used to construct a *Newton-Raphson* algorithm object which uses the Newton-Raphson method to advance to the next time step;
- Newton with Line Search Algorithm: it is used to construct a new search algorithm object which uses the Newton-Raphson method with line search to advance to the next time step;
- Modified Newton Algorithm: it is used to construct a *Modified Newton* algorithm object which uses a modified version of the Newton-Raphson method to advance to the next time step because the tangent stiffness is not updated at each step;
- Krylov-Newton Algorithm: it is used to construct a *KrylovNewton* algorithm object which uses a modified Newton method with Krylov subspace acceleration to advance to the next time step;

- BFGS Algorithm: it is used to construct a *Broyden–Fletcher–Goldfarb–Shanno* algorithm object which performs successive rank-two updates of the tangent at the first iteration of the current time step;
- Broyden Algorithm: it is used to construct a *Broyden* algorithm object for general unsymmetric systems which performs successive rank-one updates of the tangent at the first iteration of the current time step.

5.3.3.6   Integrator command

The Integrator object is used to determine the predictive step for time t+dt; specify the tangent matrix and residual vector at any iteration and determine the corrective step based on the displacement increment dU. The type of integrator used in the analysis is dependent on whether it is a static analysis or transient analysis. In the case of static analysis the type of integrator available are:

- − LoadControl integrator: the load increment at iterations i is related to the load increment at i-1;
- − DisplacementControl integrator: the displacement increment at iterations i is related to the displacement increment at i-1;
- − MinUnbalDispNorm integrator: the load increment at iterations i is related to the load increment at i-1;
- − ArcLength integrator: it is used to enable the algorithm to pass limit points at which the stability of the numerical system is dependent on whether the analysis is performed under load or displacement control.

For transient analysis, whereas, the integrators available are:

- − Newmark: the damping matrix is specified as a combination of stiffness and mass-proportional damping matrices;
- − Hilbert-Hughes-Taylor Method: it is used to construct a Transient Integrator object of type Hilbert-Hughes-Taylor or Hilbert-Hughes-Taylor. The damping matrix is specified as a combination of stiffness and mass-proportional damping matrices.

5.3.3.7   Analysis command

This command is used to define what type of analysis is to be performed. The following options are available in OpenSees:

− Static Analysis: it solves the F=KU problem, without the mass or damping matrices. The default component objects are the following:

Table 5.2: Default component for static analysis

Component object	Default object
SolutionAlgorithm	NewtonRaphson (tol=1e-6; max iter.=25)
Test	CTestNormUnbalance
ConstraintHandler	PlainHandler
DOF_Numberer	RCM
LinearSolver	profiled symmetric positive definite
StaticIntegrator	LoadControl

− Transient Analysis: it solves the time-dependent analysis with a constant time step. The default component objects are the following:

Table 5.3: Default component for transient analysis

Component object	Default object
SolutionAlgorithm	NewtonRaphson (tol=1e-6; max iter.=25)
Test	CTestNormUnbalance
ConstraintHandler	PlainHandler
DOF_Numberer	RCM
LinearSolver	profiled symmetric positive definite
TransientIntegrator	Newmark with γ=0.5 and β=0.25

− Variable Transient Analysis: it performs the same analysis type as the Transient Analysis object but with a variable time step. The default component objects are the following:

Table 5.4: Default component for variable transient analysis

Component object	Default object
SolutionAlgorithm	NewtonRaphson (tol=1e-6; max iter.=25)
Test	CTestNormUnbalance
ConstraintHandler	PlainHandler
DOF_Numberer	RCM
LinearSolver	profiled symmetric positive definite
TransientIntegrator	Newmark with γ=0.5 and β=0.25

5.3.4   Recorder Object

The Recorder commands are used to monitor user-defined parameters in the model during the analysis. In particular, they monitor the state of a domain component (node, element, etc.) at selected intervals of the analysis and write this state in text files in a way that can be easily post-processed. Several Recorder objects can be created:

- Node Recorder: it records the displacement, velocity, acceleration and incremental displacement at the nodes;
- EnvelopeNode Recorder: it records the envelope (minimum, maximum and maximum absolute value) of displacement, velocity, acceleration and incremental displacement at the nodes;
- Drift Recorder: it records the displacement drift between two nodes, i.e. the ratio between the relative displacement and the distance between them;
- Element Recorder: it records the response of a number of elements. The response recorded is element-dependent:

  - Beam-Column Elements: element resisting force in global or local coordinates (without inertial forces);
  - Sections: force, deformation, stiffness, stress-strain response.

- EnvelopeElement Recorder: it records the extreme values of the response (minimum, maximum and maximum absolute value) of a number of elements.

5.4   Software Environment

The automatic procedure has been implemented in MATLAB (MATrix LABoratory) [320] that enables to quickly create and distribute numerical applications or software components. It is a multi-paradigm numerical computing environment that allows matrix manipulations, plotting of functions and data, implementation of algorithms, and it is able to interface with programs written in other languages, including C, C++, Java, Fortran, and Python.

The main reason for using MATLAB instead of other technically possible language is that it is rarely a software development environment that is, on the one hand, a high-level language, and on the other hand a computation and visualization engine [321].

There is a significant number of built-in functions on scientific computations in MATLAB, all standardized and well-documented and, hence, very handy to use. This important feature significantly reduces the time and effort required for programming. Unlike C++ or FORTRAN, variables in MATLAB are not necessary to be pre-defined. Many complex operations, such as array searching, can be done by adding a single command line.

MATLAB allows storing a sequence of instructions in an M-file which can be of two types: script or functions. The former one contains a sequence of instructions and uses all previously defined variables. The latter group a sequence of instructions within a single block and execute a specific (and generally more complex) operation or processing.

The source code developed to solve the problem described above (Eq. 5.1-5.2) is contained within the main M-file called "RunProcedure.m" and is composed of a series of subroutines that perform a specific phase of the procedure. Figure 5.8 shows the flow-chart that schematically summarizes the whole procedure.

The steps related to the optimization algorithm are highlighted with a different color than those necessary to perform seismic analysis and post-processing stage. Each step of the proposed software package will be better described in the following Section.
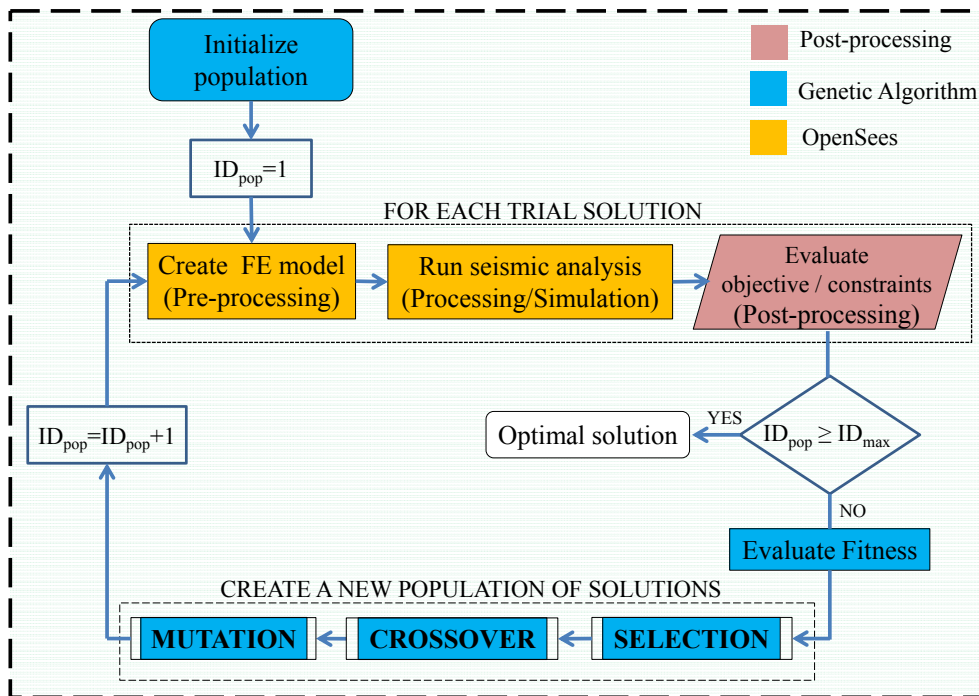

Figure 5.8: Flow-chart of the proposed procedure and classification of the steps

6. Implementation of the Soft-Computing procedure

6.1   Population representation and initialization

As known, genetic algorithms belong to the population-based optimization family that operates on a number of potential solutions, called individuals. The proposed procedure starts by generating a set of candidate solutions as shown in Figure 6.1.
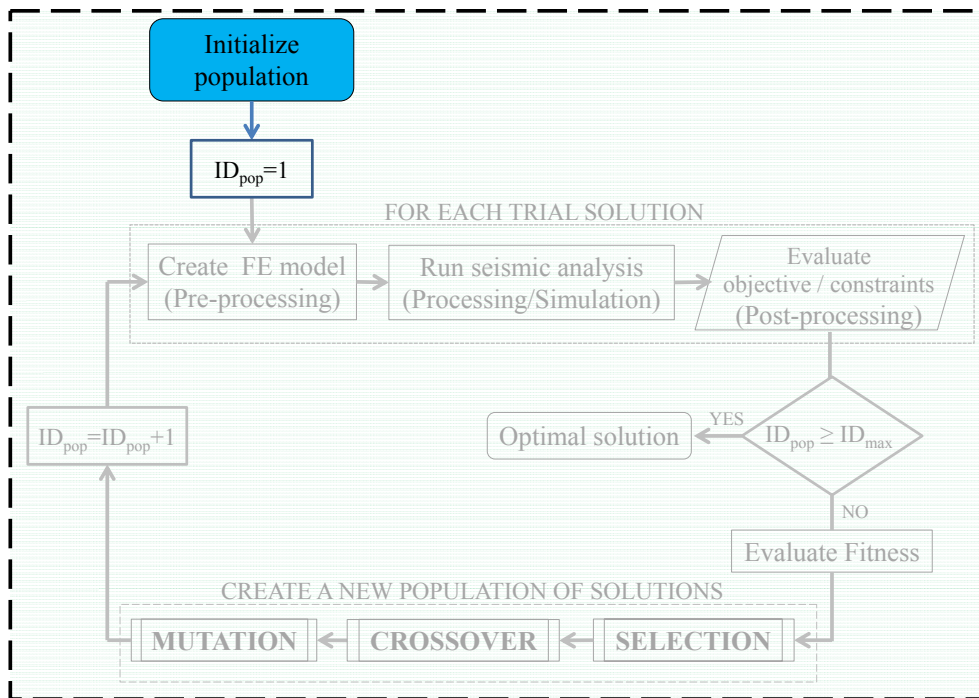
Figure 6.1: Initialization step within the proposed procedure

The search process of GA operates on the encoding of the decision variables describing the problem, rather than the decision variables themselves. Hence, the individuals are encoded as strings composed over some alphabet so that the genotypes are uniquely mapped onto the decision variable domain (phenotype). Although other representation methods can be used (e.g. ternary, gray, integer,

real-valued etc. [322][323][324][325]) the coding based on the alphabet {0, 1} [326] is actually adopted in the present work: each individual of such a population is herein represented through a simple "chromosome-like" array of bits.

To continue the genetic analogy, each chromosome (i.e. candidate solution) is composed of several genes (variables). Since the problem described in Eq. (5.1) has more than one variable, the "chromosome" describing the retrofitting intervention is structured by concatenating the set of variables that represent it.

In the present work, a generic retrofit intervention is conceived as a synergistic combination of both FRP confinement of single RC columns and concentric steel bracings installed in parallel with the existing structure (Figure 6.2).
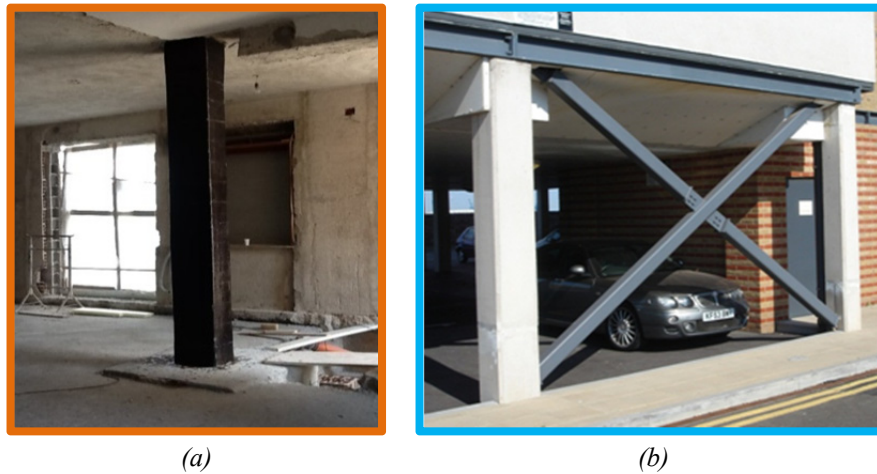

(a)   *(b)*

Figure 6.2: Example of local confinement (a); and global intervention (b)

For this reason, the vector **x** of the design variables, defining the generic interventions, consists of variables describing the local and global intervention, respectively in the first part and in the second part of the chromosome.

The set of variables are symbolically grouped in a row vector, as shown in Figure 6.3 where $n_{L,hk}$ is the number of FRP wraps at column h and story k while $ID_{sec,Nb}$ is the label of a steel profile's cross-section to be employed for realizing the bracing system between two column connected by the beam N_b.

$$x = \left[n_{L,11}, n_{L,12}, n_{L,13} \dots, \dots, \dots, \dots, \dots, \dots, \dots, \dots, \dots, n_{L,hk}, ID_{sec,1}, \dots, \dots, \dots ID_{sec,N_{bt}} \right]$$
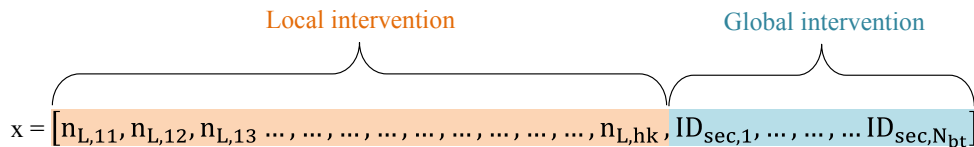
Figure 6.3: Row vector assembling the design variables of a generic intervention

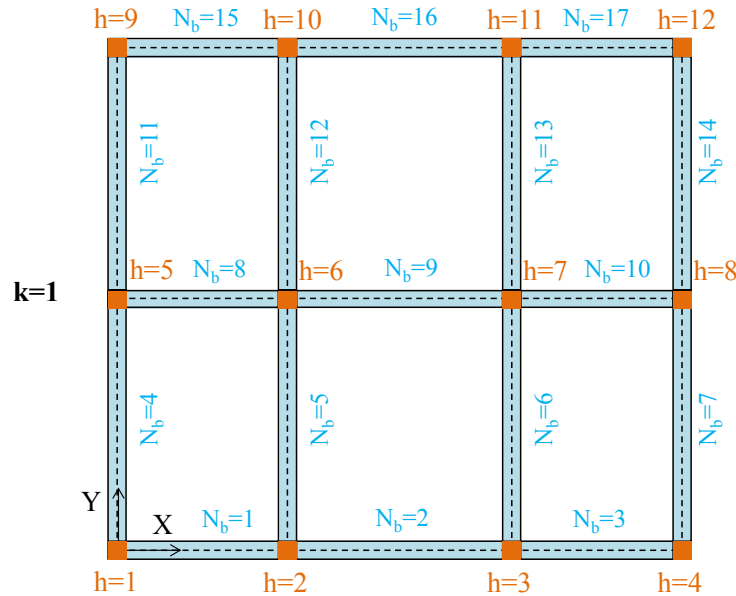The way of numbering columns and beams considered in the current implementation is shown in Figure 6.4.

Figure 6.4: Example of numbering adopted in the procedure

On the one hand, the inter-story local strengthening intervention is supposed to be realized along the whole height of the columns. On the other hand, steel bracings system representing the global intervention are supposed to be possibly built between each couple of columns connected by a beam.

These assumptions are intended at keeping the cardinality of the vector **x** as small as possible. As a matter of fact, if the length of chromosome increases it could adversely affect the convergence rate of the algorithm.

In the first part of the chromosome, for each decision variable, the procedure employs a couple of bits, that encodes the number of FRP layers possibly employed for confining the corresponding column. Hence, in the first part of the chromosome, a total of $2 *N_{col}$ bits is contained, N_{col} being the number of column elements in the structural model of the existing frame. It is worthwhile to mention here that with two bits there are only 2^2 or 4 possible distinct sub-strings.

Moreover, in the second part of the chromosome, the proposed procedure employs three bits for each design variable describing the steel diagonal bracings. Hence, in the second part of the genotype a total of $3*N_{beam}$ bits is contained, where N_{beam} is the number of beam elements in the structural model of the existing frame

at the first floor. With three bits only $2^3 = 8$ codes are available to describe the section of diagonals possibly installed at the first level, in correspondence of a generic beam. Figure 6.5 depicts an example of binary coding.
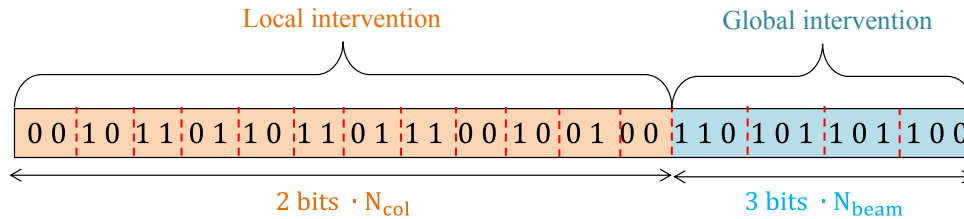

Figure 6.5: Example of binary genotype for encoding a retrofitting intervention x

Once the representation of an individual has been formalized, the procedure starts with generating a first population of candidate solutions.

The population size, i.e. the number of individuals N_{ind} belonging to the population, depends on the nature of the problem. By varying this parameter the convergence of the problem may be altered: a large size would result in a long epoch time, restricting how many chances each individual has to explore its neighborhood, whereas with a small size might be an insufficient coverage of the search space [327].

The general understanding is that increasing the number of chromosomes automatically increases the chances of finding the global optimum of an objective function [327]. In other words the probability of finding the position of global minimum increases to exactly one when the number of trials becomes infinite (covering the entire search space).

However, for all practical purposes, it is necessary to keep the population size as small as possible since more numerous populations require more computing time and more computer memory.

It is a common belief that it is necessary to assign appropriate values to N_{ind} in order to maintain the "robustness" of the algorithm. The proposed implementation employs a population with a number of individuals equal to 100 assumed being constant over the evolutionary process (Section 6.9). Hence, each population can be represented by a matrix with N_{ind} rows (chromosomes) and $N_{bit,tot}$ columns (genes) filled with ones and zeros.

The first subroutine is aimed at calculating the total number of design variables and, hence, the length of the chromosome. In principle it is useful to have a highly diverse composition of the first population, this can be achieved by generating the

required number of individuals by using a random number generator that uniformly distributes numbers in the desired range, allowing the entire range of possible solutions. This strategy ensures the search to be robust and unbiased, as it starts with a wide range of points spread uniformly over the search space.

An alternative way to generate the first population can be based on the assumption that individuals are concentrated in the most promising regions. Some evolutionary computing users have in fact "seeded" the initial population with some individuals that are known to be in the vicinity of the optimal solution [328][329].

Such techniques, such as like Nearest Neighbor (NN) [330], Gene Bank (GB) [331], Selective Initialization (SI) [332], Sorted population (SP) [333], have the benefits of generating good fitness individuals and fast convergence to the optimal solution.

Moreover, these approaches are only applicable if the nature of the problem is well understood beforehand or if the GA is used in conjunction with a knowledge-based system. Therefore, it is known the efficiency of using heuristic initialization functions that can help the algorithm to get the near optimal solution easily.

However, the excessive use of them could decrease the exploration capacity of the GA, trapping the population in local optimums quickly. Therefore, the key is to maintain a balance between individuals initialized by heuristic and individuals generated randomly.

For this reason, in the current implementation, the first population comes from two different initializing strategies with the aim to ensure such balance between the background knowledge of the user (which can mostly produce good quality individuals) and the randomness (which can produce also poor quality individuals).

The first strategy generates a random N_{rand} x $N_{bit,tot}$ matrix of uniform bit numbers. The number of individuals generated in accordance with this strategy is given by the Eq. (6.1):

$$N_{rand} = \alpha_{rand} \cdot N_{ind} \tag{6.1}$$

where the parameter $\alpha_{rand} \in [0\text{-}1]$.

The second strategy, as said, is intended at narrowing the search space towards a preferential/allowable area in the vicinity of the optimal solution by encoding the users' knowledge (or even the other sources of constraints) in a N_{seed} x $N_{bit,tot}$ matrix shown in Figure 6.6.

As already pointed out, some kind of intelligence could lead the searching algorithm much faster to the desired solution than completely "blind" trials. In the present work, the "seeded" initial population has a number of rows equal to:

$$N_{seed} = (1 - \alpha_{rand}) \cdot N_{ind} \qquad (6.2)$$

To this end, after the detailed assessment of the seismic response of the existing building in its as-built configuration a specific subroutine handles the pushover curve. More specifically, by comparing the bilinear Capacity Spectrum with the given Inelastic Demand Spectrum in ADRS format, the subroutine evaluates the required increase in strength λ_S, the increase in ductility λ_D to achieve the performance objectives and the expected inter-story drift; 2) compares them with empirical limiting values and 3) selects an appropriate retrofit strategy among the heuristic table proposed by Baros and Dritsos [94] (Section 3.2.4.).

The optimal retrofit strategy is then "translated" into a triad of real value parameters [α_{loc}, α_{glob}, α_{mix}] whose sum is equal to 1.
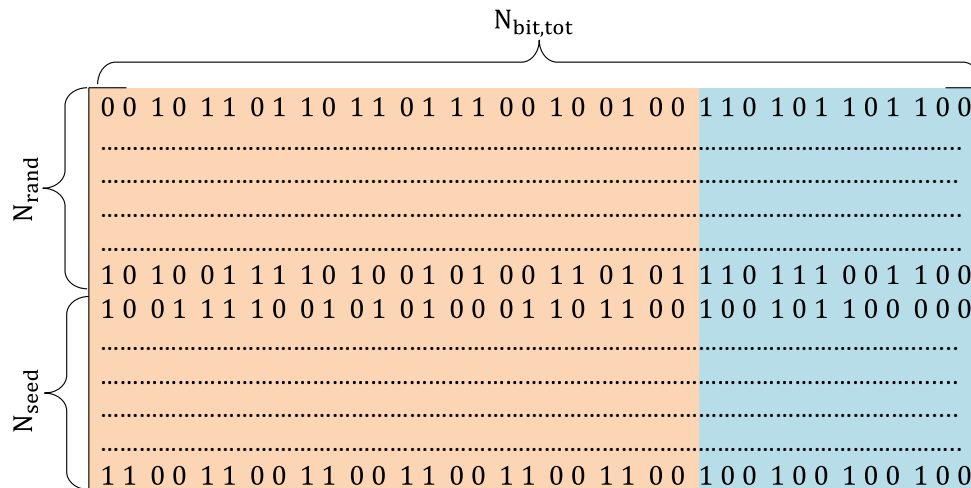
Figure 6.6: Example of the binary population composed of both random and seeded parts

For instance, if the suggested retrofit strategy is denoted with letter "A" (meaning strategy whose basic aim is to improve the overall ductility of the existing building), the corresponding triad will be [1, 0, 0]. Conversely, if the retrofit strategy is denoted with letter "B" (meaning strategy whose basic aim is to improve the lateral stiffness and strength of the existing building), the corresponding triad is [0, 1, 0].

Once α_{loc}, $\alpha_{glob,}$ and α_{mix} parameters are known, they are employed to calculate the number of chromosome in the "seeded" population which codify, respectively, purely local interventions, purely global interventions and "mixed" interventions theoretically needed to realize the selected strategy, as stated in the following relationships:

$$N_{loc} = \alpha_{loc} \cdot N_{seed}$$
$$N_{glob} = \alpha_{glob} \cdot N_{seed} \qquad\qquad (6.3)$$
$$N_{mix} = \alpha_{mix} \cdot N_{seed}$$

Therefore, in addition to the random binary matrix, the subroutine generates three different population accounting the individuals above mentioned.

In particular, the sub-matrix N_{loc} x $N_{bits,tot}$ is characterized by all zeros bits in the second part of the strings, whereas random bit is generated in the first part describing local intervention.

The sub-matrix N_{glob} x $N_{bits,tot}$ is characterized by all zeros bits in the first part of the strings, whereas random binary numbers are generated in the second part of the chromosomes which codify the global intervention.

Conversely, the sub-matrix N_{mix} x $N_{bits,tot}$ is characterized by random bits in the whole chromosome.

6.2 Creation of Finite Element Models (Pre-processing)

After the initialization of the population of candidate solutions, the next step is the building of mathematical models and the development of an appropriate finite element mesh to predict the mechanical behavior and to approximate the geometry of the given structure in retrofitted configuration with a sufficient degree of accuracy, as shown in Figure 6.7.
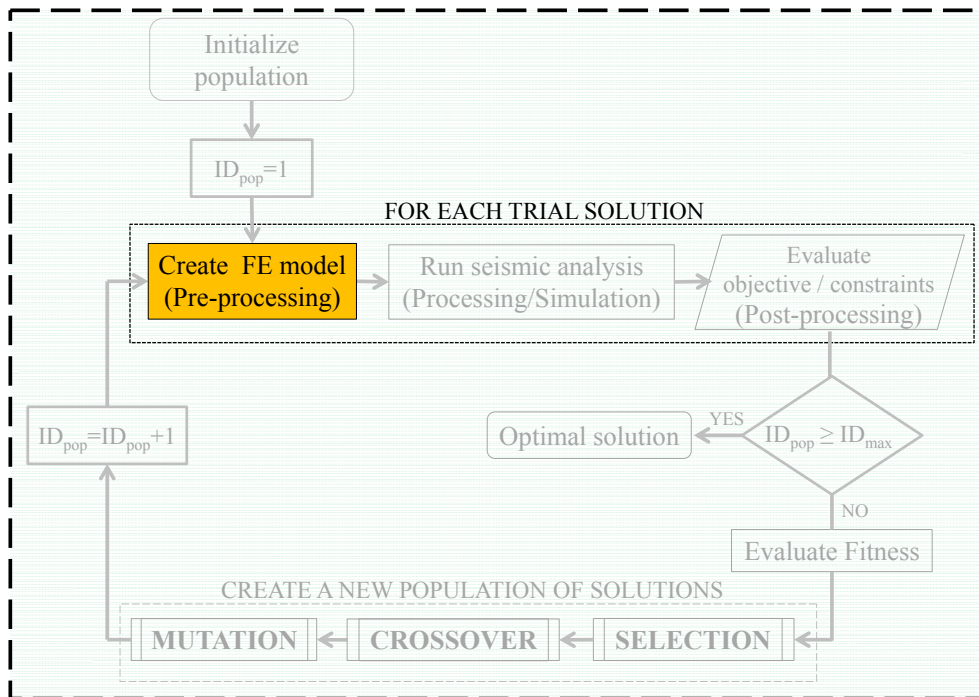
Figure 6.7: Pre-processing stage of the proposed procedure

To this end, it is previously necessary to define a finite element model of the existing building in its as-built state through a collection of Tcl text files which describe the physical problem to be executed in OpenSees (Figure 6.8).

In particular, the procedure requires a three-dimensional model to capture the response of the entire structural system and individual components under specific seismic demand. Having a 3D model enables correct evaluation of the capacity and ductility of the system under seismic loads acting along any given direction, not necessarily aligned with the principal axis of the structure.

Starting from the known model, it is then possible to obtain its "modified" (i.e. enhanced) version.

```
source "WipeAsBuilt.tcl"
source "BeamColNode.tcl"
Source "ColumnUnconfinedMaterial.tcl"
source "BeamMaterial.tcl"
source "BuildRCsection.tcl"
source "ColumnSection.tcl"
source "BeamSection.tcl"
source "Wsection.tcl"
source "ColumnElement.tcl"
source "BeamElement.tcl"
source "TrussElement.tcl"
source "Transformation.tcl"
source "Constraints.tcl"
source "GravLoadPushOver.tcl"
source "PushOverLoad.tcl"
source "RecorderOutPushOver.tcl"
source "StaticAnalisy.tcl"
source "PushOverAnalisyAsBuilt.tcl"
```

Main tcl file

Model

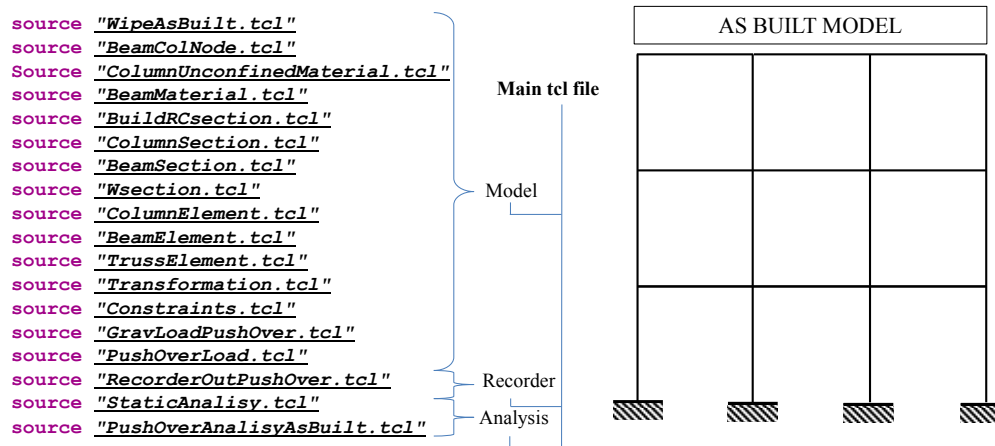Recorder

Analysis

AS BUILT MODEL

Figure 6.8: Example of a collection of Tcl files user-defined for OpenSees'analysis

As already said, each row of the binary matrix shown in Figure 6.9 represents a possible retrofitting intervention. Each chromosome of the population is composed of several genes which represent the design variables to be optimized.

Int. 1 → 0 0 1 0 1 1 0 1 1 0 1 1 0 1 1 1 0 0 1 0 0 1 0 0 1 1 0 1 0 1 1 0 1 1 0 0

...
...
...
...
...
...
...
...
...

Int. 100 → 1 1 0 0 1 1 0 0 1 1 0 0 1 1 0 0 1 1 0 0 1 1 0 0 1 0 0 1 0 0 1 0 0 1 0 0
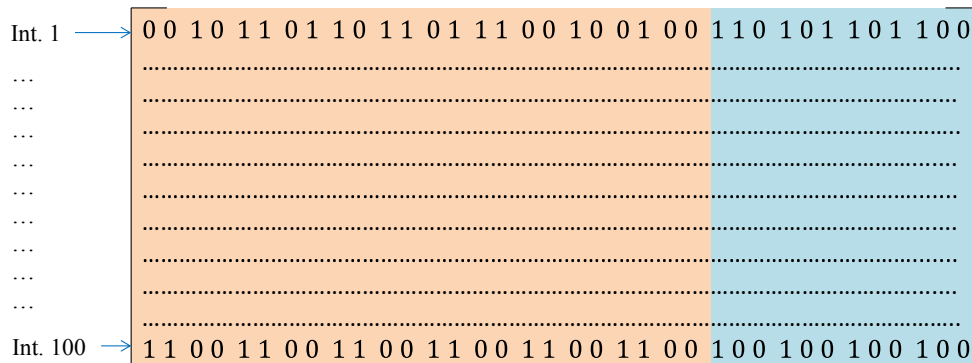
Figure 6.9: Correspondence between matrix rows and retrofit interventions

In particular, in the first part of the string, each design variable ranges between zero (as-built configuration denoted by a couple of bits "00") and 3 (denoted by a couple of bits "11").

Each couple of bits contains a code related to the number of FRP layers possibly employed for confining the corresponding column of the structure under consideration. In the second part of the genotype, whereas, the design variables which describe the global intervention range between 0 (denoted by the triad "000") and 7 (denoted by the triad "111") as shown in Figure 6.10.

Figure 6.10: Example of conversion from binary to decimal genotype

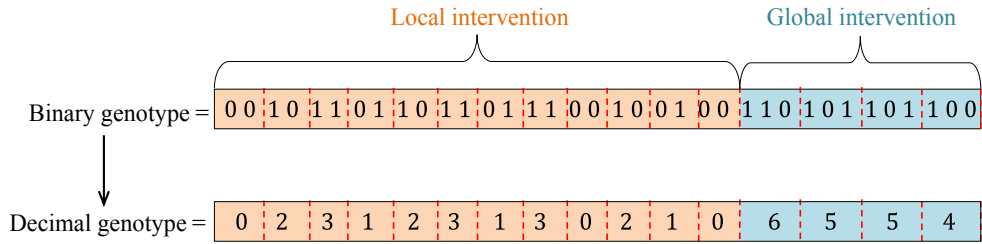However, examining the single chromosome string no information about the problem under consideration can be directly understood. It is only with the decoding of the chromosome into its phenotype that any meaning can be found in the representation.

In principle, the mapping genotype → phenotype is not part of the algorithm. It is rather problem dependent and should be supplied/invented by the user. Figure 6.11 depicts how a sequence of zeros in the genotype codifies nothing else than the as-built configuration.
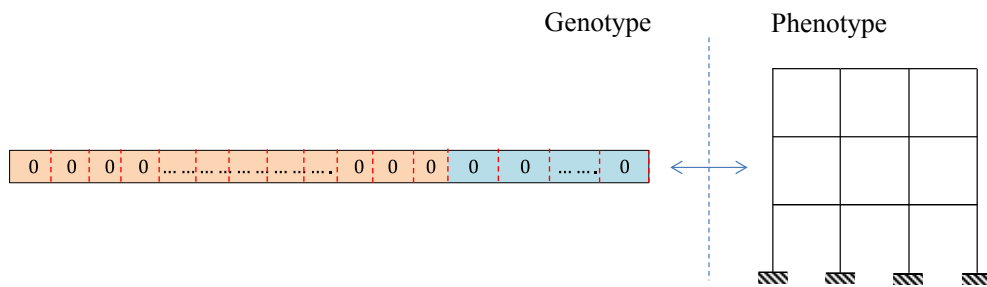
Figure 6.11: Example of mapping genotype ↔ phenotype for as-built configuration

Then, starting from the model of the existing structure, a specific subroutine of the procedure reads the population row by row (i.e. the genotype of the candidate solution) and automatically makes some modifications to the "as-built" model to include both possible local and global interventions (Figure 6.12).
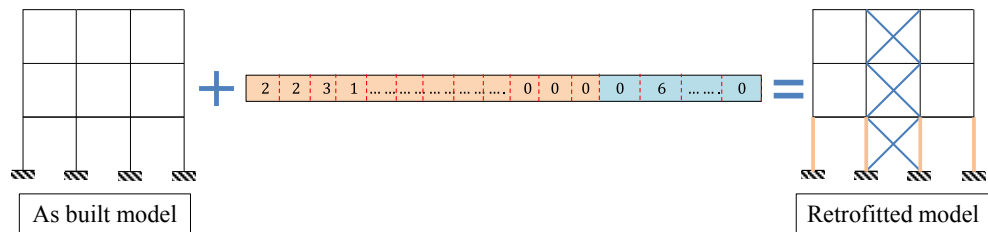
Figure 6.12: Schematization of building a retrofitted model starting from as-built one

6.2.1   Modeling of local intervention

The data collected in the first part of the chromosome are employed for modifying the original (unconfined) stress-strain relationship describing the material behavior for each column, as schematically shown in Figure 6.13.
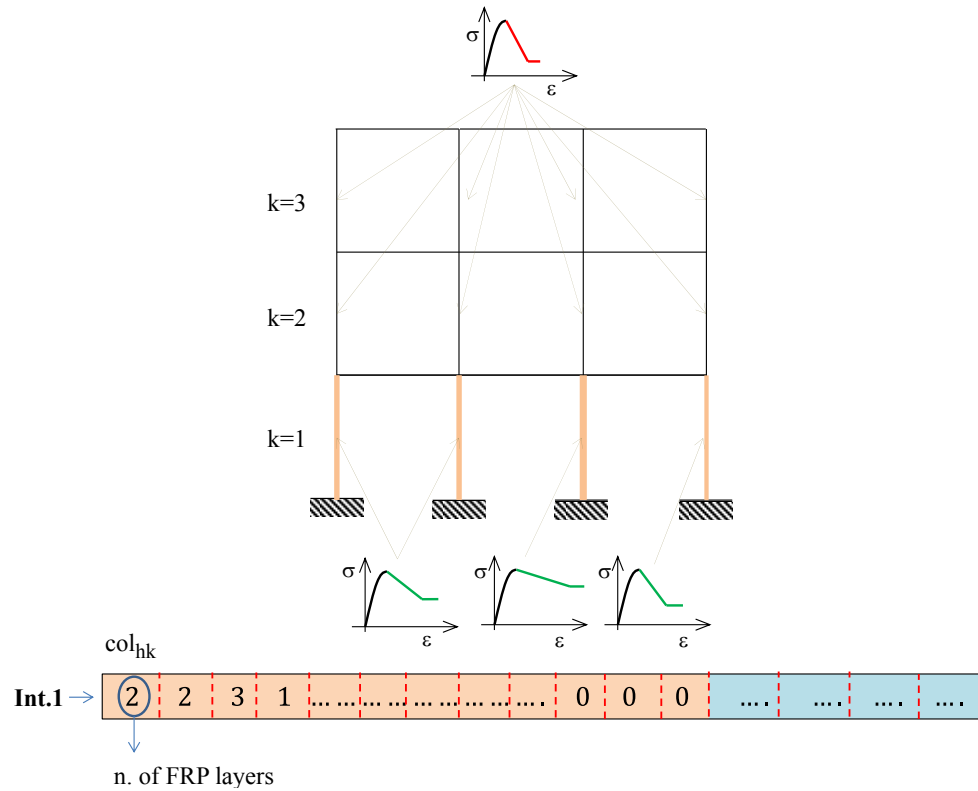
Figure 6.13: Modification of columns' material according to the corresponding FRP wraps

The command *Concrete01* available in OpenSees library is used to construct a uniaxial Kent-Scott-Park [334] concrete material object with a degraded linear unloading/reloading stiffness and no tensile strength in accordance to the work of Karsan and Jirsa [335].

The parameters needed to define such constitutive model are the concrete compressive strength at 28 days; the strain at maximum strength, the crushing strength and the strain at crushing strength. According to the aforementioned model, the effects of confinement are taken into account increasing the ductility as shown in Figure 6.14.

Based on several parameters such as the number of FRP layers, the shape of transverse section and the type of FRP considered, the original mechanical parameters describing the concrete behavior for each column are duly modified to define the non-linear mechanical behavior of the confined section.

For this purpose, a function updates the values of the crushing strength and the strain at crushing point in accordance with the number of FRP wraps found in the chromosome.
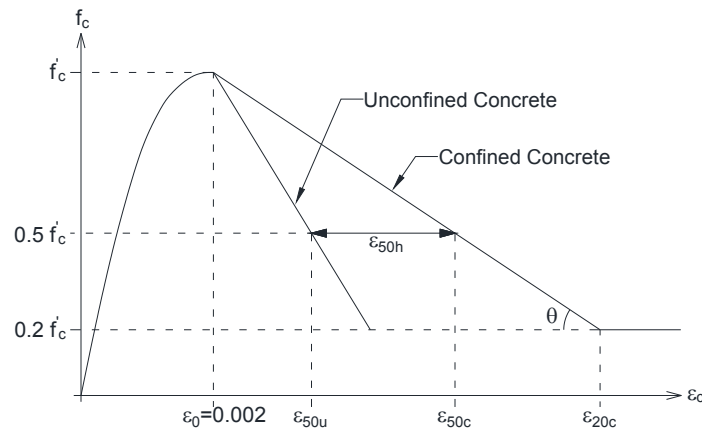
Figure 6.14: Kent and Park model [334] available in OpenSEES [317]

6.2.2   Modeling of global intervention

The information collected in the second part of the chromosomes are employed for modeling a new steel bracing system properly added for working in parallel with the existing building.

The *Steel01* command available in OpenSees' library is used to construct a uniaxial bilinear material object with kinematic hardening representative of the elastic-plastic behavior of steel. The following assumption is intended for keeping the number of design variables describing the global intervention as small as possible:

1. the transverse section of the diagonal members is identified by means of a label corresponding to a commercial steel profile (Figure 6.15);
2. only the steel profiles of the first story level (A_1) are reported in the chromosomes, as shown in Figure 6.16.

As for the first assumption, the current implementation of the proposed procedure

employs three bits for each variable. Hence, only $2^3 = 8$ choices are available to select the profile of diagonals possibly installed at the first story level along the corresponding beam.
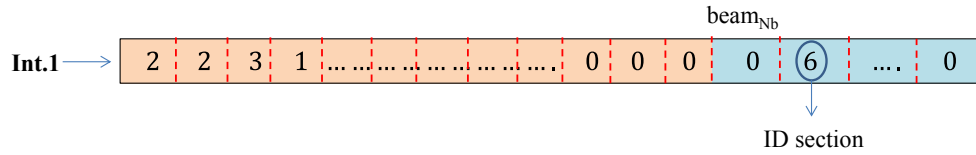
Figure 6.15: Encoding of diagonal's profile (1ˢᵗ floor) in the second part of chromosome

As already seen, the design variables in the second part of genotype represent a label which can range from 0 (absence of bracing system) to 7. It points to a position in a commercial steel profile table containing a list of commercial profiles with their relevant geometric properties available therein (Figure 6.16).
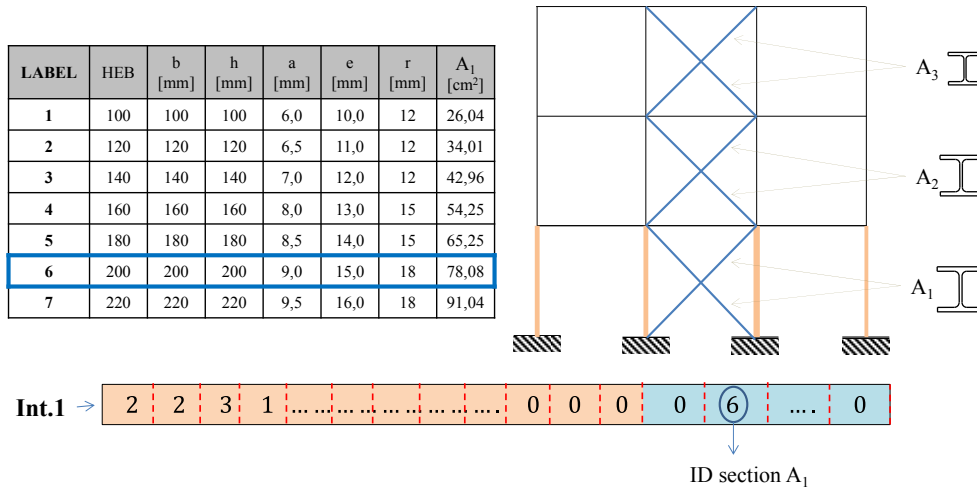
Figure 6.16: Set of commercial steel profiles and corresponding labels

A simple relationship is assumed between the section of steel members at the first level and the section of steel bracings at upper levels are defined according to the Eq. (6.4):

$$A_{k,des} = \frac{\sum_{j=k}^{n} h_j \cdot W_j}{\sum_{i=1}^{n} h_i \cdot W_i} \cdot A_1 \tag{6.4}$$

where h_j represents the position in height of the story with respect to the foundation

level, n is the total number of stories, W_j is the seismic mass of the j-th floor, A_1 is the area of the cross-section of the bracing elements at the first level and $A_{k,des}$ is the theoretical area of the bracing cross section required at the k-th floor.

The obtained areas are then rounded by taking into account the available ones among the commercial profiles. It is worth highlighting that any other consistent design criteria, defining the upper-level sections depending on the first level ones, might be possibly adopted in lieu of Eq. (6.4). Hence, once the theoretical areas are known, a specific subroutine searches for the steel commercial section whose area is just greater than $A_{k,des}$ within the available table.

It is clear that the greater the number of bits used to code the design variables of the global interventions, the more choices the profile table should have. For instance, if four bits are employed for each variable, $2^4 = 16$ alternative steel profiles should be included in the table.

Once the nominal geometric properties of the bracing members are known, the procedure uses the well-known fiber section [336] approach for better accounting the material inelasticity. In particular, the H-shaped cross-section of bracing elements is divided into three sub-regions: two horizontal regions also known as "flanges", and one vertical region termed "web".

Each region is discretized into a number of fibers which comply with beam kinematics (Figure 6.17). Each fiber, in turn, follows its own constitutive model.
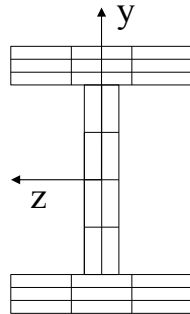
Figure 6.17: Fiber section for modeling material inelasticity in bracing members

Force-based spread plasticity elements are used to model the concentric steel bracings. In particular, the command *nonlinearBeamColumn* available in OpenSees library is used to consider the spread of plasticity along the element.

Each bracing element is discretized into a number of sections located at the Gauss-Lobatto quadrature integration points. To represent accurately the nonlinear material response of a force-based beam-column element, four to six Gauss–

Lobatto integration points are typically used [337]. In the current application, the number of integration points chosen is five: two integration points at the element end and three in the middle (Figure 6.18).
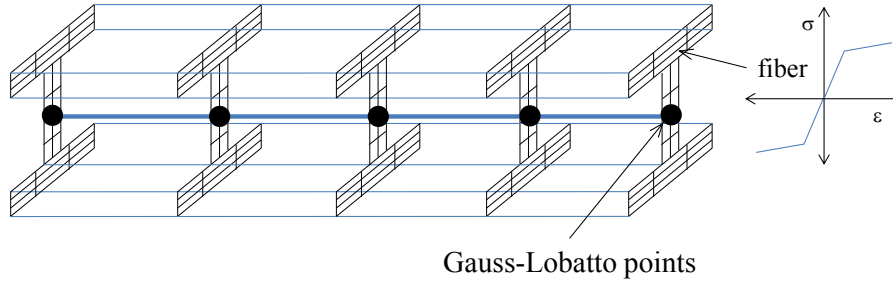
Figure 6.18: Representation of integration points in the bracing members

Moreover, an accidental eccentricity is assigned to the middle points of diagonal elements (out of the plane where the bracing system lies) according to EN 1993-1-1 [338] in order to simulate buckling in the compressed member. Hence, each diagonal is discretized into two members as shown in Figure 6.19.
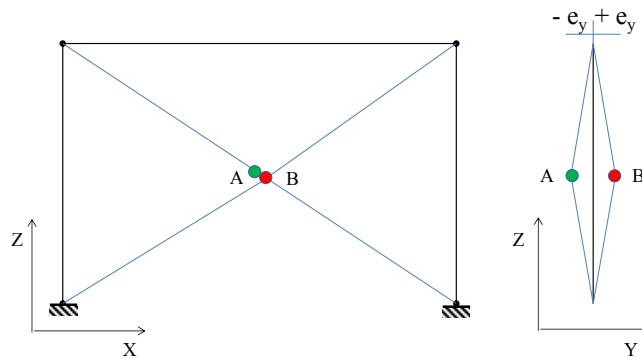
Figure 6.19: Eccentric middle points in diagonal members

Due to the cyclic nature of the equivalent seismic actions, as schematically shown in the Figure 6.20, therefore, the compressive axial force will occur once in the diagonal member connecting the points Q and S, and once in the diagonal member connecting the points P and R.

For this reason, the concentric bracing system, for each plane frame, is discretized into four elements: element 1 and 2 are connected in the eccentric middle point A, while the elements 3 and 4 are connected in the eccentric middle point B.
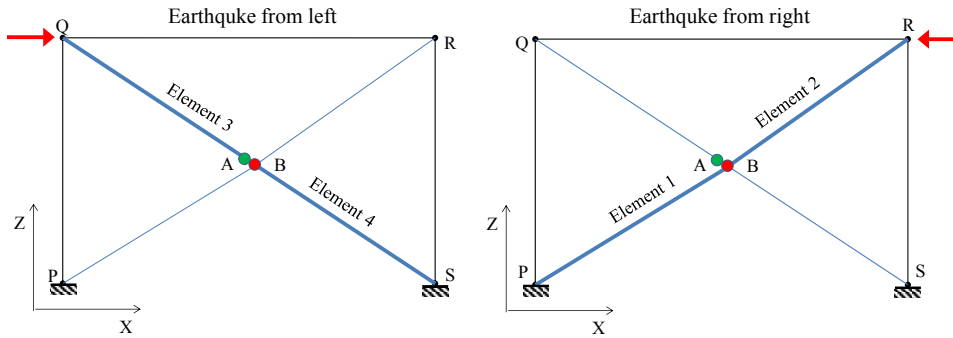
Figure 6.20: Representation of diagonals susceptible to buckling phenomena

That said, the purpose of the pre-processing step is to translate each candidate solution included in the population into its corresponding phenotype by building an appropriate finite element model as shown in Figure 6.21.
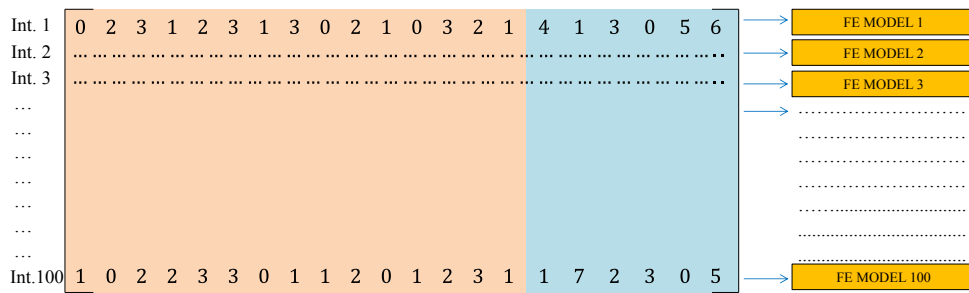
Figure 6.21: Correspondence between a decimal genotype and an FE model

The decoding basically consists in writing new Tcl files which describe both local and global techniques, in compliance with the described assumptions (Figure 6.22).
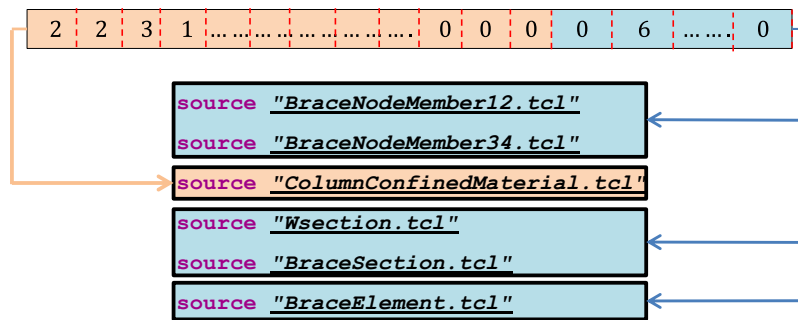
Figure 6.22: Writing of new Tcl files describing both local and global interventions

6.3   Seismic analysis (Processing)

In the procedure, the processing stage is carried out exclusively by the OpenSees framework that is capable to provide an extensive and reliable simulation of the structural response by mean of a seismic analyses solver (Figure 6.23). It is worth noting that such time-consuming task is a "black box" process because the user cannot see what's going on.
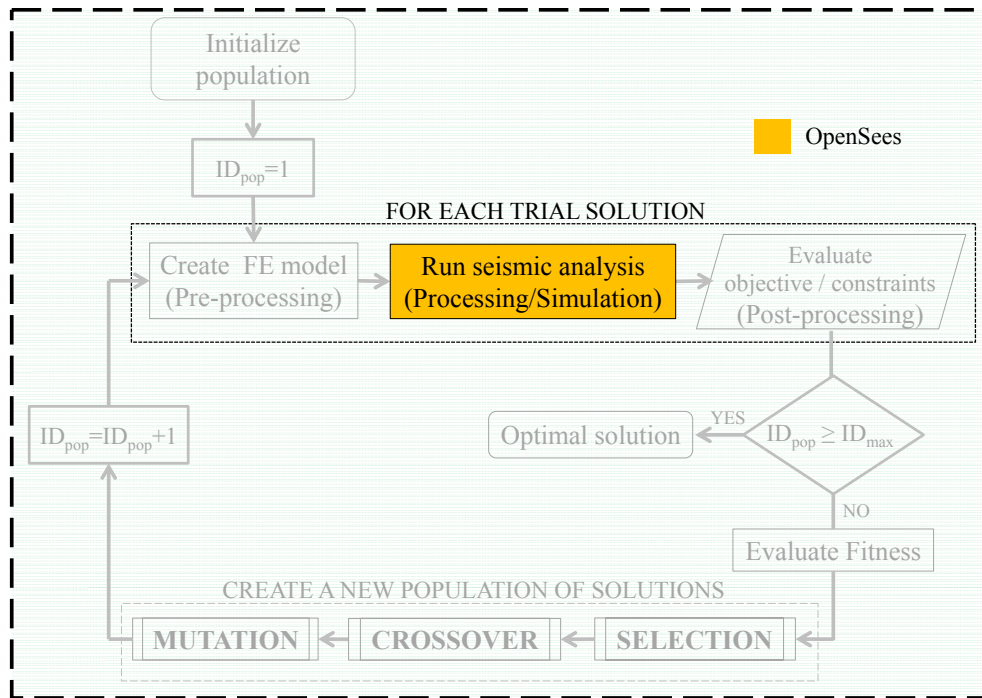
Figure 6.23: Simulation step within the proposed procedure

OpenSees is able to accommodate any advanced - linear or nonlinear, static or dynamic - analysis procedure. However, according to the Performance-Based Design approach, the procedure relies on a seismic non-linear analysis of the building in order to estimate the probable performance of the retrofitted building under various scenario events.

Such kind of analysis is required to predict inelastic deformations (i.e. to assess the damage status). In fact, the non-linear analysis allows more accurate determination of stresses, strains, inelastic deformations, forces, and displacements of critical components, results that can be utilized for the assessment of the global capacity and the ductility of the structure.

Structural engineers are usually driven by the need for accurate prediction of the building's internal forces and deformations along with the need for reducing the computational effort for the analysis.

Due to this reasons, the Non-Linear-Time-History analysis cannot be considered as the most suitable method for seismic analysis of existing structures within the proposed optimization procedure which requires a high number of iterations.

On the contrary, non-linear static (pushover) analyses, which nowadays have widespread applicability in the field of assessment of existing building, can be preferred as they require neither accelerometric signals nor accurate stress-strain relationships under cyclic actions.

However, it is worth to remind that the non-linear static procedure is only permitted to be used on structures with certain characteristics: it is typically only valid for the "first mode dominated" structures because the procedure fails to account accurately for higher mode dynamic effects. In fact, only the first mode of vibration is considered and, hence, this method is theoretically not suitable for irregular buildings for which higher modes become important.

Non-linear static procedure is intended at determining a capacity curve which provides the simplified trend of the equivalent lateral global force as a function of the lateral displacement of the structure in a control node when a system of lateral forces is applied to the structure and increased proportionally until collapse.

The lateral force distribution is determined by multiplying the mass matrix by an acceleration profile. According to Italian building standard NTC2008 [15], two acceleration profiles should be used: the first one is coincident to the first mode shape, while the second one is constant. In the preliminary applications of the proposed procedure, the capacity curve of regular structures (whose response is clearly dominated by the first mode of vibration) is determined through an incremental static analysis on a nonlinear model of the structure subjected only to lateral loads distribution with an inverted triangle (first mode) shape.

This assumption is aimed at reducing the computational time: further force distributions might be easily taken into account for performing the seismic analysis, although the introduction of another pattern of lateral loads obviously will double the computational effort. In particular, the response of the structures is investigated in the main orthogonal stiffness directions, also taking into account the possible inversion of the seismic action.

Therefore, for each candidate solution, the OpenSees framework executes four pushover analyses: the magnitude of the horizontal forces is monotonically

increased in the direction of a given degree-of-freedom, as schematically shown in the Figure 6.24. Hence, for each individual four incremental pushover analyses are carried monitoring the displacement of the control node in X towards positive, X towards negative, Y towards positive and Y towards negative, respectively.
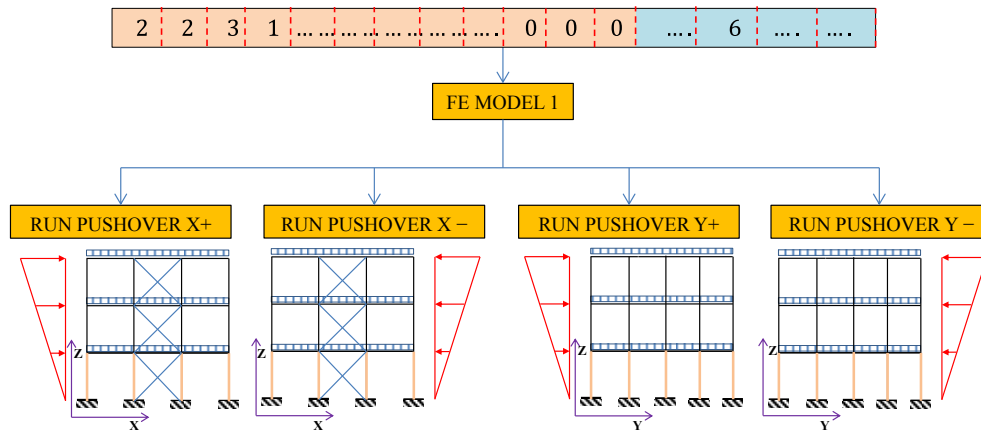
Figure 6.24: Load patterns accounted for pushover analysis

Once the gravity loads have been applied in a force-control strategy, they are held constant because they always act on the structure. A displacement control strategy is then adopted to perform the pushover analysis. A maximum displacement D_{maxU} equal to $0.03*H_{tot}$ (total height of the building) is sought, while the displacement increment is set to 1% of the desired maximum displacement. In other words, the maximum number of load steps for the non-linear static analysis is 100. However, if the analysis fails to reach the desired displacement, the procedure iteratively reduces the value of D_{maxU} until it is reached at the control node.

Moreover, as the nonlinear models do not always converge for the analysis options of choice, it is necessary to check for convergence at each step and trying different options if the analysis fails at any particular step.

In the current implementation, the pushover analysis includes an incremental iterative procedure which tries different solutions to improve the chances of convergence. Specifically, at each step, if the analysis fails using the current solving algorithm, another strategy using initial stiffness iterations is attempted. Subsequently, in case of convergence failure of the previous one, the solving algorithms (among those available from OpenSees library) are used in the following order:

1. Krylov-Newton Algorithm which uses a modified Newton method with Krylov subspace acceleration to advance to the next time step;

2. Newton-Rapson Algorithm which is, on the one hand, the most widely used and most robust iterative method for solving systems of nonlinear algebraic equations but, on the other hand, it is also the most demanding in terms of computational effort, because the stiffness matrix need to be updated at each iteration step;

3. Broyden Algorithm which is generally used in critical cases only, because the algorithm densifies the iterations in correspondence of the points where the solution has difficulty to converge;

4. Newton-Rapson with Line Search Algorithm which introduces the line search to solve the nonlinear residual equation and does not update the stiffness matrix at each step with a reduced computational effort but a greater number of iterations required.

In conclusion, since the genetic algorithm works with a population of independent solutions and the proposed procedure in the pre-processing step create as many separate structural models as the rows of the matrix, it is worth noting that this step can be run completely in parallel (Figure 6.25) exploiting the potential of any multi-core processor. This aspect will be discussed in detail in Section 6.10.
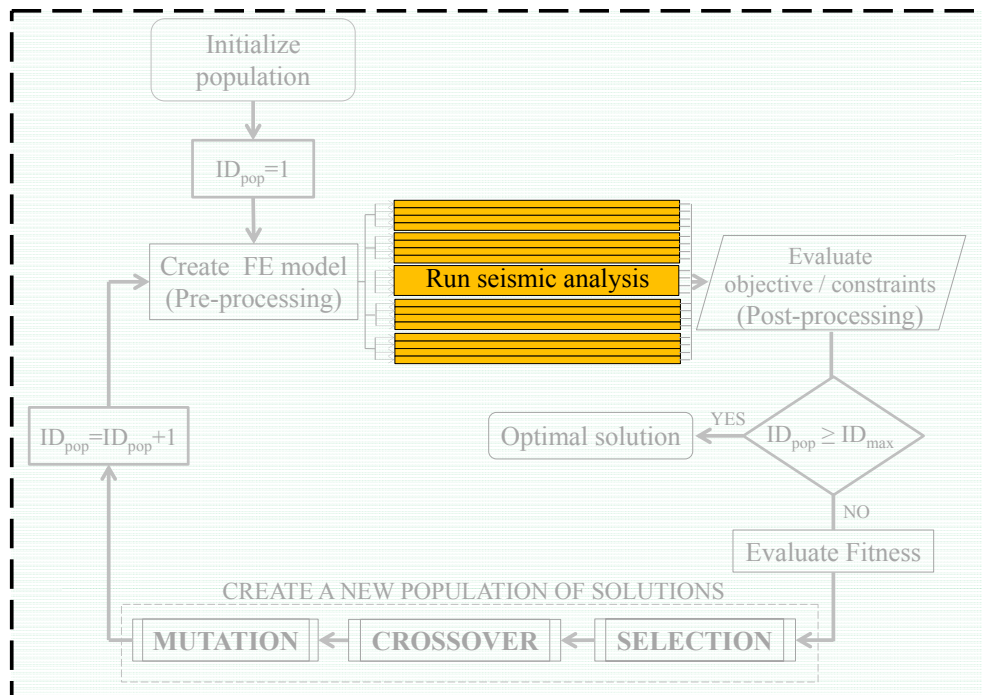
Figure 6.25: Parallel execution of seismic analyses

6.4   Post-processing

Within the proposed procedure, the post-processing stage plays the fundamental role of a "bridge" between simulation and optimization problems as described in the flow-chart of Figure 6.26.

This phase of the procedure basically interprets the output files obtained from the simulation stage in order to evaluate the objective (cost function) and the constraints (performance checks) for each trial solution.
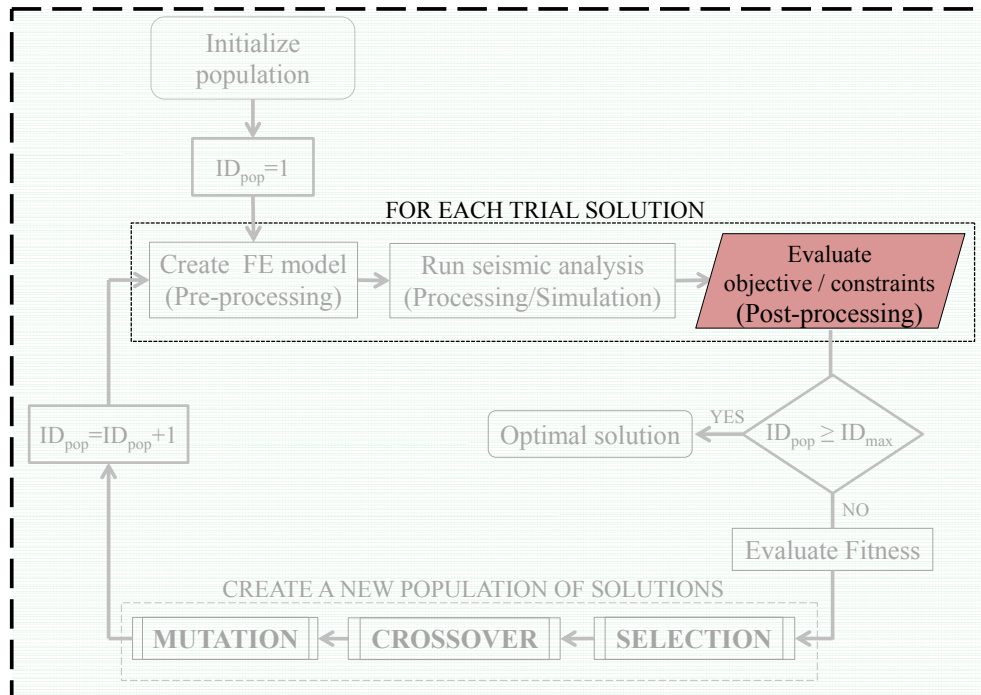
Figure 6.26: Post-processing step within the proposed procedure

6.4.1   Evaluation of constraints

In accordance with Eq. 5.2, the procedure evaluates the Limit State function g_{LS} which is the difference between the capacity $C_{LS,i}$ of the strengthened structure and the corresponding demand $D_{LS,i}$ at both the Limit State of Damage Limitation and Life Safety.

In particular, the outcomes of the incremental static analysis on the nonlinear model of the structure (subjected to a triangular distribution of lateral forces) are therein handled to describe the global inelastic behavior of the whole system in

terms of force-displacement relationship and to depict the so-called capacity curve (Figure 6.27). The force and displacement parameters selected by the subroutine to build the afore-mentioned curve are the shear base and the average displacement of a control node chosen in the vicinity of the center of gravity of the top floor.
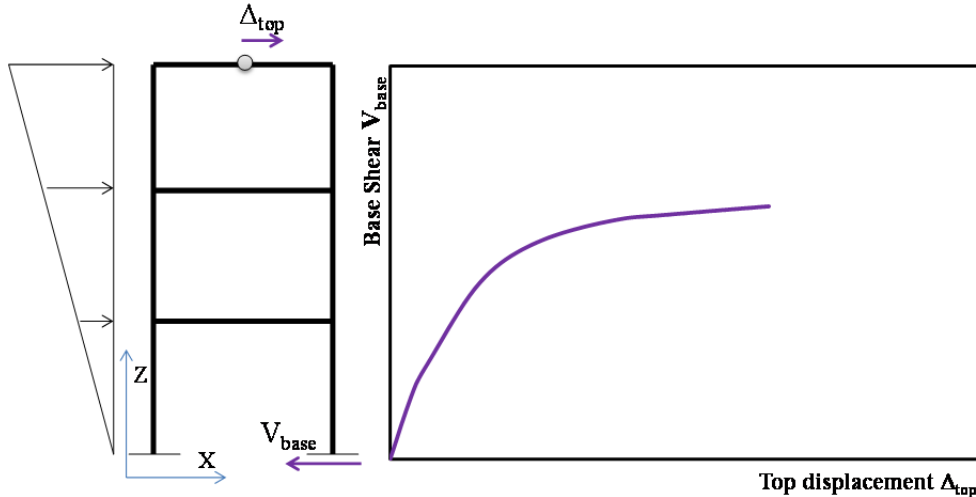
Figure 6.27: Static Non-Linear Analysis (left) and Capacity curve (right)

For the calculation of the seismic capacity C_{LS}, it is worth to remind the difference between two parameters that could be taken into account as damage indexes: the chord rotation and the inter-story drift. The former is the angle between the tangent to the axis at the yielding end and the chord connecting that end with the zero-curvature point. It is expressed by the geometrical relationships shown in Figure 6.28:

$$\theta_{ij,Y}^{(d)} = \frac{\Delta x_i}{L_{V_{iY}}} = \frac{\phi_{Yi}L_{V_{iY}} - \delta_i\left(L_{V_{iY}}\right) + \delta_{Xi}}{L_{ij} - L_{V_{iY}}}$$

(6.5)

$$\theta_{ji,Y}^{(d)} = \frac{\Delta x_j}{L_{V_{jY}}} = \frac{\phi_{Yj}L_{V_{jY}} - \delta_j\left(L_{V_{iY}}\right) + \delta_{Xj}}{L_{ij} - L_{V_{jY}}}$$

(6.6)
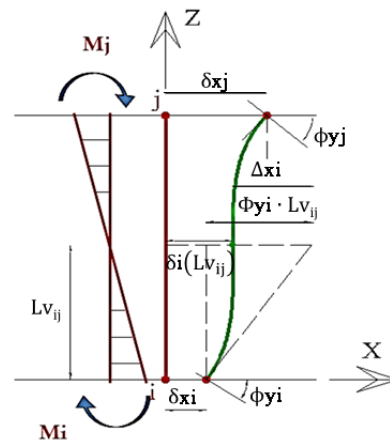
Figure 6.28: Geometric definition of the chord rotation

Likewise, the inter-story drift is defined as the ratio between the relative displacement and the specified distance between two given nodes:

$$\theta = \frac{\left|\delta_{Xi} - \delta_{Xj}\right|}{L_{ij}} \tag{6.7}$$

In the simplified assumption of "soft-story" mechanism (read Section 1.2.2.2.), where the diagram of the bending moment in the columns has a flag-like shape, the shear length tends to be equal to L/2 so that the chord rotation can be approximated with the inter-story drift (see Figure 6.29).

| Chord rotation ≈ Inter-storey Drift | Chord rotation ≠ Inter-storey Drift |
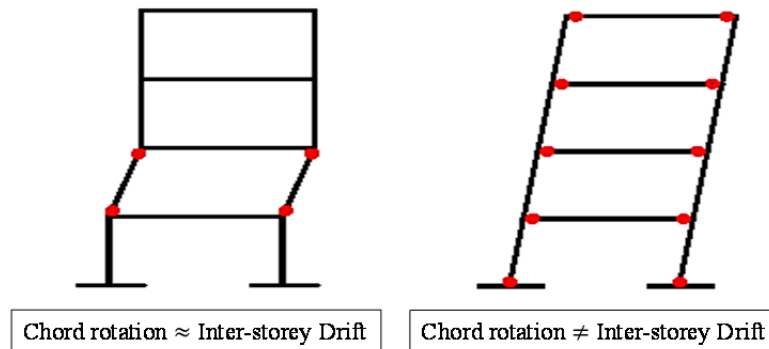
Figure 6.29: Example of soft-story (left) and global mechanism (right)

Therefore, inter-story demand drifts are considered herein as damage index in order to find the pushover step at which the Limit States are achieved. In accordance with the above-mentioned assumption, the structure reaches the Limit State at the exceeding of certain thresholds capacity value.

To this end, the drift capacity δ_C of frame elements at SLD and SLV is defined in terms of chord rotation at yielding θ_y and collapse conditions θ_{um}, respectively. With regard to the latter, the capacity chord rotation θ_{um} is herein assessed by the empirical formulation stated in Eq. (6.8) [339]:

$$\delta_{C,SLV} = \theta_{um} = \frac{1}{\gamma_{el}} \cdot 0{,}016 \cdot \left(0{,}3^{v}\right) \cdot \left[\frac{\max(0{,}01;\omega')}{\max(0{,}01;\omega)} \cdot f_c\right]^{0{,}225} \cdot \left(\frac{L_v}{h}\right)^{0{,}35} \cdot 25^{\left(\alpha\rho_{sx}\frac{f_{yw}}{f_c}\right)} \cdot \left(1{,}25^{100 \cdot \rho_d}\right)$$

(6.8)

where h is the depth of cross-section, L_v is the ratio moment/shear at the end section, a is the confinement effectiveness factor, ω (ω') is the mechanical reinforcement ratio of the tension (compression) longitudinal reinforcement, v is

the dimensionless axial force, ρ_d is the steel ratio of diagonal reinforcement, f_c and f_{wc} are the concrete compressive strength and the stirrup yield strength, respectively. Similarly, the procedure calculates the chord rotation at yielding θ_y in accordance with the empirical relationship:

$$\delta_{C,SLD} = \theta_y = \left(\theta_{um} - \theta_{um}^{pl}\right) \tag{6.9}$$

where the term θ_{um}^{pl} is represented below:

$$\theta_{um}^{pl} = \frac{1}{\gamma_{el}} \cdot 0{,}0145 \cdot \left(0{,}25^v\right) \cdot \left[\frac{\max(0{,}01;\omega')}{\max(0{,}01;\omega)} \cdot f_c\right]^{0,35} \cdot f_c^{0,25} \cdot \left(\frac{L_v}{h}\right)^{0,35} \cdot 25^{\left(\alpha\rho_{sx}\frac{f_{yw}}{f_c}\right)} \cdot \left(1{,}275^{100\cdot\rho_d}\right)$$
(6.10)

Since the magnitude of global axial force changes during the incremental static analysis, the subroutine calculates the value of θ_y and θ_{um} for each pushover step. Moreover, the evaluation of the seismic response takes into account the existence of two displacement components along the two main directions.

Hence, the subroutine defines a curvilinear eligibility domain for the drifts exceeding which the Limit State is reached. In particular, the analytical equation of the domain contains a variable exponent α which varies in the range [1-2]. An average value of 1.5 is herein assumed as shown in Eq. (6.11).

$$\left(\frac{\delta_D}{\delta_{C,LSi}}\right)_x^\alpha + \left(\frac{\delta_D}{\delta_{C,LSi}}\right)_y^\alpha \leq 1 \quad \text{with } \alpha = 1.5 \tag{6.11}$$

Once the steps of Limit States are found, the subroutine locates the point on the pushover curve and extracts the displacement Capacity value C_{LS} (Figure 6.30).
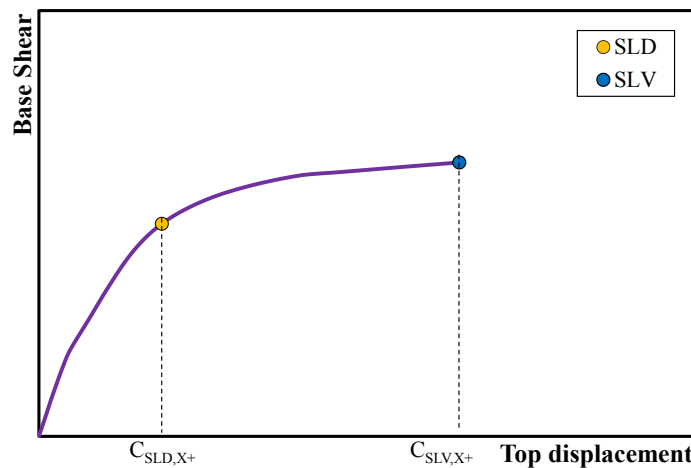
Figure 6.30: Achievement of displacement Capacity during the pushover analysis

Obviously, the greater number of load steps the user set for the incremental analysis, the more accurate the calculation will be. The subroutine repeats the calculation of C_{LS} at all the performance level of interest and for the other load patterns accounted (Table 6.1).

Table 6.1: Displacement capacity values

	P.L.	**PUSHOVER X+**	**PUSHOVER X-**	**PUSHOVER Y+**	**PUSHOVER Y-**
FE MODEL 1	SLD	$C_{SLD,X+}$	$C_{SLD,X-}$	$C_{SLD,Y+}$	$C_{SLD,Y-}$
	SLV	$C_{SLV,X+}$	$C_{SLV,X-}$	$C_{SLV,Y+}$	$C_{SLV,Y-}$

On the other hand, the procedure includes the N2-Method to estimate the maximum displacement demand D_{LS} for the structure of interest. In order to determine the so-called "performance point", the post-processing subroutine converts the pushover curve to a Capacity Spectrum which should be represented in the Acceleration-Displacement-Response-Spectra (ADRS) format characterized by spectral acceleration $S_{ae}(T)$ on the y-axis and spectral displacement $S_{de}(T)$ on the x-axis. The multi-degrees-of-freedom (MDOF) system is transformed into an equivalent single-degree-of-freedom (SDoF) system as shown in Figure 6.31.
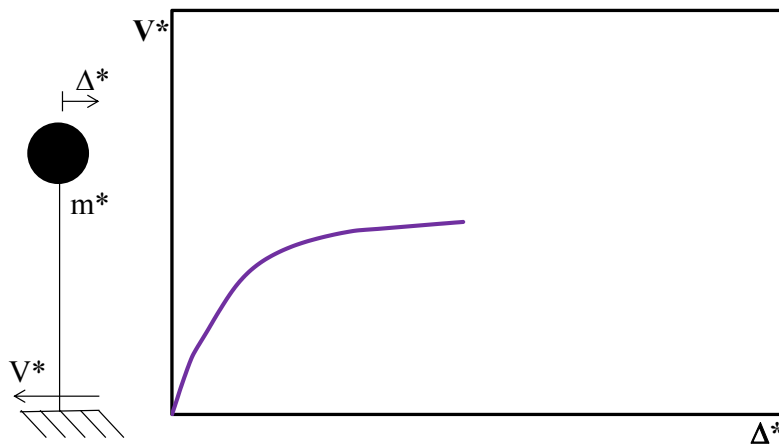
Figure 6.31: Equivalent SDoF system (left) and its response curve (right)

Force V* and displacement Δ* of the equivalent SDOF system are related to the corresponding parameters V and D which describe the global behavior of the real system by the following relationships:

$$V^* = \frac{V}{\Gamma}$$

$$\Delta^* = \frac{\Delta}{\Gamma}$$

(6.12)

where Γ is the modal participation factor, defined as:

$$\Gamma = \frac{\Phi^T M_\tau}{\Phi^T M \Phi}$$

(6.13)

where M_τ is the seismic mass of each story, M is the total mass of the structure and Φ is the vector whose components describe the shape of lateral load pattern.

This curve depicts the global behavior of a simplified oscillator and is characterized by a trend similar to the pushover curve representative of the MDoF system.

As known, N2-Method provides direct relationships between ductility demand, elastic period and reduction factor (which represents the dissipative capacity of the structure) based on well-established rules derived by analyzing the hysteretic response of bilinear SDOF [86].

Therefore, the above-mentioned V*-D* curve is simplified in order to obtain a bilinear relationship. In particular, secant stiffness k* of the SDOF (or the elastic period T*) is identified by imposing the passage of the bilinear curve for the point with an ordinate equal to 0.6 V_{bu}* as shown in Figure 6.32.
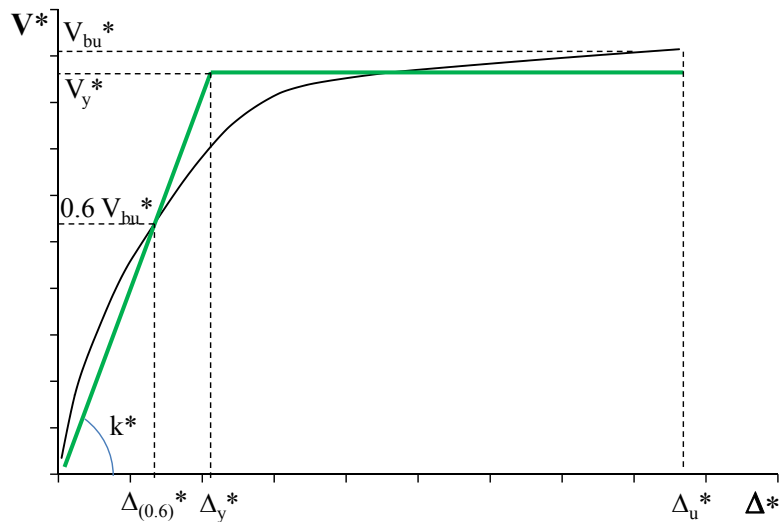
Figure 6.32: Elastic-plastic behavior of equivalent SDoF after the bilinearization

The ultimate displacement Δ_u^* is defined as the point corresponding either to a reduction of base shear up to 85% of the structural strength V_{bu}^* or to the peak strength (if the base shear does not decrease after the peak).

Hence, the plastic branch is uniquely identified by the yield displacement point which marks the transition between the elastic and plastic fields. Such point is found by equating the areas under the capacity curve A^* and the bilinear curve, according to the following system of equations:

$$\begin{cases} A^* = 0.5 \cdot V_y^* \cdot \Delta_y^* + V_y^* \cdot \left(\Delta_u^* - \Delta_y^* \right) \\ V_y^* = k^* \cdot \Delta_y^* \end{cases} \tag{6.14}$$

where V_y^* is the yielding force which depends on the yielding displacement. Since the system of equations leads to a nonlinear expression of the unknown value Δ_y^*, the subroutine iteratively searches for such displacement value in the range [0-Δ_u^*] until the difference between the area A^* and the area under the bilinear curve is lower than a given tolerance. Once all the parameters describing the bilinear curve are known, the subroutine calculates the displacement demand Δ_{max}^* for the equivalent SDOF as the intersection point between the Capacity Spectrum and the Inelastic Response Demand Spectrum (IRDS).

The latter is obtained starting from the Elastic Response Demand Spectrum (ERDS), scaled by the reduction factor R_μ^* of the SDOF. According to the Italian Code [15], the parameters needed to describe the branches of the ERDS depend on the seismic hazard level which is based on the geographical coordinates (Figure 6.33) of the construction site, the nature of subsoil/soil and nominal life of the building and its "importance".
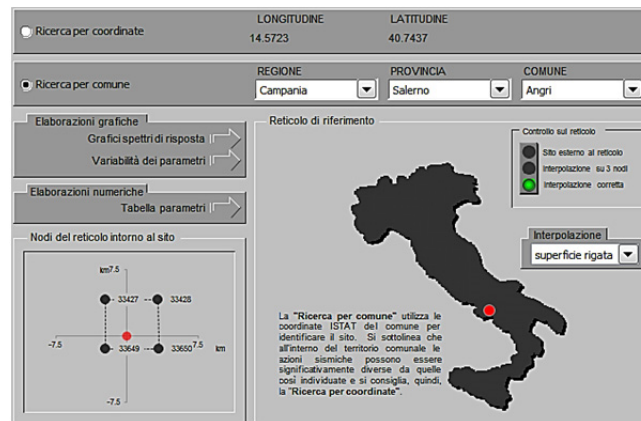
Figure 6.33: Example of searching for geographical coordinates

To this end, in addition to a FE model of the existing building it is necessary to specify the seismic risk reference parameters needed to build the four branches of the aforementioned ERS (Table 6.2).

Table 6.2: Example of risk reference parameters

Performance Level	Exceedance probability during the Nominal Life	a_g [g]	F_0 [-]	Tc [s]
SLD	63%	0.258	2.291	0.545
SLV	10 %	0.354	2.288	0.576

The force reduction factor R_μ, whereas, depends on whether the elastic period T^* is lower or greater than the period Tc which represents the transition period between the constant pseudo-acceleration and constant pseudo-velocity branch. According to the following direct μ-T-R_μ relationship:

$$R_\mu = \begin{cases} 1 + (\mu - 1) \cdot \dfrac{T^*}{T_C} & \Rightarrow T^* < T_C \\ \mu & \Rightarrow T^* \geq T_C \end{cases}$$

(6.15)

if $T^* > T_C$ (flexible system), the equal displacement rule [90] is applied. In this case, the inelastic displacement demand required by the equivalent SDOF system S_d^* is equal to the maximum displacement S_{de}^* that the system would undergo in case of linear elastic behavior as shown in Figure 6.34.
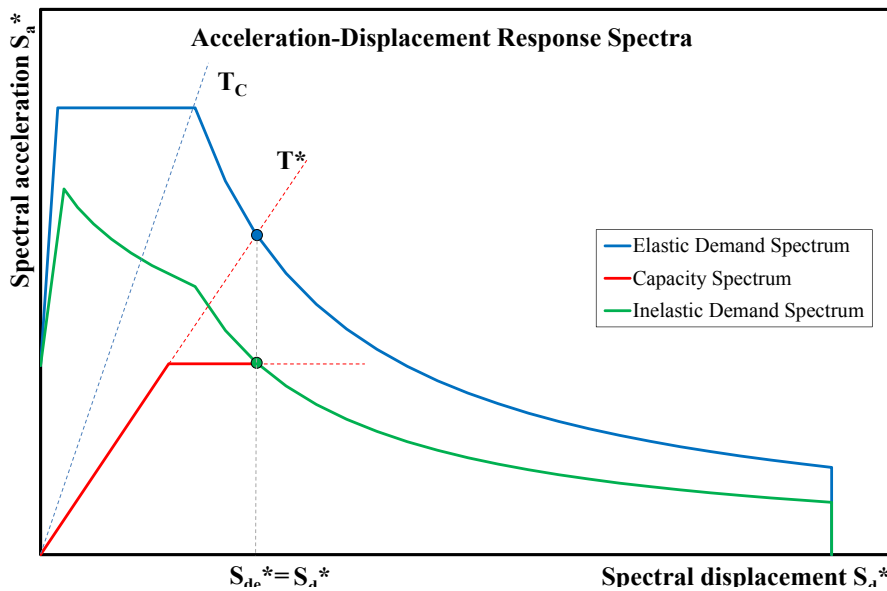
Figure 6.34:Equal displacement rule and performance point

If $T^* < T_C$ (rigid system) the equal energy rule is applied: the inelastic displacement demand required by the equivalent inelastic SDOF system is greater than the maximum displacement that the system would undergo in linear elastic behavior as shown in Figure 6.35.
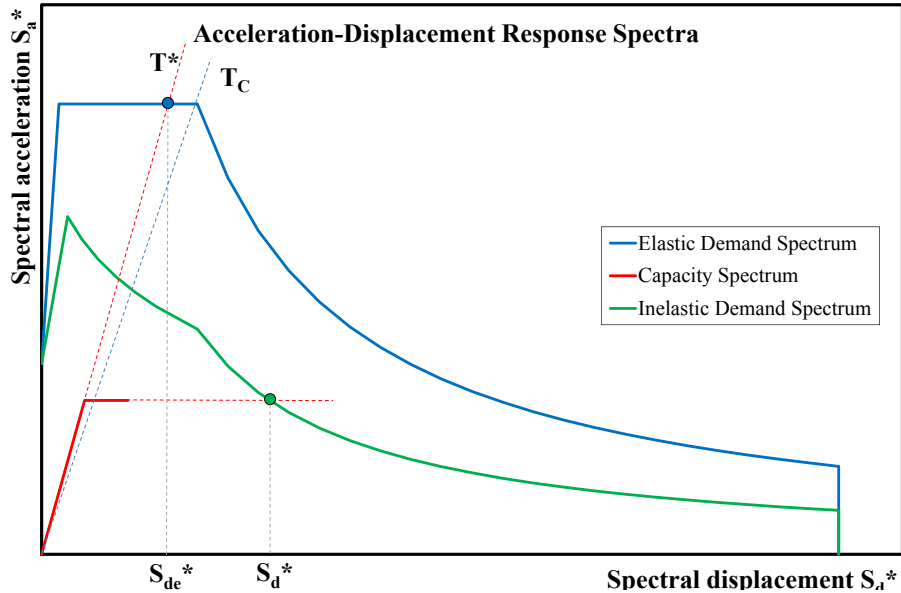
Figure 6.35: Equal energy rule and performance point

As the last step of N2-Method, the procedure converts the inelastic displacement demand of the equivalent SDOF system $S_d^*{}_{max}$ to the global inelastic displacement demand of the original multi-degree-of-freedom system according to the relationship below:

$$D_{LS,i} = \Gamma \cdot S_{d,max}^*$$ (6.16)

Taking into account two relevant Limit States and four lateral load patterns, a total of 8 values of displacement demand are determined (Table 6.3).

Table 6.3: Displacement demand values

	P.L.	**PUSHOVER X+**	**PUSHOVER X-**	**PUSHOVER Y+**	**PUSHOVER Y-**
FE MODEL 1	SLD	$D_{SLD,X+}$	$D_{SLD,X-}$	$D_{SLD,Y+}$	$D_{SLD,Y-}$
	SLV	$D_{SLV,X+}$	$D_{SLV,X-}$	$D_{SLV,Y+}$	$D_{SLV,Y-}$

6.4.2   Evaluation of the objective function

In addition to the evaluation of technical effectiveness, the post-processing stage aims also at estimating the economic viability of each retrofit solution. In particular, the current implementation takes into account only the actual direct costs C_{tot} of the intervention. The total cost is defined as follows:

$$C_{tot}(x) = C_{loc}(x) + C_{glob}(x) + C_{found}(x) \tag{6.17}$$

where x is the vector of design variables defining the generic interventions (Figure 6.2), C_{loc} is the total cost of local strengthening of columns through FRP, C_{glob} is the actual cost of global intervention realized by installing a set of steel bracing systems, and C_{found} is the total cost of possible enlargement of the foundation system.

The cost of local intervention is calculated as the sum of three terms:

$$C_{loc}(x) = \sum_{i=1}^{N_{col}} \left[C_{dem,loc}(x) + C_{rest,loc}(x) + C_{FRP,layer}(x) \right] \tag{6.18}$$

where the term $C_{dem,loc}$ refers to the cost of demolition of the existing infill walls (or partition) and is calculated according to the following equation:

$$C_{dem,loc}(x) = A_{dem,loc}(x) \cdot C_{dem,unit} \tag{6.19}$$

where $A_{dem,loc}$ is the area to be demolished and $C_{dem,unit}$ is the unit cost for demolition operation [340]. The term $C_{rest,loc,}$ whereas, is the cost of reconstruction of the masonry once the local intervention is completed and is calculated as follow:

$$C_{rest,loc}(x) = A_{rest,loc}(x) \cdot C_{rest,unit} \tag{6.20}$$

where $A_{rest,loc}$ is the area of masonry to be restored and $C_{rest,unit}$ is the unit cost for reconstruction operation. The term $C_{FRP,layer}$ represents the cost of the fiber reinforced polymeric material and its application in layers to confine the "weak" columns.

The procedure accounts for the possibility to strengthen the columns by the application of several layers. Two unit costs terms are distinguished, namely $C_{FRP,1layer,unit}$ and $C_{FRP,2+layer,unit}$ to evaluate in a different way the cost of single layer confinement from the other cases, respectively. In fact, the term $C_{FRP,layer}$ is calculated as below:

$$C_{FRP,layer}(x) = A_{1layer}(x) \cdot C_{FRP1layer,unit} + A_{2+layer}(x) \cdot C_{FRP2+layer,unit} \tag{6.21}$$

where A_{1layer} and $A_{2+layer}$ are the totals of FRP applied as the first layer and as subsequent layers, respectively. Moreover, the post-processing subroutine calculates the cost of global intervention according to the following sum:

$$C_{glob}(x) = \sum_{i=1}^{N_b} \left[C_{dem,glob,i}(x) + C_{rest,glob,i}(x) + C_{SteelB,i}(x) \right] \tag{6.22}$$

The term $C_{dem,glob}$ refers to the cost of demolition of the existing infill walls (or partition) needed to realize the global intervention and it is equal to:

$$C_{dem,glob}(x) = A_{dem,glob}(x) \cdot C_{dem,unit} \tag{6.23}$$

where $A_{dem,glob}$ is the area to be demolished to realize the global intervention and $C_{dem,unit}$ is the unit cost for demolition operation. The term $C_{rest,glob}$ is the cost of reconstruction of the masonry once the global intervention is completed:

$$C_{rest,loc}(x) = A_{rest,loc}(x) \cdot C_{rest,unit} \tag{6.24}$$

where $A_{rest,loc}$ is the area of masonry to be restored and $C_{rest,unit}$ is the unit cost for the operation. The term C_{SteelB} represents the cost of commercial steel profiles and their installation as a bracing system to work in parallel with the existing building. Since not all the steel members of the bracing system are characterized by the same geometrical properties, the above-mentioned term is calculated by the following equation:

$$C_{SteelB,i}(x) = \sum_{i=1}^{Nmemb} W_{SteelP,i}(x) \cdot L_{SteelP,i}(x) \cdot C_{SteelB,unit} \tag{6.25}$$

where N_{memb} is the number of steel members composing the bracing system, W_{SteelP} is the linear weight of the member depending on the profile's size, L_{SteelP} is the length of the member and $C_{steelB,unit}$ is the unit cost of steel material.

Moreover, the procedure account also for the cost of the possible intervention on the existing foundation system (supposed to be made with micro-piles) needed to respond to the possible increase in vertical and horizontal reactions at the base of the retrofitted structure.

In fact, the seismic actions on the retrofitted model can result in the increment (with respect to the gravitational loads only) of the reactive axial force at the bottom of each column. It's worth to say that the tensile axial forces (with a negative value) are assumed to do not affect the intervention of foundation system.

To this end, the post-processing subroutine compares the envelope axial force at the base of each column (extracted from the output files of the four seismic simulations) with the maximum axial force obtained under gravitational loads only.

The amplitude of the strengthening intervention on the foundation system is proportional to the difference of the above axial forces ΔN_i: the greater the difference, the number of micro-piles will be necessary. However, in the current assumption, if the increase in axial forces is less than 25% (with respect to the gravitational condition), any enlargement intervention is required.

Once the diameter D_{mp}, the length L_{mp} and the construction type of the micro-pile are fixed, its bearing capacity $Q_{lim,mp}$ is uniquely determined [341]. Therefore, the subroutine determines the number of micro-piles needed at the base of each column according to the following ratio:

$$N_{mp,col,i} = \frac{\Delta N_i(x)}{Q_{lim,mp}}$$ (6.26)

Hence, the cost $C_{found}(x)$ stems out from the relationship shown below:

$$C_{found}(x) = \sum_{i=1}^{N_{COL}} \left[\frac{\Delta N_i(x)}{Q_{lim,mp}} \cdot \left(C_{micropile} + C_{excav} + C_{concrete} \right) \right]$$ (6.27)

where N_{COL} is the total number of columns in the existing structure, $C_{micropile}$ is the unit cost for the installation of single micro-pile (including the shuttering and the longitudinal reinforcing steel profile), C_{excav} is the excavation unit cost (with the hypothesis that a soil volume of 0.6 m^3/micro-pile must be removed to build the plinth) and $C_{concrete}$ is the unit cost of concrete needed to build the plinth.

6.4.3   Evaluation of the penalty

It is worth to remind that the constrained optimization problem under consideration is formulated according to the following equation:

$$\overline{x}_{opt} = \underset{x}{\mathrm{argmin}}\left[C_{tot}(x) \right] \quad \text{with } \overline{x}_{opt} \in \Omega_f \subseteq S$$ (6.28)

subject to a certain number of nonlinear inequality constraints:

$$g_{LS,i}(x) = C_{LS,i}(x) - D_{LS,i}(x) \geq 0 \quad \forall i = 1,...\, n_{LS}$$ (6.29)

where n_{LS} is the number of relevant Limit States, x_{opt} the vector of the optimal solution, S is the whole search space and Ω_f is the feasible region consisting of all the feasible solutions that satisfy the above constraints. Once the structural model

for each trial retrofit solution has been created (Section 6.2) its seismic response has been simulated (Section 6.3), the post-processing stage evaluates the Limit State function g_{LS} for all the pushover directions and for all the performance levels of relevance, as reported in Table 6.4.

Table 6.4: Limit State function for all the accounted "combinations"

	P.L.	**PUSHOVER X+**	**PUSHOVER X-**	**PUSHOVER Y+**	**PUSHOVER Y-**
FE MODEL 1	SLD	$(C\text{-}D)_{SLD,X+}$	$(C\text{-}D)_{SLD,X-}$	$C\text{-}D)_{SLD,Y+}$	$(C\text{-}D)_{SLD,Y-}$
	SLV	$(C\text{-}D)_{SLV,X+}$	$(C\text{-}D)_{SLV,X-}$	$(C\text{-}D)_{SLV,Y+}$	$(C\text{-}D)_{SLV,Y-}$

Therefore, a candidate solution is considered belonging to the feasible region if the minimum difference among all the 8 combinations (4 pushovers and 2 Limit States) meets the condition below:

$$x \in \Omega_f \subseteq S \quad \text{if } \min_{dir}\left[\min_{LS}\left(C(x) - D(x)\right)\right] > 0 \tag{6.30}$$

However, since the genetic algorithm is directly applicable only to unconstrained optimization, it is necessary to use an additional method that keeps the solutions in the feasible region. During the past few years, several methods have been proposed for handling constraints by GAs [342][343][344][345][346].

The most popular approach in the GA community to handle constraints is to use penalty functions that penalize infeasible solutions and transform constrained problem to unconstrained one. The proposed procedure relies on an additive penalty consistent with the most common method followed among the GA community:

$$\text{eval}(x) = \begin{cases} C_{tot}(x), & \text{if } x \in \Omega_f \\ C_{tot}(x) + p(x) & \text{if } x \notin \Omega_f \end{cases} \tag{6.31}$$

where *eval(x)* is the new objective function to minimize and p(x) is a *penalty* term.

As known, one of the major challenges in any application of penalty function concerns the achieving an appropriate balance of the penalty value.

On the one hand, large penalty values discourage algorithm from exploring infeasible regions despite the search is quickly moved inside the feasible region.

On the other hand, low penalty values do not prohibit algorithm from searching infeasible regions most of the time.

Several approaches based on penalty functions exist in the scientific literature: Death Penalty [347]; Static Penalties [348]; Dynamic Penalties [349]; Annealing Penalties [350]; Adaptive Penalties [351][352]; Segregated GA [353] and Co-evolutionary Penalties [354].

As a result of these findings, the current implementation employs a "Death Penalty Function" which immediately rejects infeasible solutions from the population [355]: if no violation occurs, the penalty term will be zero, while if the solution does not meet the constraint, a high penalty term will be added to cost function such that the search is pushed back towards to the feasible region.

In particular, in the present work, the penalty term is chosen to be a function of the total cost of the intervention. In fact, such term is calculated according to the following relationship:

$$p(x) = \begin{cases} \beta \cdot C_{tot}(x) & \text{if } \min_{dir}\left[\min_{LS}(C(x)-D(x))\right] \leq 0 \\ \\ 0 & \text{if } \min_{dir}\left[\min_{LS}(C(x)-D(x))\right] > 0 \end{cases} \tag{6.32}$$

It is worth noting that the β-factor needs to be calibrated in order to produce high penalty term for those solutions that don't meet the performance requirements. In the current implementation, the parameter β is either zero or 1000000. The feasible and unfeasible regions are shown conceptually in Figure 6.36.
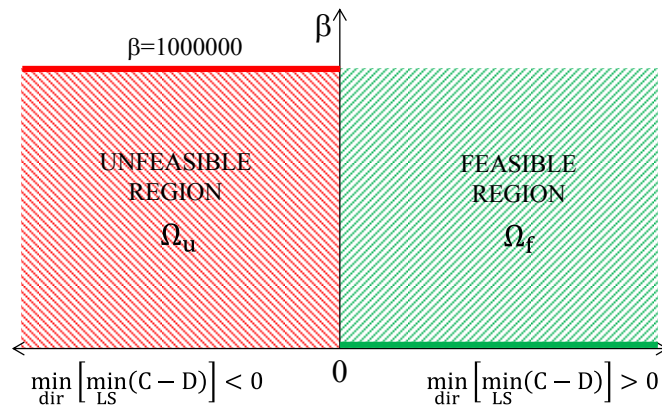
Figure 6.36: Values of b-factor in both unfeasible and feasible region

Once both penalty and cost functions are evaluated, the N_{ind} individuals of the population are sorted according to their value of new objective function eval(x): the

candidate solution characterized by the lowest value of the objective function, is saved as the temporary "best" intervention (Table 6.5).

Table 6.5: Example of individual's sorting

Individual	Chromosome	C_{loc} [€]	C_{glob} [€]	C_{found} [€]	C_{tot} [€]	p [€]	eval [€]
#1	1 3 1 0 3 2 0 1 2 2 1 3 4 6 2 5	…	…	…	…	…	min
#2	0 1 2 1 3 1 1 2 3 2 0 1 6 5 1 7	…	…	…	…	…	…
#3	3 1 1 1 2 1 0 1 2 3 3 3 6 1 0 1	…	…	…	…	…	…
…	…………………………...	…	…	…	…	…	…
#100	2 1 2 1 2 1 2 1 2 0 1 0 6 5 5 7	…	…	…	…	…	max

6.5 Selection

As said in Section 5.2, GAs search for the optimum solution "improving" initial population of candidate solutions in accordance with the "survival of the fittest" principle. The first operator involved in the evolution process is the "selection" of parents according to the flow-chart depicted in Figure 6.37.
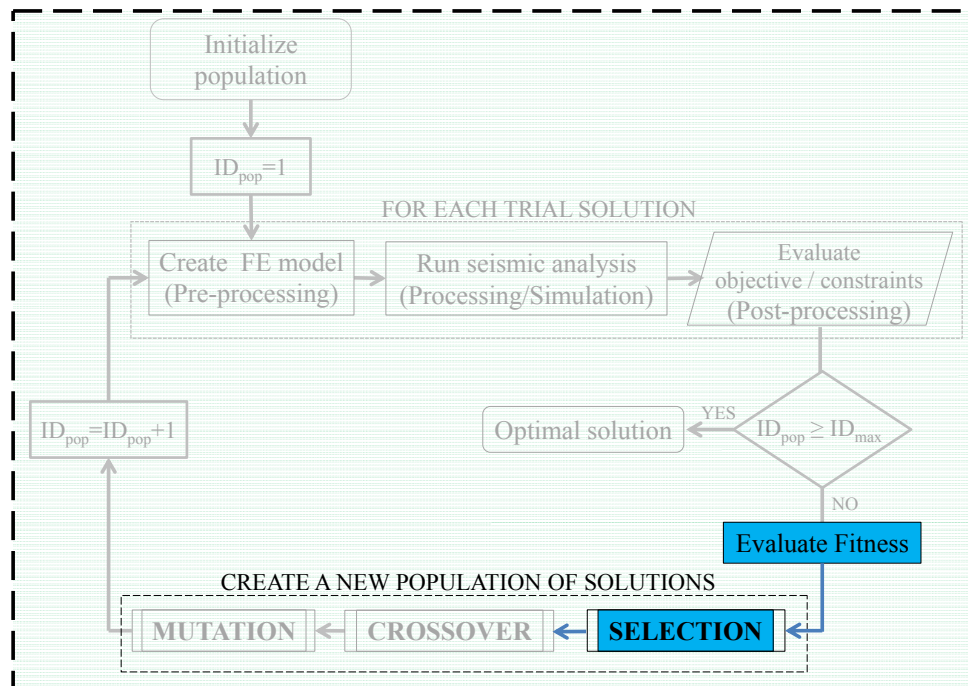
Figure 6.37: Selection of "parents" within the proposed procedure

As a matter of fact, the selection of the parents, which is essential in the progress of GA, needs to be driven by the fitness of individuals, sometimes even called "reproductive fitness" [356], rather than by their objective function values, which can vary orders of magnitude across the spectrum of optimization tasks.

Hence, once the total cost and the Limit State function $g_{LS,i}$ have been evaluated for all N_{ind} individuals of the population, the proposed procedure maps the objective function to fitness function form.

As known, the fitness function assigned to each solution "measures" the capability of the i-th individual to "compete" with the other individuals of the same population in achieving the objective of the optimization problem under consideration.

It measures the reproductive efficiency of the chromosome, i.e. the number of offspring that an individual can expect to produce in the following generation.

The selection of parents has to conform with the basic idea of giving higher chances of reproduction to better fitted individuals with the aim of realizing the "survival of the fittest" principle, which is the basis of the evolution theory [256].

The transformation "objective function value" $\rightarrow$ "fitness" is called "scaling" of the objective function and is not a trivial operation.

The proposed procedure employs a proportional fitness assignment as transformation. The fitness is computed as the individual's raw performance relative to the whole population, as stated below:

$$F(x_i) = \frac{\min\limits_{i=1..N_{ind}} [eval(x_i)]}{eval(x_i)} \qquad (6.33)$$

As can be easily understood from Eq. (6.33) the fitness function is generally smaller than 1, as the unit value corresponds to the "best" individual (characterized by the minimum value of the objective function).

Therefore, it is chosen as a real-valued and monotonic function of the objective function, ranging within the interval [0;1].

The monotonicity assures that fitness always improves with decreasing values of the objective. Then, once the N_{ind} chromosomes are ranked from lowest fitness to highest fitness value, only the best individuals survive for mating, while the worst individuals (solution that either have a high cost or doesn't comply with the seismic checks) are discarded to make room for the new "offspring" trial solutions into the new population.

As known, the selection of "parents" can be divided into two categories: elite and non-elite strategies.

On the one hand, elite methods assure that the best individuals of the population go to the next population and makes them produce more children.

It is a common belief that for optimization problems with exactly one solution the elite strategy should not be harmful. However, if the search landscape is very rugged with many local minima, then the elite strategy can significantly delay the discovery of the best point in the search space.

For this reason, the selection strategy is herein implemented through a non-elite selection method called "roulette-wheel" [357]. In particular, the number of "protected" chromosomes in each generation is given by the equation:

$$N_{keep} = X_{rate} \cdot N_{ind} \tag{6.34}$$

where X_{rate} is the fraction of N_{ind} that survives for the next step of mating, while the difference N_{ind}-N_{keep} is discarded. X_{rate} needs to be tuned (Section 6.9) because it is somewhat arbitrary: keeping too many chromosomes allows bad performers a chance to contribute their traits to the next generation.

Contrary to the hard selection methods which grant to become a parent only to those chromosomes that are fitter than a predefined threshold, this methods is rather soft as it makes possible to proliferate the genetic material contained in any chromosome. In fact, the poorly fitted individuals retain non-zero chance to become parent and transmit their genetic material to the future generations.

The essential idea is that individuals are picked out of the current population and, based on probabilistic assumptions, they are included in a mating pool, of course with fitter individuals to have higher chances of reproduction.

The fitness function of each individual is employed for determining the "probability of survival" of each candidate solution, i.e the probability that the i-th individual is "selected" within the current generation to be part of the mating pool and, hence, "reproduce" itself into the following generation. Such probability is calculated as follows:

$$p(x_i) = \frac{F(x_i)}{\sum_{i=1}^{N_{ind}} F(x_i)} \tag{6.35}$$

It is evident that, by definition, the values of $p(x_i)$ range between 0 and 1. The individuals characterized by higher values of $p(x_i)$ have the higher probability to be selected as "parents" for generating "offspring" solutions.

According to the roulette-wheel rule, the circular sections are marked proportionally to the probability of survival of each individual as shown in Figure 6.38: the individual #3 is the fittest individual and, hence, it corresponds to a wider interval, while the individual #2 is the least fit and, correspondingly, it has the smallest interval.

Individual	Chromosome	Probability	Cumulative P.
■ #1	00101011101011101011010	0.18	0.18
■ #2	10101010101010101010011	0.07	0.25
■ #3	00001011001001101001010	0.36	0.61
■ #4	11101011001011101011111	0.25	0.86
■ #5	11001011101010101111110	0.14	1.00
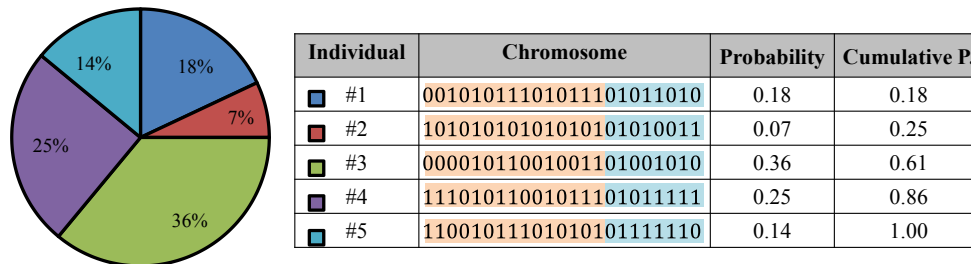
Figure 6.38: Working principle of roulette wheel selection rule

A random number in the range [0,1] is then generated. Starting from the top of the list, the first chromosome with a cumulative probability greater than the random number is selected for the mating pool. For instance, if the random number is r = 0.57, then chromosome 3 is selected because $0.25 < r \leq 0.61$.

Since the GA imitates the mammal's way of reproduction which requires two parents, two chromosomes are selected from the mating pool to produce two new offspring. Pairing takes place until N_{RW} offspring are born to replace the discarded chromosomes, being N_{RW} the number of the individual to be selected according to the roulette-wheel method.

However, due to the application of a "death" penalty function, the algorithm more likely tends to pick the solutions that are in the feasible region of the search space preventing to find better genetic features which could lay in the unfeasible region. For this reason, another selection strategy based on a random selection is added in order to prevent the loss of important genetic information contained in poorly fitted individuals (Figure 6.39).

In particular, the second pairing is aimed at generating a number of offspring individuals N_{RP} and it takes place between the "father" selected according to the roulette-wheel and the "mother" whose rank is randomly selected among the discarded individuals.
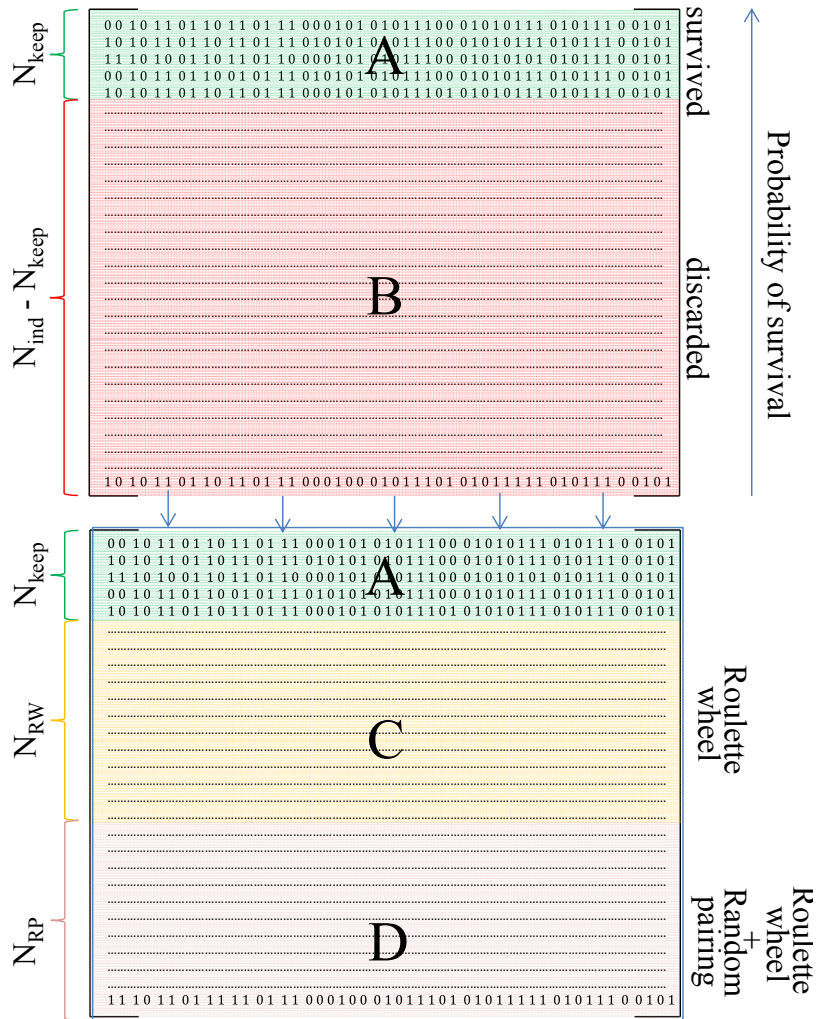
Figure 6.39: Replacement of discarded individuals (B) with offspring (C+D)

6.6 Crossover

Once $N_{RW} + N_{RP}$ chromosomes are selected according to the roulette wheel and random pairing strategy, the crossover stage occurs to create new individuals by mixing genetic information extracted from the selected parents (Figure 6.40).

The crossover is a genetic operator mainly responsible for the search of new strings, possibly better (fitter) than the old ones.
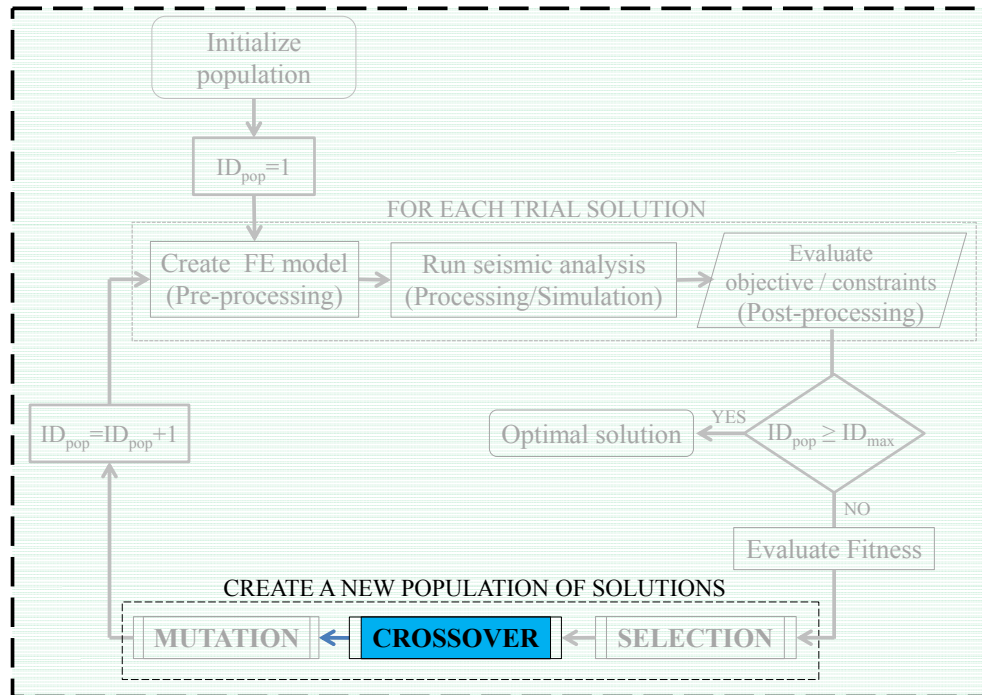
Figure 6.40: Crossover operator within the proposed procedure

Like its ideal counterpart in nature, the two genotype strings of the individual participating in the crossover are selected as "parents" and the resulting strings, similar to their parents, i.e. retaining their features, are defined as "offspring". In this way, the parents produce a total of N_{ind} - N_{keep} offspring, so the size of the population is now back to N_{ind}.

Crossover operator "mixes" the segments of each pair and the genetic information contained between these segments is exchanged. The segments are delimited by the so-called "crossover points" (or "kinetochore") which are herein located between two successive genes, so no gene can be modified or divided during the crossover.

The influence of the number of crossover points on the resulting efficiency is a key aspect, whose discussion is outside the scope of this work. However, interested readers may refer to Spears [358][359] for further details. Moreover, several methods can be used for choosing the length and location of exchange sites: one-point, two-point, and uniform crossover methods are some possibilities.

Unlike single and two-point crossover, the uniform crossover enables the parent chromosomes to contribute the bit level rather than the segment level. The

proposed algorithm relies on a modified version of uniform crossover. Empirical evidence suggests that it is a more exploratory approach to a crossover than a traditional exploitative approach that maintains longer segments.

Figure 6.41 shows the working principle of the operator with two parents and the resulting offsprings.
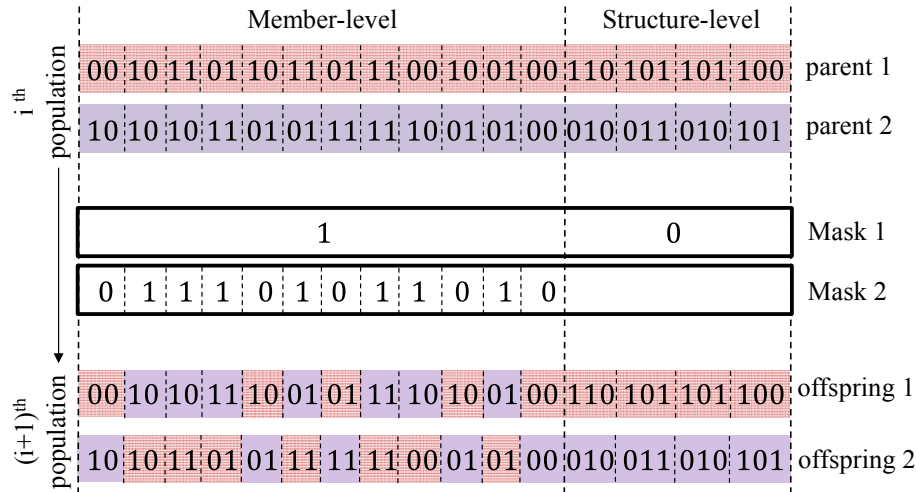
Figure 6.41: Working principle of the proposed crossover operator

As shown, two crossovers "masks" are created at random. The mask 1 is an array of two bits, like the number of techniques (local and global techniques) that synergistically coexist in the generic retrofit intervention.

The first mask indicates which part of the genotype will be exchanged between the pair of parents: the first and/or the second part of the parents' genotype will be involved by the crossover if the corresponding mask's bit is 1, otherwise the first and/or the second part will be not involved in the crossover process.

Conversely, the crossover mask 2 has as many bits as the number of design variables (delimited with dashed lines). It indicates which parent ("parent 1" or "parent 2") will contribute to the offspring's genotype with which gene: offspring 1 is produced by taking the gene from parent 1 if the corresponding bit in the mask is 0, or taking the segment from parent 2 if the bit in the mask is 1.

Offspring 2 is created using the inverse of the mask or, equivalently, swapping the gene of parent 1 (father) and parent 2 (mother).

6.7   Mutation

Figure 6.42 points out the mutation stage, i.e the second operator employed in GA to explore the design space: it makes possible to reach the regions, which might be not accessible at all without it. Hence, GA needs the mutation operator because the crossover alone cannot guarantee to find the optimal region in a search space.
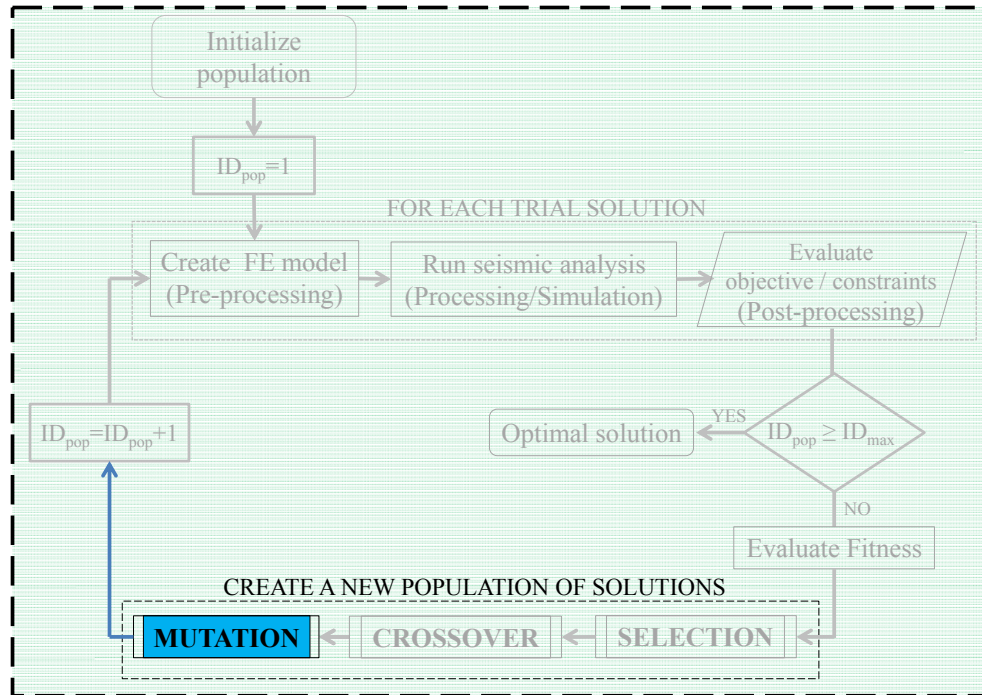
Figure 6.42: Mutation step within the proposed procedure

As a matter of fact, it may easily happen that well adapted chromosomes - the ones most likely allowed to reproduce - do not contain some bits that might be present in the desired near-optimal solution, but those bits are present in very poorly adapted individual that may be rarely selected for reproduction, as their fitness is very small. Therefore, their valuable genetic material would be lost.

The only way to recover good genetic material that may be lost through the repeated use of selection and crossover operators is the mutation.

This operator provides a guarantee that the probability of searching any given string will never be zero, acting as a "safety net" [315]. It basically introduces diversity not in the original population by executing some random changes into newly created offspring individuals.

168

Under the operational standpoint, mutation acts at the bit level of the genotype: it is nothing but negating (flipping) bit selected at random in the newly created chromosomes so that they become the bearer of features not present earlier in their predecessors nor in the population they belong to.

It is clearly expected that if weak strings are created they will be discarded by the reproduction operator in the next generation and if good strings are created, they will be increasingly emphasized.

To this end, in the present work, the number of mutations assumed to occur is equal to:

$$N_{mut} = \mu_{mut} \cdot (N_{ind} - N_{keep}) \cdot N_{bits,tot} \tag{6.36}$$

where μ_{mut} is a parameter belonging to the range [0-1]. Such parameter plays an important role in the genetic algorithm: with a high number of mutations the population will never stabilize; too little and the population will end up with homogeneity.

It is a problem-dependent parameter to be tuned (Section 6.9). Moreover, the fraction of effectively mutated bits in the entire population is chosen to be an increasing function of time: starting from a value of $\mu_{mut,1}$ applied for the first generation, the parameter μ_{mut} increases linearly up to $2*\mu_{mut,1}$ attained at the last generation, as shown in Figure 6.43.
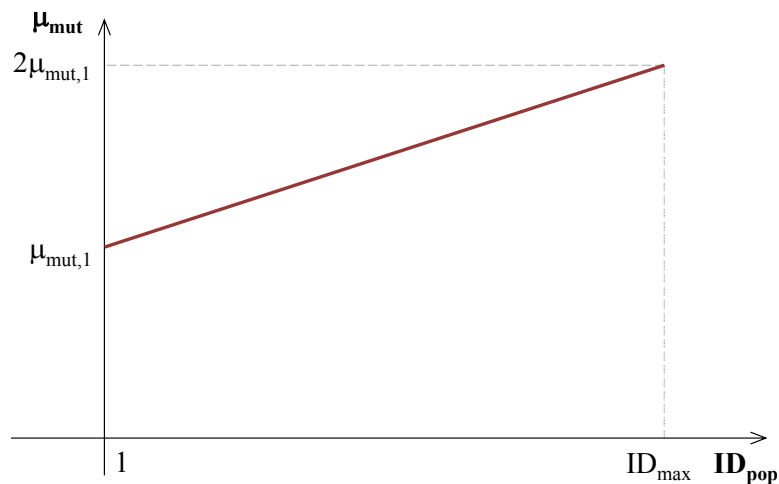
Figure 6.43: Relationship between the number of mutations and generation

This is done in order to increase the algorithm's freedom to search outside the current region of variable space and to improve its ability to "escape" from local

optima. Once μ_{mut} is set, a random number generator creates N_{mut} pairs of integers that correspond to the rows and columns of the bits to be mutated.

$$n_{row} = [n_{row1}, n_{row2}, ... n_{row,N_{mut}}]$$
$$n_{col} = [n_{col1}, n_{col2}, ... n_{col,N_{mut}}] \tag{6.37}$$

For example, if the random pair is (12, 14), thus the bit in row 12 and column 14 of the binary matrix is switched from 1 to 0 (or vice versa).

As can be seen in Figure 6.44, mutation is not allowed on the "protected" solutions: they survive as "elite" solutions destined to propagate unchanged. Moreover, it is also possible that a given binary string may be mutated at more than one point.
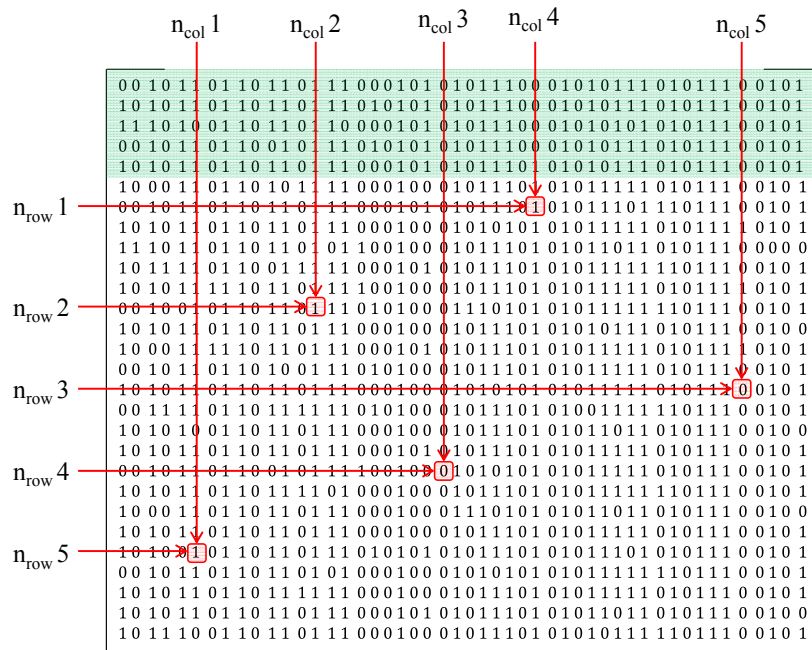
Figure 6.44:   Examples of mutation points

In conclusion, mutation is needed to distract the GA from converging too fast at local optima before sampling the entire solution space (premature convergence). It aims at creating points in the neighborhood of the current point, thereby achieving a local search around the current solution.

Therefore, without random mutations (if mutation rate μ_{mut} is set to 0), then the proposed GA would not be able to escape from local optima and may never find the optimal solution.

6.8 Convergence criteria

After a new population is created, then both the cost and penalty functions associated with the descendant individuals are evaluated.

For each candidate solution, the procedure saves the corresponding genotype, the objective and constraints values in a matrix whose dimensions are updated over the evolution process. This is done because the individuals of future populations may be identical to some old individuals. In this way, if a discarded individual reappears through the pairing process, the seismic simulation does not need to be executed again in OpenSees.

The flow-chart described above is iterated, yielding to offspring solutions that are gradually getting closer and closer to the desired solution until the stopping criteria are met. As known, when no gradient information is available, it becomes problematic to formally specify convergence criteria. An exhaustive taxonomy of heuristic stopping criteria for multi-objective evolutionary algorithms is available in the scientific literature [360].

A common practice is to terminate the GA after a predefined number of generations. In compliance with the above criterion, the proposed GA evolves until the counter of population ID_{pop} reaches a maximum value ID_{max} (Figure 6.45).
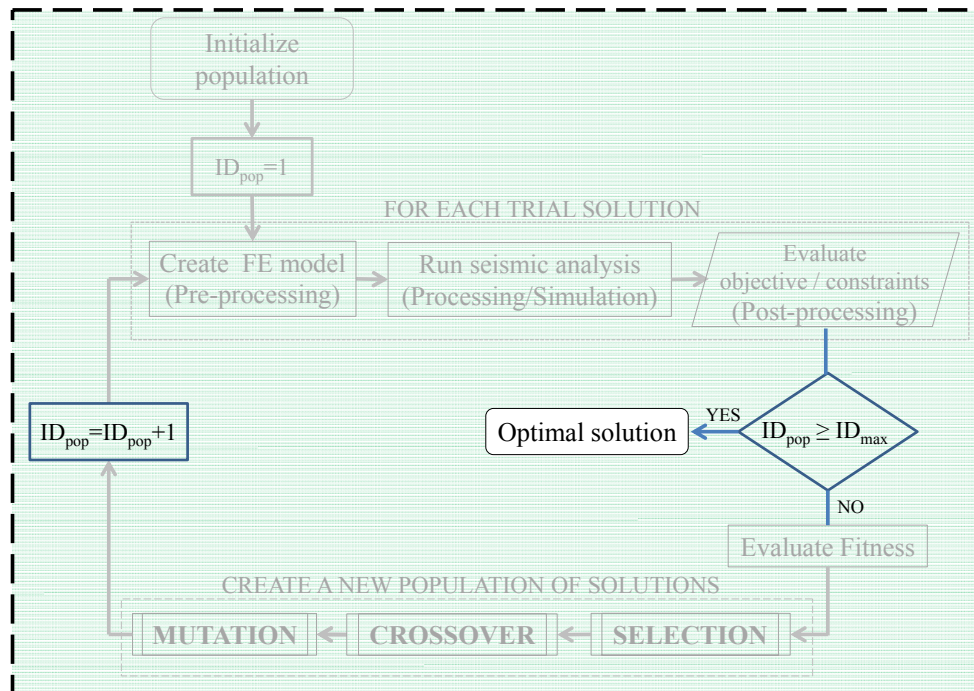
Figure 6.45: Termination criteria for the proposed procedure

6.9   Tuning of the GA parameters

Evolutionary computing researchers and practitioners all acknowledge that algorithm design can be approached as an optimization problem because the selection of appropriate details, also known as "parameters", is essential to get faster convergence and better results.

To this end, it is important to remind that the problem of setting parameters is commonly divided into two cases: parameter tuning (offline parameter search - before the algorithm is run) and parameter control (online parameter tweaking - during the algorithm run) [361].

Common belief [362] is that tuning is better suited for most cases because the parameter values are not changing during a run, hence only a single value per parameter is required. In general terms, the tuning of parameters could help the algorithm not to get trapped at local optima and to improve the solution's quality. It is aimed to decide the trade-off between wide exploration and deep exploitation of solutions during the evolutionary process.

Moreover, the evolutionary algorithm developers typically distinguish qualitative and quantitative sub-parameters [363]. In fact, for qualitative parameters (such as the type of selection, crossover and mutation operator) with a finite domain with no sensible distance metric or order, the only option to find the most appropriate parameter is sampling because the domain has no exploitable structure.

For the quantitative parameters that have a domain with a distance metric, or at least partially ordered, (such as the crossover rate, mutation rate, offspring number, population size) heuristic search and optimization methods can be used to find optimal values for parameters because the domain is a subset of real numbers.

The proposed GA is a parameter-sensitive algorithm like most of the meta-heuristics evolutionary algorithms. Regarding the qualitative parameters, the crossover strategy described in Section 6.6 has been chosen after several attempts: first the one-point crossover and then the multi-point types which, however, have led to poor results. This has been possible because the number of attempts to perform was low and did not require a large computational effort.

On the other hand, for a simple application by assigning trial values of 0.5 and 0.01 to the quantitative parameters X_{keep} and μ_{mut} respectively, it has been observed that the objective function reached a plateau, i.e. a local minimum that did not represent the desired solution for the given instance. In fact, a retrofit intervention

with a significantly lower cost has been found through a "manual" search based on the author's intuition.

The cost curve shown in Figure 6.46 points out two aspects: 1) the algorithm achieved a premature convergence after a small number of generations (symbolically referred as $N_{GEN,CONV}$), and 2) the objective function did not undergo any further improvement beyond the $N_{GEN,CONV}$th generation assuming a very high value referred herein as C_{CONV}.

This means that the quality of the solution found is significantly affected, among other factors, even by the value of the pair $[X_{keep}, \mu_{mut}]$.
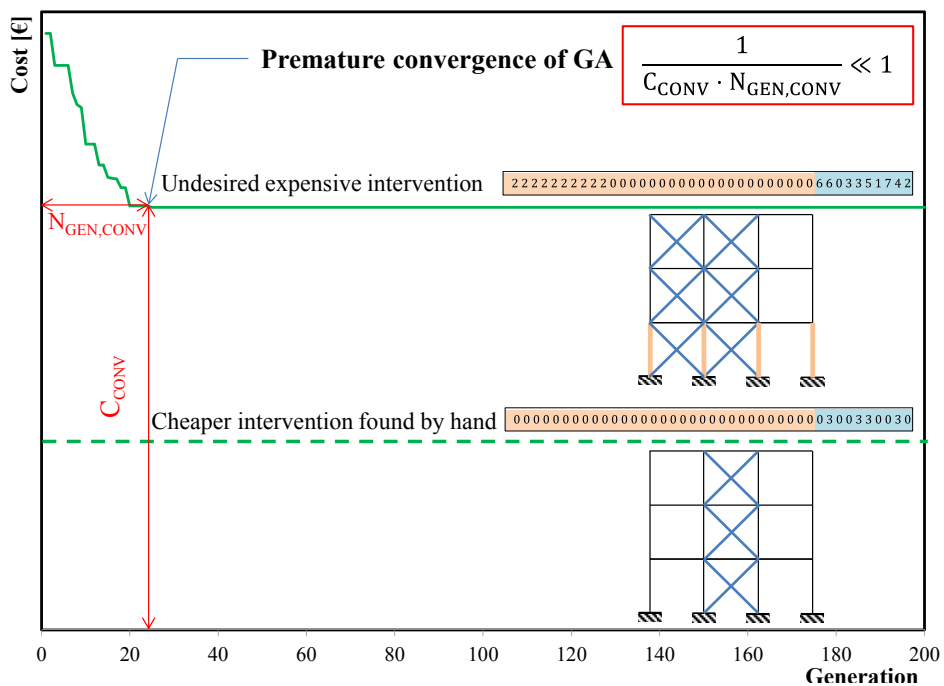
Figure 6.46: Example of premature convergence

It is clear that before being able to use the procedure described in the previous chapter, it has been necessary to address also the fundamental tuning step (Figure 6.47) for selecting the most appropriate parameters.

Similarly to the evolutionary algorithm that looks for the best candidate solution according to the fitness value, the problem of parameter tuning can be seen as a search problem in the parameter space. Solutions of the tuning procedure are parameter vectors with maximum "utility", where the utility can be related to some

definition of algorithm performance and to the objective function of the problem instances to be solved.

The former is usually referred to any sensible measure of the computational search effort, such as the number of fitness evaluations or the number of generation to achieve the convergence.
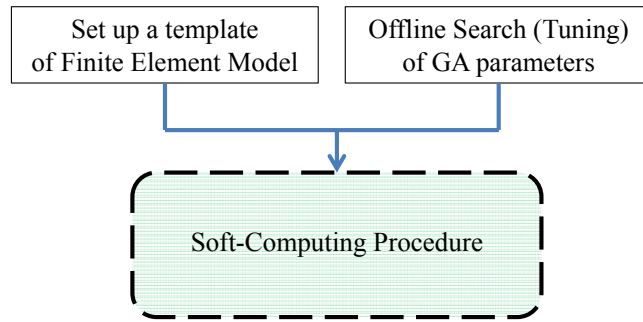
Figure 6.47: Main steps prior to the employment of the procedure

There is wide literature about how one can find these appropriate parameters [364]. Obviously, good tuning procedure should try to find a good parameter vector with the least possible effort.

6.9.1 Proposal of fast tuning strategy

Identifying a suitable pair of parameters for the proposed algorithm is primarily a very hard task. In fact, the proposed soft-computing procedure aims at solving a computationally expensive optimization problem characterized by a simulation step which is part of evaluating the objective function.

Trial-and-error searching for the best GA parameters would take months due to the high computational burden required for the evaluation of the effective objective function (cost function). However, computationally expensive optimization problems with a single objective have been frequently addressed in the literature by employing "surrogate" models [365] which are a computationally cheap approximation of the expensive objective function [366].

Likewise, the tuning method proposed by the author is nothing more than the use of the same flow-chart used in the procedure but aimed at minimizing an "auxiliary" objective function, which does not require the execution of seismic analyzes in OpenSees, as shown in Figure 6.49.

In fact, the new objective function is assumed as "gap" (or "difference") between a "target" string x_{targ} that represents the decimal genotype of a desired retrofit intervention (Figure 6.48) and the trial chromosome x_{trial} generated by the genetic algorithm over the evolution process.

Figure 6.48: Example of target string needed to define a new objective function

It is worth noting that such method does not necessarily require that the target string has to be the optimal solution towards which the soft-computing procedure should converge for a given instance, but rather it can represent the decimal genotype of a low-cost solution proved not violating the feasibility constraints.

The new objective function represents a measure of the "error" that the tuning strategy has the purpose of minimizing. The more the error is, the less the "quality" of the candidate string.

In particular, starting from the first gene of the chromosome the error function is defined as a real integer number obtained by adding the square difference between the trial and the target (known) gene's value, according to the following equation:

$$f(x_{trial}) = error(x_{trial}) = \sum_{i=1}^{N_{VAR}} \left(x_{trial,i} - \overline{x}_{targ,i} \right)^2 \tag{6.38}$$

where $N_{VAR} = N_{col} + N_{beam}$ is the total number of design variables describing the generic retrofit intervention. Once the target string for a given instance has been fixed, the proposed tuning strategy employs again the same flow-chart described in Section 5.4 with the aim to solve a computationally cheap auxiliary (or "surrogate") optimization problem.

The proposed tuning is characterized by iteratively generating a population of trial strings, seeking the one "closest" (in terms of the absolute value) to the target string. As shown in Figure 6.49, the advantage of this simplified approach is the

possibility to "delete" the simulation step of the FEM model which requires a prohibitively large number of seismic analysis.

The selection and mutation operators need the definitions of the pair of parameters [X_{keep}, μ_{mut}] whose values affect the "speed" of the algorithm in generating strings characterized by errors gradually smaller over the generations.
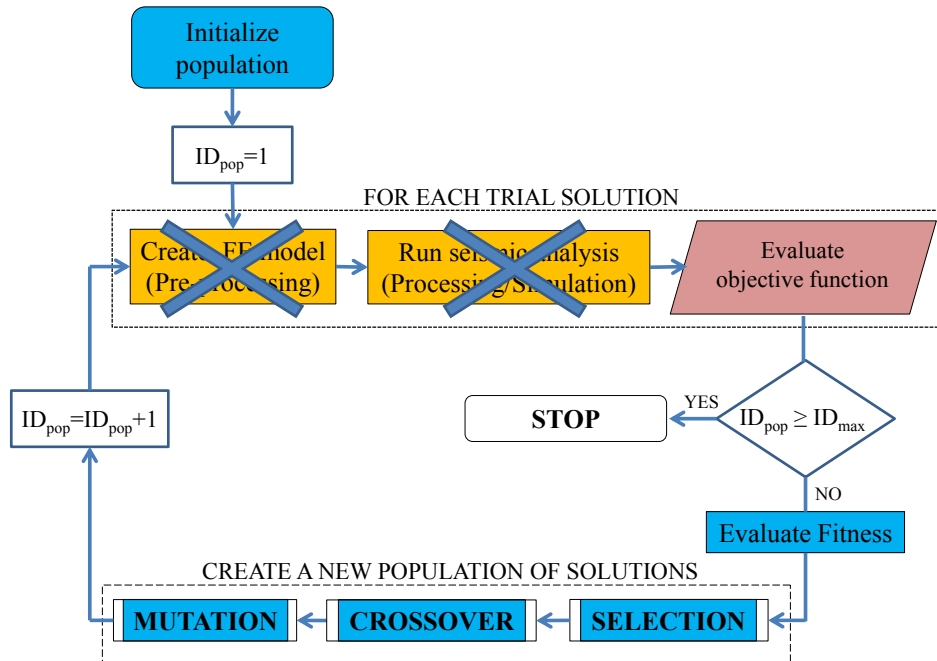
Figure 6.49: Flow-chart of the tuning strategy

Hence, it is possible to obtain "variants" of the same genetic algorithm by just modifying the combination of the above-mentioned quantitative parameters, as shown in Table 6.6.

Table 6.6: Example of GA variants

	GA 1	**GA 2**	**GA 3**	**GA 4**	**….**	**…..**	**….**	**….**	**GA n**
X_{keep}	0.05	0.05	0.05	0.05	…..	…..	…..	…..	0.50
μ_{mut}	0.001	0.001	0.001	0.001	….	….	….	…..	0.01

As said, such quantitative parameters largely influence the performance of the algorithm: a GA with good parameter values can be orders of magnitude better than one with poorly chosen parameter values as shown in Figure 6.50.
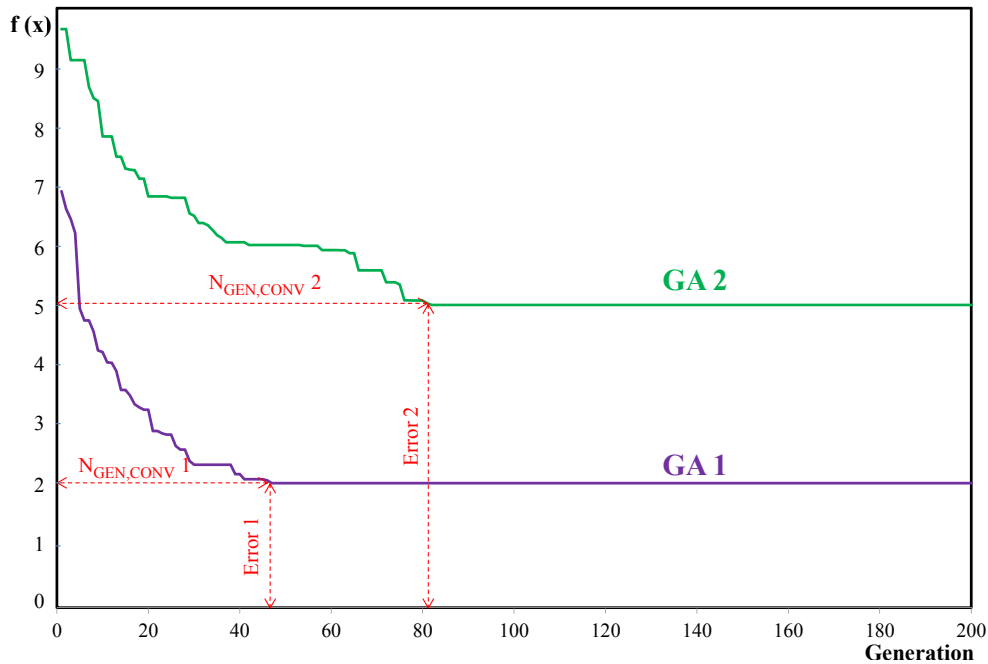
Figure 6.50: Example of comparison between two variants of GA

In line with the usual evolutionary computing terminology, the term "utility" is herein used to denote the "quality" of parameter vector [X_{keep}, μ_{mut}] which reflects the performance of the GA variant.

Solutions of the parameter tuning problem can then be defined as parameter vectors with maximum utility. In the proposed tuning procedure, the utility function is based on a trade-off between two criteria: the objective function (error function) and the convergence time $N_{GEN,CONV}$ (the number of generations above which no further improvement of the objective function is achieved):

$$\text{utility}\big[GA\big(X_{keep}, \mu_{mut}\big)\big] = \frac{1}{\text{Error} \cdot N_{GEN,CONV}} \tag{6.39}$$

the utility function takes into account not only convergence time but also the error made at the reached convergence, i.e. a measure of the algorithm's ability to minimize the difference between the target string and the "fittest" string generated through the genetic operators (selection, crossover, mutation).

As stated above, the greater utility, the better quality of the quantitative parameter. However, if exists a variant capable to find a string exactly equal to the

desired string, a conventional error equal to 1 is taken in order to avoid infinite value of utility.

A parametric tuning of X_{keep} and μ_{mut} has been carried out with the aim to search their best combination through the parameter space.

A wide range of variation for both X_{keep} and μ_{mut} has been taken into account: the former has been assumed to vary between 0.05 and 0.50 with a 0.05 increment, while the latter has been assumed to range in the interval [0.001, 0,01] with a 0.001 increment.

Hence, a total of 10x10=100 "variants" of GA have been obtained (Table 6.7).

Table 6.7: Utility function for each GA variant

	GA 1	**GA 2**	**GA 3**	**GA 4**	**….**	**…..**	**….**	**….**	**GA 100**
X_{keep}	0.05	0.05	0.05	0.05	…..	…..	…..	…..	0.50
μ_{mut}	0.001	0.001	0.001	0.001	….	….	….	…..	0.01
Error	1	1	2	1	….	….	….	….	4
$N_{GEN,CONV}$	21	19	48	16	…	…	….	….	118
Utility	0.047	0.053	0.010	0.062	…	…	….	….	0.002

The auxiliary minimization problem has been solved as many times as the GA variants, iteratively changing just the pair of values [X_{keep}, μ_{mut}].

All the variants search for the chromosome that minimizes the "error" from the target string. However, each variant is characterized by a different convergence history curve which is sufficient to evaluate the minimum error, the number of generation for convergence $N_{GEN,CONV}$ and, hence, the utility function.

Due to the stochastic nature of GA, multiple runs on the same problem should be necessary to get a good estimate of utility. Moreover, the algorithm designers are often interested in so-called "robust" algorithm, that is an algorithm that works well on a "wide range of problems".

In terms of parameters, this requires a "robust" parameter settings. To this end, Figure 6.51 shows a set of three instances and three corresponding desired retrofit solutions selected to test and evaluate the variant algorithms.

The aim is to deliver a GA that is able to find a very good solution on a wide range of problem instances.
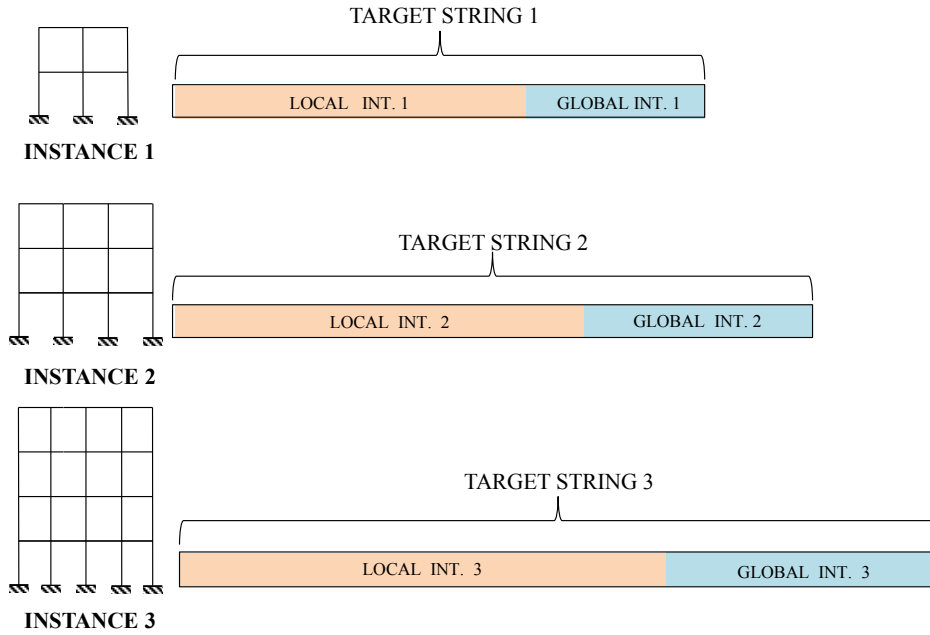
Figure 6.51: Selected instances and corresponding target strings

Once the parametric field, the number of instances and the corresponding target strings have been defined, the flow-chart shown in Figure 6.49 has been run a total number of times equal to 10 (n. of X_{keep} values) x 10 (n. of μ_{mut} values) x 3 (instances)=300 (Table 6.8).

Table 6.8: Collection of utility values for each variant and for each instance

Instance 1									
	GA 1	**GA 2**	**GA 3**	**GA 4**	**….**	**…..**	**….**	**….**	**GA 100**
X_{keep}	…..	…..	…..	…..	…..	…..	…..	…..	…..
μ_{mut}	…..	…..	…..	…..	….	….	….	…..	…..
Utility	…..	…..	…..	…..	…	…	….	….	…..
Instance 2									
	GA 1	**GA 2**	**GA 3**	**GA 4**	**….**	**…..**	**….**	**….**	**GA 100**
X_{keep}	…..	…..	…..	…..	…..	…..	…..	…..	…..
μ_{mut}	…..	…..	…..	…..	….	….	….	…..	…..
Utility	…..	…..	…..	…..	…	…	….	….	…..
Instance 3									
	GA 1	**GA 2**	**GA 3**	**GA 4**	**….**	**…..**	**….**	**….**	**GA 100**
X_{keep}	…..	…..	…..	…..	…..	…..	…..	…..	…..
μ_{mut}	…..	…..	…..	…..	….	….	….	…..	…..
Utility	…..	…..	…..	…..	…	…	….	….	…..

Hence, far from being "magic numbers", the quantitative parameters of the proposed genetic algorithm have been chosen on the basis of the results shown in the following Figure 6.52-Figure 6.55.

The diagrams separately show how the value assumed by the X_{keep} and μ_{mut} parameters influence the performance of the algorithm.

In particular, the diagram in Figure 6.52 relates the number of generations to convergence $N_{GEN,CONV}$ with the X_{keep} parameter.
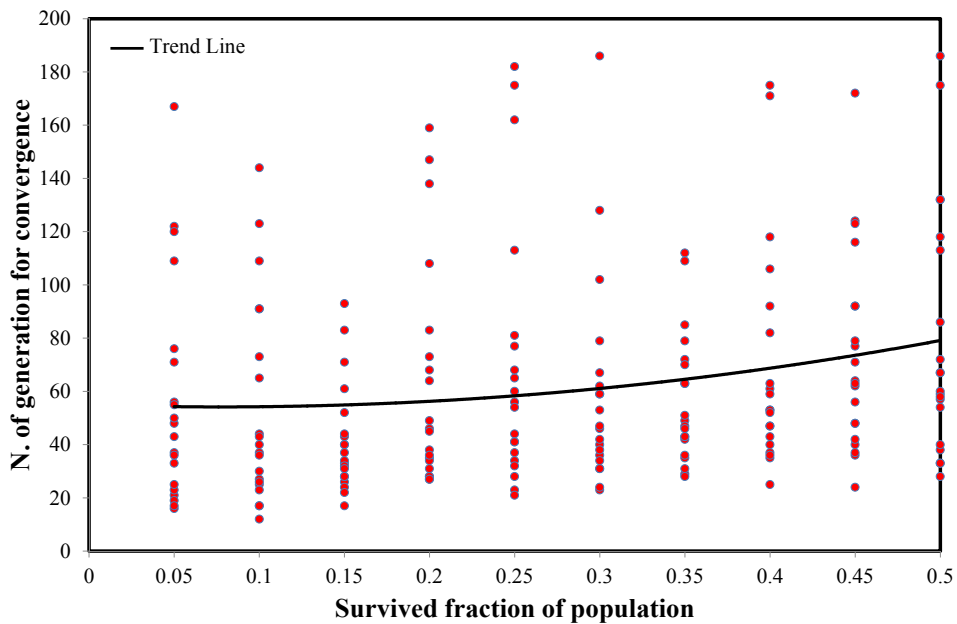
Figure 6.52: Number of generations for convergence vs survived fraction of population

As can be seen, the points are aligned vertically because, for each fixed value of X_{keep}, there are other 10 GA variants in which only the parameter μ_{mut} changes for a given instance.

Likewise, Figure 6.53 shows a relationship between $N_{GEN,CONV}$ with the parameter μ_{mut}. Again, for each fixed value of μ_{mut} there are 10 combinations in which only the parameter X_{keep} varies in its range.

For the same combination described above, Figure 6.54 and Figure 6.55 show value of the objective function value once the convergence is achieved.

It is clear that with the same residual error value, the lower the number of generations for convergence the greater the utility of the genetic algorithm.
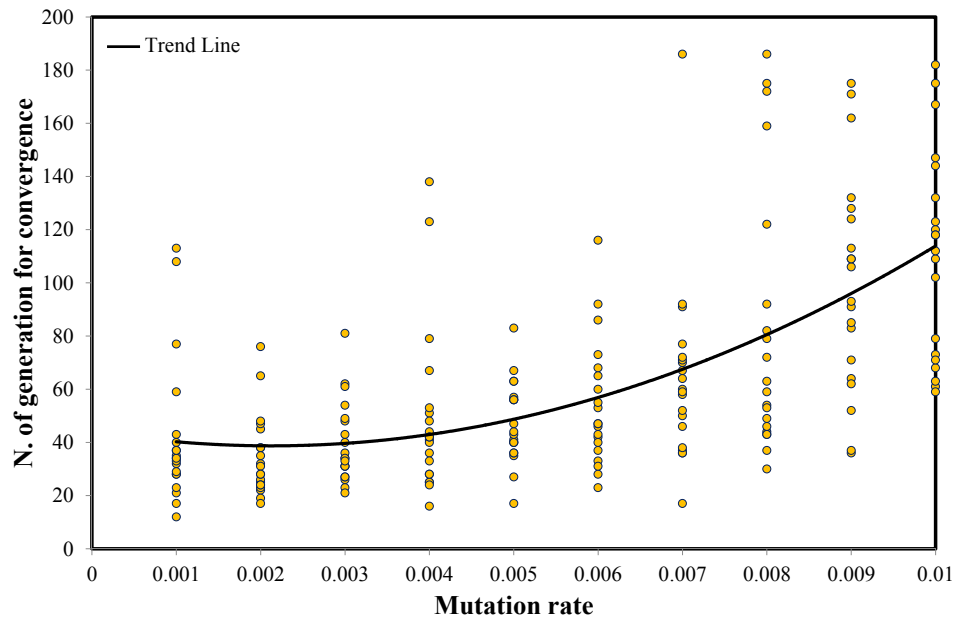
Figure 6.53: Number of generations for convergence vs mutation rate

Since tuning is intended to obtain "robust" quantitative parameters that can suit for a wide range of instances, they have been "aggregated" on trend lines that can be averagely representative of the influence of the unknown parameters on the algorithm's performance.

To this end, the points in Figure 6.52 and Figure 6.53 have been aggregated on polynomial trend lines, while linear trend line has been used to "average" the errors value.

By observing these curves, the best values selected for the quantitative parameters X_{keep} and μ_{mut} are 0.05 and 0.002, respectively.
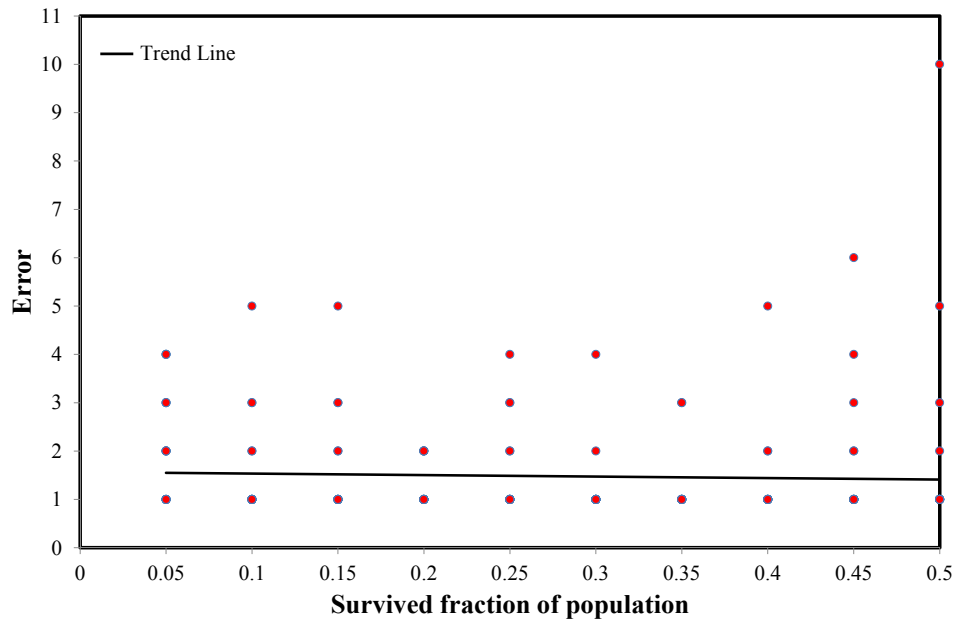
Figure 6.54: Magnitude of error vs survived fraction of the population
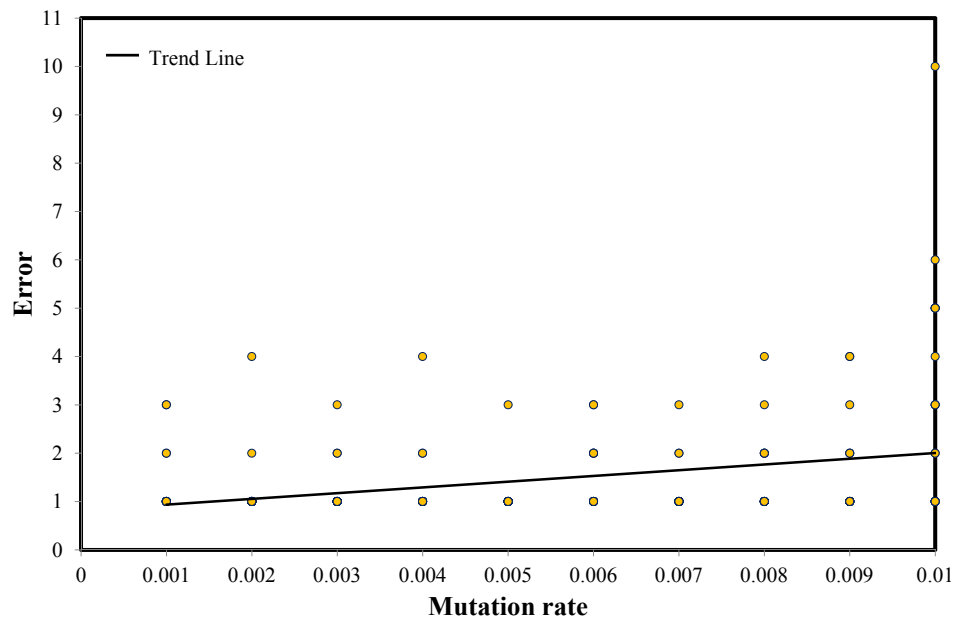
Figure 6.55: Magnitude of error vs mutation rate

6.10 Parallel computing

As already seen in the previous chapter, the proposed GA searches parallel from a population of N_{ind} individuals. To evaluate the objective function of each candidate solution, a simulation step carried out through the OpenSees framework is needed.

In particular, four pushover analyses are executed to simulate the response of each structural finite element model in the main orthogonal stiffness directions (Figure 6.56).
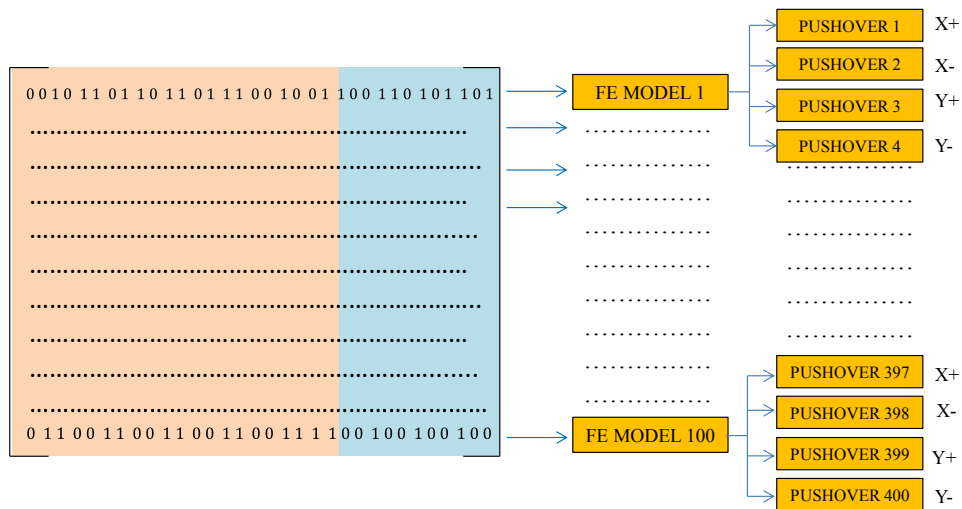
Figure 6.56: Total number of pushover analyses for each population

Since a total number of $4*N_{ind}$ seismic analyses are required for each population, the simulation is a very time-consuming task which represents the most time-consuming step. Hence, great attention has been focused on this stage to look for a way to speed up the procedure.

To this end, it is worth to say that for each individual of the population, 4 separate TCL files are automatically created to execute the seismic analyzes of the retrofitted configuration (X+, X-,Y+,Y-). All the TCL files needed to execute the seismic analysis for the entire population have been numbered by an incremental counter starting from "Pushover1.tcl".

As known, each pushover analysis can be separately executed because each TCL file concerns seismic analysis on a different model whose results do not depend on each other. Hence, working with a population of independent possible

solutions makes GA naturally suited for parallel computing which helps the fast processing of a large amount of data.

The term "parallel calculation" means the use of multiple computational processing units to solve problems. It is a form of computation in which many calculations are carried out simultaneously, operating on the principle that large problems can often be divided into smaller ones, which are then solved concurrently "in parallel".

A problem is decomposed into independent parts (tasks) that can be solved concurrently (in parallel). Each part is "split" into sequences of instructions to be executed at the same time instant on different CPUs as shown in Figure 6.57.
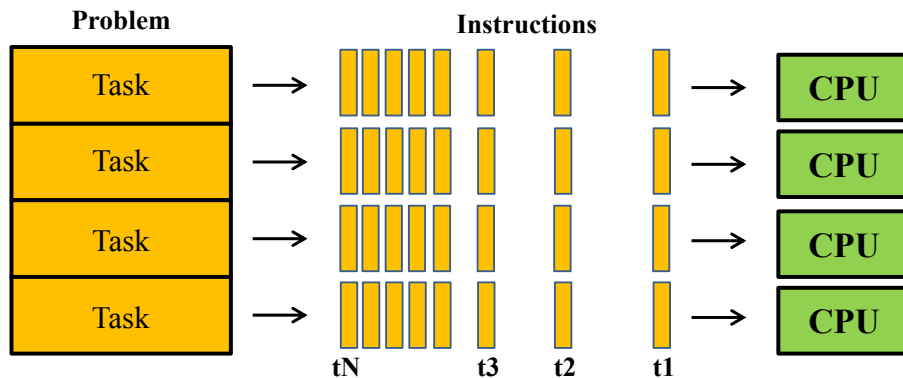
Figure 6.57: Working principle of basic parallel computing

Historically, parallel computing has been seen as a paradigm that can save time and reduce costs (use of several economic processors instead of 1 more expensive).

There are lots of different types of parallelism that allow to speed-up the execution of the above-mentioned analysis as much as possible. These programming models are not specific to a particular type of machine or memory architecture but can be theoretically implemented on any architecture.

The hardware architecture of workstations available at the University of Salerno and employed to validate the procedure is characterized by "multicore" processor (Figure 6.58).

Until 2003 such family of processors did not exist because the limit size of the transistors was still at 130 nm and did not "physically" allow the presence of 2 cores mounted on a single package.

Starting from 2005, the miniaturization of transistors, taken to the size of 10-20 nanometers, did save enough space in the single chip to integrate other cores in addition to the one already present.

Figure 6.58: Processor Intel Core i7 employed to run the procedure

Hence, a multi-core CPU is nothing other than a single computing component with two or more independent "physical" central processing units (called "cores"), which are the units that read and execute program instructions and can access to system memory (Figure 6.59).

This type of architecture compared to the single core allows an increase of the computing power of a CPU without increasing the working clock frequency.

CENTRAL PROCESSING UNIT (CPU)
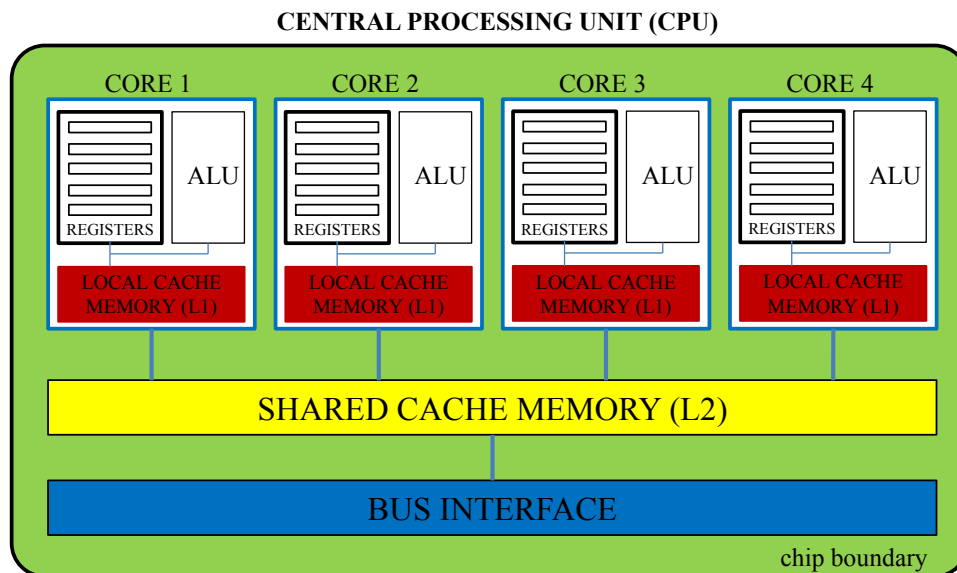
Figure 6.59: Example of multi-core CPU

The parallel programming model usually associated with multi-core shared memory architectures is the multi-threaded model. In a multi-threaded model, a single process can create some execution units called "threads" that the operating system schedules concurrently (in competition).

Each thread shares all the resources associated with the process that generated it (including its memory location), has its own memory area and communicates with the other threads through the global memory space. Synchronization operations are necessary to avoid that, at the same time, more than one thread tries to update a global memory location.

Single-threaded programs (that is generally the default behavior of a code developer) execute one line of code at a time, then move onto the next line in sequential order.

Multi-threaded programs, whereas, are executing from two or more locations in the program at the same time (or at least, with the illusion of running at the same time).

This approach differs from multi-processing: where multi-processing systems include multiple complete CPUs all working at the same time, multi-threading aims to increase utilization of a single core by using thread-level as well as instruction-level parallelism.

Therefore, multithreading is considered a form of parallel computing in that it allows things like memory references to execute at the same time as unrelated instructions, but it's essentially a variant on pipelined execution. It is worth saying that on single-core processors, the threads will be time-sliced by the operating system in the same way processes are in a multi-tasking environment and all run on the single core, so there is no effective performance gain.

In contrast, if the processor has multiple cores, and the operating system supports it, creating a new thread will cause the new thread to be executed on an unused or least busy core. Since the employed processor has multiple cores, the threads can be executing really simultaneously.

Therefore, running a multi-threaded application on multi-core processor can enable a several-fold performance increase on complex tasks. Obviously, with the same task, the relation between the number of cores and CPU usage is shown in Figure 6.60.
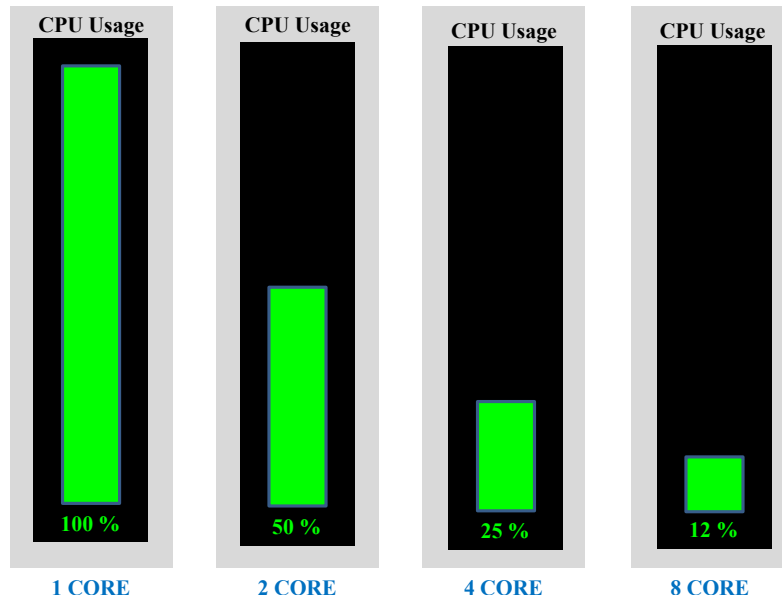
Figure 6.60: Variation of CPU usage with increasing of number of cores

6.10.1 MATLAB's multi-threaded libraries

MATLAB allows the user to benefit from the built-in parallelism provided by the multi-threaded nature of many libraries.

The speedup of the simulation step has been thus possible. In fact, thanks to the Parallel Computing Toolbox in MATLAB, it has been possible to leverage the full processing power of multi-core processor by running applications on locally independent MATLAB sessions called "workers".

Moreover, MATLAB offers the "*parfor*" loop to split the execution of for-loop over several workers provided that each iteration in the *parfor* loop is independent on the results of all others and the loop index is consecutive integers.

A *parfor*-loop can provide significantly better performance than its analogous for-loop, because several MATLAB workers can compute simultaneously on the same loop. *Parfor* divides the loop iterations into groups so that each thread can execute one group of iterations. In general terms, the *parfor*-loop can be useful if many loop iterations that take a long time to execute exist: *parfor* divides the loop iterations into groups so that each worker executes simultaneously some portion of the total number of iterations.

By default, *parfor* automatically opens a "parallel pool" of workers (if it does not already exist) on the local machine. The *parpool* command enables the full

functionality of the parallel loop in MATLAB by creating a special job on a pool of workers, and connecting the MATLAB client to the parallel pool. Data starts on base "client" workspace, and automatically copied to workers' workspaces. The client sends the necessary data on which *parfor* operates to workers, where most of the parallel computation is executed.

The results are then sent back to the client and assembled. MATLAB handles the actual scheduling of the workers for the user who doesn't need to say what goes where (details are intentionally opaque to the user). The workers evaluate iterations in no particular order and independently of each other.

They can be used interactively and communicate with each other during the lifetime of a job. The *parpool* command starts a set of workers using the default cluster profile, with the pool size specified by the user's parallel preferences. The user can change pool size and the cluster in the Parallel menu.

Moreover, the command *parpool (poolsize)* overrides the number of workers specified in the preferences or profile and starts a pool of exactly that number of workers, even if it is necessary to wait for them to be available. If the number of workers is equal to the number of loop iterations, each worker performs one iteration of the loop.

If there are more iterations than workers, some workers perform more than one loop iteration; in this case, a worker might receive multiple iterations at once to reduce communication time. If the number of iterations does not exceed the number of workers, the user cannot use all workers available and some workers perform no work. If the user requests more workers than the number of available workers, then Matlab uses the maximum number of workers available at the time of the call. If *parfor* cannot run on multiple workers because no parallel pool exist (for example, if only one core is available), Matlab executes the loop in a serial manner.

It is worth noting that when determining the default size of the local cluster, Matlab uses the number of true ("physical") cores available because the so-called "hyper-threading" is ignored. Hyper-threading is the commercial name given by Intel to its implementation of the Simultaneous Multi-Threading technology used to improve the performance of the processors by duplicating some internal processing units of the chips, so as to simultaneously execute certain threads.

Hence, a single ("physical") core processor with Hyper-Threading technology is indistinguishable from a dual ("logical") core processor. For example, a quad-core processor without Hyper-threading technology is characterized by 4 physical core

and 4 logical core (Intel Core i5); a quad-core with Hyper-Threading has 4 physical core and 8 logical core (Intel Core i7) and so on.

It is generally best practice to have the same number of workers as true cores on the user's machine. Opening more workers than cores don't usually improve performance.

Figure 6.61shows an example: if a quad-core processor is available then a local cluster with 4 workers should be preferred.
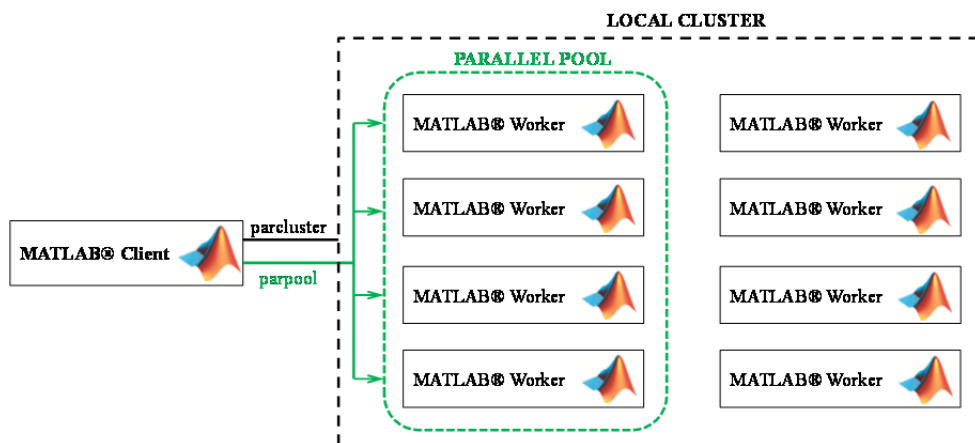
Figure 6.61: Example of parallel pool suggested in a quad-core processor

However, it is worth highlighting that running *parfor* on four workers threads will not necessarily be about three times faster than the corresponding for-loop calculation.

The speed-up is smaller than the ideal (linear) speed-up of a factor of four on four workers. This is due to the so-called "parallel overhead" which includes the time required for communication, coordination parallel task and data transfer, sending and receiving data from client to workers and back.

Hence, there is a trade-off between the number of workers and their actual use due to communication times: as the number of workers grows, the amount of data to be exchanged increases, and, therefore, the average time each worker is waiting for data.

This effect is described by Amdahl's law [367] that can be used to calculate how much a computation can be sped up by running part of the program in parallel. According this law, let p be the number of cores available, α the fraction of the program that is strictly serial (the fraction of operations that can be performed only

sequentially), for a problem of fixed size, the maximum speedup S achievable by a parallel computing is a function of the number of cores applied for the execution and the fraction (1-α) of the program that can be run in parallel on multiple cores, according to the following equation:

$$S = \frac{1}{\alpha + \frac{1}{p} \cdot (1 - \alpha)} \tag{6.40}$$

Although the ideal linear speedup ($S=p$) is not achievable, the so-called "embarrassingly" parallel problems may realize speedup factors near the number of cores. The sub-linear speed-up occurs in most real situations (Figure 6.62).
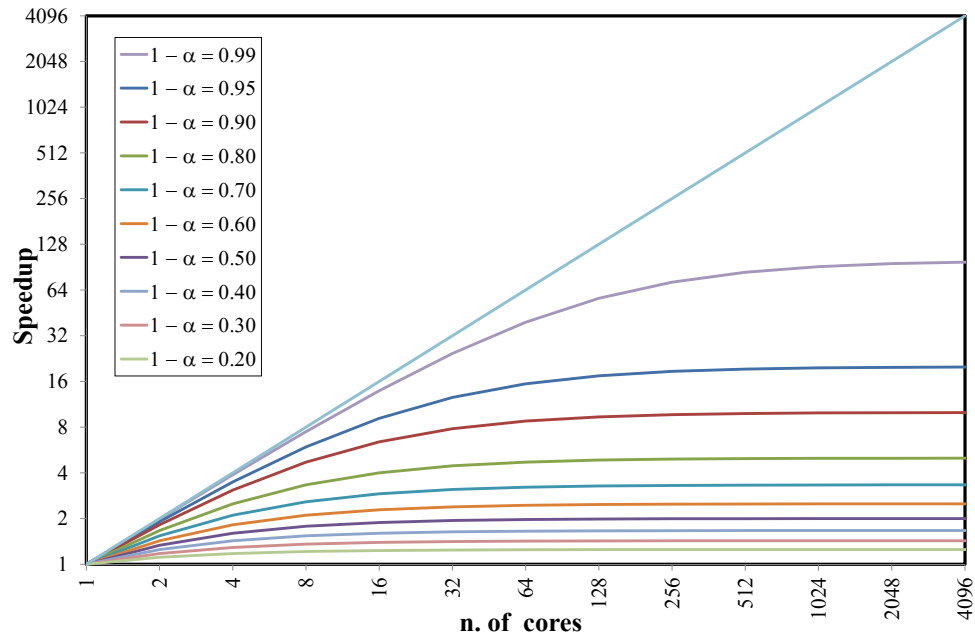
Figure 6.62: Relationship between speedup and number of cores (Amdahl's law [367])

7. Applications

The working details and the actual potential of the proposed optimization procedure can well outline considering the sample applications reported in this section. The applications concern some structures obtained through simulated design according to practices and techniques in force in the 60s and 70s of the last century.

Such structures can be defined as "case studies", which are the result of some simulated designs that follow the old regulatory codes, therefore, without complying with the rules of the seismic regulations. Both the LSs of Life Safety (SLV) and Damage Limitation (SLD) are considered (n_{LS}=2).

The considered structures are characterized by a certain initial level of vulnerability and thus require a seismic retrofitting. The structures have a very simple construction typology, as they have a rectangular plan composed of frames in both directions.

However, the presence of frames in both directions was not customary at the construction time, but for the purposes of the present thesis, it is appropriate to use this type of structural system.

The next paragraph will be devoted to the geometric description of the structures taken as "case study". In fact, two simple 3D frames, named "Structure 1" and "Structure 2", regular in plan and in elevation, are taken as preliminary examples for applying the software package proposed herein.

The Structure 1

The plan of "Structure 1" is characterized by a length of the long side and the short side respectively of 25.00 m and 15.00 m and an inter-floor height equal to 3.50 m.

A global coordinate system is used: the global Z-axis is the vertical direction of the structure, the global Y-axis is orthogonal to the horizontal plane, representing the transverse direction, while the global X-axis is denoted as the longitudinal direction. The structure is composed of four frames parallel to the X direction, four

parallel to the direction Y, forming an orthogonal grid, with 15 bays for each deck, with warping parallel to the Y-axis.

This structure is composed of four decks each having the same geometric characteristics, as shown in Figure 7.1. Regarding the concrete, reference was made to a resistance class C20/25 where the 20 means the cylindrical resistance f_{ck} while 25 indicates the cubic resistance R_{ck}.

As for steel for re-bars, a modulus of elasticity of steel is chosen equal to 210 GPa and the yield stress is F_y=220 MPa. Regarding the load analysis, the following applications are characterized by a classic slab scheme widely used in existing buildings, i.e. the brick-cement one: the floor is characterized by a height of 24 cm where 20 cm as the size of the pot and 4 cm of solid concrete slab, the distance between the single joists is 50 cm for a total of two joists and two bricks for each meter.

The analysis of the loads, carried out for a square meter of the floor, has led to the following results: the permanent load is G=5.00 kN/m^2 and the live load is Q=2.00 kN/m^2. The gravity loads are contributed from an effective area of 375 m^2.
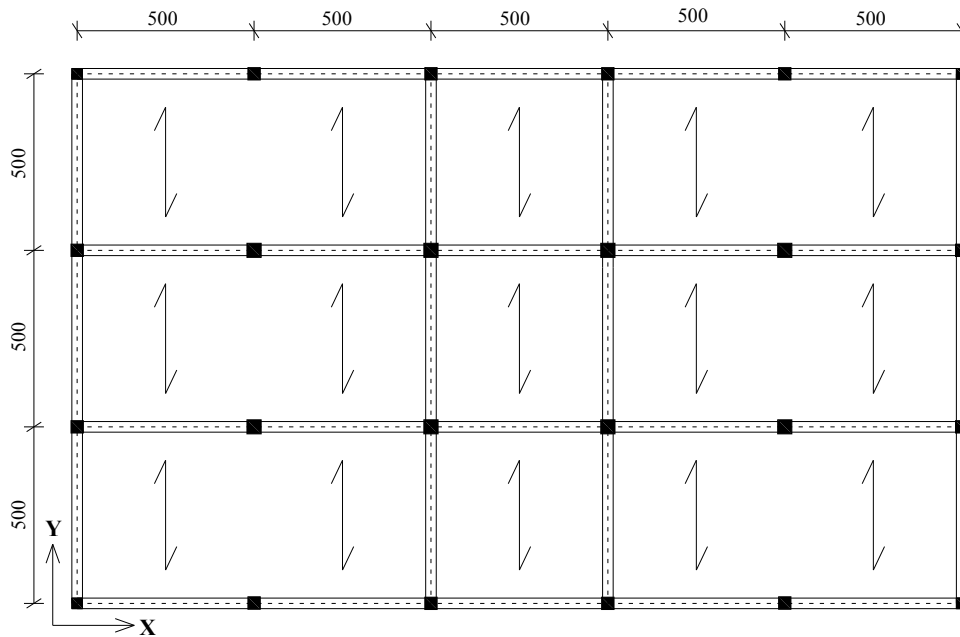
Figure 7.1: In-plane configuration of "structure 1"

Three cross-sectional areas employed for vertical members are shown in Figure 7.2.
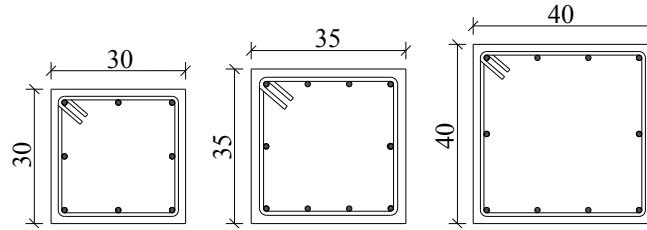
Figure 7.2: Cross-section of column elements in "structure 1"

The following Table 7.1 list all the labels of the column elements.

Table 7.1: Labels and sections of each column at each floor in "structure 1"

1ST FLOOR		2ND FLOOR		3RD FLOOR		4TH FLOOR	
Label	Section	Label	Section	Label	Section	Label	Section
1	30x30	101	30x30	201	30x30	301	30x30
2	35x35	102	35x35	202	35x35	302	35x35
3	35x35	103	35x35	203	35x35	303	35x35
4	35x35	104	35x35	204	35x35	304	35x35
5	35x35	105	35x35	205	35x35	305	35x35
6	30x30	106	30x30	206	30x30	306	30x30
7	35x35	107	35x35	207	35x35	307	35x35
8	40x40	108	40x40	208	40x40	308	40x40
9	40x40	109	40x40	209	40x40	309	40x40
10	40x40	110	40x40	210	40x40	310	40x40
11	40x40	111	40x40	211	40x40	311	40x40
12	35x35	112	35x35	212	35x35	312	35x35
13	35x35	113	35x35	213	35x35	313	35x35
14	40x40	114	40x40	214	40x40	314	40x40
15	40x40	115	40x40	215	40x40	315	40x40
16	40x40	116	40x40	216	40x40	316	40x40
17	40x40	117	40x40	217	40x40	317	40x40
18	35x35	118	35x35	218	35x35	318	35x35
19	30x30	119	30x30	219	30x30	319	30x30
20	35x35	120	35x35	220	35x35	320	35x35
21	35x35	121	35x35	221	35x35	321	35x35
22	35x35	122	35x35	222	35x35	322	35x35
23	35x35	123	35x35	223	35x35	323	35x35
24	30x30	124	30x30	224	30x30	324	30x30

The following Table 7.2 list all the labels of the beam elements.

Table 7.2: Labels and sections of each beam at each floor in "structure 1"

1ST FLOOR		2ND FLOOR		3RD FLOOR		4TH FLOOR	
Label	Section	Label	Section	Label	Section	Label	Section
1101	30x50	2201	30x50	3301	30x50	4401	30x50
1102	30x50	2202	30x50	3302	30x50	4402	30x50
1103	30x50	2203	30x50	3303	30x50	4403	30x50
1104	30x50	2204	30x50	3304	30x50	4404	30x50
1105	30x50	2205	30x50	3305	30x50	4405	30x50
1106	30x50	2206	30x50	3306	30x50	4406	30x50
1107	30x50	2207	30x50	3307	30x50	4407	30x50
1108	30x50	2208	30x50	3308	30x50	4408	30x50
1109	30x50	2209	30x50	3309	30x50	4409	30x50
1110	30x50	2210	30x50	3310	30x50	4410	30x50
1111	30x50	2211	30x50	3311	30x50	4411	30x50
1112	30x50	2212	30x50	3312	30x50	4412	30x50
1113	30x50	2213	30x50	3313	30x50	4413	30x50
1114	30x50	2214	30x50	3314	30x50	4414	30x50
1115	30x50	2215	30x50	3315	30x50	4415	30x50
1116	30x50	2216	30x50	3316	30x50	4416	30x50
1117	30x50	2217	30x50	3317	30x50	4417	30x50
1118	30x50	2218	30x50	3318	30x50	4418	30x50
1119	30x50	2219	30x50	3319	30x50	4419	30x50
1120	30x50	2220	30x50	3320	30x50	4420	30x50
1121	30x50	2221	30x50	3321	30x50	4421	30x50
1122	30x50	2222	30x50	3322	30x50	4422	30x50
1123	30x50	2223	30x50	3323	30x50	4423	30x50
1124	30x50	2224	30x50	3324	30x50	4424	30x50
1125	30x50	2225	30x50	3325	30x50	4425	30x50
1126	30x50	2226	30x50	3326	30x50	4426	30x50
1127	30x50	2227	30x50	3327	30x50	4427	30x50
1128	30x50	2228	30x50	3328	30x50	4428	30x50
1129	30x50	2229	30x50	3329	30x50	4429	30x50
1130	30x50	2230	30x50	3330	30x50	4430	30x50
1131	30x50	2231	30x50	3331	30x50	4431-2	30x50
1132	30x50	2232	30x50	3332	30x50		

All the beams forming the frame are characterized by a 30x50 cm^2 cross-section depicted in Figure 7.3.
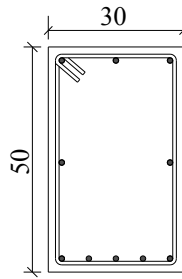
Figure 7.3: Cross-section of beam members in "structure 1"

The elevation configuration of the structure in the <ZX> plane and in the <ZY> plane are shown in Figure 7.4 and in Figure 7.5.
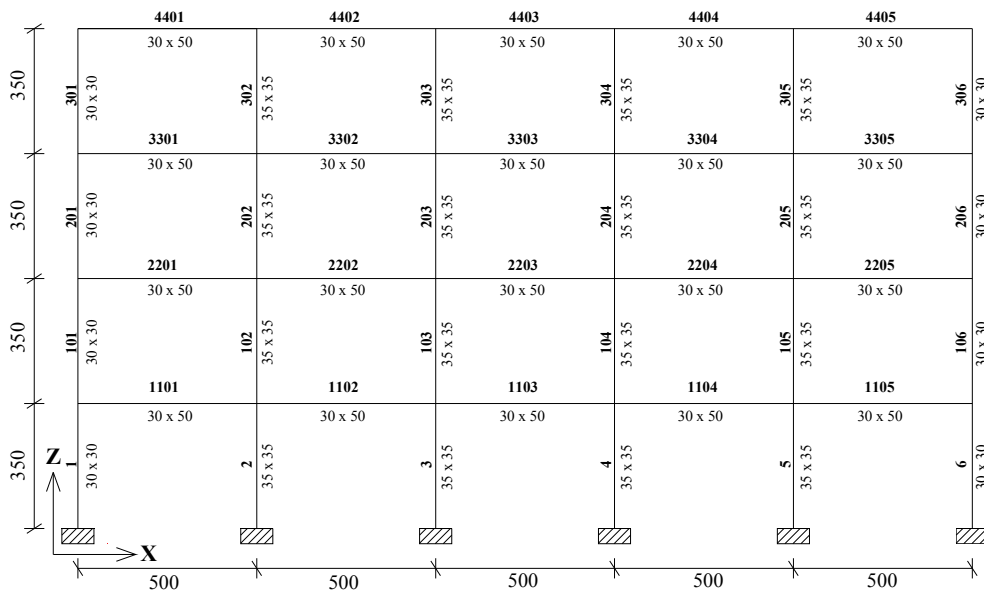
Figure 7.4: Configuration of <ZX> elevation of "structure 1"
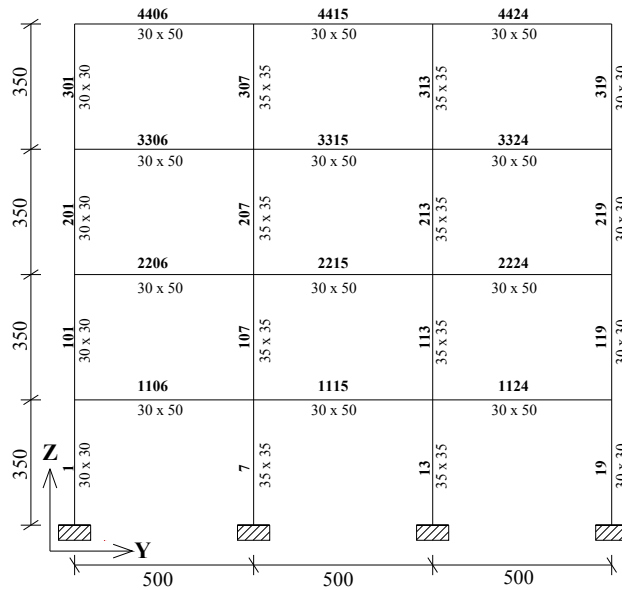
Figure 7.5: Configuration of <ZY> elevation of "structure 1"

The total number of design variables considered in the example is 128 (Figure 7.6): 4 x 24 "member-level" variables (24 columns for each floor), plus 32 "structure-level" variables (20 beams in X-direction and 12 in the Y-direction).
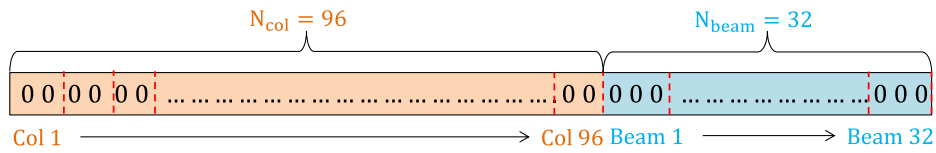
Figure 7.6: Binary genotype and number of design variables for "structure 1"

Hence, the entire search space consists of $4^{96} \cdot 8^{32}$ candidate solutions (Figure 7.7).
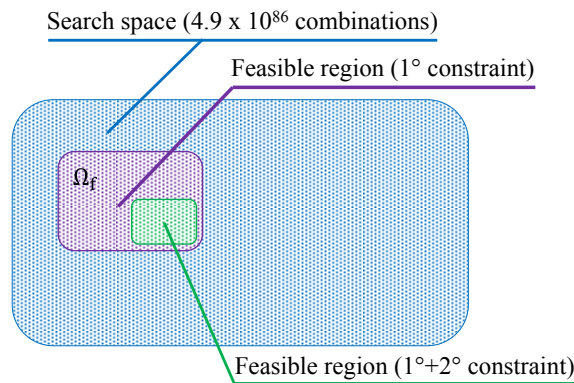
Figure 7.7: Entire search space and feasible region

As shown, the search space to which the minimum cost solution belongs may be further "restricted" by adding another constraint. In fact, the feasible region is the space of solutions that satisfy the following inequality:

$$g_{LS,i}(x) = C_{LS,i}(x) - D_{LS,i}(x) \geq 0 \quad \forall i = 1...n_{LS} \tag{7.1}$$

In the present Thesis, a further constraint within the feasible region of the seismic retrofitting solutions is accounted.

This limitation is analytically described by the following inequalities:

$$\left| \min_i \left[\frac{C_{LS,i}(x)}{D_{LS,i}(x)} \right]_{dirX+} - \min_i \left[\frac{C_{LS,i}(x)}{D_{LS,i}(x)} \right]_{dirX-} \right| < \varepsilon \text{ (tolerance)} \tag{7.2}$$

$$\left| \min_i \left[\frac{C_{LS,i}(x)}{D_{LS,i}(x)} \right]_{dirY+} - \min_i \left[\frac{C_{LS,i}(x)}{D_{LS,i}(x)} \right]_{dirY-} \right| < \varepsilon \text{ (tolerance)} \tag{7.3}$$

where the terms dirX+, dirX-, dirY+ and dirY- refer to the pushover directions.

The structure 2

The plan of "Structure 2" is characterized by a length of the long side and the short side respectively of 20.00 m and 15.00 m and an inter-floor height equal to 3.50 m.

It is composed of four frames parallel to the X direction, five parallel to the direction Y, forming an orthogonal grid, with 12 bays for each deck, with warping parallel to the X-axis.

This structure is composed of three decks each having the same geometric characteristics, as shown in Figure 7.8. Concrete and steel materials are the same chosen for structure 1. Both permanent and live loads too.

The gravity loads are contributed from an effective area of 300 m^2.
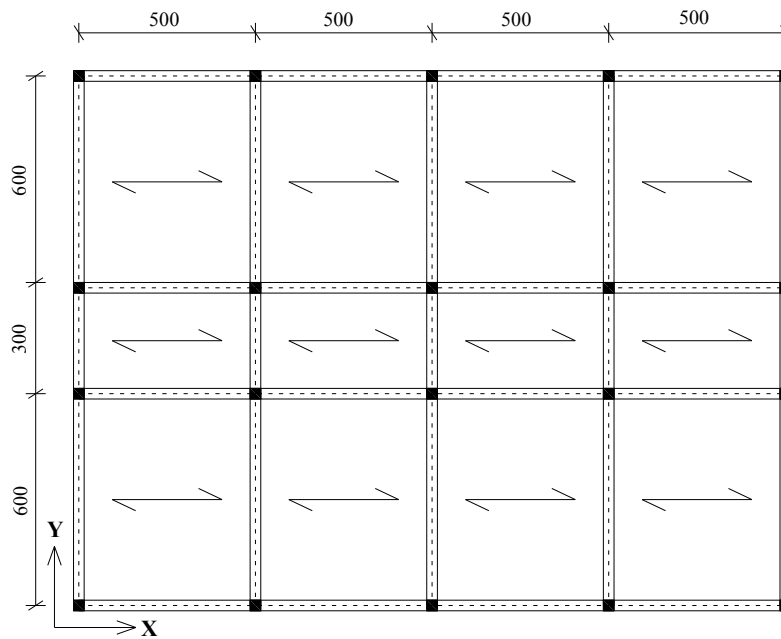
Figure 7.8: In-plane configuration of "structure 2"

All the columns are characterized by the same cross-section whose size is shown in Figure 7.9. They are reinforced through 8 longitudinal re-bars with ϕ12 diameters.
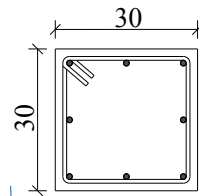
Figure 7.9: Cross-section of columns element in "structure 2"

The following Table 7.3 collects all the labels of the column elements.

Table 7.3: Labels and sections of each column at each floor in "structure 2"

1ST FLOOR			2ND FLOOR			3RD FLOOR	
Label	Section		Label	Section		Label	Section
1	30x30		101	30x30		201	30x30
2	30x30		102	30x30		202	30x30
3	30x30		103	30x30		203	30x30
4	30x30		104	30x30		204	30x30
5	30x30		105	30x30		205	30x30
6	30x30		106	30x30		206	30x30
7	30x30		107	30x30		207	30x30
8	30x30		108	30x30		208	30x30
9	30x30		109	30x30		209	30x30
10	30x30		110	30x30		210	30x30
11	30x30		111	30x30		211	30x30
12	30x30		112	30x30		212	30x30
13	30x30		113	30x30		213	30x30
14	30x30		114	30x30		214	30x30
15	30x30		115	30x30		215	30x30
16	30x30		116	30x30		216	30x30
17	30x30		117	30x30		217	30x30
18	30x30		118	30x30		218	30x30
19	30x30		119	30x30		219	30x30
20	30x30		120	30x30		220	30x30

The longitudinal reinforcement of beams is assumed to be composed of 8 bars $\phi12$, as shown in the Figure 7.10.
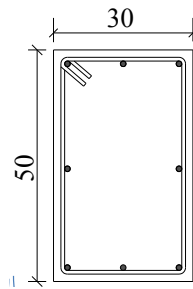
Figure 7.10: Cross-section of beam members in "structure 2"

Table 7.4 collects all the labels of the beam members and their section.

Table 7.4: Labels and sections of each beam at each floor in "structure 2"

1ST FLOOR			2ND FLOOR			3RD FLOOR	
Label	Section		Label	Section		Label	Section
1101	30x50		2201	30x50		3301	30x50
1102	30x50		2202	30x50		3302	30x50
1103	30x50		2203	30x50		3303	30x50
1104	30x50		2204	30x50		3304	30x50
1105	30x50		2205	30x50		3305	30x50
1106	30x50		2206	30x50		3306	30x50
1107	30x50		2207	30x50		3307	30x50
1108	30x50		2208	30x50		3308	30x50
1109	30x50		2209	30x50		3309	30x50
1110	30x50		2210	30x50		3310	30x50
1111	30x50		2211	30x50		3311	30x50
1112	30x50		2212	30x50		3312	30x50
1113	30x50		2213	30x50		3313	30x50
1114	30x50		2214	30x50		3314	30x50
1115	30x50		2215	30x50		3315	30x50
1116	30x50		2216	30x50		3316	30x50
1117	30x50		2217	30x50		3317	30x50
1118	30x50		2218	30x50		3318	30x50
1119	30x50		2219	30x50		3319	30x50
1120	30x50		2220	30x50		3320	30x50
1121	30x50		2221	30x50		3321	30x50
1122	30x50		2222	30x50		3322	30x50
1123	30x50		2223	30x50		3323	30x50
1124	30x50		2224	30x50		3324	30x50
1125	30x50		2225	30x50		3325	30x50
1126	30x50		2226	30x50		3326	30x50
1127	30x50		2227	30x50		3327	30x50
1128	30x50		2228	30x50		3328	30x50
1129	30x50		2229	30x50		3329	30x50
1130	30x50		2230	30x50		3330-1	30x50
1131	30x50		2231	30x50			

Figure 7.11 and in Figure 7.12 show the elevation configuration of the structure in the <ZX> plane and in the <ZY> plane, respectively.
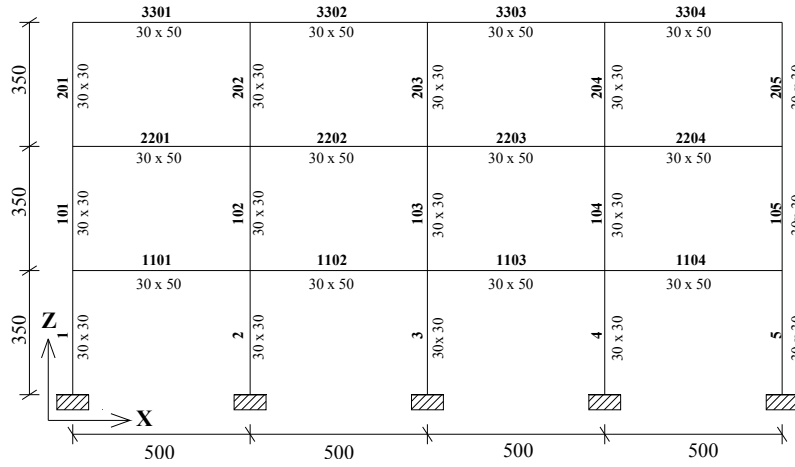
Figure 7.11: Configuration of <ZX> elevation of "structure 2"
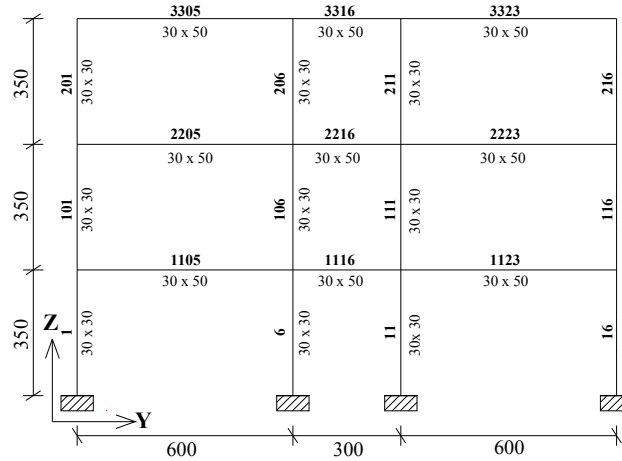
Figure 7.12: Configuration of <ZY> elevation of "structure 2"

The total number of design variables considered in this example is 91 (Figure 7.13): 3 x 20 "member-level" variables (20 columns for each floor), plus 31 structure-level variables (16 beams in X-direction and 15 in the Y-direction).
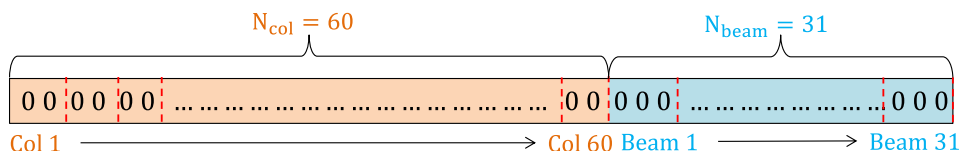
Figure 7.13: Binary genotype and number of decision variables for "structure 2"

The entire search space, therefore, consists of a number of candidate solutions equal to $4^{60} \cdot 8^{31}$. It is clear that also in this case the search for the optimal solution through an exhaustive exploration of the design space is impractical to solve for any computer because it would require years of work.

Figure 7.14 shows the total number of combination belonging to the search space.
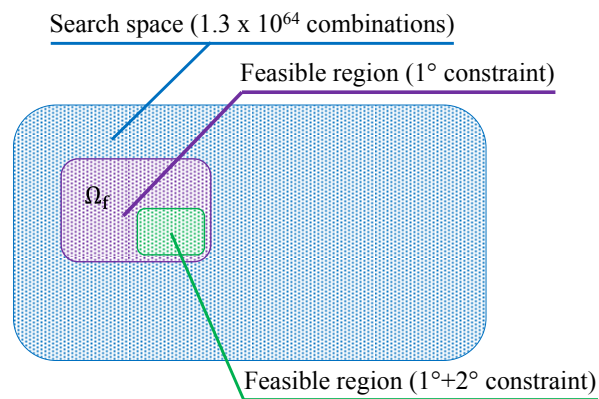
Figure 7.14: Entire search space and feasible region

It seems clear that the application of a second constraint could make infeasible the solutions that satisfy only the first constraint.

For this reason, the solving of a constrained minimum problem becomes theoretically more and more complicated as the number of nonlinear constraints to be met increases.

The Elastic Demand spectra

It is assumed that the existing structures were built in the municipalities falling in different seismic zones corresponding to the seismic actions currently expected in three Italian places, namely L'Aquila (zone 1), Lioni (zone 1) and Angri (zone 2).

These municipalities are characterized by Elastic Response Spectra (represented in the ADRS format) with decreasing severity levels (Figure 7.175-7.17). A ground type C is chosen for L'Aquila and Angri, while type B in the case of Lioni.

Table 7.5: Seismic risk parameters of ERS for L'Aquila – soil category C

	PGA	S	T_B	T_C	T_D	ε	F_0	S_S	T_C^*
SLD	0.104	1.500	0.150	0.449	2.017	5	2.332	1.500	0.281
SLV	0.261	1.330	0.172	0.516	2.643	5	2.364	1.330	0.347
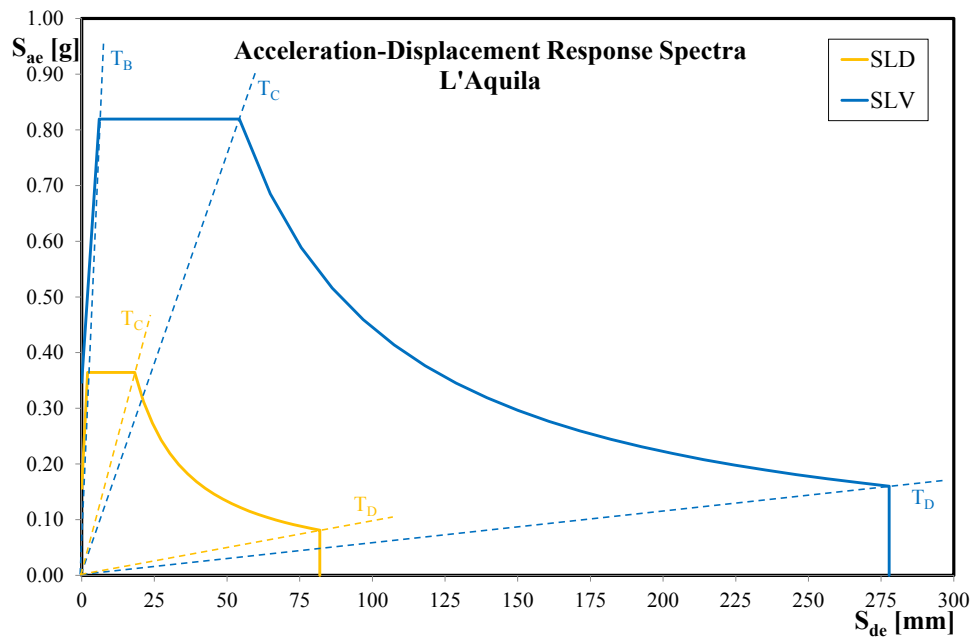
Figure 7.15:Elastic Demand Spectra for L'Aquila (ADRS format)

Table 7.6: Seismic risk parameters of ERS for Lioni – soil category B

	PGA	S	T_B	T_C	T_D	ε	F_0	S_S	T_C*
SLD	0.080	1.200	0.138	0.414	1.919	5	2.346	1.200	0.295
SLV	0.258	1.163	0.168	0.503	2.633	5	2.291	1.163	0.376
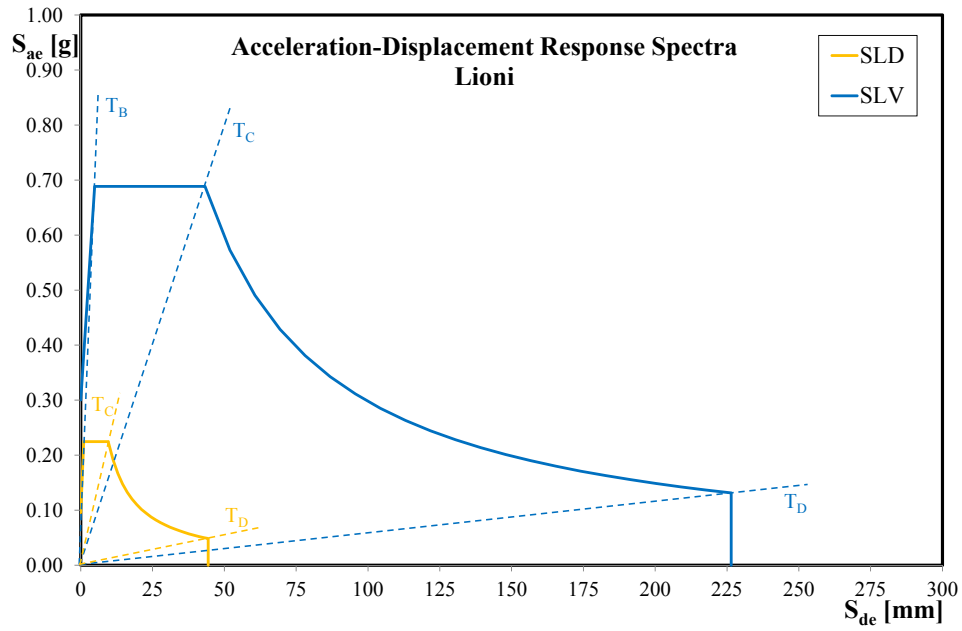
Figure 7.16: Elastic Demand Spectra for Lioni (ADRS format)

Table 7.7: Seismic risk parameters of ERS for Angri – soil category C

	PGA	S	T_B	T_C	T_D	ε	F_0	S_S	T_C^*
SLD	0.053	1.500	0.164	0.492	1.811	5	2.356	1.500	0.322
SLV	0.125	1.500	0.185	0.555	2.102	5	2.498	1.500	0.386
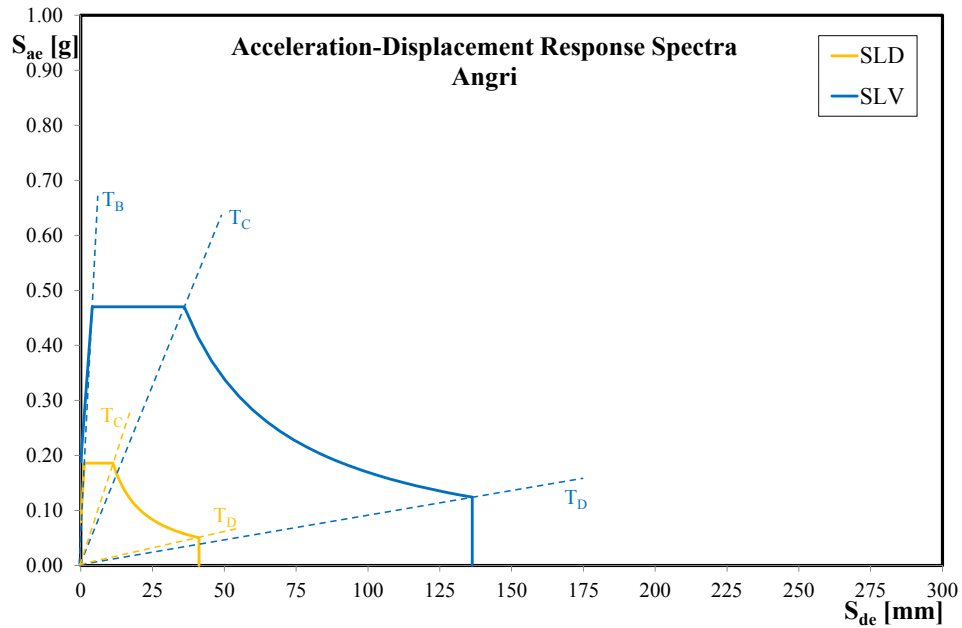
Figure 7.17: Elastic Demand Spectra for Angri (ADRS format)

The unit costs

The unit costs needed to calculate the objective function described in Section 6.4.2 are summarized in the following Table.

Table 7.8: List of unit costs

$C_{dem,unit}$	8.45	€/m^2
$C_{rest,unit}$	47.45	€/m^2
$C_{FRP,1layer,unit}$	207.20	€/m^2
$C_{FRP,2+layer,unit}$	168.00	€/m^2
$C_{steelB,unit}$	3.05	€/kg
$C_{micropile}$	1058.10	€/micro-pile
C_{excav}	144.05	€/m^3
$C_{concrete}$	122.00	€/m^3

7.1   The "case studies"

In order to evaluate the "robustness" of the proposed procedure, it is necessary to assess its sensitivity to changes in input data.

By varying the geometry of structure under examination, the construction site, the presence (or absence) of the enlargement intervention on the foundation system, and the presence (or absence) of a penalty term that further reduces the search space, a total of 15 "combinations" have been obtained (Table 7.9).

Table 7.9: List of "scenarios"

Case	Existing Structure	Construction Site	Ground Type	Foundation intervention	Penalty Eq. 7.2-7.3
1	5X 3Y 4Z	Lioni	B	No	No
2	5X 3Y 4Z	Lioni	B	Yes	No
3	5X 3Y 4Z	Lioni	B	Yes	Yes
4	5X 3Y 4Z	L'Aquila	C	No	No
5	5X 3Y 4Z	L'Aquila	C	Yes	No
6	5X 3Y 4Z	L'Aquila	C	Yes	Yes
7	4X 3Y 3Z	Lioni	B	No	No
8	4X 3Y 3Z	Lioni	B	Yes	No
9	4X 3Y 3Z	Lioni	B	Yes	Yes
10	4X 3Y 3Z	L'Aquila	C	No	No
11	4X 3Y 3Z	L'Aquila	C	Yes	No
12	4X 3Y 3Z	L'Aquila	C	Yes	Yes
13	4X 3Y 3Z	Angri	C	No	No
14	4X 3Y 3Z	Angri	C	Yes	No
15	4X 3Y 3Z	Angri	C	Yes	Yes

The sensitivity analysis consists in evaluating the effects on the results provided by the procedure induced by changes in the values of the input variables. Generally speaking, analysis "by scenarios" is used, where a scenario represents one of the possible combinations of values assumed by the variables.

The sensitivity analysis, therefore, aims to answer questions such as: how much would the final retrofit solution change if the cost of intervention on the foundation is added? The standard way to perform a sensitivity analysis is to vary one variable at a time while keeping the other variables constant. This done, the impact that a variation of each variable determines on the best seismic retrofit solution can be analyzed.

7.1.1   The Finite Element Model for as built-configurations

As seen above, the procedure requires a three-dimensional finite element model to capture the response of the entire structural system and individual elements under specific seismic demand characteristics.

However, the magnitude of the approximations made in the geometry, material's behavior, boundary conditions and loads, determines how much the numerical model corresponds to the physical problem to be analyzed.

Although the user can model an existing structure according to his level of experience and judgment, the following paragraphs show several assumptions used in the preliminary applications shown in this chapter.

The assumption

The uniaxial Kent-Scott-Park model with degraded linear unloading/reloading stiffness and no tensile strength [334] is assumed for modeling the behavior of concrete and the effect of FRP confinement. A bilinear stress-strain curve is adopted for describing the elastic-plastic behavior of steel.

The well-known *fiber* section approach (Figure 7.18) is used for accounting the material inelasticity in reinforced concrete members (both columns and beams).
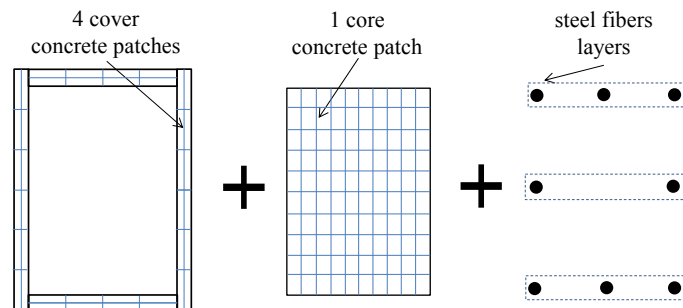
Figure 7.18: Fiber section approach for RC elements

The geometric configuration is formed by discretizing of the cross-section into sub-regions of simpler, regular shapes called "patches" for which the material stress-strain response is integrated to give resultant behavior.

A generalized subroutine is employed to build rectangular section with 4 cover concrete patches, 1 core concrete patch and 3 reinforcing layers of longitudinal re-bars: top and bottom layer reinforcement, 1 intermediate skin reinforcement layers.

The core concrete patch is considered to be not confined by the transversal stirrups (due to their wide spacing) and it is discretized into 100 fibers. Each section is divided into a number of fibers, which comply with beam kinematics and each follows its own constitutive model.

However, the fiber section itself only handles axial and flexural force-deformations relationship and their interaction is already considered. Since the shear and torsion are assumed to be coupled with the flexural and the axial response, an *Aggregator* object takes into account also shear and torsion deformation in the fiber section definition.

It is used to create a new section, taking the previously-defined uniaxial elastic material to represent the shear force-deformation along both y-and-z local axis, and the torsion force-deformation relationships (Figure 7.19).

Aggregator adds them to the existing section where the moment-curvature and axial force-deformation interaction is already accounted.

Figure 7.19: Working principle of an aggregator object

Both beam and column members are modeled with a distributed plasticity approach. *BeamWithHinges* command is selected from OpenSees library to construct a force-based nonlinear element: the internal force fields are expressed as functions of the nodal forces resulting from virtual force work in which a rigorous
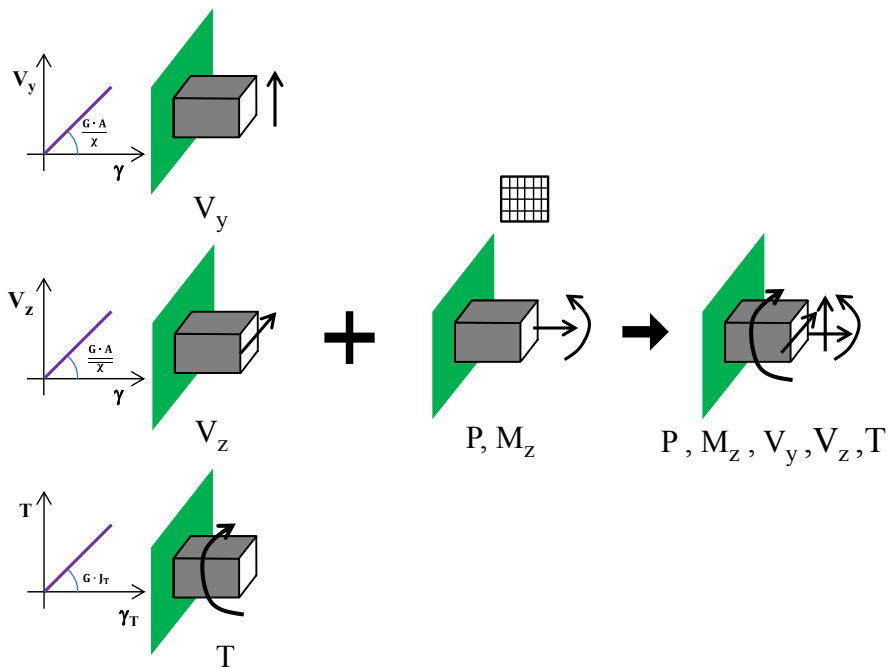
force function maintains the equilibrium and no restraints are placed on the development of inelastic deformations throughout the member.

The *BeamWith Hinges [368]* command is based on the flexibility formulation and considers plasticity to be assigned at the end element in the so-called "plastic-hinges" region with a finite length L_p, while the central part of the beam is simulated by a linear elastic element as shown in Figure 7.20. The compatibility relationship is separated into three integrals, one for each hinge region, where plasticity develops, and one for the interior region of the element.
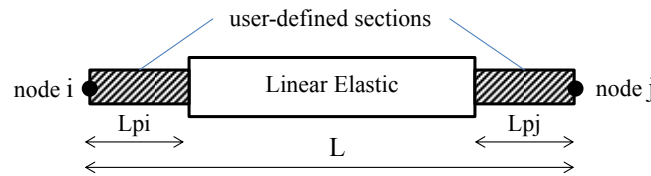
Figure 7.20: Distributed plasticity approach for RC members

Several formulae are available in the literature [369] to evaluate plastic hinge length L_p. In the present work, the plastic hinge length is chosen to be equal to the cross-section's height of the element.

For the existing structures, the floor (which is one of the most important elements for distribution of seismic actions) has been schematized with diagonals members made of a linear elastic material (with Young modulus E) because it cannot be considered infinitely rigid in its plane.

To this end, truss elastic elements hinged at the ends are used (Figure 7.21).

$$E \cdot b_{floor} \cdot h_{floor} = \frac{E \cdot h_{floor}}{10} \cdot \frac{\left(L_x^2 + L_y^2\right)^{\frac{3}{2}}}{L_x \cdot L_y}$$
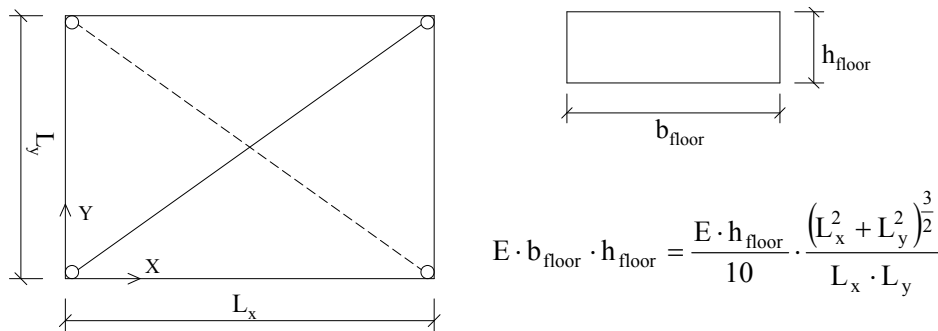
Figure 7.21: Diagonal elastic trusses for modeling floor slabs

Truss elements, by definition, are two-node members which transmit axial force only (like a real pendulum) and, in general, have a constant cross-sectional area.

The axial stiffness of diagonal truss must be consistent with the membrane's stiffness of the slab. In fact, in the present work, the derivation of the cross-sectional properties of the diagonal members is based on a reliable and widespread formula in the literature, proposed by Yettram and Hussain [370].

The whole frame is assumed to have rigid joints for simulating beam-to-column connections. Foundation is not simulated but fixed supports are considered.

Non-structural elements are not included in the FE model. Since the OpenSees interpreter does not process units, millimeters, Newton and seconds are used for length, force and time, respectively.

7.1.2   As-built conditions

According to the aforementioned assumption, the following paragraph collects the results of pushover analysis in as-built configuration (Figure 7.22-7.23) and both the displacement Capacity and Demand that the existing structure exhibit at the performance level considered herein.
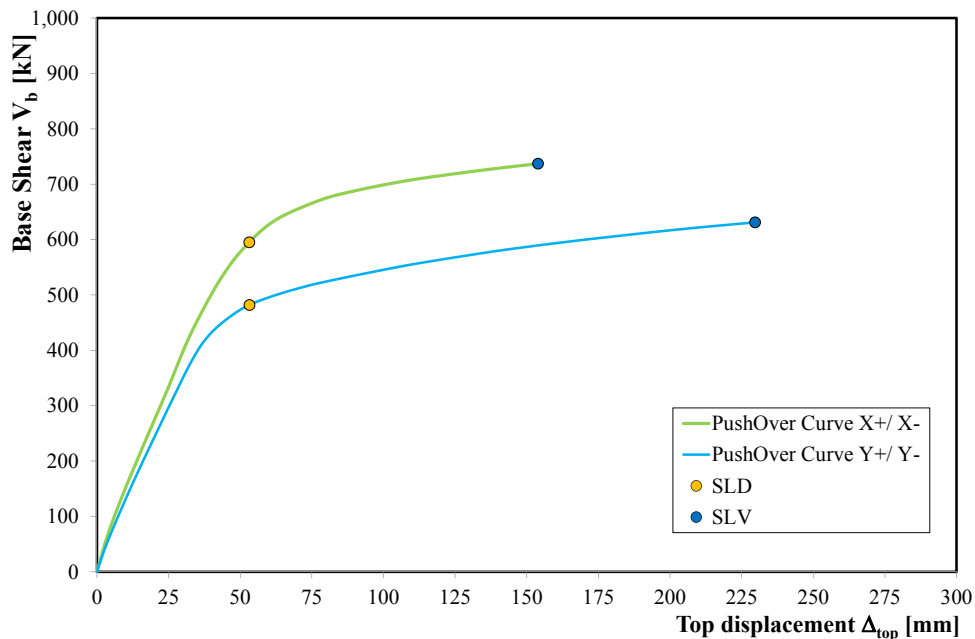
Figure 7.22: Pushover curve of "structure 1" in its as-built configuration
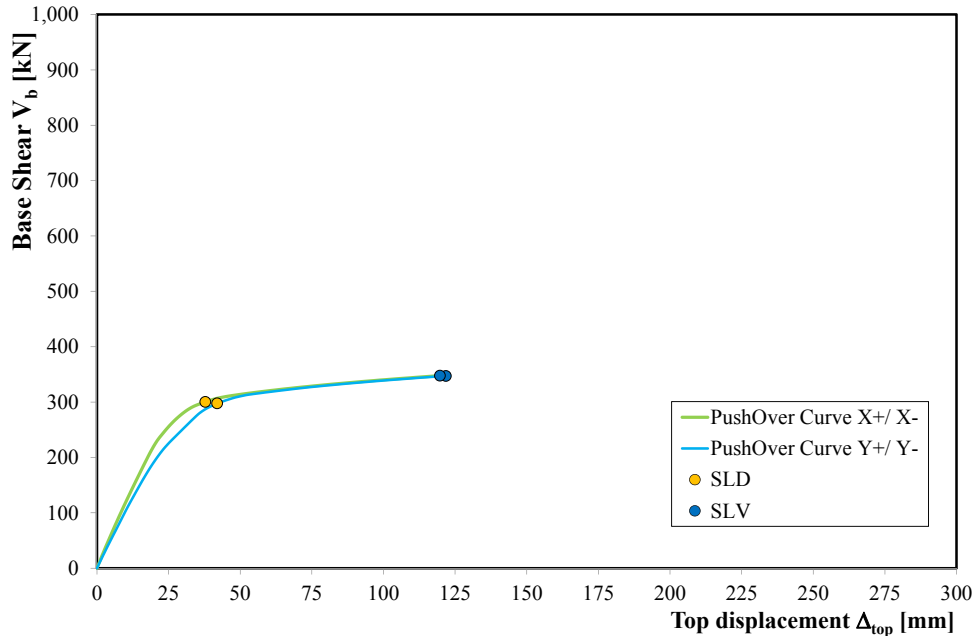
Figure 7.23: Pushover curve of "structure 2" in its as-built configuration

Once known, the pushover curves have been transformed in Capacity Spectrum in the ADRS diagram (Figure 7.24-7.28) in order to evaluate the demand.
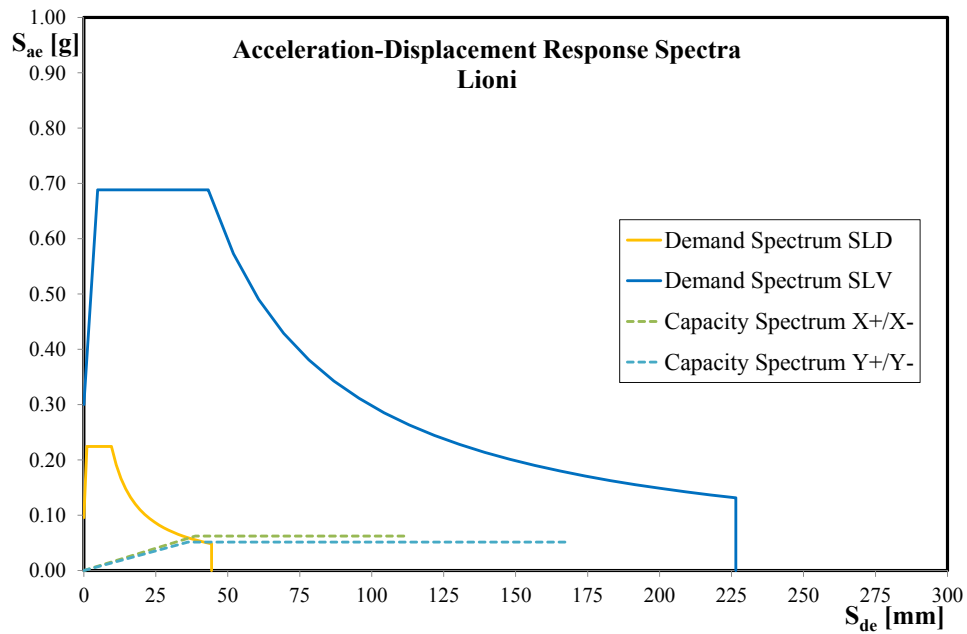
Figure 7.24: Intersection between Capacity (structure 1) and Demand Spectra of Lioni
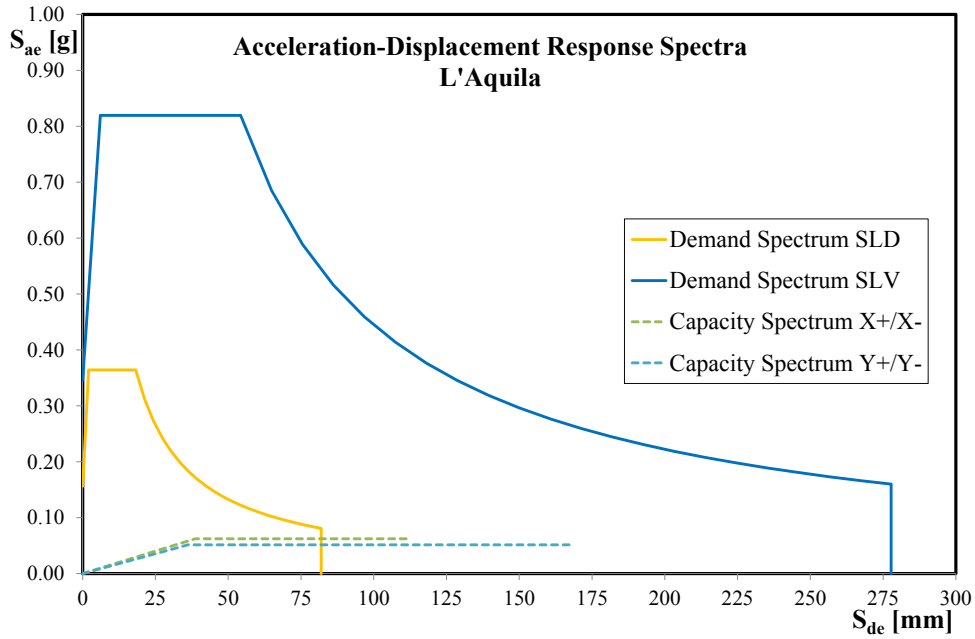
Figure 7.25: Intersection between Capacity (structure 1) and Demand Spectra of L'Aquila
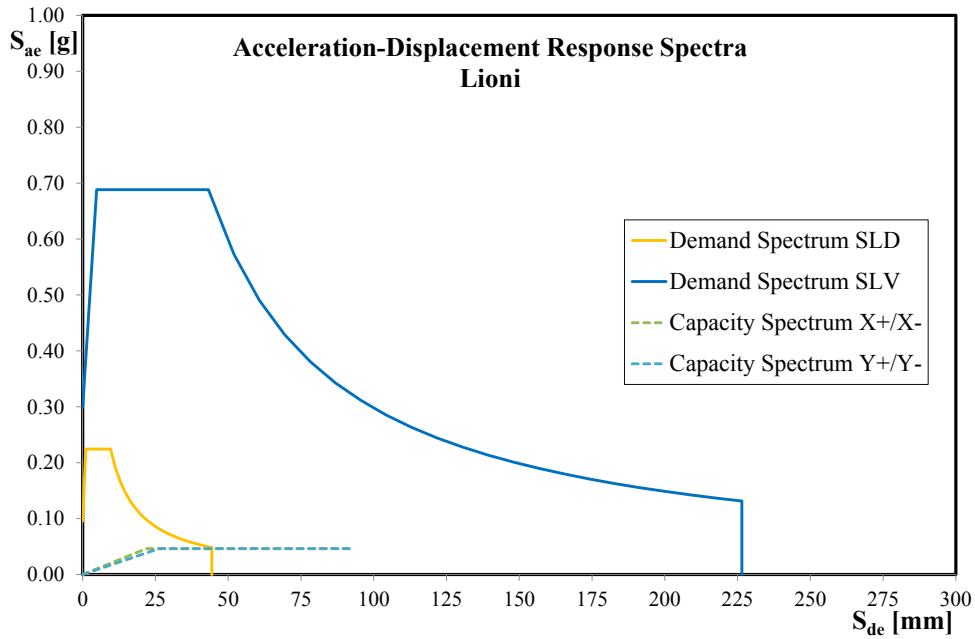
Figure 7.26: Intersection between Capacity (structure 2) and Demand Spectra of Lioni
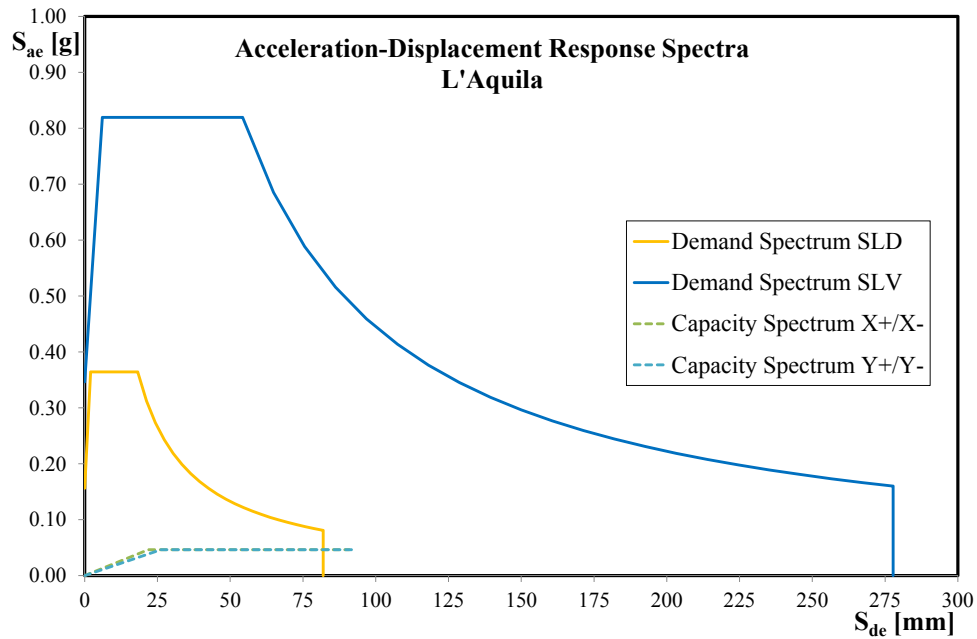
Figure 7.27: Intersection between Capacity (structure 2) and Demand Spectra of L'Aquila
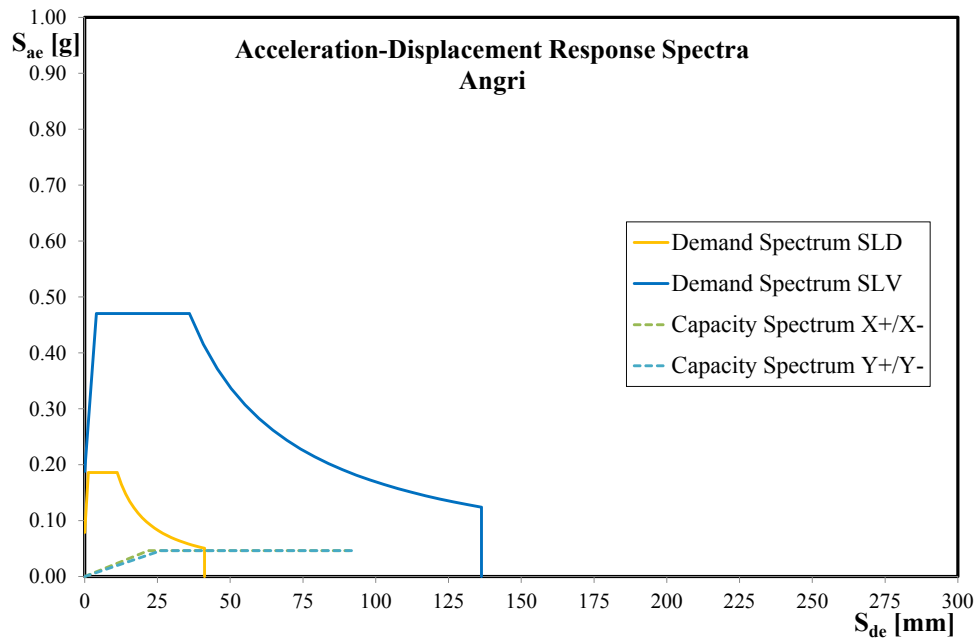
Figure 7.28: Intersection between Capacity (structure 2) and Demand Spectra of Angri

Once the performance point has been identified through the application of the N2-Method and having identified the pushover step corresponding to the achievement of a given Limit States in the as-built conditions of the structures, it has been possible to compare the Demand and Capacity in terms of displacement.

Their values are shown in Table 7.10-7.24.

Table 7.10: Displacement Demand and Capacity in as-built condition for case 1

		Pushover X+	Pushover X-	Pushover Y+	Pushover Y-
SLD	D [mm]	50.1	50.1	***53.3***	***53.3***
	C [mm]	53.2	53.2	***53.2***	***53.2***
SLV	D [mm]	***185.7***	***185.7***	197.5	197.5
	C [mm]	***153.9***	***153.9***	229.6	229.6

Table 7.11: Displacement Demand and Capacity in as-built condition for case 2

		Pushover X+	Pushover X-	Pushover Y+	Pushover Y-
SLD	D [mm]	50.1	50.1	***53.3***	***53.3***
	C [mm]	53.2	53.2	***53.2***	***53.2***
SLV	D [mm]	***185.7***	***185.7***	197.5	197.5
	C [mm]	***153.9***	***153.9***	229.6	229.6

Table 7.12: Displacement Demand and Capacity in as-built condition for case 3

		Pushover X+	Pushover X-	Pushover Y+	Pushover Y-
SLD	D [mm]	50.1	50.1	***53.3***	***53.3***
	C [mm]	53.2	53.2	***53.2***	***53.2***
SLV	D [mm]	***185.7***	***185.7***	197.5	197.5
	C [mm]	***153.9***	***153.9***	229.6	229.6

Table 7.13: Displacement Demand and Capacity in as-built condition for case 4

		Pushover X+	Pushover X-	Pushover Y+	Pushover Y-
SLD	D [mm]	***100.0***	***100.0***	***106.4***	***106.4***
	C [mm]	***53.2***	***53.2***	***53.2***	***53.2***
SLV	D [mm]	***259.3***	***259.3***	***275.8***	***275.8***
	C [mm]	***153.9***	***153.9***	***229.7***	***229.7***

Table 7.14: Displacement Demand and Capacity in as-built condition for case 5

		Pushover X+	Pushover X-	Pushover Y+	Pushover Y-
SLD	D [mm]	*100.0*	*100.0*	*106.4*	*106.4*
	C [mm]	*53.2*	*53.2*	*53.2*	*53.2*
SLV	D [mm]	*259.3*	*259.3*	*275.8*	*275.8*
	C [mm]	*153.9*	*153.9*	*229.7*	*229.7*

Table 7.15: Displacement Demand and Capacity in as-built condition for case 6

		Pushover X+	Pushover X-	Pushover Y+	Pushover Y-
SLD	D [mm]	*100.0*	*100.0*	*106.4*	*106.4*
	C [mm]	*53.2*	*53.2*	*53.2*	*53.2*
SLV	D [mm]	*259.3*	*259.3*	*275.8*	*275.8*
	C [mm]	*153.9*	*153.9*	*229.7*	*229.7*

Table 7.16: Displacement Demand and Capacity in as-built condition for case 7

		Pushover X+	Pushover X-	Pushover Y+	Pushover Y-
SLD	D [mm]	*42.0*	*42.0*	*46.0*	*46.0*
	C [mm]	*37.8*	*37.8*	*42.0*	*42.0*
SLV	D [mm]	*155.9*	*155.9*	*170.7*	*170.7*
	C [mm]	*119.7*	*119.7*	*121.8*	*121.8*

Table 7.17: Displacement Demand and Capacity in as-built condition for case 8

		Pushover X+	Pushover X-	Pushover Y+	Pushover Y-
SLD	D [mm]	*42.0*	*42.0*	*46.0*	*46.0*
	C [mm]	*37.8*	*37.8*	*42.0*	*42.0*
SLV	D [mm]	*155.9*	*155.9*	*170.7*	*170.7*
	C [mm]	*119.7*	*119.7*	*121.8*	*121.8*

Table 7.18: Displacement Demand and Capacity in as-built condition for case 9

		Pushover X+	Pushover X-	Pushover Y+	Pushover Y-
SLD	D [mm]	*42.0*	*42.0*	*46.0*	*46.0*
	C [mm]	*37.8*	*37.8*	*42.0*	*42.0*
SLV	D [mm]	*155.9*	*155.9*	*170.7*	*170.7*
	C [mm]	*119.7*	*119.7*	*121.8*	*121.8*

Table 7.19: Displacement Demand and Capacity in as-built condition for case 10

		Pushover X+	Pushover X-	Pushover Y+	Pushover Y-
SLD	D [mm]	*84.0*	*84.0*	*91.9*	*91.9*
	C [mm]	*37.8*	*37.8*	*42.0*	*42.0*
SLV	D [mm]	*217.7*	*217.7*	*238.3*	*238.3*
	C [mm]	*119.7*	*119.7*	*121.8*	*121.8*

Table 7.20: Displacement Demand and Capacity in as-built condition for case 11

		Pushover X+	Pushover X-	Pushover Y+	Pushover Y-
SLD	D [mm]	*84.0*	*84.0*	*91.9*	*91.9*
	C [mm]	*37.8*	*37.8*	*42.0*	*42.0*
SLV	D [mm]	*217.7*	*217.7*	*238.3*	*238.3*
	C [mm]	*119.7*	*119.7*	*121.8*	*121.8*

Table 7.21: Displacement Demand and Capacity in as-built condition for case 12

		Pushover X+	Pushover X-	Pushover Y+	Pushover Y-
SLD	D [mm]	*84.0*	*84.0*	*91.9*	*91.9*
	C [mm]	*37.8*	*37.8*	*42.0*	*42.0*
SLV	D [mm]	*217.7*	*217.7*	*238.3*	*238.3*
	C [mm]	*119.7*	*119.7*	*121.8*	*121.8*

Table 7.22: Displacement Demand and Capacity in as-built condition for case 13

		Pushover X+	Pushover X-	Pushover Y+	Pushover Y-
SLD	D [mm]	*41.6*	*41.6*	*45.5*	*45.5*
	C [mm]	*37.8*	*37.8*	*42.0*	*42.0*
SLV	D [mm]	117.2	117.2	*128.3*	*128.3*
	C [mm]	119.7	119.7	*121.8*	*121.8*

Table 7.23: Displacement Demand and Capacity in as-built condition for case 14

		Pushover X+	Pushover X-	Pushover Y+	Pushover Y-
SLD	D [mm]	*41.6*	*41.6*	*45.5*	*45.5*
	C [mm]	*37.8*	*37.8*	*42.0*	*42.0*
SLV	D [mm]	117.2	117.2	*128.3*	*128.3*
	C [mm]	119.7	119.7	*121.8*	*121.8*

Table 7.24: Displacement Demand and Capacity in as-built condition for case 15

		Pushover X+	Pushover X-	Pushover Y+	Pushover Y-
SLD	D [mm]	*41.6*	*41.6*	*45.5*	*45.5*
	C [mm]	*37.8*	*37.8*	*42.0*	*42.0*
SLV	D [mm]	117.2	117.2	*128.3*	*128.3*
	C [mm]	119.7	119.7	*121.8*	*121.8*

All the cases examined have at least one pushover direction and/or one Limit State in which the Demand is greater than the Capacity and, therefore, the corresponding structure, for that case, needs a seismic retrofitting intervention.

The proposed procedure has been applied to search for the best retrofit solution. The applications have been performed using the following hardware and software:

- − Windows 10 Professional 64 bit;
- − Workstation with 8 GB of RAM;
- − Intel ® Core™ i7-2600 CPU 3.40 GHz;
- − MATLAB Version R2017b, (Academic Licence Number: 40615932).

Moreover, using the Intel's Hyper-threading technology it has been possible to activate 8 workers on Matlab, i.e. twice the number of "physical" cores available, in order to perform parallel computing.

The next paragraph collects the outcome of the proposed algorithm in terms of objective function towards the final convergence which is supposed to be achieved after 200 generations.

7.2   The outcomes of the procedure

Figures 7.29-7.43 depict the evolution of the cost function throughout generations.
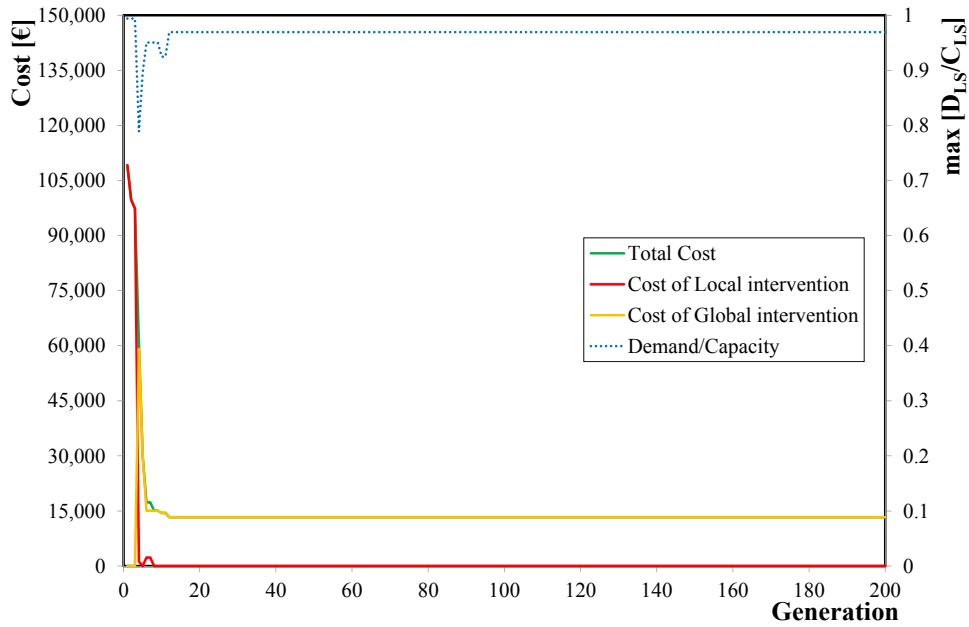

Figure 7.29: Convergence history of procedure applied for case 1 (Table 7.9)

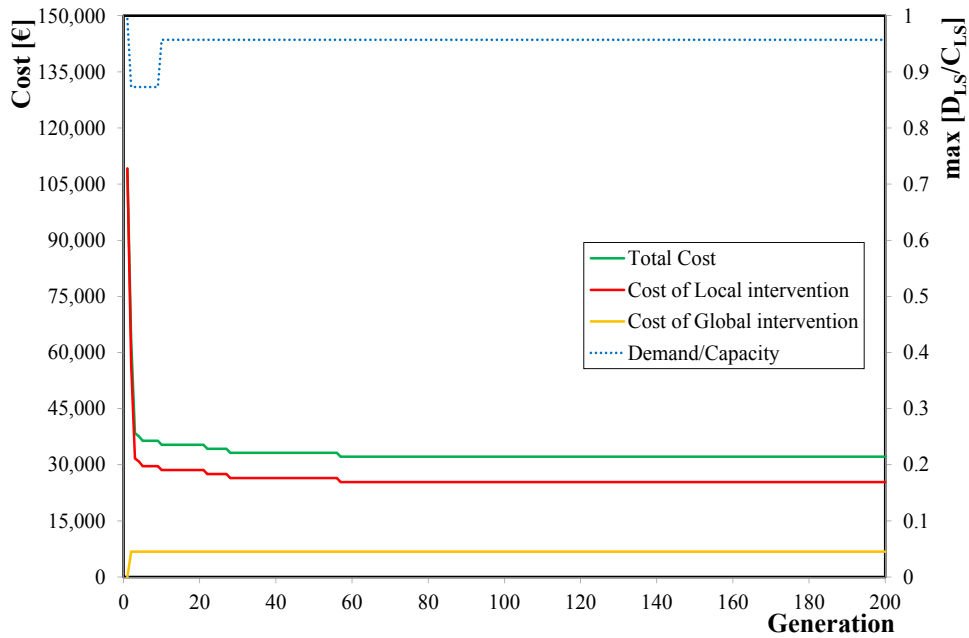*Figure 7.30: Convergence history of procedure applied for case 2 (Table 7.9)*

Figure 7.31: Convergence history of procedure applied for case 3 (Table 7.9)

The resulting optimal individual in the last population has a total cost of 34,035 €.

Figure 7.32: Convergence history of procedure applied for case 4 (Table 7.9)

The fittest individual obtained in the last population has a total cost of 49,177 €.

Figure 7.33: Convergence history of procedure applied for case 5 (Table 7.9)

The resulting optimal individual in the last population has a total cost of 56,101 €.

Figure 7.34: Convergence history of procedure applied for case 6 (Table 7.9)

The fittest individual in the last population has a total cost of 126,284 €.

Figure 7.35: Convergence history of procedure applied for case 7 (Table 7.9)

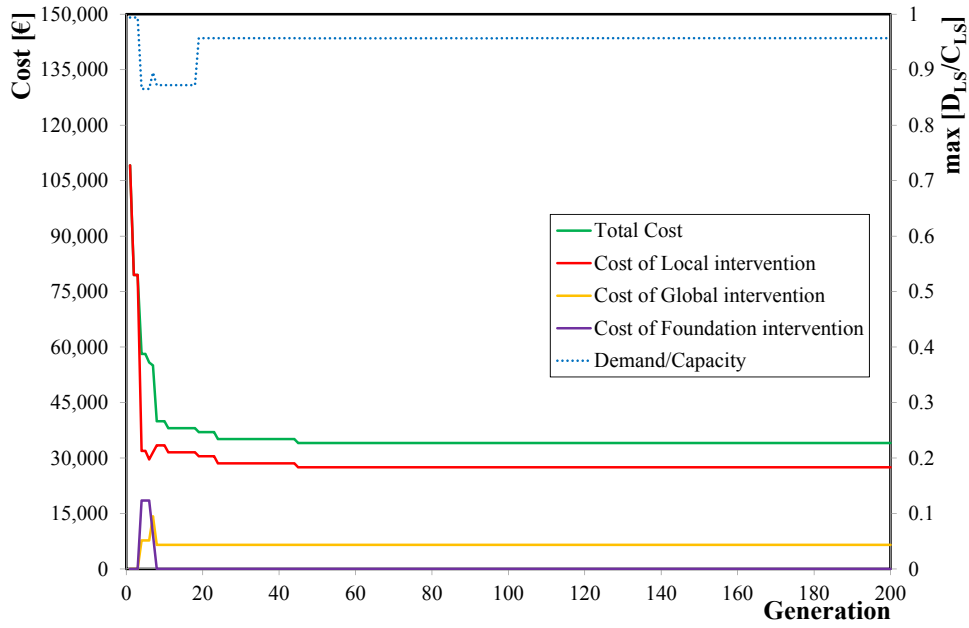As shown, the fittest individual in the last population has a total cost of 17,058 €.

Figure 7.36: Convergence history of procedure applied for case 8 (Table 7.9)

The resulting optimal individual in the last population has a total cost of 29,500 €.

Figure 7.37: Convergence history of procedure applied for case 9 (Table 7.9)

The cheapest individual created in the last population has a total cost of 57,769 €.
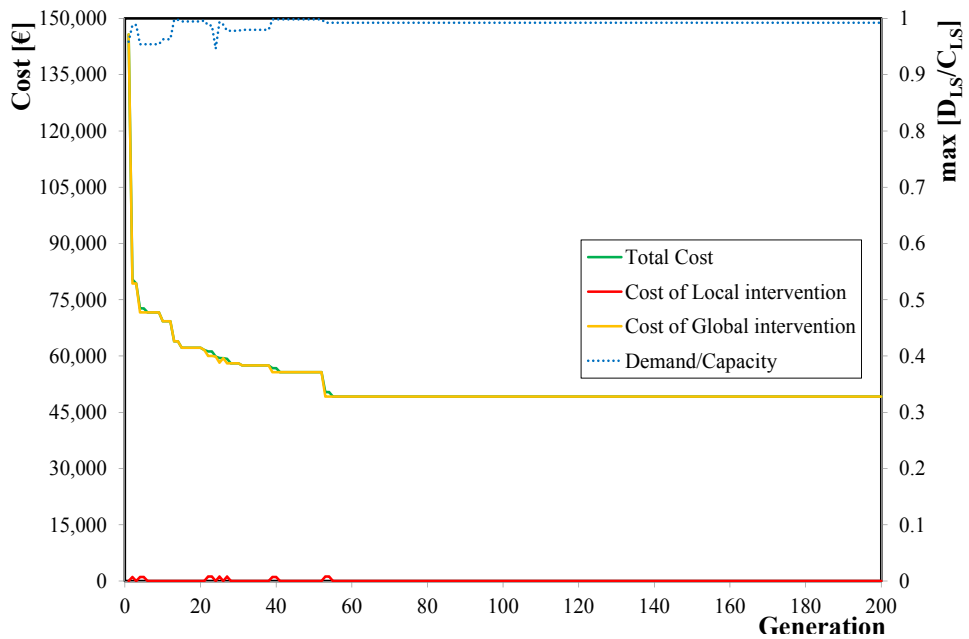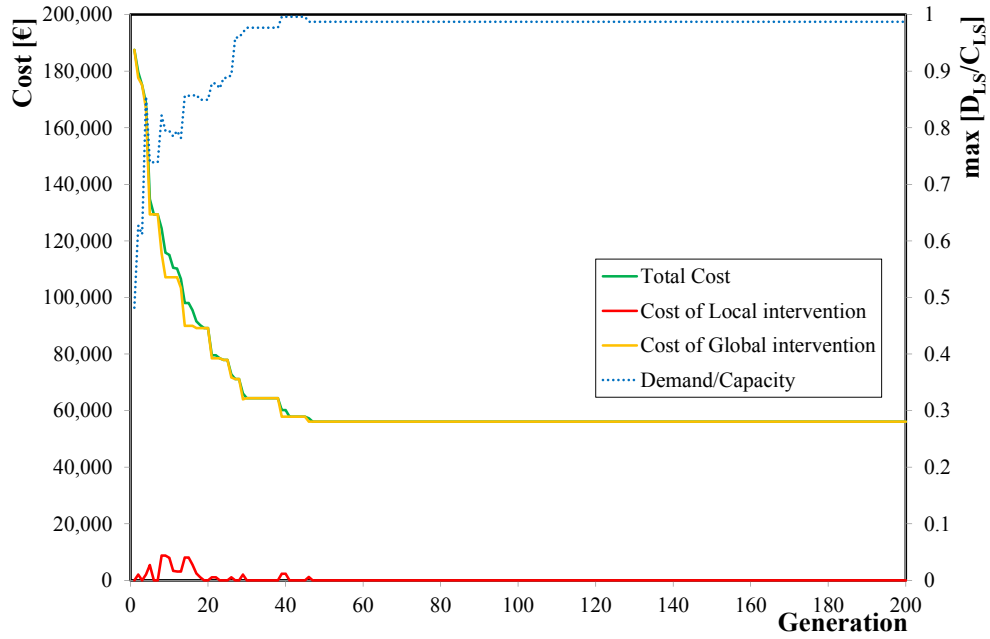

Figure 7.38: Convergence history of procedure applied for case 10 (Table 7.9)

The fittest individual obtained in the last population has a total cost of 33,907 €.
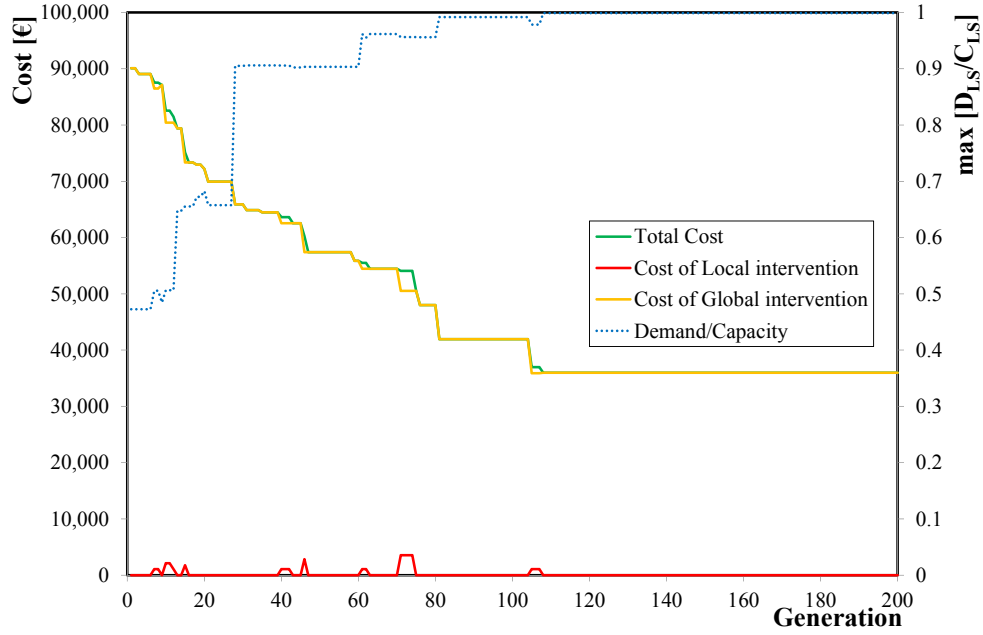
Figure 7.39: Convergence history of procedure applied for case 11 (Table 7.9)

As shown, the fittest individual in the last population has a total cost of 35,986 €.
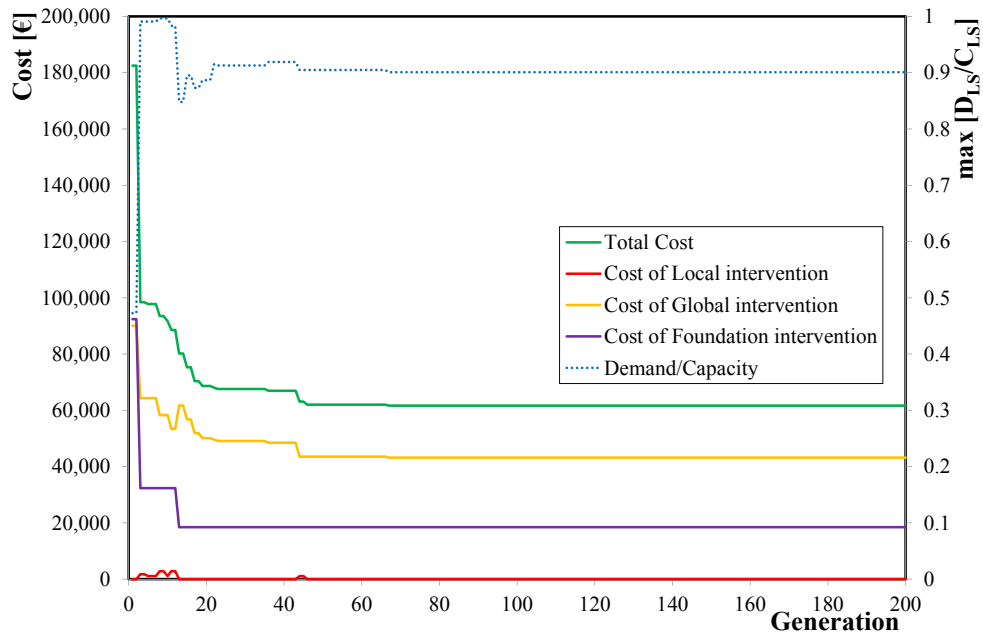
Figure 7.40: Convergence history of procedure applied for case 12 (Table 7.9)

The resulting cheapest individual in the last population has a total cost of 61,650 €.
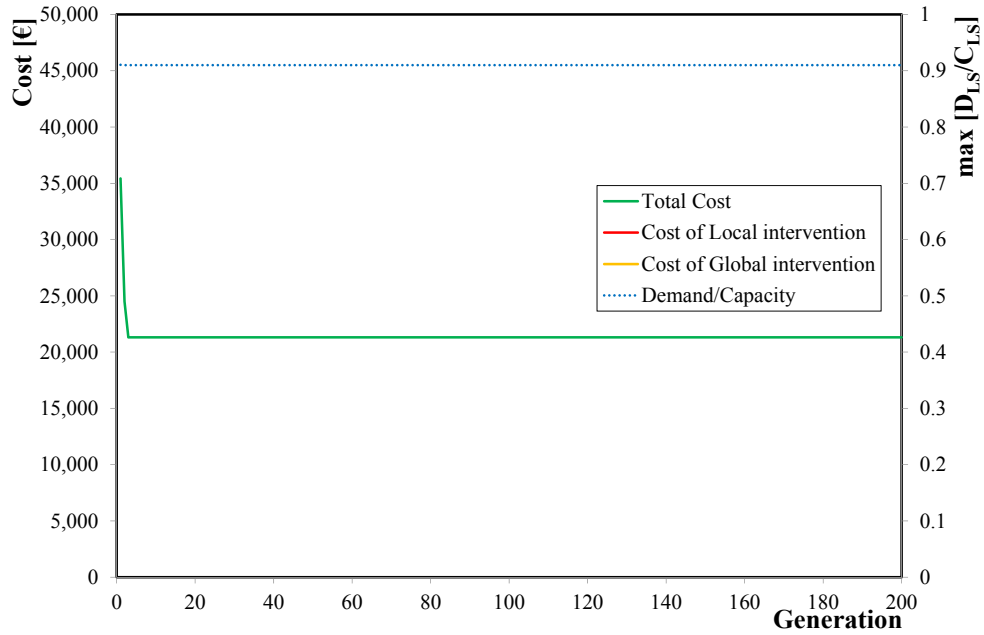
Figure 7.41: Convergence history of procedure applied for case 13 (Table 7.9)

As shown, the optimal individual in the last population has a total cost of 21,315 €.
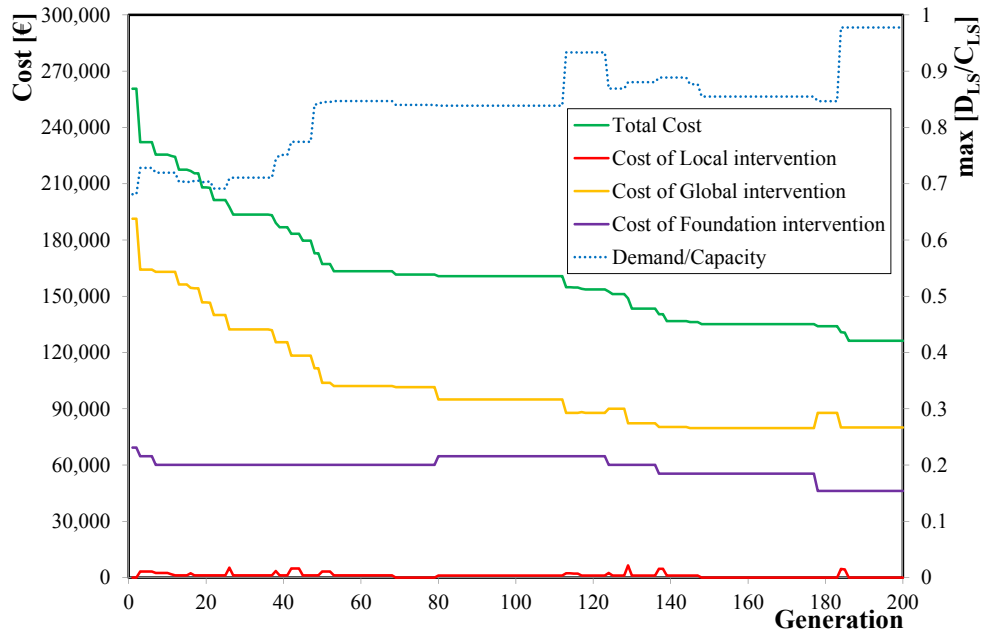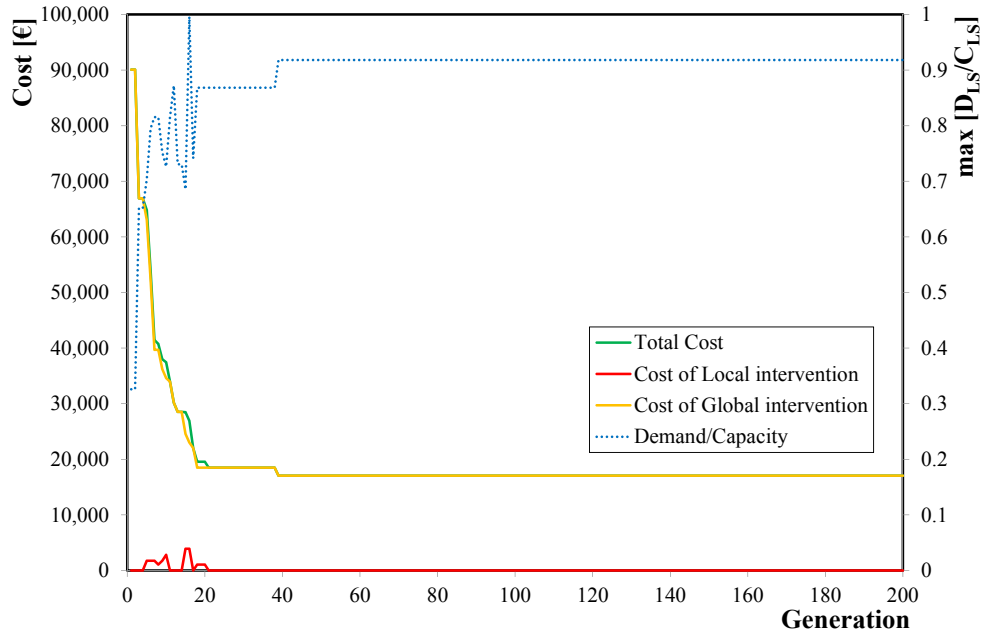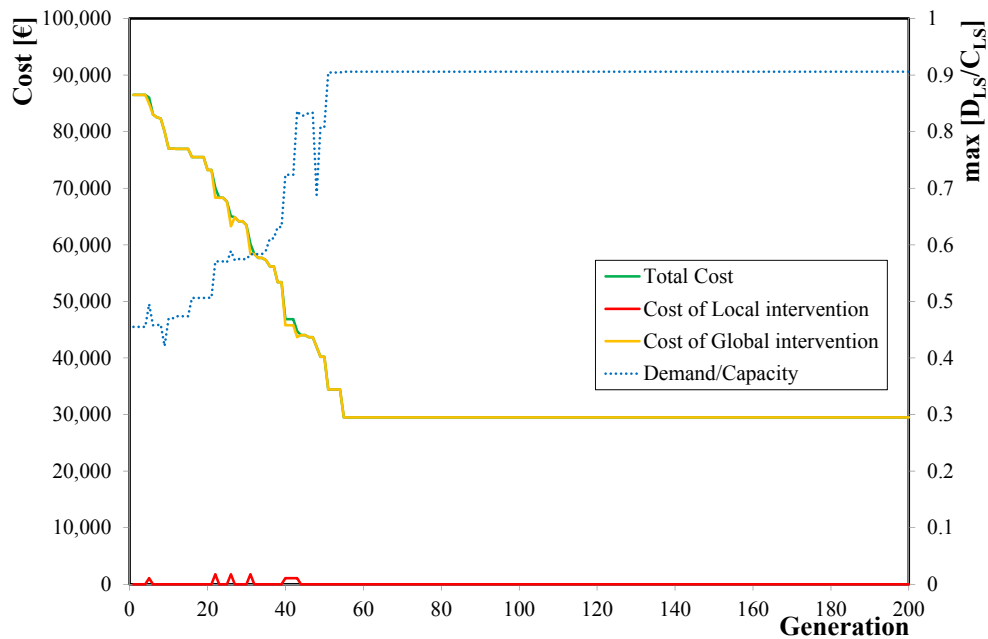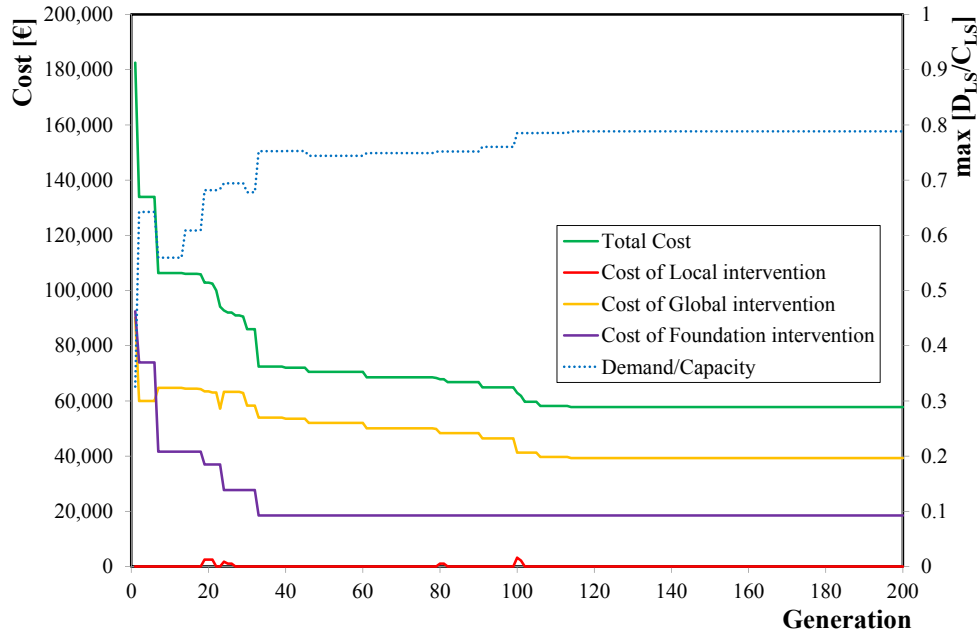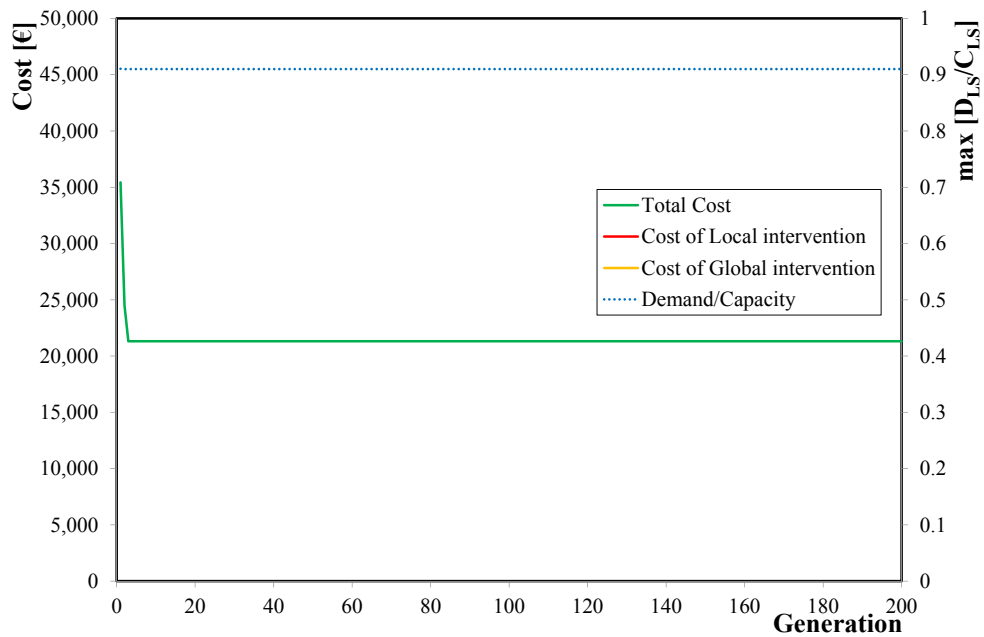

Figure 7.42: Convergence history of procedure applied for case 14 (Table 7.9)

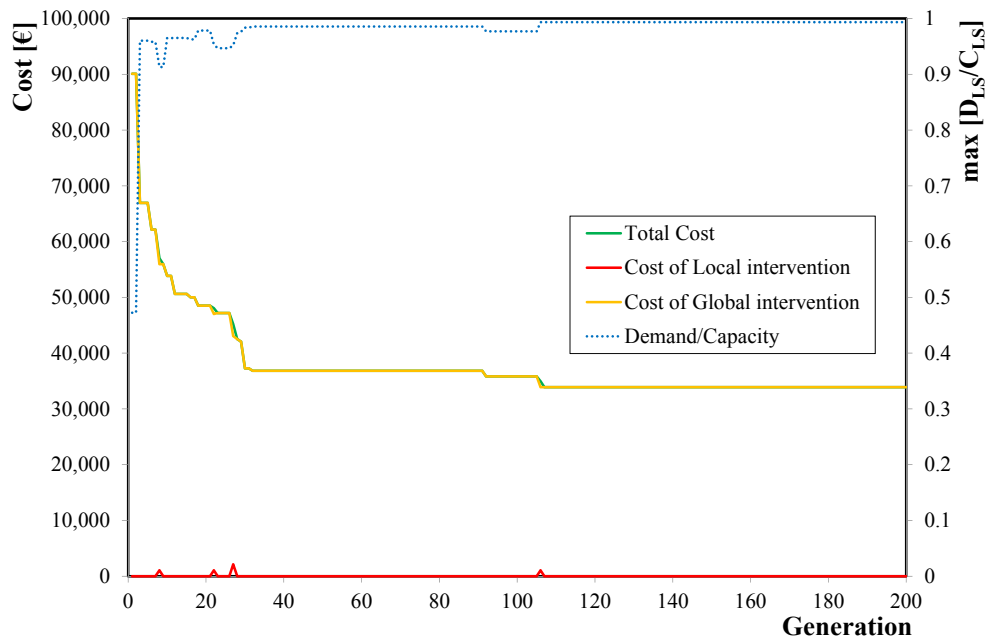The cheapest individual created in the last population has a total cost of 21,315 €.
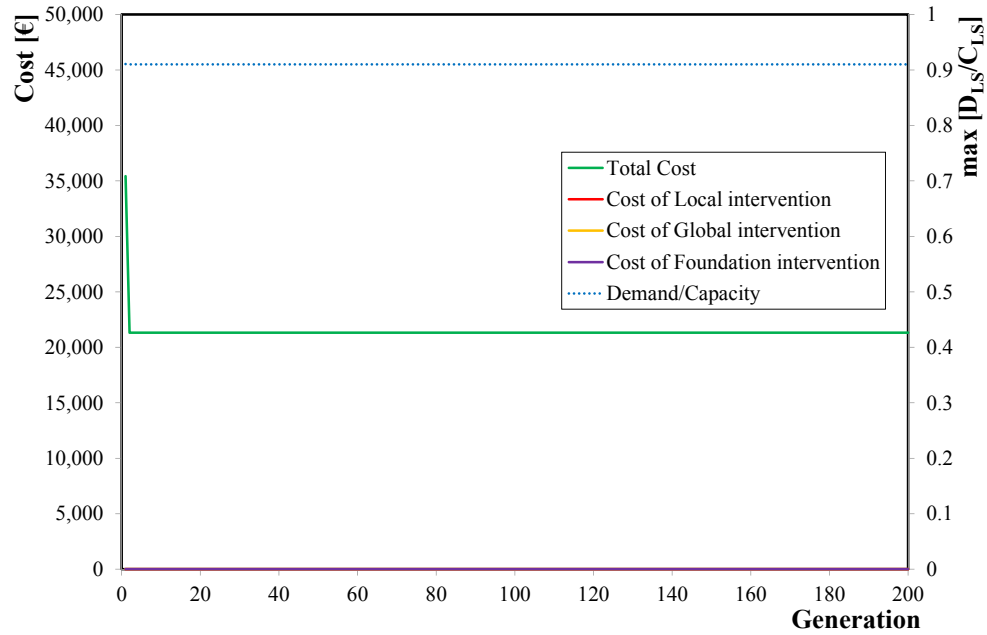
Figure 7.43: Convergence history of procedure applied for case 15 (Table 7.9)

The following table summarizes the costs calculated for all the cheapest retrofit interventions obtained by applying, for each case, the proposed procedure.

Table 7.25: Resulting costs of the cheapest retrofit solution found for each case study

Case	Cost of Local Intervention	Cost of Global Intervention	Cost of Micro-piles	Total Cost	Type of Intervention
1	€ 13,287	-	-	€ 13,287	Local
2	€ 25,376	€ 6,760	-	€ 32,137	Mix
3	€ 27,508	€ 6,527	-	€ 34,035	Mix
4	-	€ 49,177	-	€ 49,177	Global
5	-	€ 56,101	-	€ 56,101	Global
6	-	€ 80,079	€ 46,205	€ 126,284	Global
7	-	€ 17,058	-	€ 17,058	Global
8	-	€ 29,500	-	€ 29,500	Global
9	-	€ 39,287	€ 18,482	€ 57,769	Global
10	-	€ 33,907	-	€ 33,907	Global
11	-	€ 35,986	-	€ 35,986	Global
12	-	€ 43,168	€ 18,482	€ 61,650	Global
13	€ 21,315	-	-	€ 21,315	Local
14	€ 21,315	-	-	€ 21,315	Local
15	€ 21,315	-	-	€ 21,315	Local

7.2.1 The optimal genotype

For the sake of brevity, the genotype of the best intervention belonging to the last population cannot be represented here in full but it is summarized in the Table 7.26-7.38. For each column, the n. of FRP wraps needed for confinement is reported, while at each story the steel profile needed for the bracing system is specified.

Table 7.26: Decimal genotype of the fittest individual found in case 1 (Table 7.9)

Column	n. FRP layers	Beam		IDsec	Profile
1-24	0	17	1st story	2	HE 120 B
			2nd story	-	HE 100 A
			3rd story	-	HE 100 A
			4th story	-	HE 100 A
25-48	0	21	1st story	1	HE 100 B
			2nd story	-	HE 100 A
			3rd story	-	HE 100 A
			4th story	-	HE 100 A
49-72	0				
73-96	0				

Table 7.27: Decimal genotype of the fittest individual found in case 2 (Table 7.9)

Column	n. FRP layers	Beam		IDsec	Profile
1-24	0	19	1st story	2	HE 120 B
			2nd story	-	HE 100 A
			3rd story	-	HE 100 A
			4th story	-	HE 100 A
25-48	1				
49-72	0				
73-96	0				

Table 7.28: Decimal genotype of the fittest individual found in case 3 (Table 7.9)

Column	n. FRP layers	Beam		IDsec	Profile
1-24	0	19	1st story	1	HE 100 B
			2nd story	-	HE 100 A
			3rd story	-	HE 100 A
			4th story	-	HE 100 A
25-48	1				
49-72	0				
73-96	0				

Table 7.29: Decimal genotype of the fittest individual found in case 4 (Table 7.9)

Column	n. FRP layers	Beam		IDsec	Profile
1-24	0	4	1st story	1	HE 100 B
			2nd story	-	HE 100 A
			3rd story	-	HE 100 A
			4th story	-	HE 100 A
25-48	0	8	1st story	4	HE 160 B
			2nd story	-	HE 120 B
			3rd story	-	HE 100 A
			4th story	-	HE 100 A
49-72	0	11	1st story	2	HE 120 B
			2nd story	-	HE 100 A
			3rd story	-	HE 100 A
			4th story	-	HE 100 A
73-96	0	16	1st story	3	HE 140 B
			2nd story	-	HE 100 B
			3rd story	-	HE 100 A
			4th story	-	HE 100 A
		17	1st story	1	HE 100 B
			2nd story	-	HE 100 A
			3rd story	-	HE 100 A
			4th story	-	HE 100 A
		22	1st story	2	HE 120 B
			2nd story	-	HE 100 A
			3rd story	-	HE 100 A
			4th story	-	HE 100 A
		25	1st story	2	HE 120 B
			2nd story	-	HE 100 A
			3rd story	-	HE 100 A
			4th story	-	HE 100 A
		29	1st story	4	HE 160 B
			2nd story	-	HE 120 B
			3rd story	-	HE 100 A
			4th story		HE 100 A

Table 7.30: Decimal genotype of the fittest individual found in case 5 (Table 7.9)

Column	n. layers of FRP	Beam		IDsec	Profile
1-24	0	5	1st story	3	HE 140 B
			2nd story	-	HE 100 B
			3rd story	-	HE 100 A
			4th story	-	HE 100 A
25-48	0	7	1st story	2	HE 120 B
			2nd story	-	HE 100 A
			3rd story	-	HE 100 A
			4th story	-	HE 100 A
49-72	0	15	1st story	1	HE 100 B
			2nd story	-	HE 100 A
			3rd story	-	HE 100 A
			4th story	-	HE 100 A
73-96	0	16	1st story	1	HE 100 B
			2nd story	-	HE 100 A
			3rd story	-	HE 100 A
			4th story	-	HE 100 A
		18	1st story	4	HE 160 B
			2nd story	-	HE 120 B
			3rd story	-	HE 100 A
			4th story	-	HE 100 A
		32	1st story	4	HE 160 B
			2nd story	-	HE 120 B
			3rd story	-	HE 100 A
			4th story	-	HE 100 A

Table 7.31: Decimal genotype of the fittest individual found in case 6 (Table 7.9)

Column	n. layers of FRP	Beam		IDsec	Profile
1-24	0	7	1st story	1	HE 100 B
			2nd story	-	HE 100 A
			3rd story	-	HE 100 A
			4th story	-	HE 100 A
25-48	0	9	1st story	4	HE 160 B
			2nd story	-	HE 120 B
			3rd story	-	HE 100 A
			4th story	-	HE 100 A
49-72	0	15	1st story	1	HE 100 B
			2nd story	-	HE 100 A
			3rd story	-	HE 100 A
			4th story	-	HE 100 A
73-96	0	16	1st story	4	HE 160 B
			2nd story	-	HE 120 B
			3rd story	-	HE 100 A
			4th story	-	HE 100 A
		18	1st story	2	HE 120 B
			2nd story	-	HE 100 A
			3rd story	-	HE 100 A
			4th story	-	HE 100 A
		20	1st story	5	HE 180 B
			2nd story	-	HE 140 B
			3rd story	-	HE 100 A
			4th story	-	HE 100 A
		24	1st story	4	HE 160 B
			2nd story	-	HE 120 B
			3rd story	-	HE 100 A
			4th story	-	HE 100 A
		27	1st story	3	HE 140 B
			2nd story	-	HE 100 B
			3rd story	-	HE 100 A
			4th story	-	HE 100 A
		28	1st story	2	HE 120 B
			2nd story	-	HE 100 A
			3rd story	-	HE 100 A
			4th story	-	HE 100 A
		29	1st story	1	HE 100 B
			2nd story	-	HE 100 A
			3rd story	-	HE 100 A
			4th story	-	HE 100 A

Table 7.32: Decimal genotype of the fittest individual found in case 7 (Table 7.9)

Column	n. layers of FRP	Beam		IDsec	Profile
1-20	0	14	1st story	1	HE 100 B
			2nd story	-	HE 100 A
			3rd story	-	HE 100 A
21-40	0	16	1st story	1	HE 100 B
			2nd story	-	HE 100 A
			3rd story	-	HE 100 A
41-60	0	18	1st story	2	HE 120 B
			2nd story	-	HE 100 A
			3rd story	-	HE 100 A
		20	1st story	6	HE 200 B
			2nd story	-	HE 140 B
			3rd story	-	HE 100 A

Table 7.33: Decimal genotype of the fittest individual found in case 8 (Table 7.9)

Column	n. layers of FRP	Beam		IDsec	Profile
1-20	0	6	1st story	2	HE 120 B
			2nd story	-	HE 100 A
			3rd story	-	HE 100 A
21-40	0	11	1st story	5	HE 180 B
			2nd story	-	HE 120 B
			3rd story	-	HE 100 A
41-60	0	20	1st story	4	HE 160 B
			2nd story	-	HE 140 A
			3rd story	-	HE 100 A
		24	1st story	2	HE 120 B
			2nd story	-	HE 100 A
			3rd story	-	HE 100 A

Table 7.34: Decimal genotype of the fittest individual found in case 9 (Table 7.9)

Column	n. layers of FRP	Beam		IDsec	Profile
1-20	0	2	1st story	5	HE 180 B
			2nd story	-	HE 120 B
			3rd story	-	HE 100 A
21-40	0	3	1st story	1	HE 100 B
			2nd story	-	HE 100 A
			3rd story	-	HE 100 A
41-60	0	6	1st story	2	HE 120 B
			2nd story	-	HE 100 A
			3rd story	-	HE 100 A
		25	1st story	4	HE 160 B
			2nd story	-	HE 140 A
			3rd story	-	HE 100 A
		29	1st story	1	HE 100 B
			2nd story	-	HE 100 A
			3rd story	-	HE 100 A
		30	1st story	1	HE 100 B
			2nd story	-	HE 100 A
			3rd story	-	HE 100 A
		31	1st story	1	HE 100 B
			2nd story	-	HE 100 A
			3rd story	-	HE 100 A

Table 7.35: Decimal genotype of the fittest individual found in case 10 (Table 7.9)

Column	n. layers of FRP	Beam		IDsec	Profile
1-20	0	7	1st story	2	HE 120 B
			2nd story	-	HE 100 A
			3rd story	-	HE 100 A
21-40	0	16	1st story	1	HE 100 B
			2nd story	-	HE 100 A
			3rd story	-	HE 100 A
41-60	0	18	1st story	1	HE 100 B
			2nd story	-	HE 100 A
			3rd story	-	HE 100 A
		20	1st story	2	HE 120 B
			2nd story	-	HE 100 A
			3rd story	-	HE 100 A
		23	1st story	1	HE 100 B
			2nd story	-	HE 100 A
			3rd story	-	HE 100 A
		28	1st story	1	HE 100 B
			2nd story	-	HE 100 A
			3rd story	-	HE 100 A

Table 7.36: Decimal genotype of the fittest individual found in case 11 (Table 7.9)

Column	n. layers of FRP	Beam		IDsec	Profile
1-20	0	2	1st story	4	HE 160 B
			2nd story	-	HE 140 A
			3rd story	-	HE 100 A
21-40	0	14	1st story	2	HE 120 B
			2nd story	-	HE 100 A
			3rd story	-	HE 100 A
41-60	0	15	1st story	5	HE 180 B
			2nd story	-	HE 120 B
			3rd story	-	HE 100 A
		16	1st story	1	HE 100 B
			2nd story	-	HE 100 A
			3rd story	-	HE 100 A
		17	1st story	1	HE 100 B
			2nd story	-	HE 100 A
			3rd story	-	HE 100 A
		18	1st story	2	HE 120 B
			2nd story	-	HE 100 A
			3rd story	-	HE 100 A
		30	1st story	4	HE 160 B
			2nd story	-	HE 140 A
			3rd story	-	HE 100 A

Table 7.37: Decimal genotype of the fittest individual found in case 12 (Table 7.9)

Column	n. layers of FRP	Beam		IDsec	Profile
1-20	0	7	1st story	4	HE 160 B
			2nd story	-	HE 140 A
			3rd story	-	HE 100 A
21-40	0	10	1st story	1	HE 100 B
			2nd story	-	HE 100 A
			3rd story	-	HE 100 A
41-60	0	12	1st story	1	HE 100 B
			2nd story	-	HE 100 A
			3rd story	-	HE 100 A
		13	1st story	2	HE 120 B
			2nd story	-	HE 100 A
			3rd story	-	HE 100 A
		16	1st story	2	HE 120 B
			2nd story	-	HE 100 A
			3rd story	-	HE 100 A
		24	1st story	1	HE 100 B
			2nd story	-	HE 100 A
			3rd story	-	HE 100 A
		25	1st story	1	HE 100 B
			2nd story	-	HE 100 A
			3rd story	-	HE 100 A
		28	1st story	4	HE 160 B
			2nd story	-	HE 140 A
			3rd story	-	HE 100 A

Table 7.38: Decimal genotype of the fittest individual found in case 13-14-15 (Table 7.9)

Column	n. FRP layers	Beam		IDsec	Profile
1-20	1	1-31	1st story	0	-
			2nd story	-	-
			3rd story	-	-
21-40	0				
41-60	0				

7.2.2   The optimal phenotype

Starting from the genotype of the fittest individual belonging to the final population, it has been possible to "trace" the actual retrofit intervention by the mapping rule genotype → phenotype previously defined, as shown in Figure 7.44.
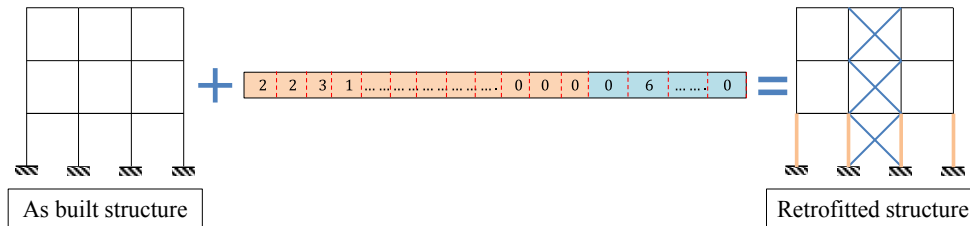

Figure 7.44: Schematization of building a retrofitted model starting from as-built one

For each case studies, the cheapest intervention that meets the constraints in Eq. 7.1, found by the procedure once the convergence is achieved, is shown in the following Figure 7.45-7.59. The beams along which the bracing systems are installed are highlighted in red.
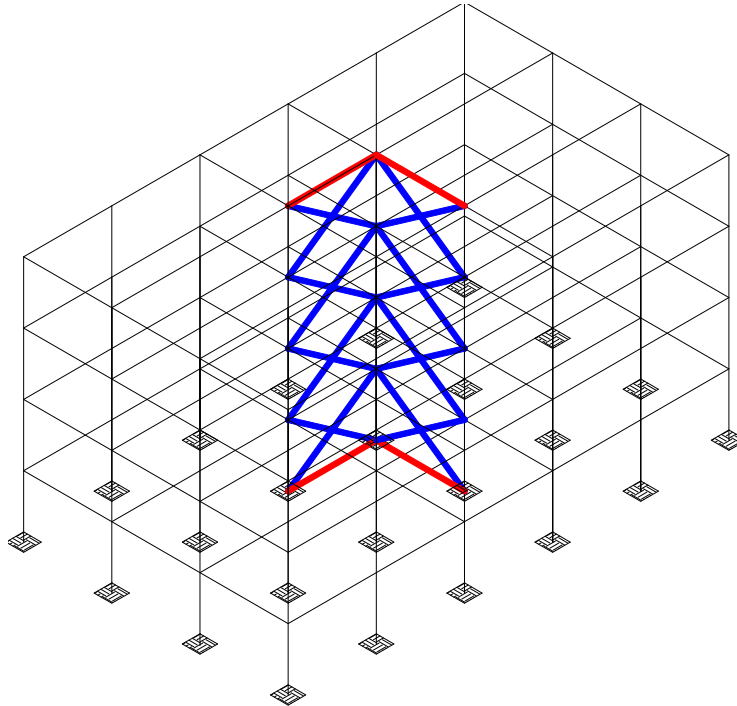
Figure 7.45: Phenotype of the fittest individual found in case 1 (Table 7.9)
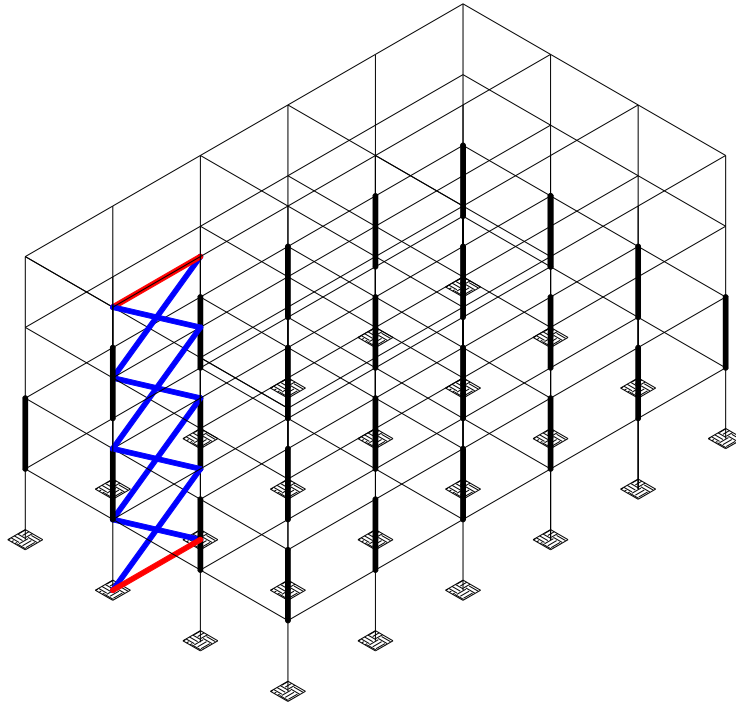
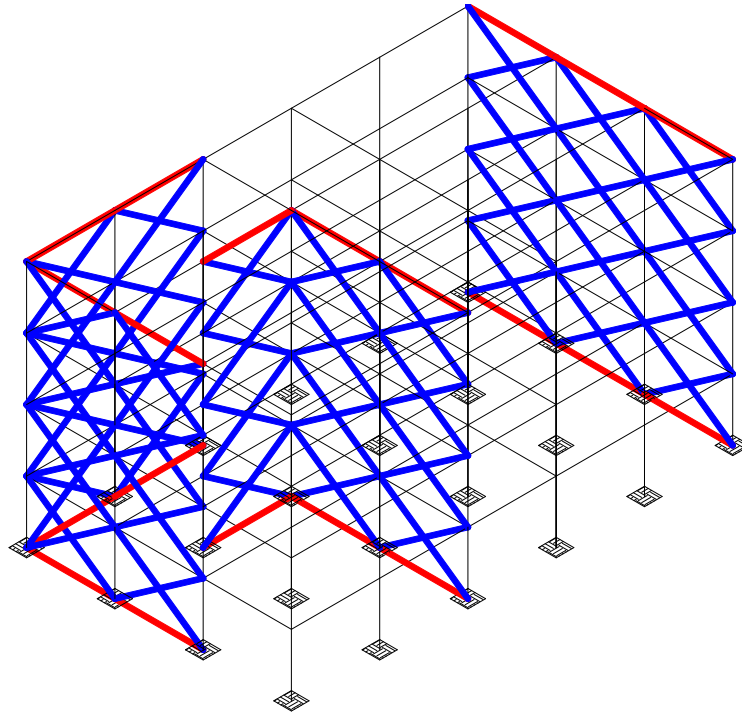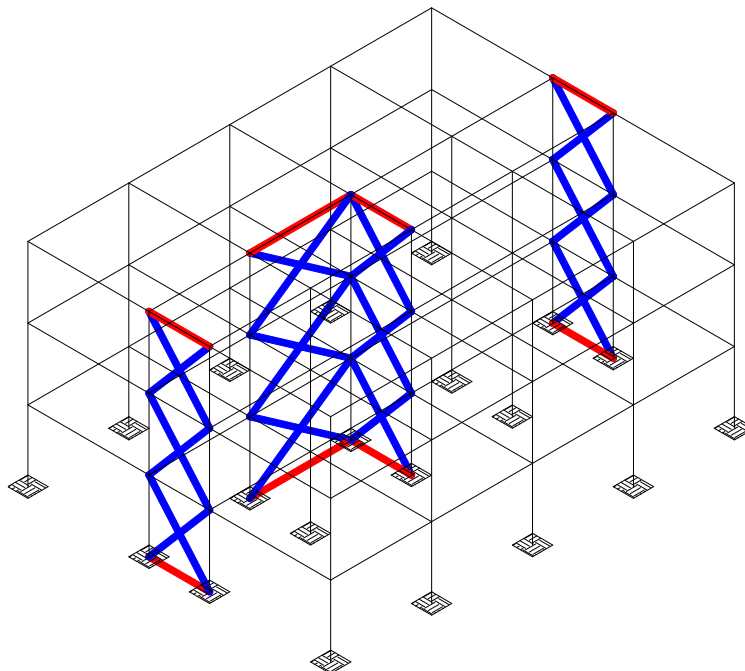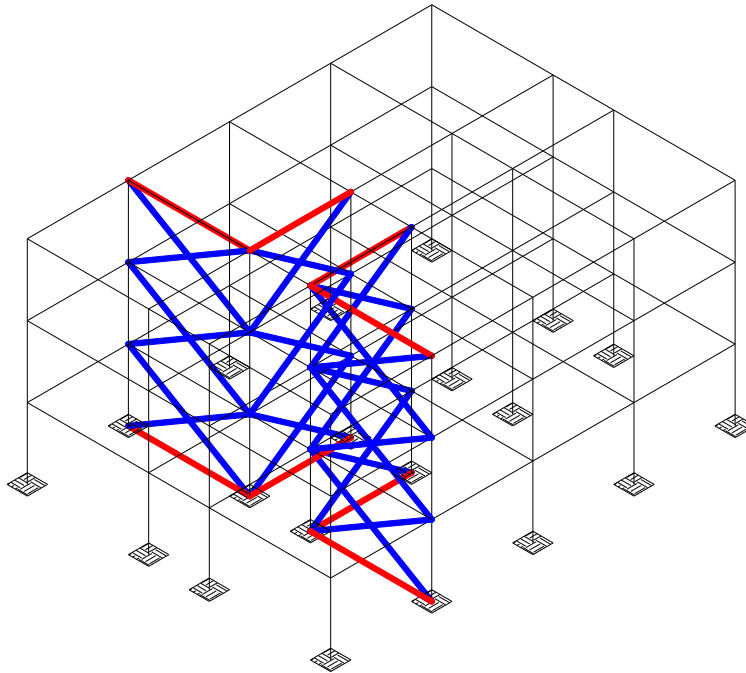*Figure 7.46: Phenotype of the fittest individual found in case 2 (Table 7.9)*
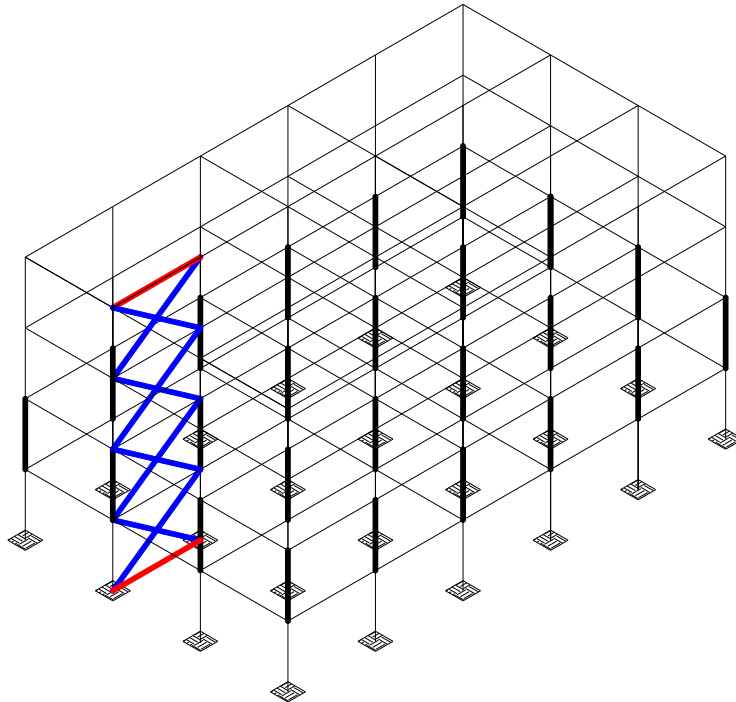
Figure 7.47: Phenotype of the fittest individual found in case 3 (Table 7.9)
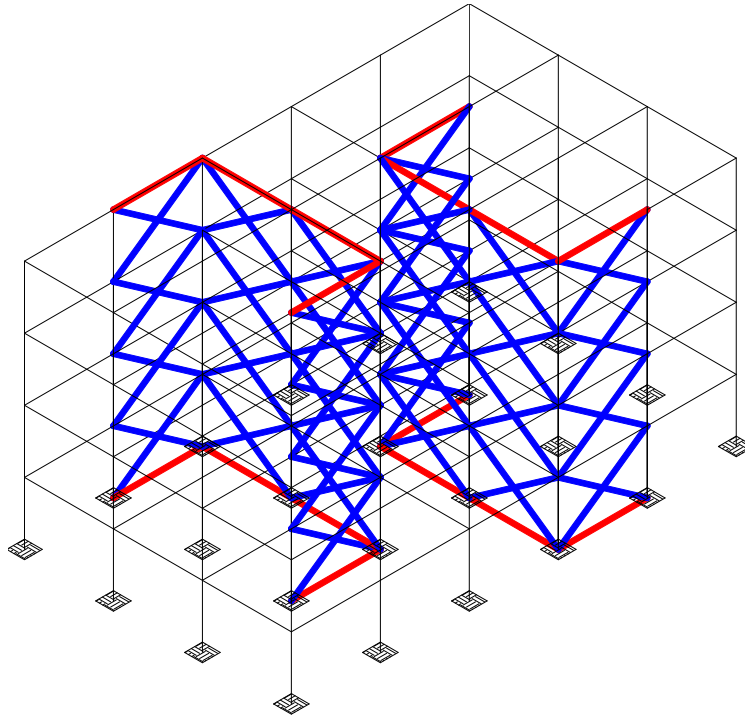
Figure 7.48: Phenotype of the fittest individual found in case 4 (Table 7.9)
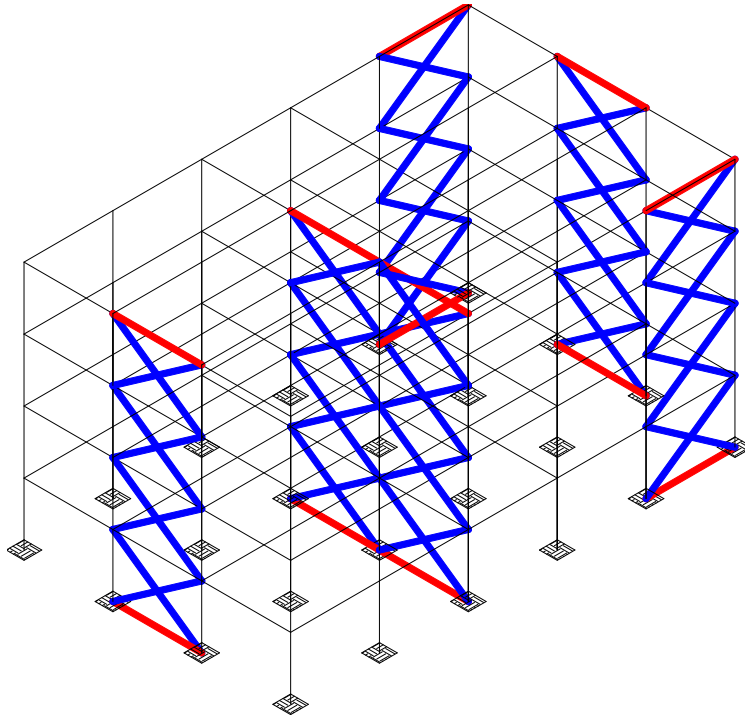
Figure 7.49: Phenotype of the fittest individual found in case 5 (Table 7.9)

Figure 7.50: Phenotype of the fittest individual found in case 6 (Table 7.9)

Figure 7.51: Phenotype of the fittest individual found in case 7 (Table 7.9)

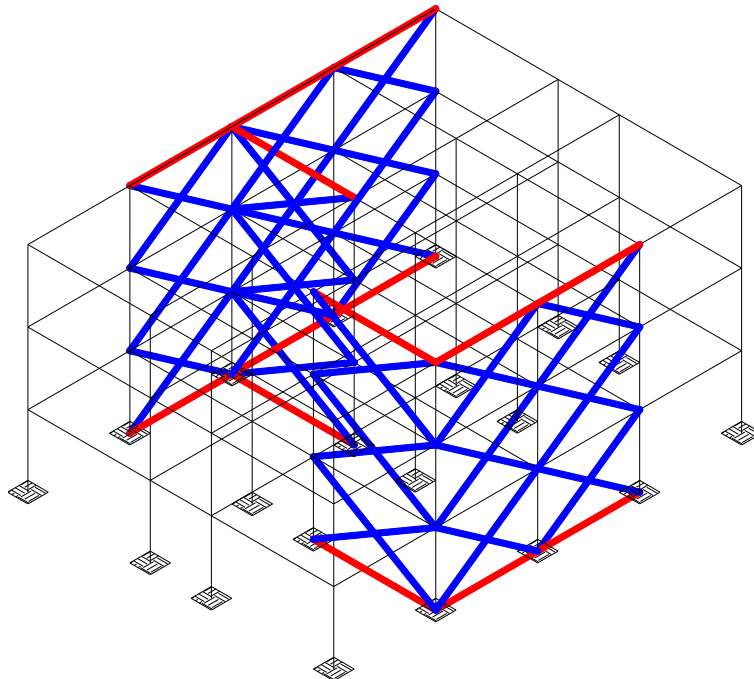*Figure 7.52: Phenotype of the fittest individual found in case 8 (Table 7.9)*

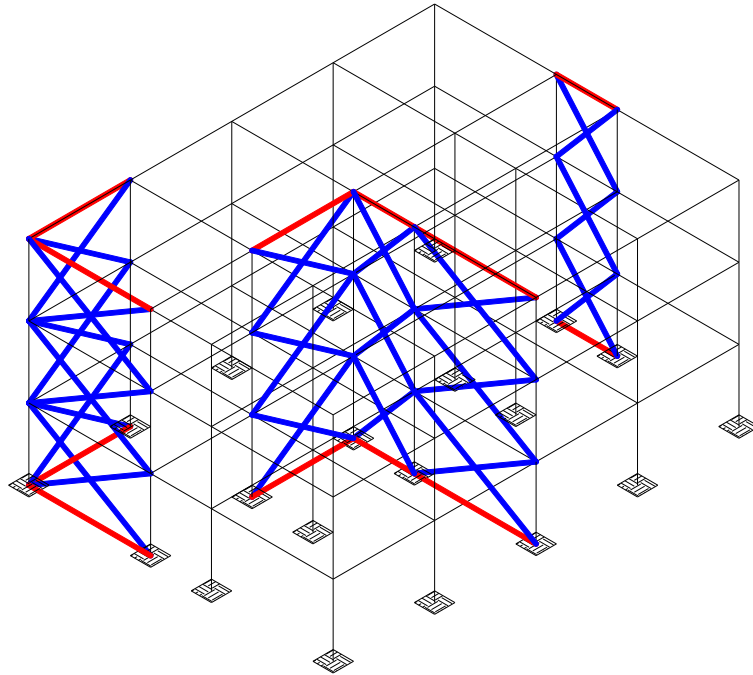*Figure 7.53: Phenotype of the fittest individual found in case 9 (Table 7.9)*

Figure 7.54: Phenotype of the fittest individual found in case 10 (Table 7.9)
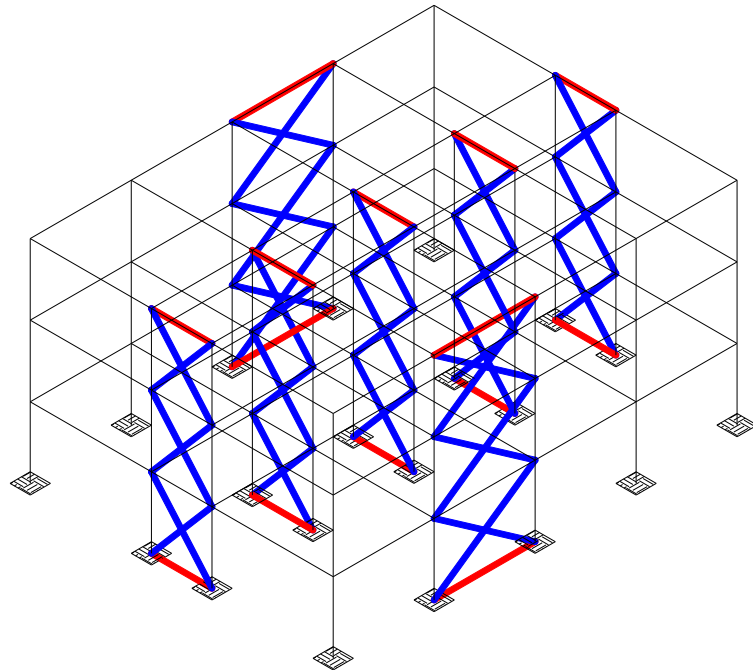

Figure 7.55: Phenotype of the fittest individual found in case 11 (Table 7.9)

Figure 7.56: Phenotype of the fittest individual found in case 12 (Table 7.9)

Figure 7.57: Phenotype of the fittest individual found in case 13 (Table 7.9)
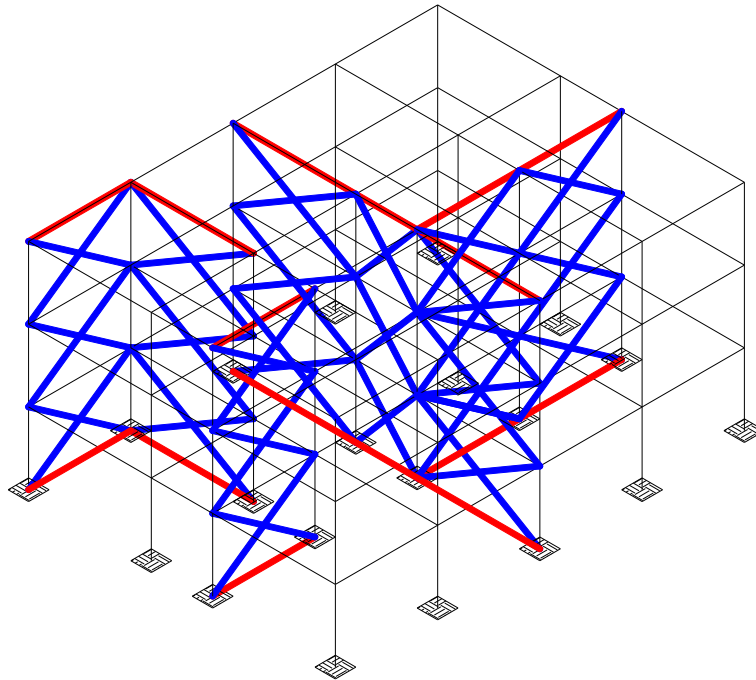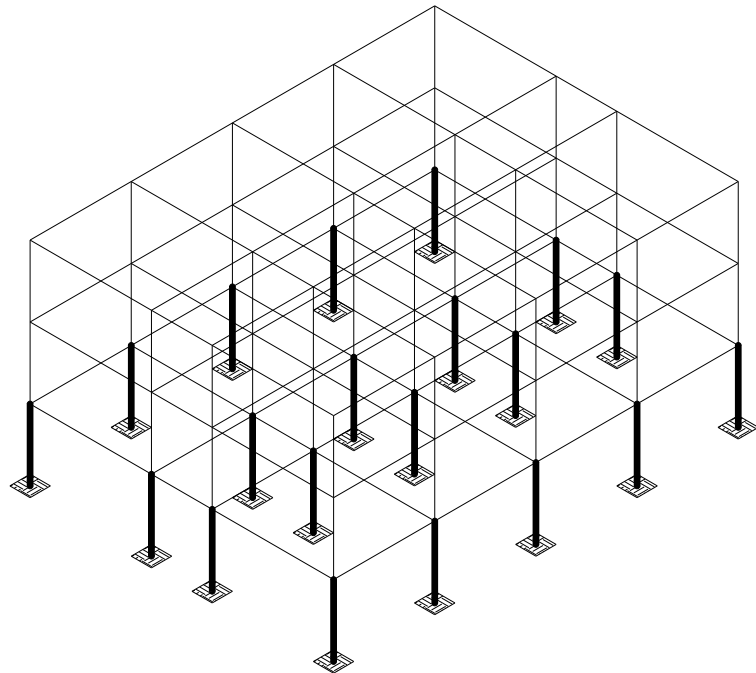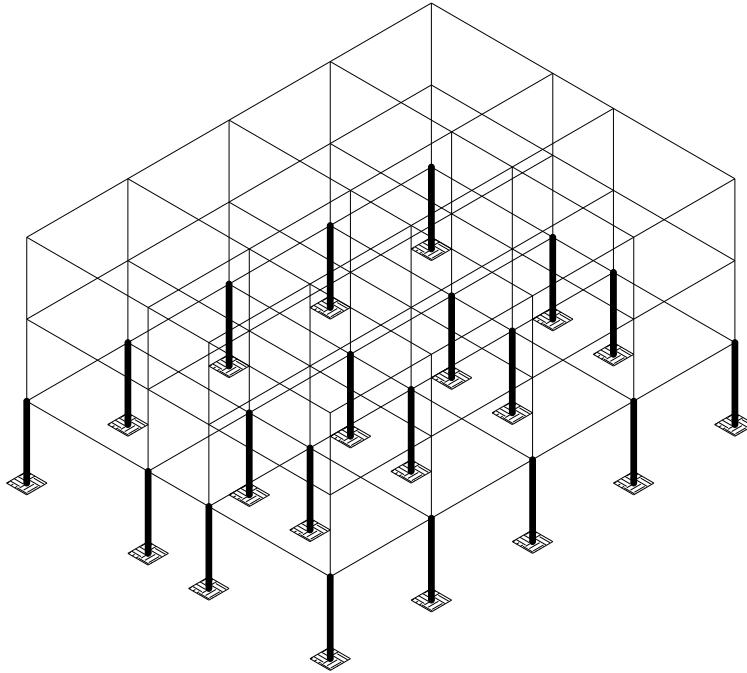
Figure 7.58: Phenotype of the fittest individual found in case 14 (Table 7.9)
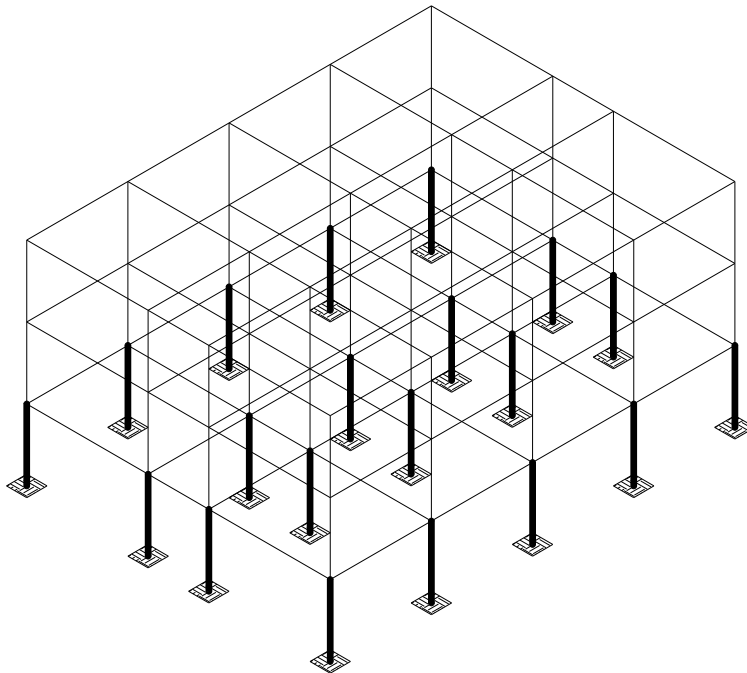
Figure 7.59: Phenotype of the fittest individual found in case 15 (Table 7.9)

7.2.3   The "retrofitted" condition

As described in Section 6.3, for each individual of the population the automatic procedure is able to assess the seismic performance of the structure in "retrofitted" configuration.

For each case study, the Figure 7.60-7.85 depict the pushover curves and the outcomes of N2-Method related to the best retrofitting solution.

Figure 7.60: Pushover curves of the cheapest retrofitting solution in case 1 (Table 7.9)

Figure 7.61: Pushover curves of the cheapest retrofitting solution in case 2 (Table 7.9)

Figure 7.62: Pushover curves of the cheapest retrofitting solution in case 3 (Table 7.9)
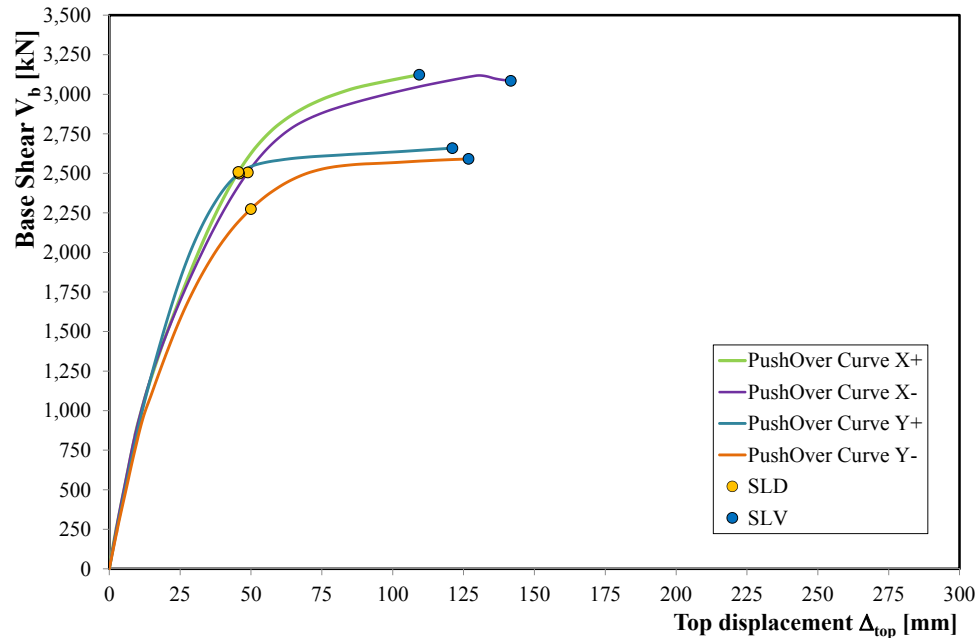
Figure 7.63: Pushover curves of the cheapest retrofitting solution in case 4 (Table 7.9)
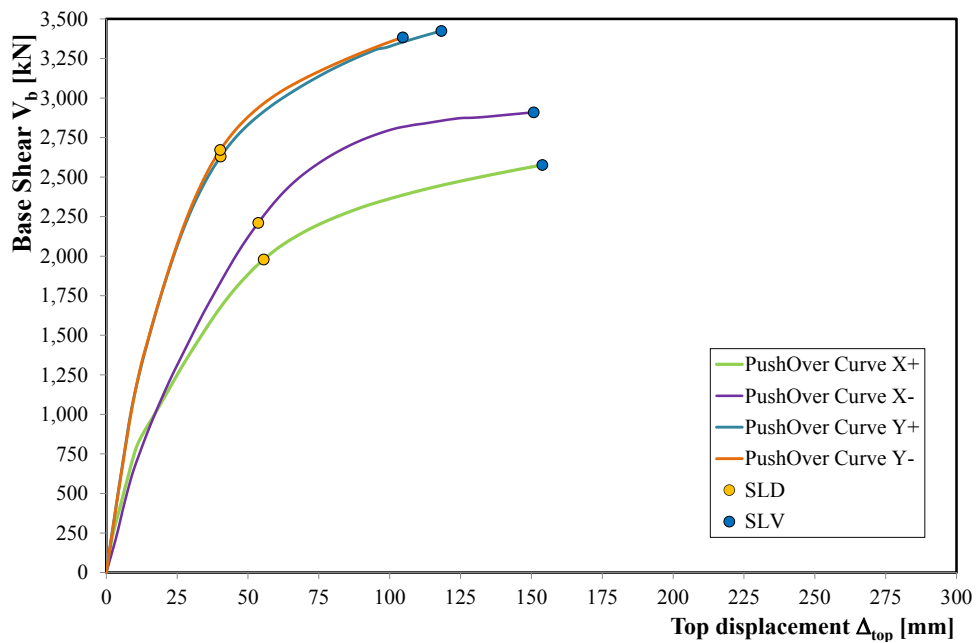
Figure 7.64: Pushover curves of the cheapest retrofitting solution in case 5 (Table 7.9)
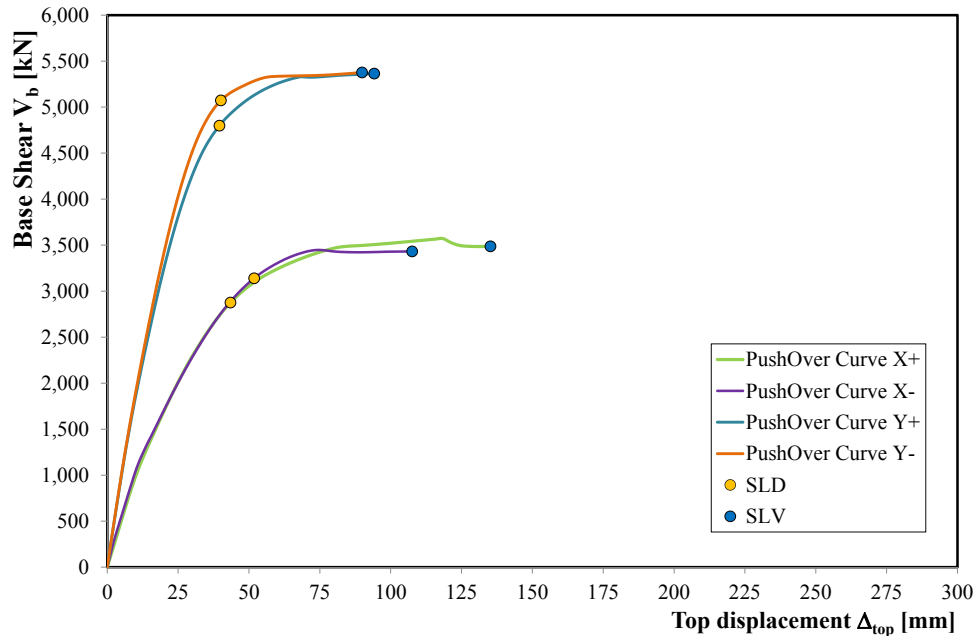
Figure 7.65: Pushover curves of the cheapest retrofitting solution in case 6 (Table 7.9)
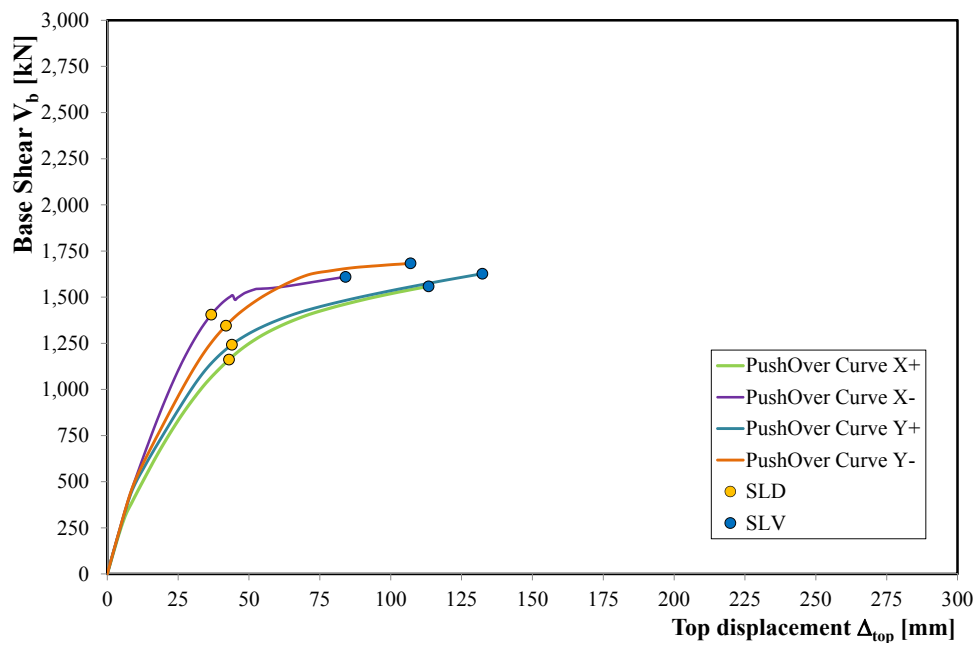
Figure 7.66: Pushover curves of the cheapest retrofitting solution in case 7 (Table 7.9)
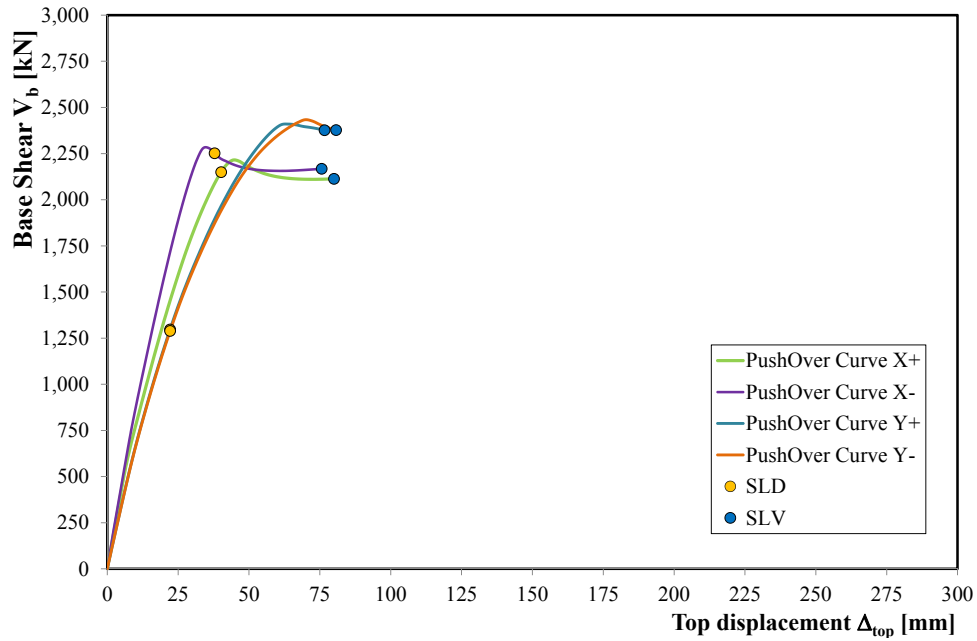
Figure 7.67: Pushover curves of the cheapest retrofitting solution in case 8 (Table 7.9)
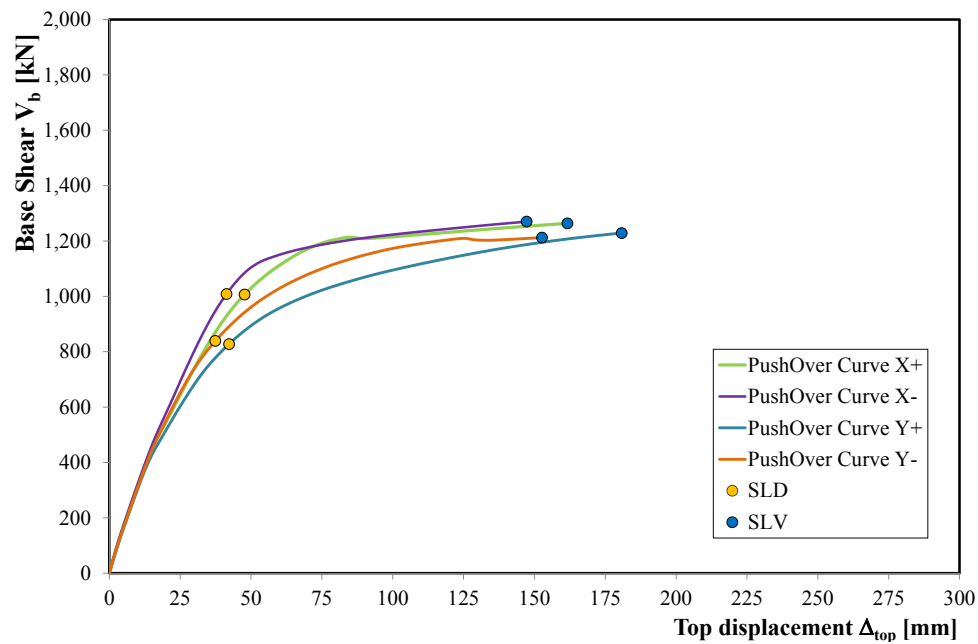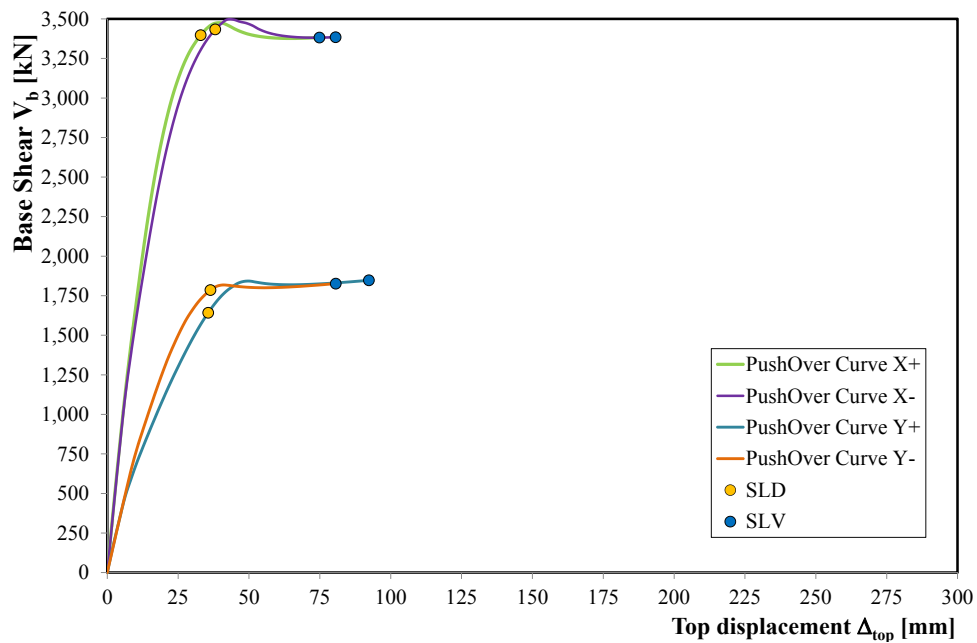

Figure 7.68: Pushover curves of the cheapest retrofitting solution in case 9 (Table 7.9)
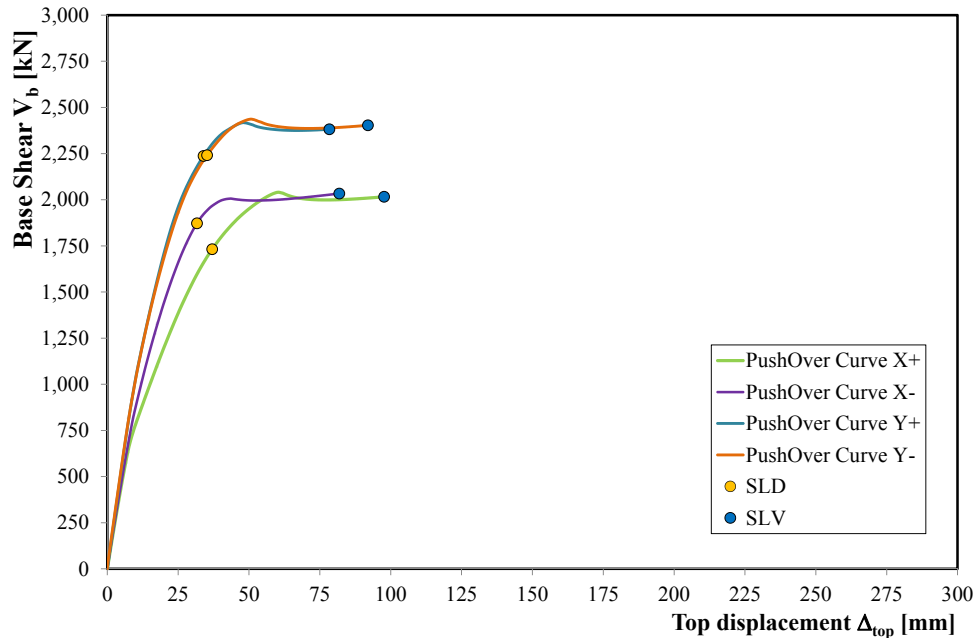
Figure 7.69: Pushover curves of the cheapest retrofitting solution in case 10 (Table 7.9)
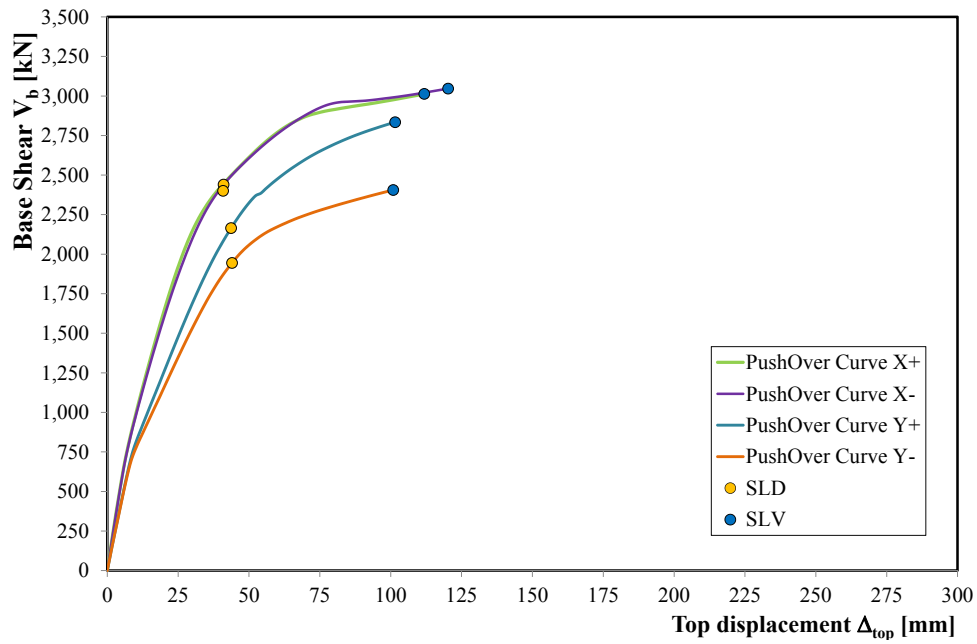
Figure 7.70: Pushover curves of the cheapest retrofitting solution in case 11 (Table 7.9)
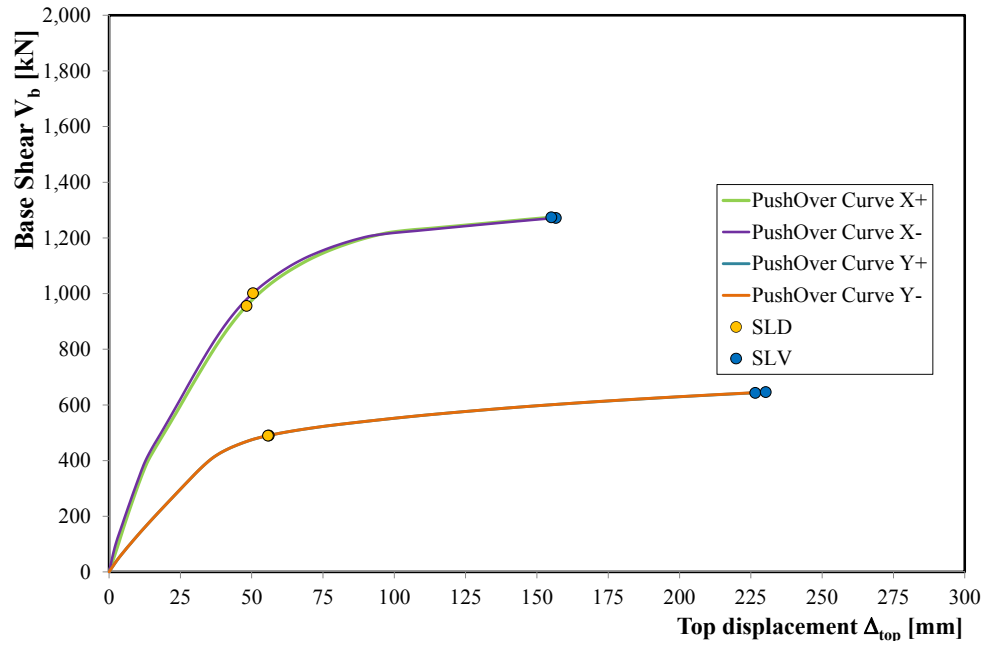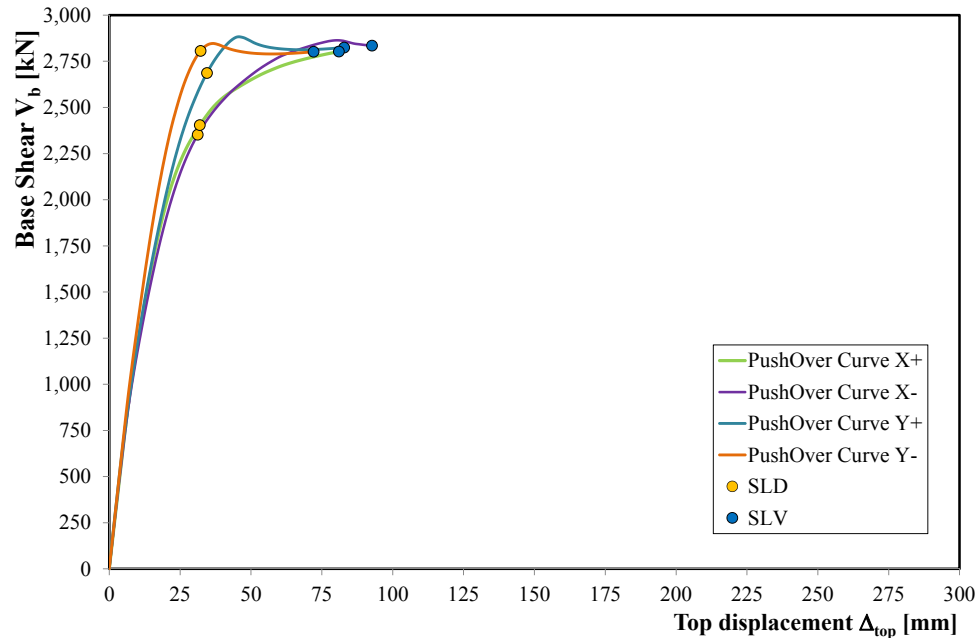
Figure 7.71: Pushover curves of the cheapest retrofitting solution in case 12 (Table 7.9)
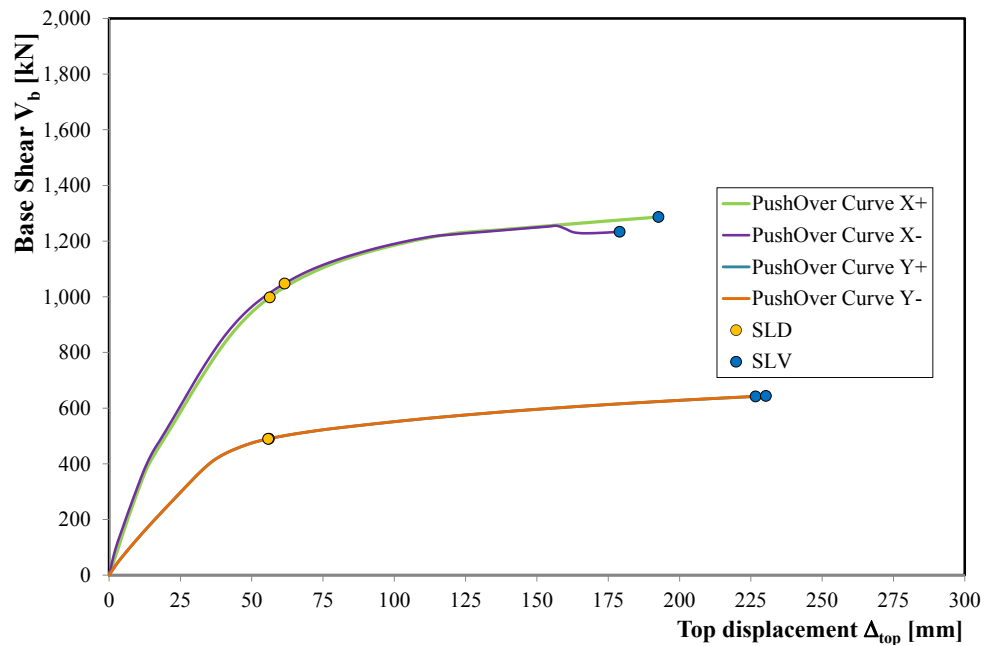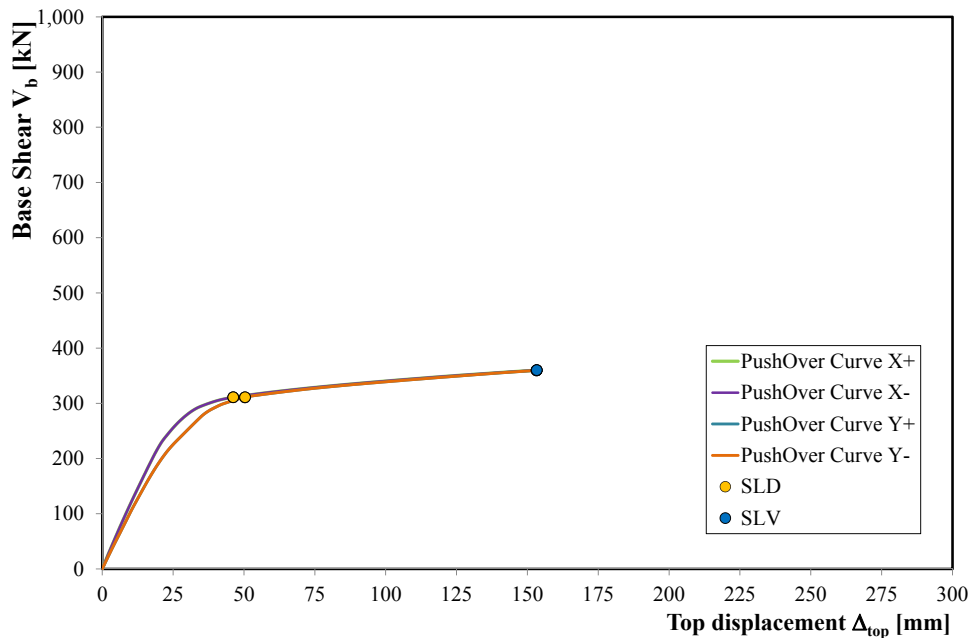

Figure 7.72: Pushover curves of the cheapest retrofitting solution in case 13-14-15
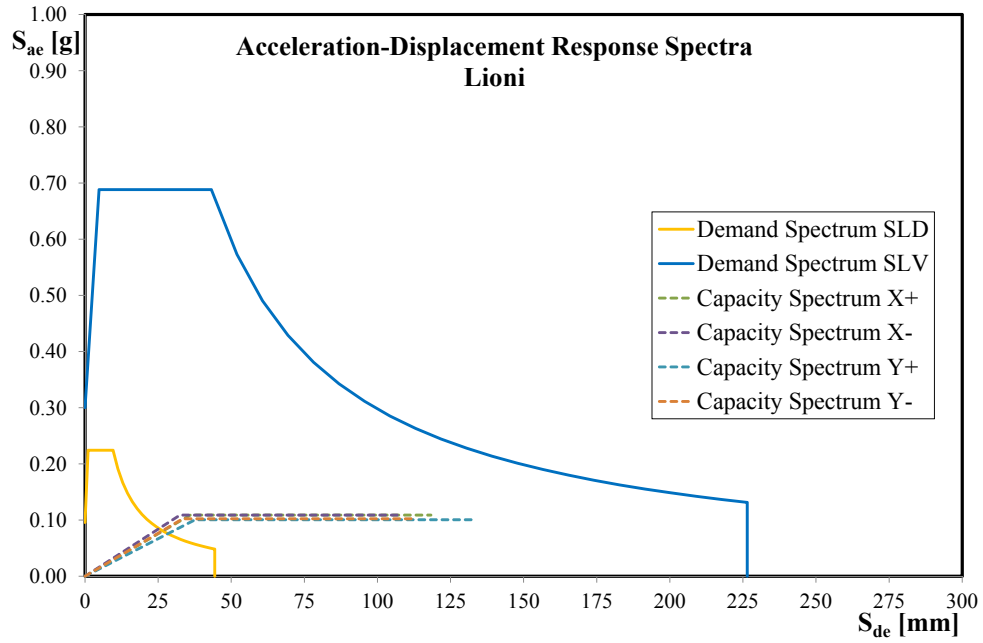
*Figure 7.73: Application of N2-Method in case 1 (Table 7.9)*
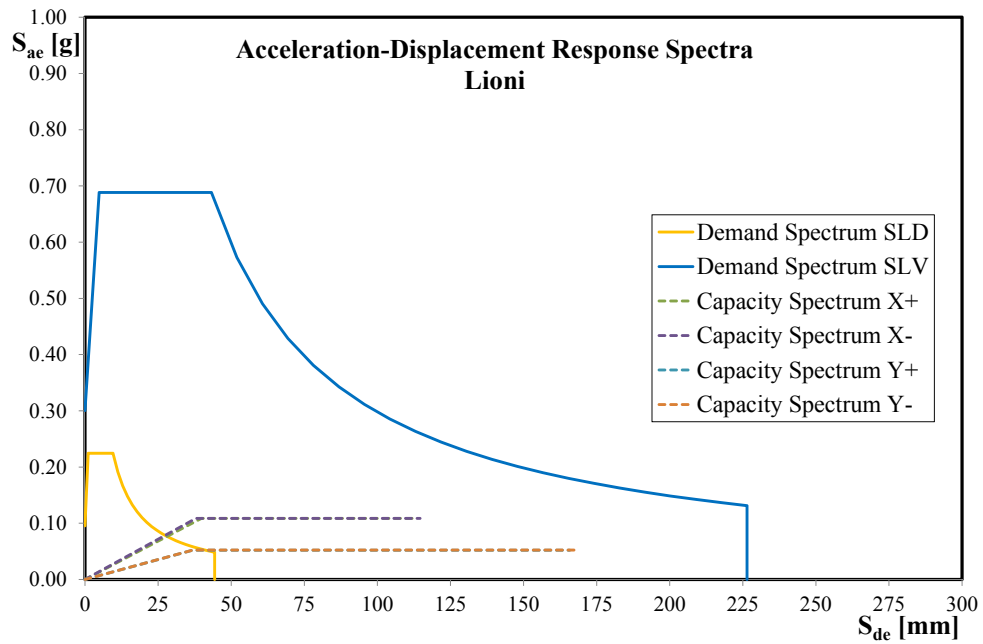
Figure 7.74: Application of N2-Method in case 2 (Table 7.9)
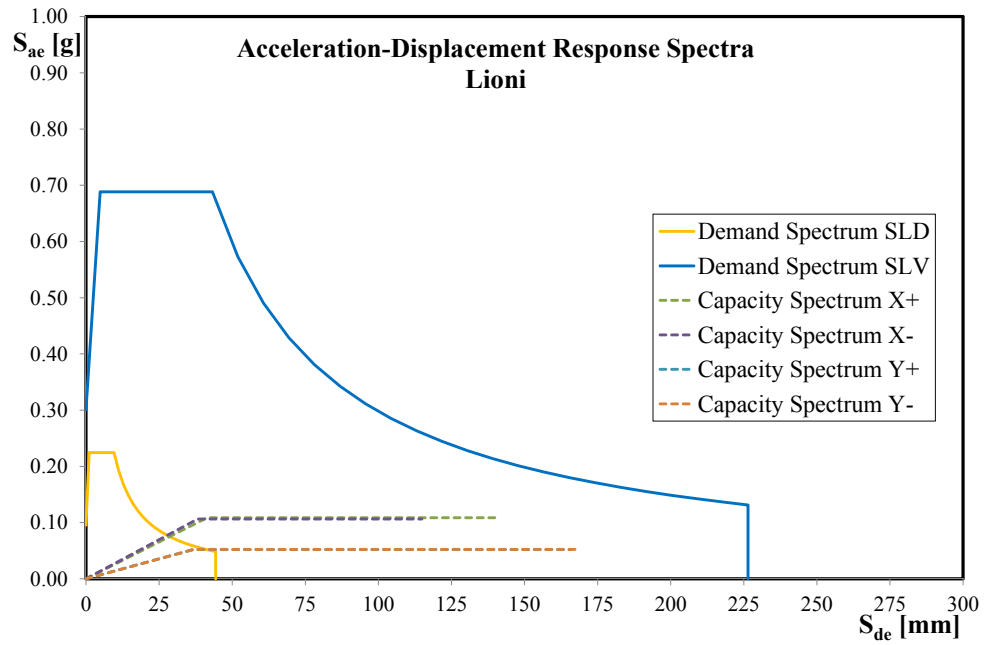
Figure 7.75: Application of N2-Method in case 3 (Table 7.9)
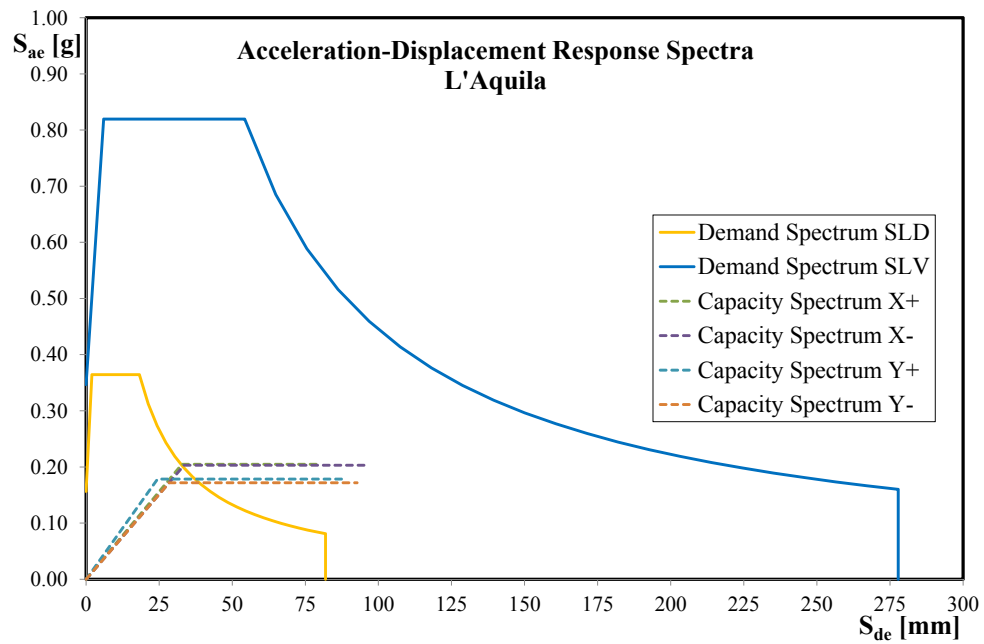
Figure 7.76: Application of N2-Method in case 4 (Table 7.9)
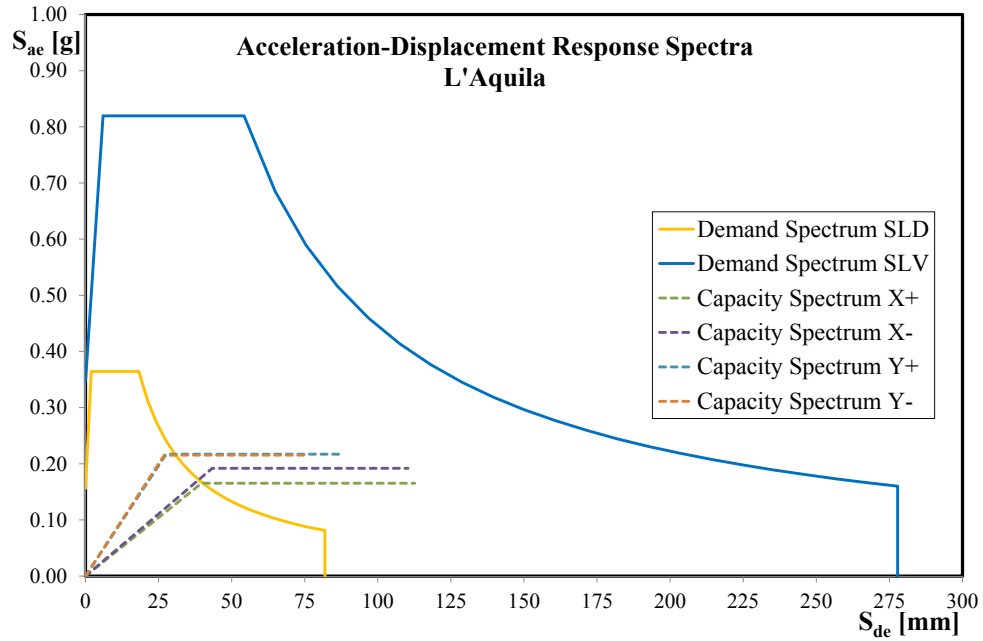
Figure 7.77: Application of N2-Method in case 5 (Table 7.9)
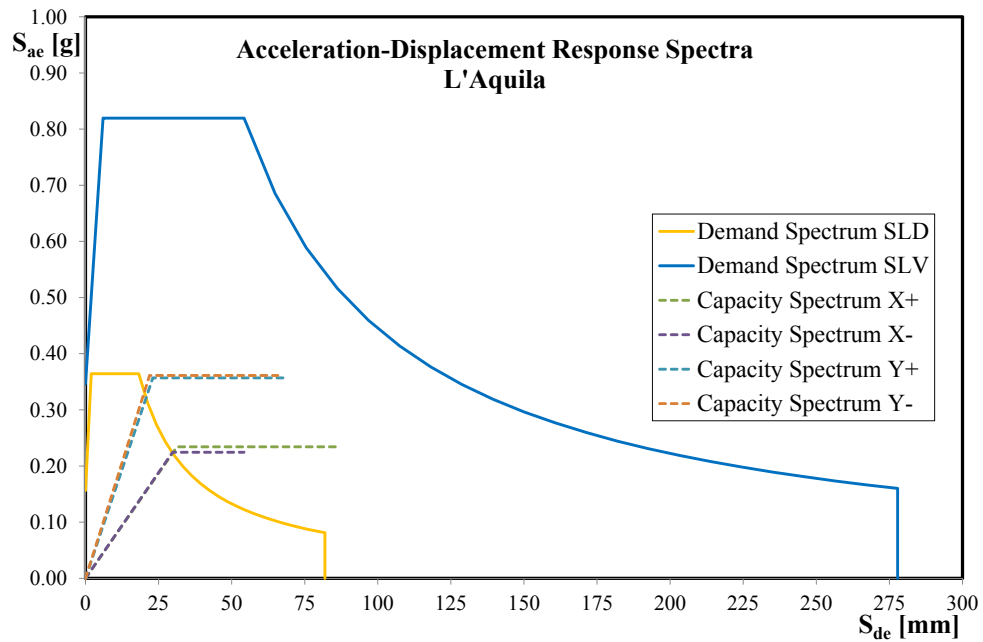
Figure 7.78: Application of N2-Method in case 6 (Table 7.9)
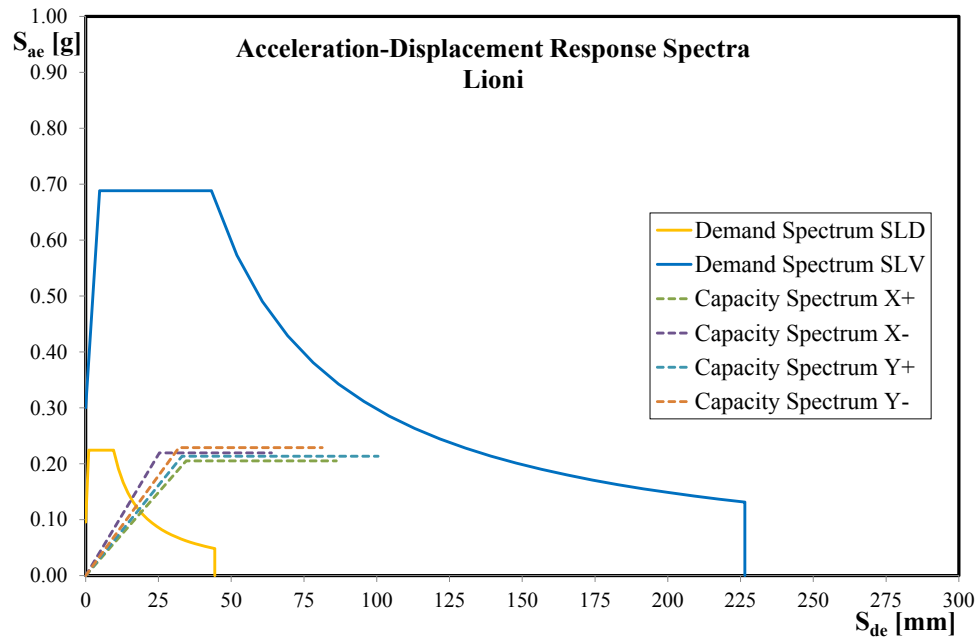
Figure 7.79: Application of N2-Method in case 7 (Table 7.9)
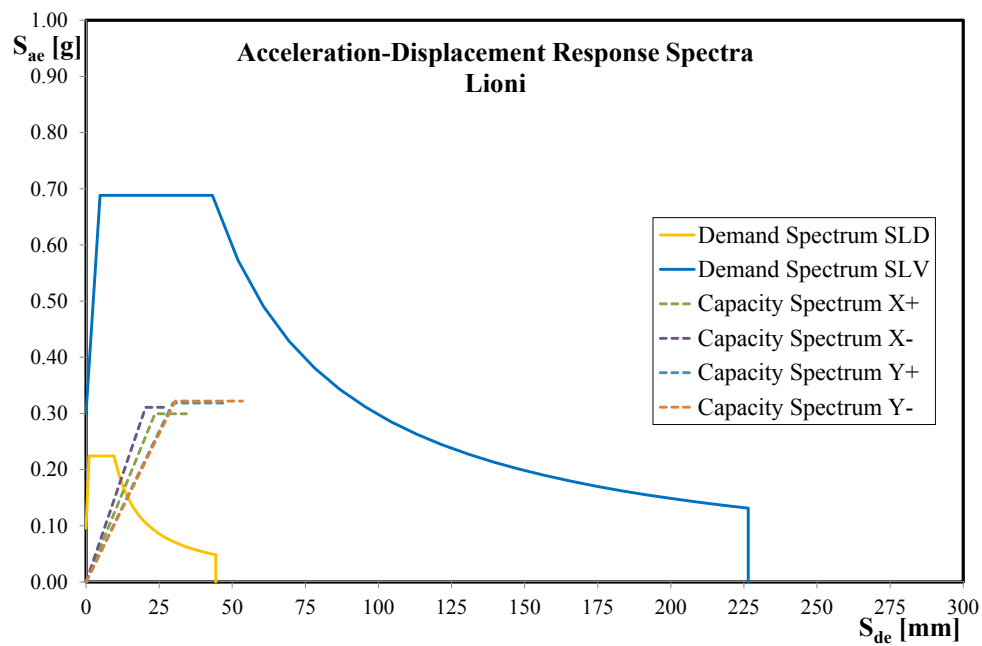
Figure 7.80: Application of N2-Method in case 8 (Table 7.9)
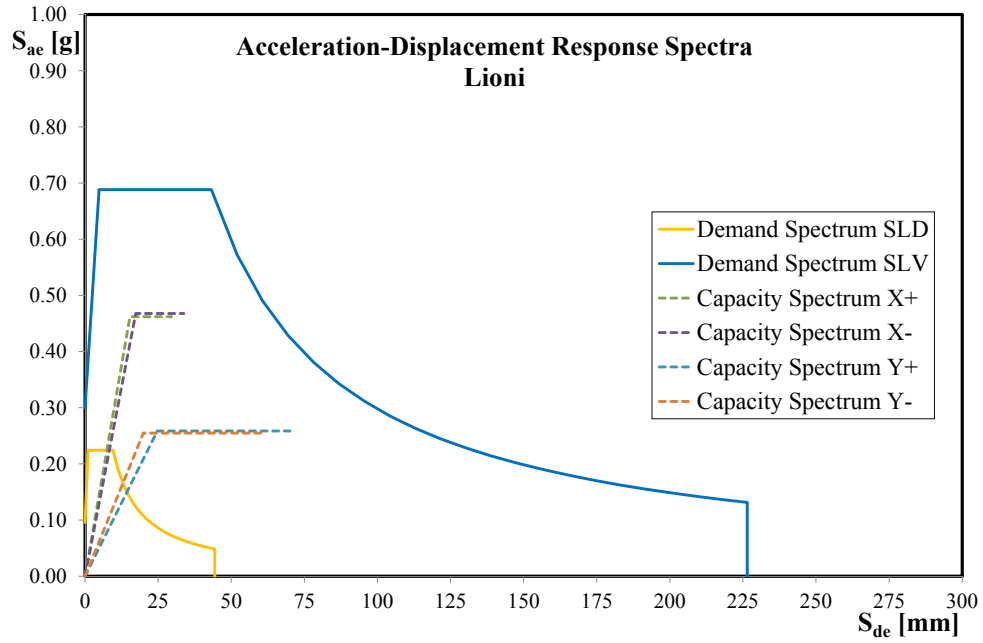
Figure 7.81: Application of N2-Method in case 9 (Table 7.9)
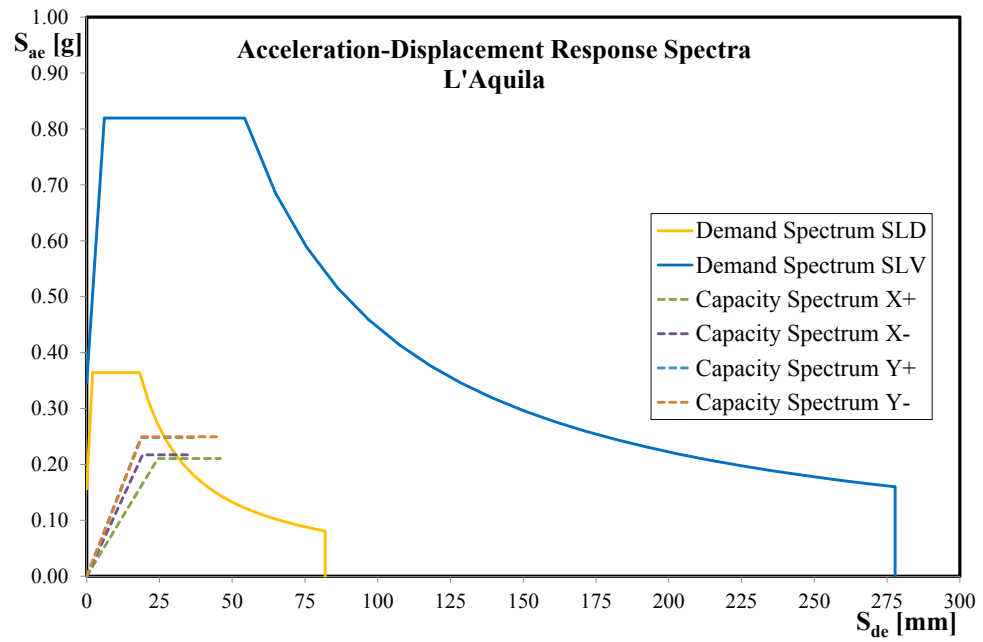
Figure 7.82: Application of N2-Method in case 10 (Table 7.9)
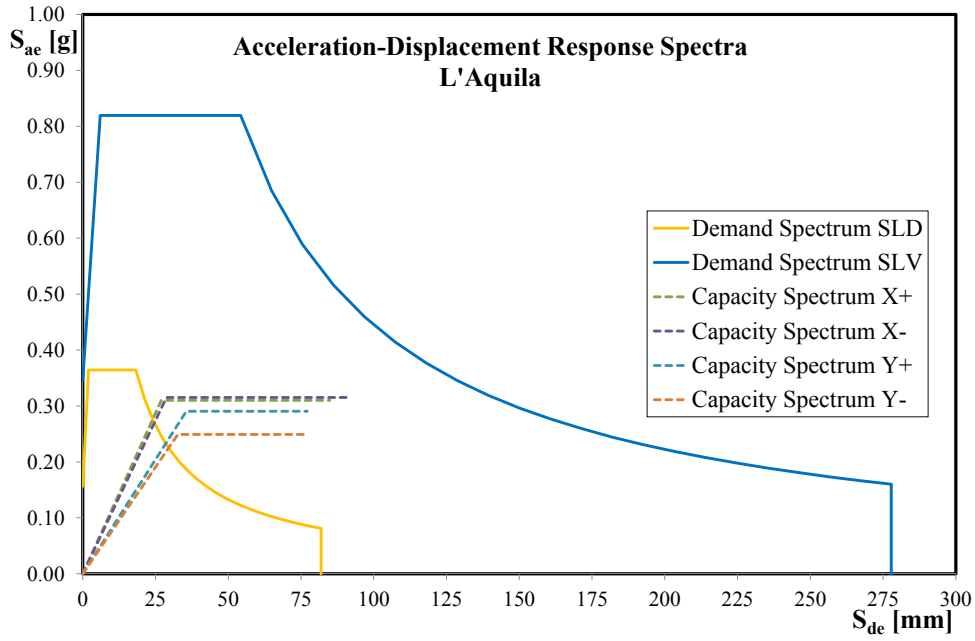
Figure 7.83: Application of N2-Method in case 11 (Table 7.9)
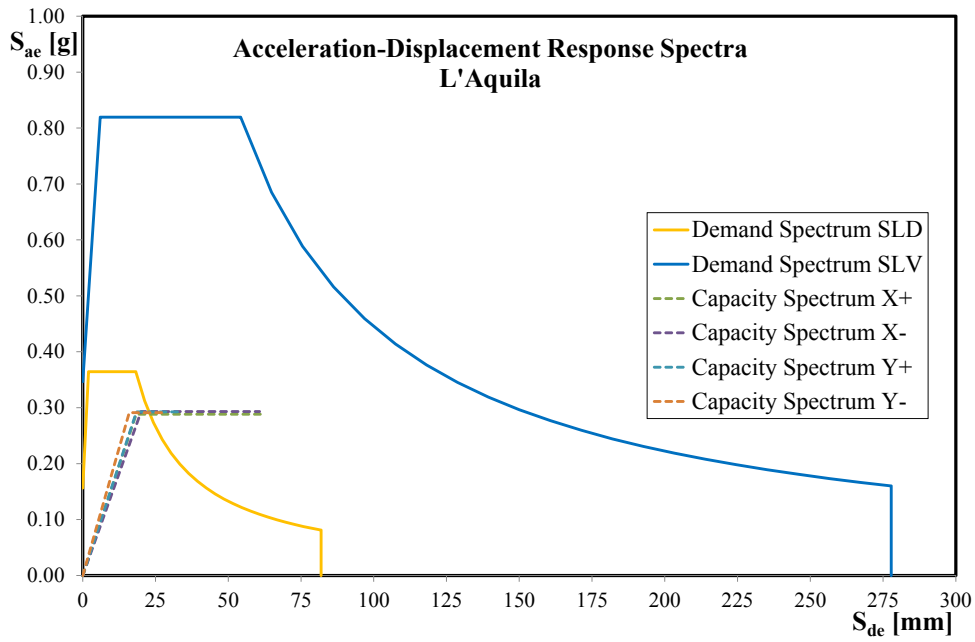
Figure 7.84: Application of N2-Method in case 12 (Table 7.9)
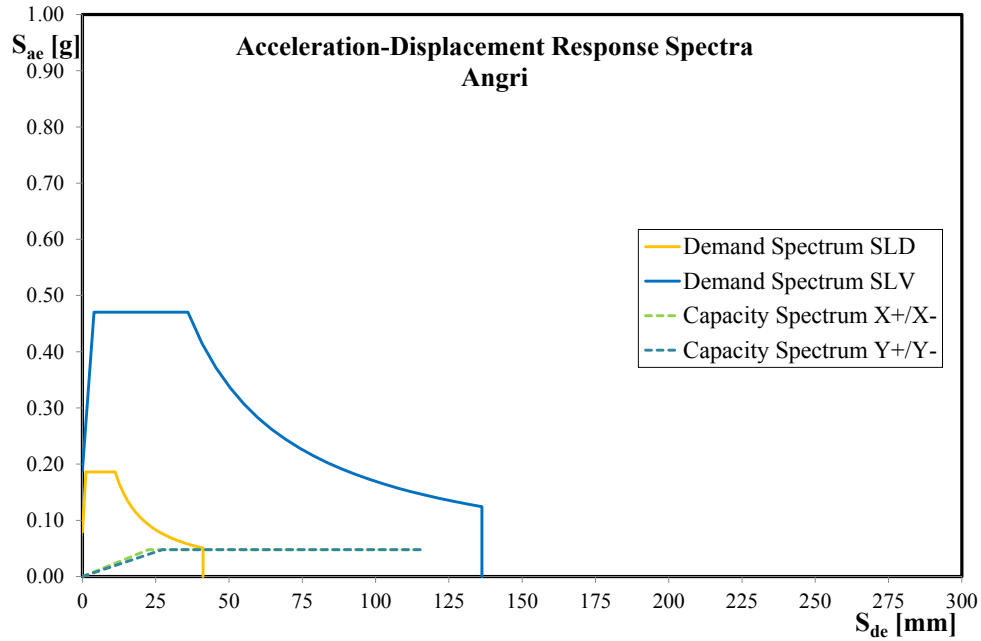
Figure 7.85: Application of N2-Method in case 13-14-15 (Table 7.9)

Table 7.39-7.53 contain the values of Demand and Capacity in terms of displacement for each Limit State and for each pushover direction. As can be seen, in all cases the inequality in Eq. 7.1 is satisfied.

Table 7.39: Displacement Demand and Capacity after retrofit intervention for case 1

		Pushover X+	Pushover X-	Pushover Y+	Pushover Y-
SLD	D [mm]	36.5	34.7	38.8	36.3
	C [mm]	47.7	41.4	42.3	37.4
SLV	D [mm]	135.5	128.8	144.0	134.6
	C [mm]	161.7	147.3	180.8	152.7

Table 7.40: Displacement Demand and Capacity after retrofit intervention for case 2

		Pushover X+	Pushover X-	Pushover Y+	Pushover Y-
SLD	D [mm]	38.5	37.5	53.3	53.4
	C [mm]	48.2	50.4	56.0	55.7
SLV	D [mm]	142.7	139.2	197.7	197.9
	C [mm]	155.0	156.6	226.5	230.2

Table 7.41: Displacement Demand and Capacity after retrofit intervention for case 3

		Pushover X+	Pushover X-	Pushover Y+	Pushover Y-
SLD	D [mm]	39.2	38.1	53.3	53.3
	C [mm]	56.3	61.6	56.0	55.7
SLV	D [mm]	145.4	141.3	197.7	197.8
	C [mm]	192.6	179.0	226.7	230.3

Table 7.42: Displacement Demand and Capacity after retrofit intervention for case 4

		Pushover X+	Pushover X-	Pushover Y+	Pushover Y-
SLD	D [mm]	44.7	45.3	41.2	45.3
	C [mm]	45.1	48.9	45.7	49.9
SLV	D [mm]	116.0	117.4	106.9	117.4
	C [mm]	129.9	141.6	118.3	126.7

Table 7.43: Displacement Demand and Capacity after retrofit intervention for case 5

		Pushover X+	Pushover X-	Pushover Y+	Pushover Y-
SLD	D [mm]	54.6	52.9	39.7	39.4
	C [mm]	55.6	53.6	40.4	40.2
SLV	D [mm]	141.5	137.2	102.9	102.2
	C [mm]	153.9	150.8	118.2	104.6

Table 7.44: Displacement Demand and Capacity after retrofit intervention for case 6

		Pushover X+	Pushover X-	Pushover Y+	Pushover Y-
SLD	D [mm]	40.7	40.6	28.3	27.4
	C [mm]	43.5	51.8	39.6	40.1
SLV	D [mm]	105.5	105.2	73.1	70.1
	C [mm]	135.2	107.6	94.2	89.9

Table 7.45: Displacement Demand and Capacity after retrofit intervention for case 7

		Pushover X+	Pushover X-	Pushover Y+	Pushover Y-
SLD	D [mm]	25.1	20.8	24.1	22.9
	C [mm]	42.9	36.7	44.0	41.9
SLV	D [mm]	93.1	77.2	89.5	84.9
	C [mm]	113.4	84.1	132.4	107.0

Table 7.46: Displacement Demand and Capacity after retrofit intervention for case 8

		Pushover X+	Pushover X-	Pushover Y+	Pushover Y-
SLD	D [mm]	17.2	15.7	18.7	18.9
	C [mm]	40.2	37.9	22.2	22.2
SLV	D [mm]	63.7	58.1	69.4	69.9
	C [mm]	80.0	75.6	76.6	80.8

Table 7.47: Displacement Demand and Capacity after retrofit intervention for case 9

		Pushover X+	Pushover X-	Pushover Y+	Pushover Y-
SLD	D [mm]	10.3	11.3	18.9	17.1
	C [mm]	33.0	38.1	35.6	36.4
SLV	D [mm]	37.6	40.3	70.2	63.5
	C [mm]	74.9	80.6	92.3	80.6

Table 7.48: Displacement Demand and Capacity after retrofit intervention for case 10

		Pushover X+	Pushover X-	Pushover Y+	Pushover Y-
SLD	D [mm]	36.6	31.9	29.4	29.6
	C [mm]	37.0	34.8	34.0	35.2
SLV	D [mm]	94.8	82.8	76.3	76.8
	C [mm]	97.7	83.1	79.2	92.0

Table 7.49: Displacement Demand and Capacity after retrofit intervention for case 11

		Pushover X+	Pushover X-	Pushover Y+	Pushover Y-
SLD	D [mm]	31.7	32.4	37.6	38.9
	C [mm]	38.8	41.1	43.7	44.0
SLV	D [mm]	82.1	84.0	97.4	100.8
	C [mm]	118.8	120.3	101.6	100.9

Table 7.50: Displacement Demand and Capacity after retrofit intervention for case 12

		Pushover X+	Pushover X-	Pushover Y+	Pushover Y-
SLD	D [mm]	27.1	28.1	27.0	25.1
	C [mm]	32.0	31.2	34.5	32.2
SLV	D [mm]	69.8	72.8	69.4	63.3
	C [mm]	81.0	92.7	82.8	72.1

Table 7.51: Displacement Demand and Capacity after retrofit intervention for case 13

		Pushover X+	Pushover X-	Pushover Y+	Pushover Y-
SLD	D [mm]	41.7	41.7	45.8	45.8
	C [mm]	46.2	46.2	50.4	50.4
SLV	D [mm]	117.7	117.7	129.3	129.3
	C [mm]	153.3	153.3	153.2	153.2

Table 7.52: Displacement Demand and Capacity after retrofit intervention for case 14

		Pushover X+	Pushover X-	Pushover Y+	Pushover Y-
SLD	D [mm]	41.7	41.7	45.8	45.8
	C [mm]	46.2	46.2	50.4	50.4
SLV	D [mm]	117.7	117.7	129.3	129.3
	C [mm]	153.3	153.3	153.2	153.2

Table 7.53: Displacement Demand and Capacity after retrofit intervention for case 15

		Pushover X+	Pushover X-	Pushover Y+	Pushover Y-
SLD	D [mm]	41.7	41.7	45.8	45.8
	C [mm]	46.2	46.2	50.4	50.4
SLV	D [mm]	117.7	117.7	129.3	129.3
	C [mm]	153.3	153.3	153.2	153.2

8. Concluding remarks and open issues

This chapter summarizes the capabilities of the proposed model, yet highlighting its "limitations" at the current state of development. Some possible modifications are discussed to enhance its efficiency and completeness.

8.1 Concluding remarks

This Thesis has been aimed at developing an automated procedure capable of selecting and designing the "best" solution for seismic retrofitting of existing RC buildings supposed be realized through the synergistic combination of both member- and structure-level techniques.

The outcomes of the preliminary applications have demonstrated that the implemented procedure is capable to converge to a solution characterized by a cost significantly lower than the initially assumed trial solutions.

As expected, the objective function curve shows a very steep slope over the first generations, whereas a slower and slower reduction of costs, often characterized by a staircase evolution, characterizes the final steps of the iterative search towards the assumed convergence condition.

In particular, as regards the member-level technique, for each column the procedure can find the minimum number of FRP layers needed to realize the local confinement.

On the other hand, with regard to the structure-level intervention, the procedure is capable to look for the optimal layout of concentric steel bracings, as well as their optimal size.

Moreover, the procedure can design a preliminary intervention on the existing foundation system through the knowledge of the number of micro-piles needed to realize the strengthening intervention. Therefore, the procedure has the potential to support engineering judgment (being far from the ambition to rule it out) in determining the "fittest" (in terms of initial costs) retrofit solution for a vulnerable RC frame. It is a promising tool for approaching a subject of high relevance.

Nevertheless, the implementation of the procedure still needs further developments: the work ahead should be intended at including the aspects that are not taken into account yet. Moreover, it should also aim at enhancing the efficiency of the procedure, whose computational cost is one of the main critical issues to be duly addressed for it be actually feasible in real applications.

8.2   Reduction of CPU time

For the case studies presented in Chapter 7, the MATLAB procedure has been profiled. In software engineering, "profiling" is a form of analysis that measures the memory or time complexity of a program or the frequency and duration of subroutine calls. It has been obtained that about 50% of the CPU time is used to perform the post-processing phase while the remaining 50% is used to execute the seismic analyses in OpenSees as shown in Figure 8.1.

Hence, the implementation of the software package should also aim at enhancing the computational efficiency of the computer procedure, whose computational cost is one of the main critical issues to be duly addressed for the proposed method be actually feasible in real applications.
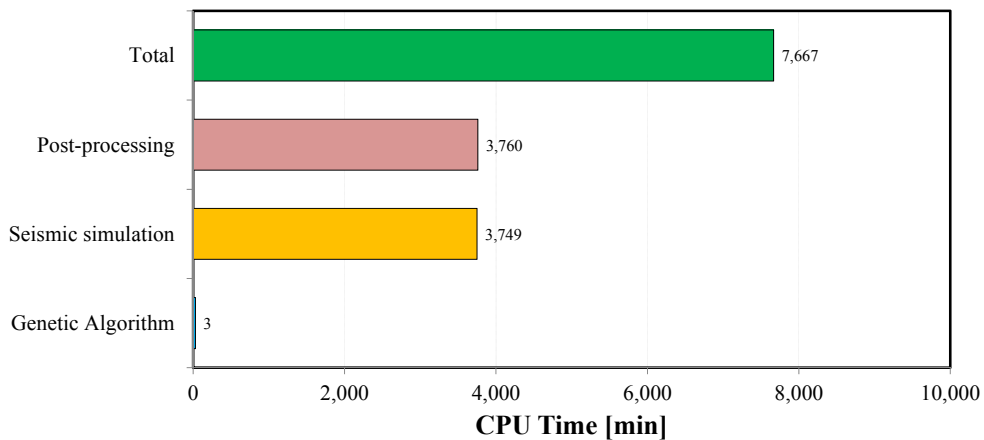

Figure 8.1: Profile summary obtained for case 1

8.2.1   Classifying the retrofit solutions through ANN

A possible way to speed up the procedure could be to replace seismic analysis with a "black box" able to immediately classify each seismic retrofit solution as either

technically feasible or unfeasible on the basis of its genotype. To this purpose, it may be possible to employ an Artificial Neural Network.

ANNs [111] are electronic networks of neurons inspired by the neural structure of the human brain. A neuron is a set of input values x_i and associated weights w_{ki}. It includes an activation function φ that sums the weights and maps the results to an output y_k (Figure 8.2).
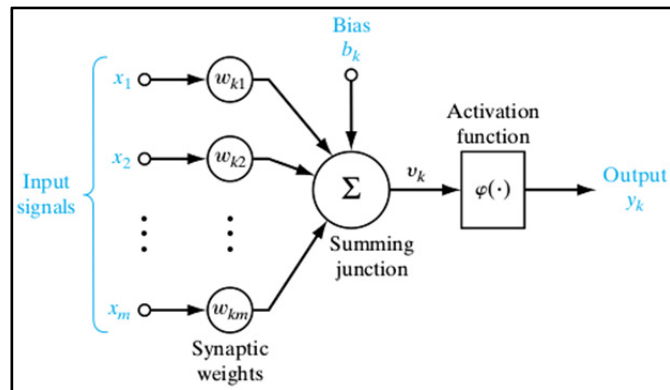
Figure 8.2: Model of an artificial neuron

Neurons are organized into layers: input, hidden and output. The input layer is composed not of full neurons but rather consists simply of the record's values that are inputted to the next layer of neurons called hidden layer. Several hidden layers can exist in one neural network. The final layer is called output layer (Figure 8.3).

Figure 8.3: A schematic architecture of a multi-layered neural network

The number of layers and the number of processing elements per layer are important decisions. There is no quantifiable answer to the layout of the network

for any particular application but only general rules picked up over time and followed by most researchers and engineers.

The back-propagation architecture is the most popular model for complex, multi-layered networks. The typical back-propagati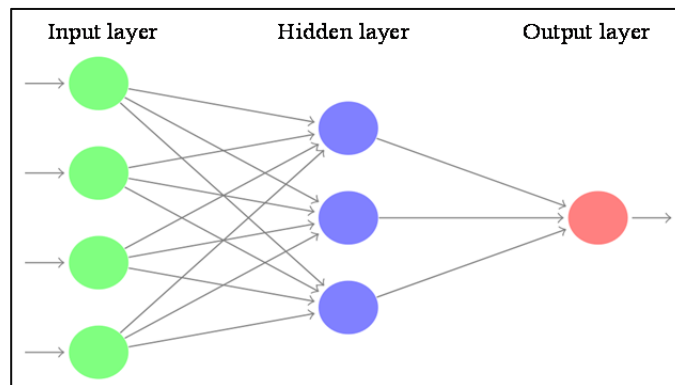on network has an input layer, an output layer, and at least one hidden layer. Each layer is fully connected to the succeeding layer.

As known, Artificial Neural Networks are also good at recognizing patterns and for solving classification problem. Its greatest strength is in non-linear solutions to ill-defined problems. In Matlab, the standard network that is used for classification is a two-layer feed-forward network [371] (Figure 8.4), with a sigmoid transfer function in the hidden layer, and a softmax transfer function in the output layer. The default number of nodes in the hidden layer is 10, as shown in Figure 8.5.
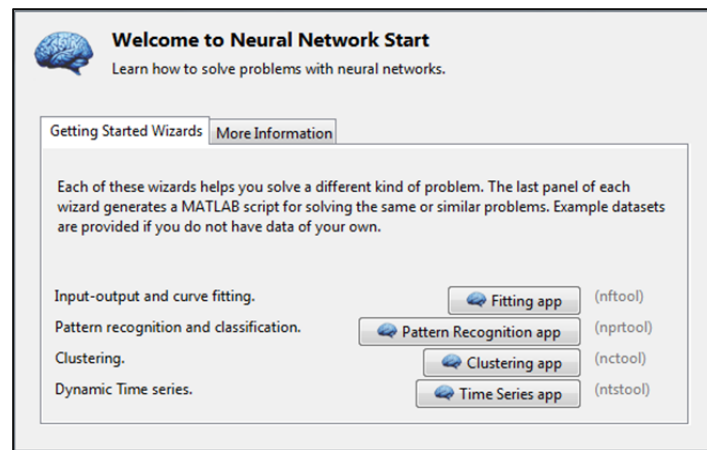
Figure 8.4: Neural Network Start in Matlab

Therefore, the ANN could be used to classify a seismic retrofit intervention as feasible or unfeasible. In this case, the number of output neurons should be set to 2, which is equal to the number of categories.

Once a network has been structured for a particular application, that network is ready to be trained, i.e. for learning from available known records.
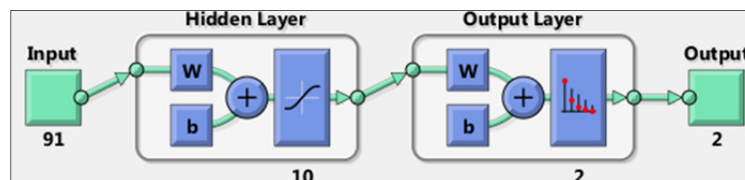

Figure 8.5: A two-layer feed-forward network

For training the two-layer feedforward network a collection of database record may be needed. The database should be composed of a set of Q input vectors (genotype) and a set of Q target vectors which indicate the classes to which the input vectors are assigned.

Table 8.1 depicts an example of data set: when there are only two categories (feasible or unfeasible), it may be necessary to set each scalar target value to either 0 or 1, indicating which class the corresponding genotype belongs to.

Table 8.1: Example of data set required for training the "classifier"

Input (genotype)	Target	
	Feasible	Unfeasible
1 3 1 0 3 2 0 1 2 2 1 3 4 6 2 5	1 (yes)	0 (no)
0 1 2 1 3 1 1 2 3 2 0 1 6 5 1 7	0 (no)	1 (yes)
3 1 1 1 2 1 0 1 2 3 3 3 6 1 0 1	0 (no)	1 (yes)
2 1 2 1 2 1 2 1 2 0 1 0 6 5 5 7	1 (yes)	0 (no)
1 1 1 1 0 2 2 2 3 3 0 1 6 0 1 3	0 (no)	1 (yes)

Such "black-box" may process one record at a time, and learn by comparing their classification of the record (resulting output) with the known actual class label of the input sample (desired output).

The errors from the initial classification of the first record are propagated back into the network and used to adjust the connection weights (usually modified by the derivative of the transfer function) each time in the hidden layers so that, during the next iteration the output values should be closer to the correct values.

This process proceeds for the previous layer(s) until the input layer is reached. The input vectors and target vectors are generally randomly divided into three sets as follows:

- 70% are used for "learning" the relationship between input sample category;
- 15% are used to validate that the trained network is generalizing;
- 15% are used as a completely independent test of network generalization.

However, some networks never learn because the input data does not contain the specific information from which the desired output is derived. Others do not converge because there is not enough data to enable complete learning.

If even more accurate results were needed, it could be possible to try any of the following approaches:

   − increase the number of hidden neurons;
   − increase the number of training vectors;
   − increase the number of input values,
   − try a different training algorithm.

That said, to point out the potential and the working principle of a neural network in the classification problem, a wide database of real example has been studied.

The number of retrofit solutions chosen in the example has been fixed equal to 3000 (30 populations with 100 individuals). For each candidate solutions, the real class (feasible or unfeasible) they belong to has been obtained by executing accurate pushover analyses in OpenSees.

Figure 8.6 shows an example of confusion matrices for training, testing, and validation, and the three kinds of data combined.

Figure 8.6: Plot of the confusion matrixes

The blue cell in the bottom right shows the total percent of correctly classified cases (in green) and the total percent of misclassified cases (in red). The lower right blue squares illustrate the overall accuracies.

The diagonal cells show the number of cases that were correctly classified, and the off-diagonal cells show the misclassified cases. Hence, the network outputs have been very accurate, due to the high numbers of correct responses in the green squares and the low numbers of incorrect responses in the red squares.

Since the results show very good recognition, such black box could be inserted within the proposed procedure to compute the network outputs and "predict" the category of the retrofit solution without waiting for seismic analysis outcomes.

8.2.2 Changing the hardware architecture

In the procedure described in Chapter 6, only the subroutine related to the seismic analysis is performed in parallel while the remaining parts of the code are executed in serial mode.

One way to optimize the code could be to exploit the potential of parallel computing and to include the post-processing stage in the parallelizable part of the code. In fact, this could contribute to increasing the term 1-α described in the Amdhal's law [367]. Furthermore, the procedure could be run on a more powerful computer, equipped with multi-core architecture and possibly with Hyper-threading technology (Figure 8.7). In this way, if the computer had more physical cores the speedup of the procedure would grow.
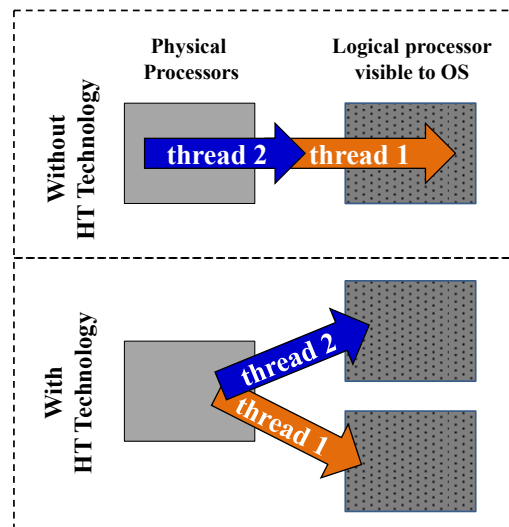

Figure 8.7: Example of how Hyper-Threading works

8.3 Future developments

8.3.1 Accurate seismic analysis

From the observation of the results obtained for simple and regular structures, another critical aspect to highlight is the tendency of the procedure to converge on retrofit solutions that do not comply with the in-plan regularity of the existing structure.

Although it could be a case of premature convergence on a local minimum that can be solved by improving the tuning of GA parameters or implementing a local search in the "neighborhood" of the optimal solution, this limitation is substantially due to the type of seismic analysis considered in the procedure.

The non-linear static analysis, in fact, was originally proposed for regular structures in plan and elevation for which the prevailing displacement components are those parallel to the direction of application of the lateral loads.

In the case of T-shaped, L-shaped or C-shaped structures where the center of gravity is far from the center of rigidity and if the analyzed structure includes "asymmetric" interventions, it is clear that the results of the canonical pushover analysis will not describe exactly the actual behavior of the structure subject to the earthquake.

Nowadays, research efforts are devoted primarily to extending the applicability of pushover methods by addressing the following issues: (i) the contributions of the higher modes of vibration, (ii) the torsional effects exhibited by plan irregular building structures.

The increasing popularity of simplified nonlinear methods in seismic design has recently led to many proposals for procedures aimed at extending pushover analysis to plan asymmetric structures: Fajfar et al. [372]; Bhatt and Bento [373]; Chopra and Goel [374]; De Stefano and Pintucchi [375].

In addition to these pushover methods, a more complex analysis such as Non-Linear Time-History (Section 2.2.4) could be used. Figure 8.8 depicts an example of accelerograms needed to perform such type of seismic analysis.
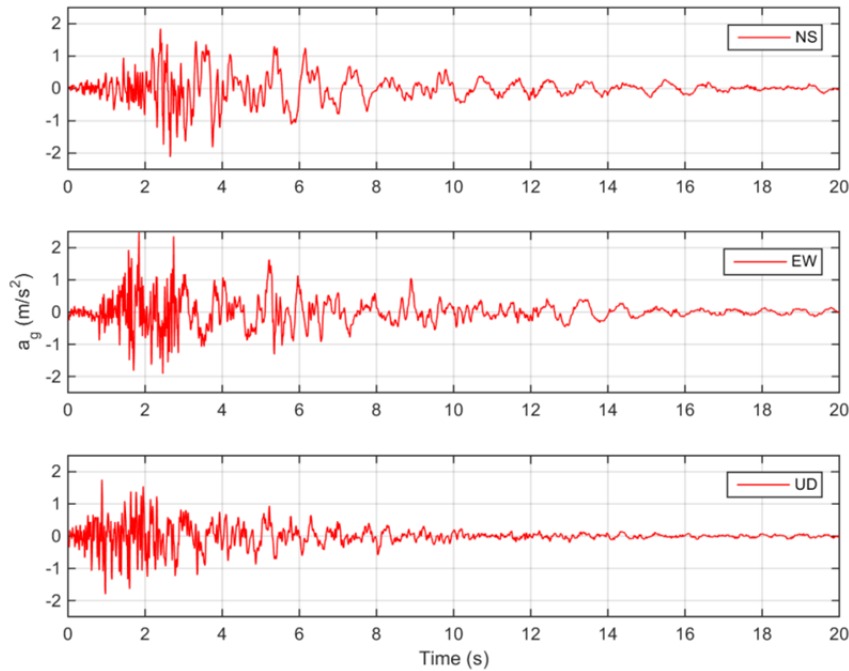
Figure 8.8: Example of acceleration time-history needed for NLTH

8.3.2   Other retrofit systems

In the proposed procedure a generic seismic retrofit intervention is conceived as a "synergistic" combination of a local intervention, aimed at increasing the displacement capacity of the structure as a whole, and a global intervention aimed at reducing the seismic demand. In particular, a confinement intervention with FRP wraps is considered to enhance only the response of the columns, while concentric bracing systems are considered as global interventions.

However, the implemented procedure could be used to optimize interventions obtained by combining any other retrofit systems belonging to the two aforementioned broad classes.

For example, steel jacketing of columns shown in Figure 8.9 could be accounted as a local intervention. Likewise, the shear r.c. walls could be considered in lieu of the steel bracing systems to work in "parallel" with the existing structure.

Obviously, by varying or adding the retrofit techniques, the design variables encoded in the chromosome could change, and therefore the length of the latter could increase/decrease along with the search space to which the optimum belongs.

Figure 8.9: Example of steel jacketing (left) and shear wall (right) intervention

8.3.3   Brittle mechanisms

As known, the assessment procedure for existing buildings should be displacement-based concerning ductile mechanisms and force- (strength-) based regarding brittle mechanisms.

In particular, in the case of R.C. structures, the ductile modes should be checked in terms of chord rotation, while the brittle mechanisms should be assessed at a section level, through the comparison of shear demand and corresponding capacity at both ends of each structural member.

However, in the current implementation, the post-processing subroutine takes into account only the ductile failure. For a more-comprehensive rational procedure, it is necessary to add another Limit State to the function g_{LS}.

Unlike the verification of ductile mechanisms, the assessment is required only at the most severe Limit State (i.e. Life Safety). To this end, it is worth noting that several brittle mechanisms can take place in existing RC buildings, such as the failure of panel zones (beam-column connections), the exceeding of shear strength in the beams, and the exceeding of shear resistance in columns.

Once at least one of these three failure modes occurs, the SLV (brittle) should be considered reached (Figure 8.10).
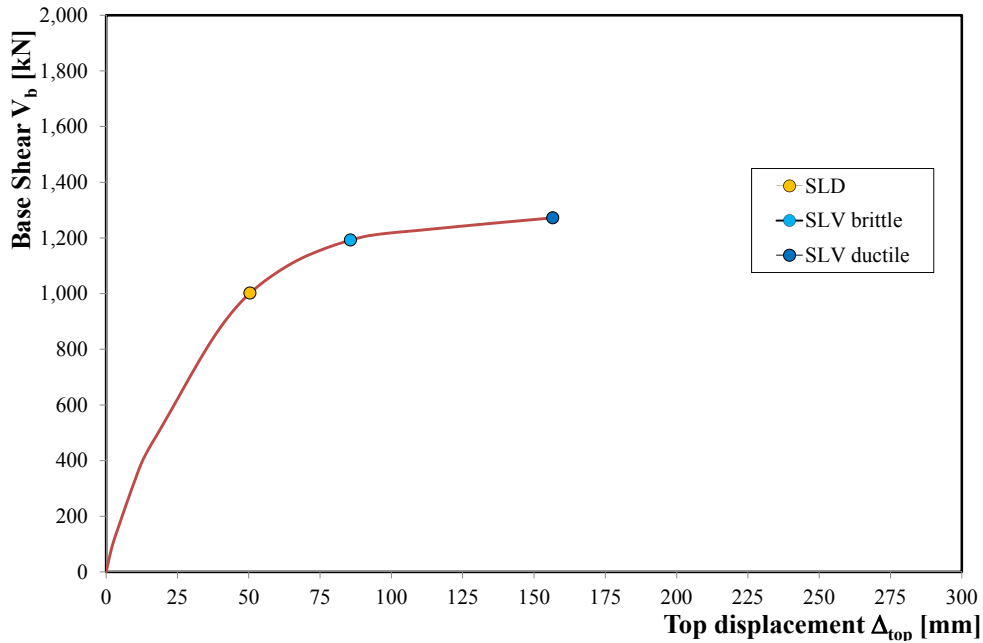
Figure 8.10: Example of pushover curve and relevant Limit States

By adding a third Limit State, and considering 4 pushover directions, 12 values of the g_{LS} function would be obtained, as shown in the following Table.

Table 8.2: Example of combinations for evaluating the Limit State function

		Pushover X+	Pushover X-	Pushover Y+	Pushover Y-
SLD	D [mm]				
	C [mm]				
SLV_{brit}	D [mm]				
	C [mm]				
SLV_{duc}	D [mm]				
	C [mm]				

8.3.4   Architectural constraints

In the proposed procedure, there are no restrictions on the search space due to the presence of architectural or technical constraints.

If a complete procedure is desired, in addition to the function g_{LS} other constraints should be accounted to search for feasible retrofit solutions (Figure 8.11). For instance, the global intervention with bracing systems should be

preferred in the perimeter part of the structure where the strengthening of the foundation system is easier (Figure 8.12).

Figure 8.11: Columns that should be "involved" in a global intervention (in green)

Conversely, the installation of the bracing systems in the inner part of the structure should be avoided since it is more complicated to build the micro-piles.
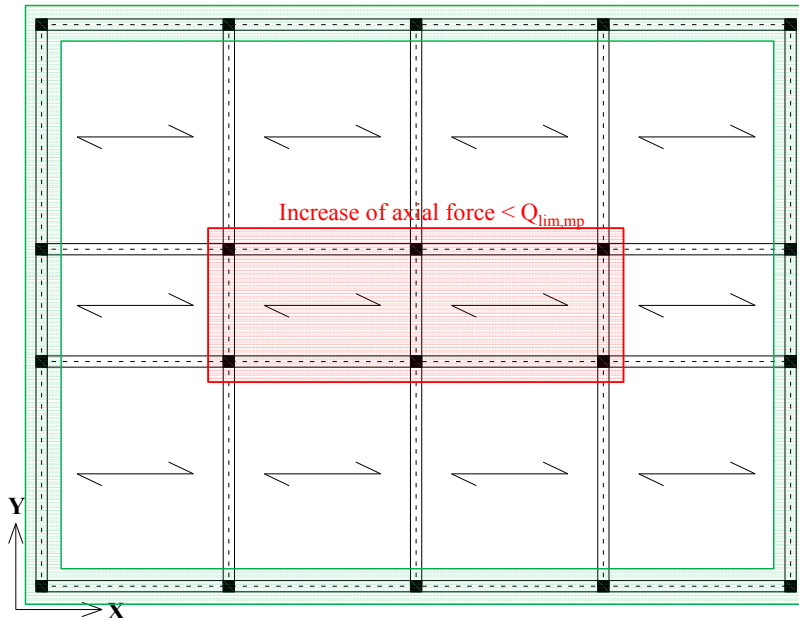

Figure 8.12: Example of strengthening of the foundation through micro-piles

8.3.5   Multi-objective function

In the present work, the actual cost of the intervention is assumed as an objective function whose minimization leads to the optimal solution for the problem of under consideration.

However, a more comprehensive and rational objective function could be obtained by taking into account not only one single objective but a series of concurrent (or conflicting) objectives.

Such objective could be based on both strictly quantitative measures (such as specific parameters related to the seismic response of the retrofitted structures or with the levels of reliability of its seismic performance) or qualitative measures, possibly related to either the users' opinion or the aesthetical aspects of the final solutions.

In that case, the procedure should be aimed at solving a multi-objective optimization problem whose goal may be to simultaneously minimize all the objectives grouped into the f(x) vector given in Eq.(8.1):

$$f(x) = \left[f_1(x), f_2(x), f_3(x), \dots f_n(x) \right] \tag{8.1}$$

However, if it has multiple objectives, it may be not possible to find an optimal solution with respect to all objectives. Combining the minimization of the actual cost of intervention and the minimization of the "risk" of intervention is an example of two objective optimization problem that has no global optimum.

For this example, it is not possible to achieve the minimal total cost f_1 and the minimal risk f_2 at the same time. In fact, in multi-objective terminology, a solution A is considered dominating another solution B if all the objectives of B are greater than ones of solution A.

Hence, in multi-objective optimization problem, all the non-dominated points belong to the so-called Pareto optimal front shown in Figure 8.13 that is normally a high dimensional area and it represents the multi-objective optimum.
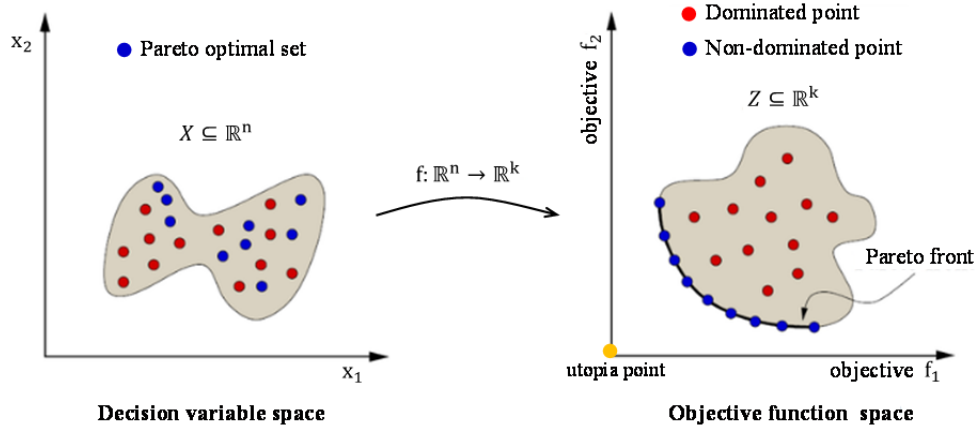
Figure 8.13: Example of the Pareto front in a two-objective optimization problem

Then the decision which solution is the best is taken with respect to other criteria and human (decision maker) need to be involved in this selection process.

Three basic approaches are commonly employed to solve a multi-objective optimization problem. The first one is to aggregate the multi-objective functions into a single objective. The mapping can be generally represented as follows:

$$f(x) = [f_1(x), f_2(x), f_3(x), ...f_n(x)] \rightarrow m(x) \tag{8.2}$$

Several different methods are available for forming multi-objective functions, such as weighted sum and fuzzy logic fitness. This single objective function can be optimized using many optimization algorithms. Such method could be suitable and very efficient if the decision maker knows how to trade-off all objectives.

The second approach called "criteria method" [376] consists in optimizing one objective at one time. A practical application could be to start multiple search processes, each of which could be driven by an algorithm to optimize one objective.

The third method is to find Pareto optimal front. Population-based search algorithms are more suitable for this task. The user should then select the final solution. To this end, the Analytical Hierarchy Process (AHP) [377] could be employed to simplify the preference ratings among decision criteria using pairwise comparisons.

References

[1].Wang, Z. 2005. A clear definition of seismic hazard and risk: a basis for hazard and risk assessment, communication, and management. In AGU Fall Meeting Abstracts.

[2].Gutenberg, B., Richter, C. F. 1944. Frequency of earthquakes in California. Bulletin of the Seismological Society of America, 34(4), 185-188.

[3].Ambraseys, N. N. 1971. Value of historical records of earthquakes. Nature, 232(5310), 375.

[4].Guidoboni, E., Stucchi, M. 1993. The contribution of historical records of earthquakes to the evaluation of seismic hazard. Annals of Geophysics, 36 (3-4).

[5].Lang, K. 2002. Seismic vulnerability of existing buildings (No. 273). vdf Hochschulverlag AG.

[6].https://it.wikipedia.org/wiki/Terremoti_in_Italia_nel_XX_secolo.

[7].Binda, L., Chesi, C., Parisi, M. A., Magi, J., Marsili, C. 2010. Monumental heritage in the L'Aquila, Italy, earthquake: considerations on a case-study. In Third Euro-Mediteranean Symposium on Advances in Geomaterials and Structures (pp. 529-534).

[8].Kaplan, H., Bilgin, H., Yilmaz, S., Binici, H., Öztas, A. 2010. Structural damages of L'Aquila (Italy) earthquake. Natural Hazards and Earth System Sciences, 10(3), 499.

[9].European Standard EN (Eurocode 8) 1998-1:2005, Design of structures for earthquake resistance, Part 1: General rules, seismic actions and rules for buildings. European Committee for Standardization (CEN), Bruxelles, 2005.

[10].Bellicoso, A. 2011. Italian anti-seismic legislation and building restoration. International Journal for Housing Science and Its Applications, 35(3), 137.

[11].Oliveto, G., Liberatore, L., Decanini, L. D. 2011. Evoluzione storica della normativa sismica italiana alla luce degli effetti causati dal terremoto dell'Aquila del 2009 (in Italian). XIV Convegno ANIDIS L'Ingegneria Sismica in Italia, Bari, Italy. DBD of an Energy Dissipating System for Masonry Structures, 501.

[12].Order of the President of the Council of Ministers no. 3274 of 20 March 2003. Primi elementi in materia di criteri generali per la classificazione sismica del territorio nazionale e di normative tecniche per le costruzioni in zona sismica, G.U.R.I. n.72 08/05/2003. (http://www.protezionecivile.it/legislazione)

[13].15th National Census of Population, 2011. Rome, ISTAT (http://www.istat.it).

[14].Elaboration of National Council of Engineers (CNI) Study Center on Istat, CRESME, and Civil Protection data. 2012.

[15].M.II.TT. 2008 D.M. 14/01/2008 "Norme tecniche per le costruzioni", G.U. n. 29 04/02/2008 (in Italian).

[16].fib .2003. Seismic assessment and retrofit of reinforced concrete buildings Bulletin No. 24 138 ISBN: 978-2-88394-054-3.

[17].May P.J. 2007. Societal Implications of Performance-Based Earthquake Engineering PEER Report 2006/12.

[18].CRESME, Fondazione Housing Sociale. 2015. Il mercato delle costruzioni 2012. XIX Rapporto Congiunturale e previsionale CRESME. Lo scenario di medio periodo (in Italian).

[19].Masi, A., Chiauzzi, L., Braga, F., Mucciarelli, M., Vona, M., Ditommaso, R. 2011. Peak and integral seismic parameters of L'Aquila 2009 ground motions: observed versus code provision values. Bulletin of Earthquake Engineering, 9(1), 139-156.

[20].Gu, Q., Barbato, M., Conte, J. P., Gill, P. E., McKenna, F. 2011. OpenSees-SNOPT framework for finite-element-based optimization of structural and geotechnical systems. Journal of Structural Engineering, 138(6), 822-834.

[21].Guerra, A., Kiousis, D.P. 2004. Design optimisation of reinforced concrete structures, Computers and Concrete, 3(5), 313-334, 2006.

[22].Thermou, G. E., Elnashai, A. S. 2006. Seismic retrofit schemes for RC structures and local-global consequences. Progress in Structural Engineering and Materials, 8(1), 1-15.

[23]. Kaplan, H., Yilmaz, S., Cetinkaya, N., Atimtay, E. 2011. Seismic strengthening of RC structures with exterior shear walls. Sadhana, 36(1), 17.

[24].Rodriguez, M., Park, R. 1991. Repair and strengthening of reinforced concrete buildings for seismic resistance. Earthquake Spectra, 7(3), 439-459.

[25].Kunisue, A., Koshika, N., Kurokawa, Y., Suzuki, N., Agami, J., Sakamoto, M. 2000. Retrofitting method of existing rein-forced concrete buildings using elastoplastic steel dampers. Proceedings of the twelfth World Conference on Earthquake Engineering (12WCEE), Paper 0648.

[26].Bordea, S., Dubina, D. 2009. Retrofitting/upgrading of reinforced concrete elements with buckling restrained bracing elements. In Proceedings of the 11th

WSEAS International Conference on Sustainability in Science Engineering, Timisoara (Romania), 27-29 May 2009, 407 (Vol. 402).

[27].EERI. 2006. Learning from Earthquakes: The Kashmir Earthquake of October 8, 2005: Impacts in Pakistan, EERI Special Earthquake Report — February 2006 (http://www.eeri.org/lfe/pdf/kashmir_eeri_2nd_report.pdf).

[28].EERI. 2008. Learning from Earthquakes: The Wenchuan, Sichuan Province, China, Earthquake of May 12, 2008, EERI Special Earthquake Report-October 2008(http://www.eeri.org/site/images/eeri_newsletter/2008_pdf/Wenchuan_C hina_Rec on_Rpt.pdf).

[29].EERI. 2010. Learning from Earthquakes: The Mw 7.0 Haiti Earthquake of January 12, 2010: Report #1, EERI Special Earthquake Report — April 2010 (http://www.eeri.org/site/images/eeri_newsletter/2010_pdf/Haiti_Rpt_1.pdf)

[30].Kaplan, H., Bilgin, H., Yilmaz, S., Binici, H., Öztas, A. 2010. Structural damages of L'Aquila (Italy) earthquake. Natural Hazards and Earth System Sciences, 10(3), 499.

[31].EERI. 2011. Learning from Earthquakes: The M 6.3 Christchurch, New Zealand, Earthquake of February 22, 2011, EERI Special Earthquake Report (http://www.eeri.org/site/images/eeri_newsletter/2011_pdf/EERI_NewZealand_EQRpt_web.p df).

[32].Elwood, K., Comartin, C., Holmes, W., Kelly, D., Lowes, L., Moehle, J. 2010. Program Plan for the Development of Collapse Assessment and Mitigation Strategies for Existing Reinforced Concrete Buildings (No. Grant/Contract Reports (NISTGCR)-10-917-7). National Institute of Standards and Technology, Gaithersburg.

[33].NISEE. The Earthquake Engineering Online Archive.

[34].Guevara, L. T., García, L. E. 2005. The captive-and short-column effects. Earthquake Spectra, 21(1), 141-160.

[35].Damaged Concrete Buildings Database.

[36].De Stefano, M., Pintucchi, B. 2008. A review of research on seismic behaviour of irregular building structures since 2002. Bulletin of Earthquake Engineering, 6(2), 285-308.

[37].Popovics, S. 1990. Analysis of concrete strength versus water-cement ratio relationship. Materials Journal, 87(5), 517-529.

[38].Özturan, T., Çeçen, C. 1997. Effect of coarse aggregate type on mechanical properties of concretes with different strengths. Cement and Concrete Research, 27(2), 165-170.

[39].Akiyama, M., Frangopol, D. M., Suzuki, M. 2012. Integration of the effects of airborne chlorides into reliability-based durability design of reinforced

concrete structures in a marine environment. Structure and Infrastructure Engineering, 8(2), 125-134.

[40].Lima, C., De Stefano, G., Martinelli, E. 2014. Seismic response of masonry infilled RC frames: practice-oriented models and open issues. Earthquakes and Structures, 6(4), 409-436.

[41].https://www.colorado.edu/engineering/CAS/courses.d/IFEM.d/IFEM.Ch06.d/IFEM.Ch06.pdf.

[42].Bathe, K. J. (2006). Finite element procedures. Klaus-Jurgen Bathe.

[43].Taucer, F., Spacone, E., Filippou, F. C. 1991. A fiber beam-column element for seismic response analysis of reinforced concrete structures (Vol. 91, No. 17). Berkekey, California: Earthquake Engineering Research Center, College of Engineering, University of California.

[44].Spacone, E. 2001. A module for analysis and design of segmental pre-stressed concrete bridges (CASI-TR-01-04), Final report of a CASI FY00 technology transfer grant. Fort Collins, CO: Colorado Advanced Software Institute.

[45].Clough, R. W. 1960. The finite element method in plane stress analysis. In Proceedings of 2nd ASCE Conference on Electronic Computation, Pittsburgh Pa., September 8 and 9.

[46].Bathe, J.K. 1982. Finite element procedures in engineering analysis. Prentice-Hall, Englewood Cliffs.

[47]. Clough, R.W. and Penzien, J. 1993. Dynamics of Structures, 2nd edition, McGraw Hill, Inc., New York.

[48].Felippa, C.A. 2000. Introduction to the finite element method – lecture notes. Boulder: University of Colorado.

[49].Goel, R.K., Chopra, A.K. 1996. Evaluation of Code Formulas for Fundamental Period of Buildings, CD-ROM, in: Proc., 11th World Conf. on Earthquake Engineering., Paper No. 1127, Elsevier Science Ltd, Oxford, U.K.

[50].Goel, R.K., Chopra, A.K. 1997. Vibration Properties of Buildings during Earthquakes, Rep. to be Published, Earthquake Engineering. Rs. Ctr., Univ. of California, Berkeley, Richmond, Calif.

[51].Goel, R. K., Chopra, A. K. 1997. Period formulas for moment-resisting frame buildings. Journal of Structural Engineering, 123(11), 1454-1461.

[52].Newmark, N.M., Rosenblueth, E. 1971. Fundamentals of Earthquake Engineering. New York: Prentice-Hall.

[53].Clough, R., Penzien. W.J. 1975. Dynamics of Structures. New York: McGraw-Hill.

[54].Thomson, W.T. 1965. Vibration Theory and Application. New York: Prentice-Hall.

[55].Wiegel, R. L., 1970. Earthquake Engineering. New York: Prentice-Hall.

[56]. ATC 40, 1996, Seismic evaluation and retrofit of concrete buildings, Vol. 1.

[57]. Krawinkler, H., Seneviratna, G.D.P.K. 1998. Pros and cons of a pushover analysis of seismic performance evaluation. Engineering structures, 20(4-6), 452-464.

[58]. Tremayne, B., Kelly, T. E. 2005. Time history analysis as a method of implementing performance based design. Holmes Consulting Group, Auckland, New Zealand.

[59]. McKenna, F., Fenves, G.L., Jeremic, B., Scott, M.H. 2000, Open system for earthquake engineering simulation (http://opensees.berkely.edu).

[60]. Clough, R.W., Penzien, J. 1993. Dynamics of Structures, 2nd Edition, McGraw-Hill Book Co., Singapore.

[61]. Beyer, K., Bommer, J.J. 2007. Selection and Scaling of Real Accelerograms for Bi-Directional Loading: A Review of Current Practice and Code Provisions, Journal of Earthquake Engineering, 11(1), 13-45.

[62]. Iervolino I, Cornell CA. 2005. Record Selection for Nonlinear Seismic Analysis of Structures. Earthquake Spectra; 21(3):685–713.

[63]. Kalkan, E., Chopra, A.K. 2010. Practical Guidelines to Select and Scale Earthquake Records for Nonlinear Response History Analysis of Structures, Earthquake Engineering Research Center, Open-File Report (available online at ⟨https://www.eeri.org/site/images/awards/ reports/ekalkan.pdf⟩).

[64]. Stefanou, G., Fragiadakis, M. 2009. Nonlinear dynamic analysis of frames with stochastic non-Gaussian material properties. Engineering Structures, 31(8), 1841-1850.

[65]. Jalayer, F., Elefante, L., Iervolino, I., Manfredi, G. 2011. Knowledge-based performance assessment of existing RC buildings. Journal of Earthquake Engineering, 15(3), 362-389.

[66]. Dides, M. A., De la Llera, J. C. 2005. A comparative study of concentrated plasticity models in dynamic analysis of building structures. Earthquake engineering & structural dynamics, 34(8), 1005-1026.

[67]. Orbison, J. G., McGuire, W., Abel, J. F. 1982. Yield surface applications in nonlinear steel frame analysis. Computer Methods in Applied Mechanics and Engineering, 33(1-3), 557-573.

[68]. Bazant, S., Bhat, P. 1977. Prediction of hysteresis in reinforced concrete members. Journal of Structural Engineering (ASCE) 103, 151–167.

[69]. Elnashai, A. S., Di Sarno, L. 2008. Fundamentals of earthquake engineering (p. 34). New York: Wiley.

[70]. Kunnath, S. K., Reinhorn, A. M., Park, Y. J. 1990. Analytical modeling of inelastic seismic response of R/C structures. Journal of Structural Engineering, 116(4), 996-1017.

[71].Spacone, E., Filippou, F.C., Taucer, F.F. 1996. Fibre beam–column model for non-linear analysis of RC frames: Part I: Formulation. Earthquake Engineering and Structural Dynamics 25, 711–725.

[72].Spacone, E., Filippou, F.C., Taucer, F.F. 1996. Fibre beam–column model for non-linear analysis of RC frames: Part II: Applications. Earthquake Engineering and Structural Dynamics 25,727–742.

[73].Iribarren, B. S., Berke, P., Bouillard, P., Vantomme, J., Massart, T. J. 2011. Investigation of the influence of design and material parameters in the progressive collapse analysis of RC structures. Engineering structures, 33(10), 2805-2820.

[74].Structural Engineers Association of California (SEAOC). 1995. Vision 2000, conceptual framework for performance-based seismic design. Recommended Lateral Force Requirements and Commentary, 1996, 6th Edition. Sacramento, CA: 391-416.

[75].Applied Technology Council (ATC), 1997. NEHRP Commentary on the Guidelines for the Seismic Rehabilitation of Buildings, published by the Federal Emergency Management Agency, FEMA 273, Washington, D.C.

[76].Applied Technology Council (ATC), 1997. NEHRP Commentary on the Guidelines for the Seismic Rehabilitation of Buildings, prepared for the Building Seismic Safety Council, published by the Federal Emergency Management Agency, FEMA 274, Washington, D.C.

[77].Applied Technology Council (ATC), 2000. NEHRP Commentary on the Guidelines for the Seismic Rehabilitation of Buildings, published by the Federal Emergency Management Agency, FEMA 356, Washington, D.C.

[78].Fajfar, P., Fischinger, M. 1987. Non-linear seismic analysis of RC buildings: implications of a case study. European Earthquake Engineering, 1(1), 31-43.

[79].Fajfar, P., Fischinger, M. 1989. N2–A method for non-linear seismic analysis of regular buildings. In: Proceedings of the 9th world conference on Earthquake Engineering, Vol. 5. Tokyo- Kyoto: Japan; p. 111–116.

[80].Fajfar, P., Vidic, T., Fischinger, M. 1990. A measure of earthquake motion capacity to damage medium-period structures. Soil Dynamics and Earthquake Engineering, 9(5), 236-242.

[81].Fajfar, P., Gašperšič, P. 1996. The N2 method for the seismic damage analysis of RC buildings. Earthquake Engineering & Structural Dynamics, 25(1), 31-46.

[82].Fajfar, P. 1999. Capacity spectrum method based on inelastic demand spectra, Earthquake Engineering & Structural Dynamics, 28(9), 979-993.

[83]. European Standard EN (Eurocode 8) 1998-3:2005, Design of structures for earthquake resistance, Part 3: Assessment and retrofitting of buildings. European Committee for Standardization (CEN), Bruxelles.

[84]. Kalkan, E., Kunnath, S. K. 2007. Assessment of current nonlinear static procedures for seismic evaluation of buildings. Engineering Structures, 29(3), 305-316.

[85]. Shibata, A., Sozen, M.A. 1976. Substitute-structure method for seismic design in R/C. Journal of the Structural Division ASCE, 102(1), 1-18.

[86]. Newmark, N.M., Hall, W.J. 1982. Earthquake Spectra and Design: Engineering Monographs on Earthquake Criteria, Structural Design, and Strong Motion Records. Earthquake Engineering Research Institute Monograph, Berkeley, CA.

[87]. Veletsos, A.S., Newmark, N.M. 1960. Effect of inelastic behaviour on the response of simple systems to earthquake motions. Proceedings of the 2nd World Conference on Earthquake Engineering, Tokyo, Japan, vol. 2, 895–912.

[88]. Vidic, T., Fajfar, P., Fischinger, M. 1994. Consistent inelastic design spectra: strength and displacement. Earthquake Engineering & Structural Dynamics, 23(5), 507-521.

[89]. Martinelli, E., Falcone, R., Faella, C. 2017. Inelastic design spectra based on the actual dissipative capacity of the hysteretic response. Soil Dynamics and Earthquake Engineering, 97, 101-116.

[90]. Veletsos, A.S., Newmark, N.M. 1964. Design procedures for shock isolation systems of underground protective structures. New Mexico: Air Force Weapons Laboratory; Technical Documentary Report No. RTD TDR-63-3096, III.

[91]. Priestley, M.J.N. 2000. Performance based seismic design, Proceedings of the 12th World Conference on Earthquke Engineering (12WCEE), Auckland (NZ), 30 January - Friday 4 February 2000, Paper 2831.

[92]. Moehle, J., Deierlein, G.G. 2004. A framework methodology for performance-based earthquake engineering. Proceedings of the 13th World Conference on Earthquake Engineering (13WCEE), August 1-6, 2004, Vancouver, B.C., Canada, Paper No. 679.

[93]. UNDP/UNIDO. 1985. Post-earthquake damage evaluation and strength assessment of buildings under seismic conditions. PR. RER/79/015, Vol. 4, Ch. 3, Vienna.

[94]. Baros, D.K., Dritsos, S. E. 2008. A simplified procedure to select a suitable retrofit strategy for existing RC buildings using pushover analysis. Journal of Earthquake Engineering, 12(6), 823-848.

[95].Kaplan, H., Yilmaz, S., Cetinkaya, N., Atimtay, E. 2011. Seismic strengthening of RC structures with exterior shear walls, Sadhana, Indian Academy of Sciences , 36(1), 17–34.

[96].Thermou, G.E., Elnashai, A.S. 2006. Seismic retrofit schemes for RC structures and local–global consequences, Progress in Structural Engineering and Materials, 8:1–15.

[97].Roy, B., 1973. How outranking relation helps multiple criteria decision making, Multiple Criteria Decision Making, Actes du Séminaire «Théorie de la Décision», Beaulieu-Sainte-Assise, Francia.

[98].Caterino, N., Iervolino, I., Manfredi, G., Cosenza, E. 2008. Multi-criteria decision making for seismic retrofitting of RC structures. Journal of Earthquake Engineering, 12(4), 555-583.

[99].Le Gauffre, P., Haidar, H., Poinard, D., Laffréchine, K., Baur, R., Schiatti, M. 2007. A multicriteria decision support methodology for annual rehabilitation programs of water networks. Computer-Aided Civil and Infrastructure Engineering, 22(7), 478-488.

[100].Faella, C., Martinelli, E., Nigro, E. 2008. A rational strategy for seismic retrofitting of RC existing buildings, Proceedings of the fourteenth World Conference on Earthquake Engineering (14WCEE), October 12-17, Beijing, China.

[101].Russell, S. J. and Norvig, P., 2003. Artificial Intelligence: A Modern Approach (2nd ed.), Upper Saddle River, New Jersey: Prentice Hall, ISBN 0-13-790395-2.

[102].Russell, S. J. and Norvig, P., 2009. Artificial Intelligence: A Modern Approach (3rd ed.). Upper Saddle River, New Jersey: Prentice Hall. ISBN 0-13-604259-7.

[103].Zadeh, L.A. Foreword, 1992. Proceedings of the Second International Conference on Fuzzy Logic and Neural Networks, Iizouka, Japan, pp. 13-14.

[104].Das, S. K., Kumar, A., Das, B., Burnwal, A., 2013. On soft computing techniques in various areas. Computer Science & Information Technology. 3, 59-68.

[105].Friedberg, R. M. 1958. A learning machine: Part I. IBM Journal of Research and Development. 2(1), 2-13.

[106].Pratihar, D.K. 2014. Soft Computing: Fundamentals and Applications.Alpha Science International Ltd., Oxford.

[107].Mitchell, T. 1997. Machine Learning, McGraw Hill Education, India.

[108]. Rudolph, S., Tuvshintur, T., Pascal H.. 2008. What is approximate reasoning?. International Conference on Web Reasoning and Rule Systems. Springer Berlin Heidelberg.

[109].Rastrigin, L.A. 1963. The convergence of the random search method in the extremal control of a many parameter system. Automation and Remote Control. 24 (10). 1337-1342.

[110].Zadeh, L.A. 1965. Fuzzy algorithms. Information and Control. Vol. 12, pp. 94-102.

[111].Hassoun, M. 2003. Fundamentals of Artificial Neural Networks. A Bradford Book.

[112].Eiben, A.E., Smith, J.E. 2003. Introduction to Evolutionary Computing. Springer-Verlag, Berlin.

[113].https://en.wikipedia.org/wiki/Structural_engineering#cite_note-1.

[114].Earthquake Engineering Research. 1982. Committee on Earthquake Engineering, Research Commission on Engineering and Technical Systems, National Research Council, National Academy Press, Washington, D.C.

[115].Chandwani, V., Agrawal, V., Nagar, R. 2013. Applications of Soft Computing in Civil Engineering: A Review. International Journal of Computer Applications. 81(10).

[116].Fister, I. et al. 2014. Soft Computing in Earthquake engineering: A short overview. International Journal of Earthquake Engineering and Hazard Mitigation (IREHM). 2.2, 42-48.

[117].Yang, X.-S., Koziel, S., Leifsson, L., 2013, Computational Optimization, Modelling and Simulation: Recent Trends and Challenge, Procedia Computer Science, 18, 855-860

[118].Pontryagin, L.S., Boltyanskii, V.G., Gamkrelidze, R.V., Mishchenko, E. 1962. The mathematical theory of optimal processes (International series of monographs in pure and applied mathematics). Interscience, New York.

[119].Sgambi, L. 2008. Artificial Intelligence: Historical Development and Applications in Civil Engineering Field. Proceedings of 3th International Conference on Bridge Maintenance, Safety and Management (IABMAS08).

[120].Klement, E.P., Slany W., 1997, Fuzzy Logic in Artificial Intelligence, Encyclopedia of Computer Science and Technology, 34 (19), 179-190.

[121].Khayut, B., Fabri, L., Abukhana, M. 2014. Knowledge representation, reasoning and systems thinking under uncertainty. In Computer Modelling and Simulation. UKSim-AMSS 16th International Conference. IEEE. pp. 163-169.

[122].Fazel Zarandi, M. H., Turksen, I. B., Sobhani, J., Ramezanianpour, A. A. 2008. Fuzzy polynomial neural networks for approximation of the compressive strength of concrete. Applied Soft Computing Journal. Vol. 8, no. 1, pp. 488-498.

[123].Doran, B., Yetilmezsoy, K., Murtazaoglu, S. 2015. Application of fuzzy logic approach in predicting the lateral confinement coefficient for RC columns wrapped with CFRP. Engineering Structures. 88, 74-91.

[124].Ozbulut O. E., Hurlebaus, S. 2009. A temperature- and strain-rate-dependent model of NiTi shape memory alloys for seismic control of bridges. Sensors and Smart Structures Technologies for Civil, Mechanical and Aerospace Systems, USA.

[125].Provenzano P., Bontempi F. 2000. Impostazione dell'analisi strutturale in presenza di informazioni imprecise attraverso logica fuzzy. Studies and Researches, Vol. 21, Politecnico di Milano.

[126].Savoia, M. 2002. Structural reliability analysis through fuzzy number approach, with application to stability. Computer and Structures. Vol. 80, No. 12, pp. 1087-1102.

[127].Biondini, F., Bontempi, F., Malerba, P.G. 2004. Fuzzy reliability analysis of concrete structures. Computers and structures. 82(13), 1033-1052.

[128].Biondini F., Bontempi F., Malerba, P.G. 2000. Fuzzy Theory and Genetically-Driven Simulation in the Reliability Assessment of Concrete Structures. Proceedings of 8-th Conference on Probabilistic Mechanics and Structural Reliability, July 24-26, Notre Dame.

[129].Möller, B., Graf, W., Beer, M. 2003. Safety assessment of structures in view of fuzzy randomness. Computers and Structures. 81(15), 1567-1582.

[130].Marano, G. C., Quaranta, G., Mezzina, M. 2008. Fuzzy time-dependent reliability analysis of RC beams subject to pitting corrosion. Journal of Materials in Civil Engineering. 20(9), 578-587.

[131].Dordoni, S., Malerba, P. G., Sgambi, L., Manenti, S. 2010. Fuzzy reliability assessment of bridge piers in presence of scouring. In Proceedings of the Fifth International Conference on Bridge Maintenance. Safety and Management. pp. 11-15.

[132].Nieto-Morote A., Ruz-Vila, F. 2011. A fuzzy approach to construction project risk assessment. International Journal of Project Management. Vol. 29, no. 2, pp. 220–231.

[133].Sobhani J., Ramezanianpour, A. A. 2011. Service life of the reinforced concrete bridge deck in corrosive environments: A soft computing system. Applied Soft Computing Journal. Vol. 11, no. 4, pp. 3333–3346.

[134].Darain, ud, Kh Mahfuz. 2015. Automated serviceability prediction of NSM strengthened structure using a fuzzy logic expert system. Expert Systems with Applications. 42.1, 376-389.

[135].Arfiadi Y. 2000. Optimal passive and active control mechanisms for seismically excited buildings. Doctor of Philosophy Thesis, Faculty of Engineering, University of Wollongong.

[136].Zhou, L., Chang, C.C., Wang, L. X. 2003. Adaptive fuzzy control for nonlinear building-magnetorheological damper system. Journal of Structural Engineering. 129(7), 905-913.

[137].Kim, Y., Hurlebaus, S., Langari, R. 2010. Model-Based Multi-input, Multi-output Supervisory Semi-active Nonlinear Fuzzy Controller. Computer-Aided Civil and Infrastructure Engineering. 25(5), 387-393.

[138].Guclu R., Yazici, H. 2008. Vibration control of a structure with ATMD against earthquake using fuzzy logic controllers. Journal of Sound and Vibration. Vol. 318, no. 1-2, pp. 36-49.

[139].Ozbulut O. E., Hurlebaus, S. 2010. Fuzzy control of piezoelectric friction dampers for seismic protection of smart base isolated buildings. Bulletin of Earthquake Engineering. Vol. 8, n. 6, 2010, pp. 1435-1455.

[140].Meng, Q., Zhang, M., Ye, J. 2011. Fuzzy control strategy based on mode identification Used in semiactive control. Applied Mechanics and Materials. Vol. 71–78, pp. 3975–3982.

[141].Zorić, N. D., Simonović, A. M., Mitrović, Z. S., Stupar, S. N., Obradović, A. M., Lukić, N. S. 2014. Free vibration control of smart composite beams using particle swarm optimized self-tuning fuzzy logic controller. Journal of Sound and Vibration. 333(21), 5244-5268.

[142].Pourzeynali S, Lavasani H.H., Modarayi A.H. 2007. Active control of high rise building structures using fuzzy logic and genetic algorithms. Engineering Structure. 29(3), 346–57.

[143].Uz, Mehmet E., Hadi M.N.S. 2014. Optimal design of semi active control for adjacent buildings connected by MR damper based on integrated fuzzy logic and multi-objective genetic algorithm. Engineering structures. 69, 135-148.

[144].Song, C., Yu, C., Xiao, Y., Zhang, J. 2017. Fuzzy logic control based on genetic algorithm for a multi-source excitations floating raft active vibration isolation system. Advances in Mechanical Engineering. 9(6), 1687814017705843.

[145].Rosko. 2011. Structural topology optimization with fuzzy constraint. In 4th International Conference on Machine Vision (ICMV ʼ11): Computer Vision and Image Analysis; Pattern Recognition and Basic Technologies, vol. 8350 of Proceedings of the SPIE, The International Society for Optical Engineering.

[146].McCelloch, W. S., Pitts, W. 1943. A Logical Calculus of the Idea Immanent in Neural Nets. Bulletin of Mathematical Biophysics. 5, 115-133.

[147].Haykin, S. 2009. Neural Networks A Comprehensive Foundation, 8th Edn., Pearson Prentice Hall, India.

[148].Rumelhart, D. E., McClelland, J. L., PDP Research Group. 1987. Parallel distributed processing. Cambridge, MA, USA. MIT press. Vol. 1, p. 184.

[149].Williams, R.J. 2008. A learning algorithm for continually running fully recurrent neural networks, Neural Computation, MIT Press. Vol. 1 n. 2, pp. 270-280.

[150].Ji, T., Lin, T., Lin, X. 2006. Concrete mix proportion design algorithm based on artificial neural networks. Cement and Concrete Research. 36(7), 1399-1408.

[151].Naderpour, H., Kheyroddin, A., Ghodrati Amiri, G. 2010. Prediction of FRP – Confined compressive concrete using artificial networks. Composite Structures. 92(12), 2817-2829.

[152].Abdollahzadeh, A., Masoudnia, R., Aghababaei, S. 2011. Predict strength of rubberized concrete using artificial neural network. WSEAS Transactions on Computers. 10(2), 31–40.

[153].Uysal, M., Tanyildizi, H. 2012. Estimation of compressive strength of self-compacting concrete containing polypropylene fibre and mineral additives

exposed to high temperature using artificial neural network. Construction and Building Materials. 27(1), 404–414.

[154].Duan, Z. H., Kou, S. C., Poon, C. S. 2013. Prediction of compressive strength of recycled aggregate concrete using artificial neural networks. Construction and Building Materials. 40, 1200–1206.

[155].Bal, L., Buyle-Bodin, F. (2013). Artificial neural network for predicting drying shrinkage of concrete. Construction and Building Materials. 38, 248–254.

[156].Ni, H. G., Wang, J. Z. 2000. Prediction of compressive strength of concrete by neural networks. Cement and Concrete Research. 30(8), 1245-1250.

[157].Oreta, A.W.C., Kawashima, K. 2003. Neural Network Modeling of Confined Compressive Strength and strain of Circular Concrete Columns. Journal of Structural Engineering. 129(4), 554-561.

[158].Gupta, R., Kewalramani, M. Goel, A. 2006. Prediction of Concrete Strength using Neural-Expert System. Journal of Materials in Civil Engineering. 18(3), 462-466.

[159].Ozturan, M., Birgul, K. Ozturan, T. 2008. Comparison of Concrete Strength Prediction Techniques with Artificial Neural Network Approach. Building Research Journal. 56(1), 23-36.

[160].Aggarwal, Y. and Aggarwal, P. 2011. Prediction of Compressive Strength of SCC containing Bottom Ash using Artificial Neural Network. World Academy of Science, Engineering and Technology, 53, 735-740.

[161].Pham, T. M., Hadi, M. N. 2014. Predicting stress and strain of FRP-confined square/rectangular columns using artificial neural networks. Journal of Composites for Construction. 18(6), 04014019.

[162].Nikoo, M., Torabian Moghadam, F., Sadowski, Ł. 2015. Prediction of concrete compressive strength by evolutionary artificial neural networks. Advances in Materials Science and Engineering.

[163].Demir, F. 2008. Prediction of elastic modulus of normal and high strength concrete by artificial neural networks. Construction and Building Materials. 22(7), 1428-1435.

[164].Parichatprecha, R., Nimityonskul, P. 2009. Analysis of durability of high performance concrete using artificial neural networks. Construction and Building Materials. 23(2), 910-917.

[165].Chandwani, V., Agrawal, V., Nagar, R. 2015. Modeling slump of ready mix concrete using genetic algorithms assisted training of Artificial Neural Networks. Expert Systems with Applications. 42(2), 885-893.

[166].Sanad, A. Saka, M. 2001. Prediction of Ultimate Shear Strength of Reinforced-Concrete Deep Beams Using Neural Networks, Journal of Structural Engineering. 127(7), 818–828.

[167].Cladera, A., Mari, A.R. 2004. Shear design procedure for reinforced normal and high-strength concrete beams using artificial neural networks Part I: beams without stirrups,. Engineering Structures. 26, 917-926.

[168].Cladera, A. Mari, A.R. 2004. Shear design procedure for reinforced normal and high-strength concrete beams using artificial neural networks Part II: beams with stirrups, Engineering Structures. 26, 927-936.

[169].Lee, S., C. Lee. 2014. Prediction of shear strength of FRP-reinforced concrete flexural members without stirrups using artificial neural networks. Engineering structures. 61, 99-112.

[170].Pendharkar, U., Chaudhary, S. Nagpal, A.K. 2007. Neural network for bending moment in continuous composite beams considering cracking and time effects in concrete. Engineering Structures. 29(9), 2069-2079.

[171].Bagci, M. 2010. Neural Network Model for Moment- Curvature relationship of Reinforced Concrete sections. Mathematical and Computational Applications. 15(1), 66-78.

[172].Erdem, H. 2010. Prediction of the moment capacity of reinforced concrete slabs in fire using artificial neural networks. Advances in Engineering Software. 41(2), 270-276.

[173].Jasim, N.A. Mohammed, M.Y. 2011. Prediction of Ultimate Torsional Strength of Spandrel beams using Artificial Neural Networks. Basrah Journal for Engineering Science. 11(1), 88-100.

[174].Ghaboussi, J., Elnashai, A.S. 2007. Development of neural network based hysteretic models for steel beam column connections through self-learning simulation. Journal of Earthquake Engineering. 11, 453-467.

[175].Alacalı, S. N., Akbaş, B., Doran, B. 2011. Prediction of lateral confinement coefficient in reinforced concrete columns using neural network simulation. Applied Soft Computing, 11(2), 2645-2655.

[176].Jakubek, M. 2012. Neural network prediction of load capacity for eccentrically loaded reinforced concrete columns. Computer Assisted Methods in Engineering and Science. 19, 339-349.

[177].Asteris, P. G., Tsaris, A. K., Cavaleri, L., Repapis, C. C., Papalou, A., Di Trapani, F., Karypidis, D. F. 2016. Prediction of the fundamental period of infilled RC frame structures using artificial neural networks. Computational intelligence and neuroscience.

[178].Chou, J. S., Ngo, N. T., Chong, W. K. 2017. The use of artificial intelligence combiners for modeling steel pitting risk and corrosion rate. Engineering Applications of Artificial Intelligence. 65, 471-483.

[179].Papadrakakis, M., Papadopoulos, V., Lagaros, N. D. 1996. Structural reliability analyis of elastic-plastic structures using neural networks and Monte Carlo simulation. Computer methods in applied mechanics and engineering. 136(1-2), 145-163.

[180].Hurtado, J. E., Alvarez, D. A. 2001. Neural-network-based reliability analysis: a comparative study. Computer methods in applied mechanics and engineering. 191(1), 113-132.

[181].Rogers, J. L. 1994. Simulating structural analysis with neural network. Journal of Computing in Civil Engineering, 8(2), 252-265.

[182].Tsompanakis, Y., Lagaros, N. D., Stavroulakis, G. E. 2008. Soft computing techniques in parameter identification and probabilistic seismic analysis of structures. Advances in Engineering Software. 39(7), 612-624.

[183].Arslan, H.M. 2010. An evaluation of effective design parameters on the earthquake performance of RC buildings using neural networks. Engineering Structures. 32, 1888-1898.

[184].Liu, G. R., Xu, Y. G., Wu, Z. P. 2001. Total solution for structural mechanics problems. Computer methods in applied mechanics and engineering. 191(8), 989-1012.

[185].Zacharias, J., Hartmann, C., Delgado, A. 2004. Damage detection on crates of beverages by artificial neural networks trained with finite-element data. Computer methods in applied mechanics and engineering. 193(6), 561-574.

[186].Parhi, D. R., Dash, A. K. 2011. Application of neural network and finite element for condition monitoring of structures. Proceedings of the Institution of Mechanical Engineers, Part C: Journal of Mechanical Engineering Science. 225(6), 1329-1339.

[187].Li, J., Dackermann, U., Xu, Y. L., Samali, B. 2011. Damage identification in civil engineering structures utilizing PCA-compressed residual frequency response functions and neural network ensembles. Structural Control and Health Monitoring. 18(2), 207-226.

[188].Meruane, V., J. Mahu. 2014. Real-time structural damage assessment using artificial neural networks and anti-resonant frequencies. Shock and Vibration.

[189].Hakim, S. J. S., Razak, H. A., Ravanfar, S. A. 2015. Fault diagnosis on beam-like structures from modal parameters using artificial neural networks. Measurement. 76, 45-61.

[190].Arangio, S., Bontempi, F. 2010. Soft computing based multilevel strategy for bridge integrity monitoring. Computer-Aided Civil and Infrastructure Engineering. 25(5), 348-362.

[191].Arangio, S., Bontempi, F. 2015. Structural health monitoring of a cable-stayed bridge with Bayesian neural networks. Structure and Infrastructure Engineering. 11(4), 575-587.

[192].Adeli, H., Park, H. S. 1995. Optimization of space structures by neural dynamics. Neural networks. 8(5), 769-781.

[193].Zhang, L., Subbarayan, G. 2002. An evaluation of back-propagation neural networks for the optimal design of structural systems: Part II. Numerical evaluation. Computer Methods in Applied Mechanics and Engineering. 191(25), 2887-2904.

[194].Park, H. S., Adeli, H. 1995. A neural dynamics model for structural optimization-application to plastic design of structures. Computers and structures. 57(3), 391-399.

[195].Mukherjee, A., Despande, J.M. 1995. Modeling Initial design process using Artificial Neural Networks. Journal of Computing in Civil Engineering. 9(3), 194- 200.

[196].Yeh, I. C. 1999. Design of high-performance concrete mixture using neural networks and nonlinear programming. Journal of Computing in Civil Engineering. 13(1), 36-42.

[197].Hadi, M.N.S. 2003. Neural Network applications in Concrete Structures. Computers and structures. 81(6), 373-381.

[198].Hajela, P., Berke, L. 1991. Neurobiological computational models in structural analysis and design. Computers and Structures. 41(4), 657-667.

[199].Papadrakakis, M., Lagaros, N.D. 2002. Reliability-based structural optimization using neural networks and Monte Carlo simulation. Computer methods in applied mechanics and engineering. 191(32), 3491-3507.

[200].Ahmadkhanlou, F., Adeli, H. 2005. Optimum cost design of reinforced concrete slabs using neural dynamics model. Engineering Applications of Artificial Intelligence. 18, 65-72.

[201].Papadrakakis, M., Lagaros, N. D., Plevris, V. 2005. Design optimization of steel structures considering uncertainties. Engineering Structures. 27(9), 1408-1418.

[202].Cho, H.C., Fadali, M.S., Saiidi, S.M., Soon, L.K. 2005. Neural network active control of structures with earthquake excitation. International Journal of Control, Automation and Systems. 3(2), 202-210.

[203].Gu, Z. Q., Oyadiji, S. O. 2008. Diagonal recurrent neural networks for MDOF structural vibration control. Journal of Vibration and Acoustics. 130(6), 061001.

[204].Narasimhan, S. 2009. Robust direct adaptive controller for the nonlinear highway bridge benchmark. Structural Control and Health Monitoring. 16(6), 599-612.

[205].Laflamme, S., Connor, J. J. 2009. Application of self-tuning Gaussian networks for control of civil structures equipped with magnetorheological dampers. Society of Photo-Optical Instrumentation Engineers.

[206].Wang, N., Adeli, H. 2015. Self-constructing wavelet neural network algorithm for nonlinear control of large structures. Engineering Applications of Artificial Intelligence. 41, 249-258.

[207].Abdeljaber, O., Avci, O., Inman, D. J. 2016. Active vibration control of flexible cantilever plates using piezoelectric materials and artificial neural networks. Journal of sound and vibration. 363, 33-53.

[208].Turing, A.M. 1948. Intelligent machinery. Technical report, National Physical Laboratory, Teddington, England.

[209].Turing, A.M. 1969. Machine Intelligence 5. Edition Meltzer, B. & Michie, D. Edinburgh Univ. Press.

[210].Fogel, D.B. 1995. Evolutionary Computation: Toward a New Philosophy of Machine Intelligence. Piscataway, NJ: IEEE Press.

[211].Luke, S. 2000. Issues in scaling genetic programming: breeding strategies, tree generation, and code bloat (Doctoral dissertation, research directed by Dept. of Computer Science. University of Maryland, College Park).

[212].Blum, C., Li, X. 2008. Swarm intelligence in optimization. In Swarm Intelligence. Springer Berlin Heidelberg. pp. 43-85.

[213].Eiben, A. E., Smith, J. E. 2003. Introduction to evolutionary computing. Heidelberg: springer. Vol. 53.

[214].Zhou, M., Pagaldipti, N., Thomas, H. L., Shyy, Y. K. 2004. An integrated approach to topology, sizing, and shape optimization. Structural and Multidisciplinary Optimization. 26(5), 308-317.

[215].Kawohl, B., Pironneau, O., Tartar, L., Zolesio, J.-P. 2000. Optimal shape design. Berlin New York Heidelberg: Springer-Verlag.

[216].Allaire, G., Henrot, A. 2001. On some recent advances in shape optimization. Comptes Rendus de l'Académie des Sciences-Series IIB-Mechanics. 329(5), 383-396.

[217].Bendsøe, M. P., Sigmund, O. 2003. Topology optimization: theory, methods and applications. Springer-Verlag.

[218].Beni, G., Wang, J., 1989. Swarm intelligence. Proceedings of the Seventh Annual Meeting of the Robotics Society of Japan. RSJ Press, Tokyo, pp. 425–428.

[219].Kennedy, J., Eberhart, R. C. 1995. Particle swarm optimization, Proceedings of IEEE International Conference on Neural Networks (ICNN), Perth, Australia. Vol. IV, pp.1942-1948.

[220].Karaboga, D., Basturk, B. 2007. A powerful and efficient algorithm for numerical function optimization: artificial bee colony (ABC) algorithm. Journal of global optimization. 39(3), 459-471.

[221].X.-S.Yang, Firefly Algorithm. In X.-S. Yang, Nature-Inspired Metaheuristic Algorithms, Luniver Press, London, UK, 2008, pp. 79-90.

[222].Fister, I., Fister Jr, I., Yang, X. S., Brest, J. 2013. A comprehensive review of firefly algorithms. Swarm and Evolutionary Computation. 13, 34-46.

[223].Geem, Z. W. 2010. Recent advances in harmony search algorithm. Springer-Verlag, Berlin. Vol. 270.

[224].Dorigo, M., Di Caro, G. 1999. The Ant Colony Optimization Metaheuristic. In Corne, D. Dorigo, M., Glover, F. New Ideas in Optimization, McGraw Hill, London, UK, pp. 11-32.

[225].Poli, R., Kennedy, J.,Blackwell, T. 2007. Particle swarm optimization: An overview: Swarm Intelligence. 1, 33–57.

[226].Quaranta, G., Monti, G., Marano, G. C. 2010. Parameters identification of Van der Pol–Duffing oscillators via particle swarm optimization and differential evolution. Mechanical Systems and Signal Processing. 24(7), 2076-2095.

[227].Quaranta, G., Marano, G. C., Greco, R., Monti, G. 2014. Parametric identification of seismic isolators using differential evolution and particle swarm optimization. Applied Soft Computing. 22, 458-464.

[228].Coello, C. A. C., Pulido, G. T., Lechuga, M. S. 2004. Handling multiple objectives with particle swarm optimization. IEEE Transactions on evolutionary computation. 8(3), 256-279.

[229].Perera, R., Sevillano, E., Arteaga, A., De Diego, A. 2014. Identification of intermediate debonding damage in FRP-plated RC beams based on multi-objective particle swarm optimization without updated baseline model. Composites Part B: Engineering. 62, 205-217.

[230].Zhang, X., Gao, R. X., Yan, R., Chen, X., Sun, C., Yang, Z. 2016. Multivariable wavelet finite element-based vibration model for quantitative crack identification by using particle swarm optimization. Journal of Sound and Vibration. 375, 200-216.

[231].Chatterjee, S., Sarkar, S., Hore, S., Dey, N., Ashour, A. S., Balas, V. E. 2017. Particle swarm optimization trained neural network for structural failure prediction of multistoried RC buildings. Neural Computing and Applications. 28(8), 2005-2016.

[232].Perez, R. E., Behdinan, K. 2007. Particle swarm approach for structural design optimization. Computers and Structures. 85(19), 1579-1588.

[233].Salajegheh, E., Gholizadeh, S., Khatibinia, M. 2008. Optimal design of structures for earthquake loads by a hybrid RBF-BPSO method. Earthquake Engineering and Engineering Vibration. 7(1), 13-24.

[234].Plevris, V., Papadrakakis, M. 2011. A hybrid particle swarm-gradient algorithm for global structural optimization. Computer-Aided Civil and Infrastructure Engineering. 26(1), 48-68.

[235].Behbahan, I. 2012. Design Optimization of RC Frames under Earthquake Loads. International Journal of Optimization in Civil Engineering. 2(4), 459-477.

[236].Gholizadeh, S., Salajegheh, E. 2009. Optimal design of structures subjected to time history loading by swarm intelligence and an advanced metamodel. Computer Methods in Applied Mechanics and Engineering. 198(37), 2936-2949.

[237].Gholizadeh, S., Moghadas, R. K. 2014. Performance-based optimum design of steel frames by an improved quantum particle swarm optimization. Advances in Structural Engineering. 17(2), 143-156.

[238].Fourie, P. C., Groenwold, A. A. 2000. Particle swarms in size and shape optimization. In Proceedings of the international workshop on multidisciplinary design optimization, Pretoria, South Africa. pp. 97-106.

[239].Fourie, P. C., Groenwold, A. A. 2002. The particle swarm optimization algorithm in size and shape optimization. Structural and Multidisciplinary Optimization. 23(4), 259-267.

[240].Camp, C. V., Meyer, B. J., Palazolo, P. J. 2004. Particle swarm optimization for the design of trusses. In Structures 2004: Building on the Past, Securing the Future. pp. 1-10.

[241].Li, L. J., Huang, Z. B., Liu, F. 2009. A heuristic particle swarm optimization method for truss structures with discrete variables. Computers and Structures. 87(7), 435-443.

[242].Dimou, C. K., Koumousis, V. K. 2009. Reliability-based optimal design of truss structures using particle swarm optimization. Journal of Computing in Civil Engineering. 23(2), 100-109.

[243].Kaveh, A., Talatahari, S. 2009. A particle swarm ant colony optimization for truss structures with discrete variables. Journal of Constructional Steel Research. 65(8), 1558-1568.

[244].de Oliveira, C. J. P., Gomes, H. M. 2010. A particle swarm optimization algorithm for truss optimization on shape and size with dynamic constraints. In 2nd international conference on engineering optimization, Lisbon, Portugal.

[245].Zeng, S.K., Li, L.J. 2012. Particle Swarm-Group Search algorithm and its application to spatial structural design with discrete variables. International Journal of Optimization in Civil Engineering. 2(4):443-458.

[246].Felkner, J., Chatzi, E., Kotnik, T. 2013. Interactive particle swarm optimization for the architectural design of truss structures. In Computational Intelligence for Engineering Solutions. IEEE Symposium on (pp. 15-22).

[247].Kaveh, A., Javadi, S. M. 2014. Shape and size optimization of trusses with multiple frequency constraints using harmony search and ray optimizer for enhancing the particle swarm optimization algorithm. Acta Mechanica. 225(6), 1595-1605.

[248].Leung, A. Y., Zhang, H., Cheng, C. C., Lee, Y. Y. 2008. Particle swarm optimization of TMD by non-stationary base excitation during earthquake. Earthquake Engineering and Structural Dynamics. 37(9), 1223-1246.

[249].Shayeghi, H., Kalasar, H. E., Shayanfar, H. A., Shayeghi, A. 2009. PSO Based TMD Design for Vibration Control of Tall Building Structures. In IC-AI. pp. 273-279.

[250].Ali, S. F., Ramaswamy, A. 2009. Optimal fuzzy logic control for MDOF structural systems using evolutionary algorithms. Engineering Applications of Artificial Intelligence. 22(3), 407-419.

[251].Schmidt, A. 2010. The Design of an Active Structural Vibration Reduction System Using a Modified Particle Swarm Optimization. In ANTS Conference. pp. 544-551.

[252].Marinaki, M., Marinakis, Y., Stavroulakis, G. E. 2010. Fuzzy control optimized by PSO for vibration suppression of beams. Control Engineering Practice. 18(6), 618-629.

[253].Raju, V., Maheswari, D., Patnaik, S. K. 2012. Active vibration control of piezo actuated cantilever beam using PSO. In Electrical, Electronics and Computer Science (SCEECS), IEEE Students' Conference. pp. 1-5.

[254].Sorkhabi, R. V., Naseri, A., Naseri, M. 2014. Optimization of the Castellated Beams by Particle Swarm Algorithms Method. APCBEE Procedia. 9, 381-387.

[255].Loja, M. A. 2014. On the use of particle swarm optimization to maximize bending stiffness of functionally graded structures. Journal of Symbolic Computation. 61, 12-30.

[256].Darwin, C. 1859. The origin of species by means of natural selection. Murray. J. London.

[257].Holland, J. H. 1975. Adaptation in natural and artificial systems. Ann Arbor, University of Michigan Press. Michigan.

[258].Schwefel, H.P. 1965. Kybernetische Evolution als Strategie der experimentelen Forschung in der Stromungstechnik. Master's thesis, Hermann Föttinger Institute for Hydrodynamics, Technical University of Berlin.

[259].Fogel, L.J., Owens, A.J., Walsh, M.J. 1966. Artificial Intelligence through simulated evolution. Chichester, UK: John Wiley.

[260].Koza, J. R. 1992. Genetic programming: on the programming of computers by means of natural selection. Cambridge, Mass. MIT Press.

[261].Storn, R., Price, K. 1997. Differential evolution–a simple and efficient heuristic for global optimization over continuous spaces. Journal of global optimization. 11(4), 341-359.

[262].Marano, G. C., Quaranta, G., Monti, G. 2011. Modified genetic algorithm for the dynamic identification of structural systems using incomplete measurements. Computer-Aided Civil and Infrastructure Engineering. 26(2), 92-110.

[263].Chisari, C., Bedon, C., Amadio, C. 2015. Dynamic and static identification of base-isolated bridges using Genetic Algorithms. Engineering Structures. 102, 80-92.

[264].Chisari, C., Macorini, L., Amadio, C., Izzuddin, B. A. 2017. Optimal sensor placement for structural parameter identification. Structural and Multidisciplinary Optimization. 55(2), 647-662.

[265].Chisari, C., Francavilla, A. B., Latour, M., Piluso, V., Rizzano, G., Amadio, C. 2017. Critical issues in parameter calibration of cyclic models for steel members. Engineering Structures. 132, 123-138.

[266].Sgambi, L., Gkoumas, K., Bontempi, F. 2012. Genetic Algorithms for the Dependability Assurance in the Design of a Long-Span Suspension Bridge. Computer-Aided Civil and Infrastructure Engineering. 27(9), 655-675.

[267].Cha, Y. J., Buyukozturk, O. 2015. Structural damage detection using modal strain energy and hybrid multiobjective optimization. Computer-Aided Civil and Infrastructure Engineering. 30(5), 347-358.

[268].Silva, M., Santos, A., Figueiredo, E., Santos, R., Sales, C., Costa, J. C. 2016. A novel unsupervised approach based on a genetic algorithm for structural damage detection in bridges. Engineering Applications of Artificial Intelligence. 52, 168-180.

[269].Goldberg, D.E., Samtani, M.P. 1986. Engineering optimization via genetic algorithm. Proceedings 9th Conference on Electronic Computation, ASCE, 471-482.

[270].Rajeev, S., Krishnamoorthy, C. S. 1992. Discrete optimization of structures using genetic algorithms. Journal of structural engineering. 118(5), 1233-1250.

[271].Azid, I. A., Kwan, A. S. K., Seetharamm, K. N. 2002. An evolutionary approach for layout optimization of a three-dimensional truss. Structural and Multidisciplinary Optimization. 24(4), 333–337.

[272].Woon, S. Y., Querin, O. M., Steven, G. P. 2001. Structural application of a shape optimization method based on a genetic algorithm. Structural and Multidisciplinary Optimization. 22(1), 57-64.

[273].Lagaros, N. D., Papadrakakis, M., Kokossalakis, G. 2002. Structural optimization using evolutionary algorithms. Computers and structures. 80(7), 571-589.

[274].Pezeshk, S., Camp, C. V. 2002. State of the art on the use of genetic algorithms in design of steel structures. In S. Burns (Ed.), Recent Advances in Optimal Structural Design. Reston, VA: American Society of Civil Engineers. 55-80.

[275].Deb, K. 1991. Optimal design of a welded beam via genetic algorithms. AIAA journal. 29(11), 2013-2015.

[276].Chau, K. W., Albermani, F. 2002. Genetic algorithms for design of liquid retaining structure. International Conference on Industrial, Engineering and Other Applications of Applied Intelligent Systems. Springer, Berlin, Heidelberg. pp. 119-128.

[277].Jarmai, K., Snyman, J. A., Farkas, J., Gondos, G. 2003. Optimal design of a welded I-section frame using four conceptually different optimization algorithms. Structural and Multidisciplinary Optimization. 25, 54–61.

[278].Fu, K. C., Zhai, Y., Zhou, S. 2005. Optimum design of welded steel plate girder bridges using a genetic algorithm with elitism. Journal of Bridge Engineering. 10(3), 291-301.

[279].Senouci, A. B., Al-Ansari, M. S. 2009. Cost optimization of composite beams using genetic algorithms. Advances in Engineering Software. 40(11), 1112-1118.

[280].Kociecki, M., Adeli, H. 2014. Two-phase genetic algorithm for topology optimization of free-form steel space-frame roof structures with complex curvatures. Engineering Applications of Artificial Intelligence, 32, 218-227.

[281].Kociecki, M., Adeli, H. 2015. Shape optimization of free-form steel space-frame roof structures with complex geometries using evolutionary computing. Engineering Applications of Artificial Intelligence. 38, 168-182.

[282].Jenkins, W. M. 1992. Plane frame optimum design environment based on genetic algorithm. Journal of Structural Engineering. 118(11), 3103-3112.

[283].Koumousis, V. K., Arsenis, S. J. 1994. Genetic algorithms in a multi-criterion optimal detailing of reinforced concrete members.

[284].Sarma, K. C., Adeli, H. 1998. Cost optimization of concrete structures. Journal of structural engineering. 124(5), 570-578.

[285].Camp, C. V., Pezeshk, S., Hansson, H. 2003. Flexural design of reinforced concrete frames using a genetic algorithm. Journal of Structural Engineering. 129(1), 105-115.

[286].Noguchi, T., Maruyama, I., Kanematsu, M. 2003. Performance based design system for concrete mixture with multi-optimizing genetic algorithm. In Proceedings of the 11th International Congress on the Chemistry of Cement, Durban.

[287].Amirjanov, A., Sobolev, K. 2005. Optimal proportioning of concrete aggregates using a self-adaptive genetic algorithm. Computers and Concrete. 2(5), 411-421.

[288].Xie, X. S., Yan, D. J., Zheng, Y. Z. 2011. Optimization Design of High-Performance Concrete Based on Genetic Algorithm Toolbox of Matlab. In Advanced Materials Research Trans Tech Publications. Vol. 250, pp. 2672-2677.

[289].Rahman, M., Jumaat, M. Z. 2012. Cost minimum proportioning of Non-Slump concrete mix using Genetic Algorithms. In Advanced Materials Research. Trans Tech Publications. Vol. 468, pp. 50-54.

[290].Aydın, Z., Ayvaz, Y. 2013. Overall cost optimization of pre-stressed concrete bridge using genetic algorithm. KSCE Journal of Civil Engineering. 17(4), 769-776.

[291].Sgambi, L., Gkoumas, K., Bontempi, F. 2014. Genetic algorithm optimization of precast hollow core slabs.

[292].Kim, Y. J., Ghaboussi, J. 2001. Direct use of design criteria in genetic algorithm‐based controller optimization. Earthquake engineering and structural dynamics. 30(9), 1261-1278.

[293].Wongprasert, N., Symans, M. D. 2004. Application of a genetic algorithm for optimal damper distribution within the nonlinear seismic benchmark building. Journal of Engineering Mechanics. 130(4), 401-406.

[294].Hejazi, F., Toloue, I., Jaafar, M. S., Noorzaei, J. 2013. Optimization of earthquake energy dissipation system by genetic algorithm. Computer‐Aided Civil and Infrastructure Engineering. 28(10), 796-810.

[295].Xu, C., Lin, S., Yang, Y. 2015. Optimal design of viscoelastic damping structures using layerwise finite element analysis and multi-objective genetic algorithm. Computers and Structures. 157, 1-8.

[296].Greco, R., Marano, G.C. 2016. Multi-objective optimization of a dissipative connection for seismic protection of wall-frame structures. Soil Dynamics and Earthquake Engineering. 87, 151-163.

[297].Greco, R., Marano, G. C., Fiore, A. 2016. Performance–cost optimization of tuned mass damper under low‐moderate seismic actions. The Structural Design of Tall and Special Buildings. 25(18), 1103-1122.

[298].Poh'Sie, G. H., Chisari, C., Rinaldin, G., Amadio, C., Fragiacomo, M. 2016. Optimal design of tuned mass dampers for a multi‐storey cross laminated timber building against seismic loads. Earthquake Engineering & Structural Dynamics. 45(12), 1977-1995.

[299].Asadi, E., da Silva, M. G., Antunes, C. H., Dias, L., Glicksman, L. 2014. Multi-objective optimization for building retrofit: A model using genetic algorithm and artificial neural network and an application. Energy and Buildings. 81, 444-456.

[300].Rodriguez, M., Park, R. 1991. Repair and strengthening of reinforced concrete buildings for seismic resistance. Earthquake Spectra, 7(3), 439-459..

[301].Ireland, M. G., Pampanin, S., Bull, D. 2007. Experimental investigations of a selective weakening approach for the seismic retrofit of rc walls.

[302].Kunisue, A., Koshika, N., Kurokawa, Y., Suzuki, N., Agami J., Sakamoto M. 2000. Retrofitting method of existing reinforced concrete buildings using elasto-plastic steel dampers, Proceedings of the twelfth World Conference on Earthquake Engineering (12WCEE), Paper 0648;

[303].Chisari, C., Bedon, C. 2017. Performance-based design of FRP retrofitting of existing RC frames by means of multi-objective optimisation. Bollettino di Geofisica Teorica ed Applicata, 58(4).

[304].Paya I., Yepes V., Gonzalez-Vidosa F., Hospitaler A. 2008. Multiobjective Optimization of Concrete Frames by Simulated Annealing, Computer-Aided Civil and Infrastructure Engineering 23 (2008) 596–610.

[305].Lee D.-C., Oh B.-K., Choi S.-W., Park H.-S. 2011. Multi-Objective Optimization for Performance-based Seismic Retrofit using Connection Upgrade, World Academy of Science, Engineering and Technology, 59, 1174-1179.

[306].Grosan, C., Abraham, A. 2007. Intelligent data analysis using multiple criteria decision making, IADIS European Conference Data Mining, Lisbon, Portugal, pp. 89-94.

[307].Wilkinson S., Ying F.J. 2007. The application of life-cycle costing for building retrofit, Proceedings of the CIB World Building Congress "Construction for Development", 14-17 May 2007, Cape Town, South Africa.

[308].FEMA 156 .1994. Typical Costs for Seismic Rehabilitation of Existing Buildings. Vol 1: Summary (Second Edition).

[309].Brandt, A. M. (Ed.). (1987). Criteria and methods of structural optimization (Vol. 1). Springer Science & Business Media.

[310].Chibani, L. 1989. Optimum Design of Structures. With Special Reference to Alternative Loads Using Geometric Programming. Berlin etc., Springer-Verlag.

[311].Box, M.J., Davies, D. Swann, W.H.; 196. Non-linear optimization techniques. In: Oliver and Boyd (Eds), Imperial Chemical Industries Monograph, Edinburgh, United Kingdom, 68 pp.

[312].Byrd, R. H., Schnabel, R. B., Shultz, G. A. 1987. A trust region algorithm for nonlinearly constrained optimization. SIAM Journal on Numerical Analysis, 24(5), 1152-1170.

[313].Wetter M. GenOpt, generic optimization program – user manual, version 3.0.0. Technical report LBNL-5419. Lawrence Berkeley National Laboratory;2009.

[314].Nguyen, A. T., Reiter, S., Rigo, P. 2014. A review on simulation-based optimization methods applied to building performance analysis. Applied Energy, 113, 1043-1058.

[315].Goldberg, D.E. 1989. Genetic algorithms in search, optimization and machine learning. Addison-Wesley Publishing Company Inc., New York, NY, USA, 432 pp.

[316].Goldberg, D.E., Korb, B., Deb, K. 1989. Messy genetic algorithms: motivation, analysis, and first results. Complex Systems, 3(5), 493-530.

[317].McKenna, F., Fenves, G. L., Scott, M. H. 2000. Open system for earthquake engineering simulation. University of California, Berkeley, CA.

[318].Mazzoni, S., McKenna, G.L, Scott, M.H, Fenves, G.L., et al. 2004. "OpenSees System for Earthquake Engineering Simulation User Manual", (http://peer.berkeley.edu/~silvia/OpenSees/examplesprimer/html/).

[319].Kaul, R and Deierlein, G. 2001. "An OpenSees Editor – TclEditor", (http://opensees.berkeley.edu/OpenSees/accessories.html).

[320].Moler, C. 2004. The origins of Matlab. Cleve's Corner (in the Mathworks Newsletter).

[321].King, J.T. 1998. "MATLAB Tutorial" accessed on July 25, 2004, Cincinnati, http://math.uc.edu/~kingjt/matlab/tutorial_v4.html

[322].Jenkins, W.M. 1991. Towards structural optimization via the genetic algorithm. Computers & Structures, 40(5), 1321-1327.

[323].Jenkins, W.M. 1991. Structural optimization with the genetic algorithm. The Structural Engineer, 69(24), 418-422.

[324].Reeves, C. R. 1993. Modern heuristic techniques for combinatorial problems. John Wiley & Sons, Inc.

[325].Hajela, P. 1993. Stochastic search in structural optimization: genetic algorithms and simulated annealing. Progress in astronautics and aeronautics, 150, 611-611.

[326].Biondini, F. 1999. Optimal limit state design of concrete structures using genetic algorithms. Studi e Ricerche, 1-30.

[327]. Gutowski, M. W. (2005). Biology, physics, small worlds and genetic algorithms. Leading Edge Computer Science Research, Nova Science Publishers, Inc. p, 165-218.

[328].Grefenstette, J. J. 1987. Incorporating Problem Specific Knowledge into Genetic Algorithms, in Genetic Algorithms and Simulated Annealing, pp. 42-60, L. Davis (Ed.), Morgan Kaufmann.

[329].D. Whitley, K. Mathias and P. Fitzhorn, 1991. Delta Coding: An Iterative Search Strategy for Genetic Algorithms. Proceeding in ICGA 4, pp. 77-84, 1991.

[330].Shubhra S.R., Sanghamitra B, Sankar K.P.. 2007. Genetic operators for combinatorial optimization in TSP and microarray gene ordering", Journal of Applied Intelligence, Kluwer Academic Publishers, Volume 26 Issue 3, pp.183 - 195.

[331].Dhavachelvan, P., Uma, G. V. 2005. Multi-agent-based integrated framework for intra-class testing of object-oriented software. Applied Soft Computing, 5(2), 205-222.

[332].Rong Yang. 1997. Solving Large Travelling Salesman Problems with Small Populations. Genetic Algorithms in Engineering Systems. Innovations and Applications, Conference Publication No. 446, 2-, pp.157-162.

[333].Yugay, O., Kim, I., Kim, B., Ko, F. I. 2008. Hybrid genetic algorithm for solving traveling salesman problem with sorted population. In Convergence and Hybrid Information Technology. ICCIT'08. Third International Conference on (Vol. 2, pp. 1024-1028). IEEE.

[334].Kent, D. C., Park, R. 1971. Flexural members with confined concrete. Journal of the Structural Division, 97(7): 1969-1990.

[335].Karsan, I. D., Jirsa, J. O. 1969. Behavior of concrete under compressive loading, Journal of Structural Division ASCE, Vol. 95.

[336].Taucer, F., Spacone, E., Filippou, F. C. 1991. A fiber beam-column element for seismic response analysis of reinforced concrete structures (Vol. 91, No. 17). Berkekey, California: Earthquake Engineering Research Center, College of Engineering, University of California.

[337].Neuenhofer, A., Filippou, F. C. 1997. Evaluation of nonlinear frame finite-element models. Journal of structural engineering, 123(7), 958-966.

[338].European Standard EN (Eurocode 3) 1993-1-1:2005, Design of steel structures, Part 1-1: General rules and rules for buildings. European Committee for Standardization (CEN), Bruxelles, 2005.

[339].Panagiotakos, T. B., Fardis, M. N. 2001. Deformations of reinforced concrete members at yielding and ultimate. Structural Journal, 98(2), 135-148.

[340].B.U.R.C., Bollettino Ufficiale della Regione Campania n.359 del 13.07.2016. "L.R. del 27 febbraio 2007, n.3 - Prezziario Regionale dei Lavori Pubblici anno 2016" (in Italian).

[341].Viggiani, C. 1993. Fondazioni. Cooperativa Universitaria Editrice Napoletana (in Italian).

[342].Coello, C. A. C., Carlos, A. 1999. A survey of constraint handling techniques used with evolutionary algorithms. Lania-RI-99-04, Laboratorio Nacional de Informática Avanzada.

[343].Coello, C.A.C. 2002. Theoretical and numerical constraint-handling techniques used with evolutionary algorithms: A survey of the state of the art, Computer Methods in Applied Mechanics and Engineering, 191, 1245-1287.

[344].Michalewicz, Z. 1995. Survey of constraint handling techniques in evolutionary computation methods, Proceedings of the 4th Annual Conference on Evolutionary Programming, 135-155.

[345].Michalewicz, Z., Fogel, D.B. 2000. How to solve it: Modern Heuristics, Springer Verlag, Berlin.

[346].Michalewicz, Z., Janikow, C.Z. 1993. Handling constraints in genetic algorithms, Proceedings of the Fourth International Conference on Genetic Algorithms, Morgan Kaufmann, 151-157.

[347].Back, T., Hoffmeister, F., Schwefel, H. P. 1991. A survey of evolution strategies. In Proceedings of the fourth international conference on genetic algorithms (Vol. 2, No. 9). Morgan Kaufmann Publishers San Mateo, CA.

[348].Morales, A. K., Quezada, C. V. 1998. A universal eclectic genetic algorithm for constrained optimization. In Proceedings of the 6th European congress on intelligent techniques and soft computing (Vol. 1, pp. 518-522).

[349].Joines, J. A., Houck, C. R. 1994. On the use of non-stationary penalty functions to solve nonlinear constrained optimization problems with GA's. In Evolutionary Computation, 1994. IEEE World Congress on Computational Intelligence., Proceedings of the First IEEE Conference on (pp. 579-584). IEEE.

[350].Michalewicz, Z., Attia, N. 1994. Evolutionary optimization of constrained problems. In Proceedings of the 3rd annual conference on evolutionary programming (pp. 98-108). World Scientific.

[351].Smith, A., Tate, D. 1993. Genetic optimization using a penalty function, Proceedings of the fifth International Conference on Genetic Algorithms, Morgan Kaufmann, 499-503.

[352].Gen, M., Cheng, R. 1996. A survey of penalty techniques in genetic algorithms. In Evolutionary Computation, 1996., Proceedings of IEEE International Conference on (pp. 804-809). IEEE.

[353].Le Riche, R., Knopf-Lenoir, C., Haftka, R. T. 1995. A Segregated Genetic Algorithm for Constrained Structural Optimization. In ICGA (pp. 558-565).

[354].Coello, C. A. C. 2000. Use of a self-adaptive penalty approach for engineering optimization problems. Computers in Industry, 41(2), 113-127.

[355].Schwefel, H.P. 1981. Numerical optimisation of computer models. John Wiley & Sons, Chichester, UK.

[356].Holmström, K., Jensen, H. J. 2004. Who runs fastest in an adaptive landscape: sexual versus asexual reproduction. Physica A: Statistical Mechanics and its Applications, 337(1-2), 185-195.

[357].Lipowski, A., Lipowska, D. 2012. Roulette-wheel selection via stochastic acceptance. Physica A: Statistical Mechanics and its Applications, 391(6), 2193-2196.

[358].Spears, W.M. 1992. Crossover or mutation? Proceedings of the Foundations of Genetic Algorithms Workshop, Vail, Colorado: Morgan Kaufmann.

[359].Spears, W.M. 1992. Adapting crossover in a genetic algorithm. Naval Research Laboratory AI Center Report AIC-92-025. Washington, DC 20375 USA.

[360].Wagner, T., Trautmann, H., Martí, L. 2011. A taxonomy of online stopping criteria for multi-objective evolutionary algorithms. In International Conference on Evolutionary Multi-Criterion Optimization (pp. 16-30). Springer, Berlin, Heidelberg.

[361].Eiben, Á. E., Hinterding, R., Michalewicz, Z. 1999. Parameter control in evolutionary algorithms. IEEE Transactions on evolutionary computation, 3(2), 124-141.

[362]. Smit, S. K., Eiben, A. E. 2009, May. Comparing parameter tuning methods for evolutionary algorithms. In Evolutionary Computation, 2009. CEC'09. IEEE Congress on (pp. 399-406). IEEE.

[363].Bartz-Beielstein, T. 2006. Experimental research in evolutionary computation—the new experimentalism. Natural Computing Series. Springer, Berlin, Heidelberg, New York.

[364].Eiben, A. E., Smit, S.K. 2011. Evolutionary algorithm parameters and methods to tune them. In Autonomous search (pp. 15-36). Springer, Berlin, Heidelberg.

[365].Müller, J. 2017. SOCEMO: Surrogate Optimization of Computationally Expensive Multiobjective Problems. Informs Journal on Computing, 29(4), 581-596.

[366].Booker, A. J., Dennis, J. E., Frank, P. D., Serafini, D. B., Torczon, V., Trosset, M. W. 1999. A rigorous framework for optimization of expensive functions by surrogates. Structural optimization, 17(1), 1-13.

[367].Amdahl, G. M. 1967. Validity of the single processor approach to achieving large scale computing capabilities. In Proceedings of the April 18-20, 1967, spring joint computer conference, pp. 483-485.

[368].Scott, M. H., Fenves, G. L. 2006. Plastic hinge integration methods for force-based beam–column elements. Journal of Structural Engineering, 132(2), 244-252.

[369].Priestley, M. J. N., Seible F., Calvi G.M., 1996. Seismic Design and Retrofit of Bridges, Wiley, New York.

[370].Yettram, A. L., Husain, H. M. 1965. Grid-Framework Method for Plates. Journal of the Engineering Mechanics Division, 91(3), 53-64.

[371].Werbos, P.J. 1974. Beyond regression: New tools for prediction and analysis in the behavioral sciences. Ph.D. Thesis, Harvard University.

[372].Fajfar, P., Marušić, D., Peruš, I. 2005. Torsional effects in the pushover-based seismic analysis of buildings. Journal of Earthquake Engineering, 9(06), 831-854.

[373].Bhatt, C., Bento, R. 2014. A 3D pushover methodology for seismic assessment of plan asymmetric buildings. Earthq Spectra Earthq Eng Res Inst, 30(2), 683-703.

[374].Chopra, A. K., Goel, R. K. 2004. A modal pushover analysis procedure to estimate seismic demands for unsymmetric-plan buildings. Earthquake engineering & structural dynamics, 33(8), 903-927.

[375].De Stefano, M., Pintucchi, B. 2010. Predicting torsion-induced lateral displacements for pushover analysis: Influence of torsional system characteristics. Earthquake Engineering & Structural Dynamics, 39(12), 1369-1394.

[376].Yin, L., Yang, W. 2001. Optimality criteria method for topology optimization under multiple constraints. Computers & Structures, 79(20-21), 1839-1850.

[377].Saaty, T. L. 1977. A scaling method for priorities in hierarchical structures. Journal of mathematical psychology, 15(3), 234-281.